



**HAL**  
open science

# The role of organic pollutants in the alteration of historic soda silicate glasses

Laurianne Robinet

► **To cite this version:**

Laurianne Robinet. The role of organic pollutants in the alteration of historic soda silicate glasses. Material chemistry. Université Pierre et Marie Curie - Paris VI; Edinburgh University, 2006. English. NNT: . tel-00088408

**HAL Id: tel-00088408**

**<https://theses.hal.science/tel-00088408>**

Submitted on 1 Aug 2006

**HAL** is a multi-disciplinary open access archive for the deposit and dissemination of scientific research documents, whether they are published or not. The documents may come from teaching and research institutions in France or abroad, or from public or private research centers.

L'archive ouverte pluridisciplinaire **HAL**, est destinée au dépôt et à la diffusion de documents scientifiques de niveau recherche, publiés ou non, émanant des établissements d'enseignement et de recherche français ou étrangers, des laboratoires publics ou privés.

THE UNIVERSITY OF EDINBURGH  
UNIVERSITE PARIS VI - PIERRE ET MARIE CURIE

JOINT THESIS

Submitted for the joint-degree of

**PhD / Doctorat**

in materials chemistry, physical chemistry and analytical chemistry

by

**LAURIANNE ROBINET**

**THE ROLE OF ORGANIC POLLUTANTS IN THE  
ALTERATION OF HISTORIC SODA SILICATE GLASSES**

Prepared at the School of Engineering and Electronics of the University of Edinburgh and at the  
Laboratoire de Dynamique Interaction et Réactivité  
(LADIR – Unité mixte de Recherche CNRS 7075 – Université Paris VI)

**18<sup>th</sup> July 2006**

Professor C. Hall	Supervisor
Professor N. Lacombe	Supervisor
Professor A. Harrison	Reviewer
Professor S. Turrell	Reviewer
Professor G. Allen	Examiner
Doctor L. Galois	Examiner
Doctor J. Tate	Guest
Doctor C. Coupy	Guest

## DECLARATION

I declare that this thesis has been composed by myself and is all my own work except where otherwise stated.

---

Laurianne Robinet

July 2006

## ACKNOWLEDGMENTS

This adventure, shared between Scotland and France, has been extremely rich and constructive in so many aspects. This richness flourished from all the meetings: with the glass material, the world of research, the Scottish culture and all those who facilitated these meetings, I would like to acknowledge them here.

Mes premiers remerciements sont adressés à une femme d'exception Claude Coupry, pour m'avoir fait partager sa connaissance et passion de la spectroscopie Raman, de l'art et de la vie; et pour m'avoir donné du courage tout au long de cette aventure. Ton aide fut précieuse, merci.

My deepest thanks to Christopher Hall, for his support and patience, for sharing his deep research knowledge and for challenging and pushing my intellectual ability. I am very grateful.

I would like to thank Nelly Lacombe (Université Pierre et Marie Curie) and Colin Pulham (University of Edinburgh) for their advice and for helping me out in all situations.

I wish to thank Sylvia Turrell from the Laboratoire de Spectrochimie Infrarouge et Raman (LASIR) of the Université des Sciences et Technologies de Lille for her valuable advice and for accepting to be a member of the jury and a reviewer of this work. I also thank Andrew Harrison from the School of Chemistry of the University of Edinburgh for agreeing to be a reviewer of this thesis and a member of the jury. I am grateful to Geoffrey Allen from the Interface Analysis Centre of the University of Bristol, and Laurence Galois from the Institut de Minéralogie et de Physique des Milieux Condensés of the Université de Paris VI and Paris VII for accepting to be members of this jury and therefore sharing their knowledge.

I am much indebted to Katherine Eremin and Jim Tate from, or originally from, the National Museums of Scotland (NMS) for their help, advice and encouragement throughout this research. I am also very grateful for the support of colleagues or friends at the NMS and in the Conservation and Analytical Research team. I would like to thank in particular Belen Cobo del Arco for introducing me to the alteration of historic glass in the NMS, Ulrike Al-Khamis and Brenda McGoff for giving me access to the cellars, always with a smile, and David Peggie for his energy, advice and for making me discover his Scottish culture.

I would like to say ‘merci’ to the team at the Laboratoire de Dynamique Interactions et Réactivité of the CNRS in France for making this three years a lively experience, in particular I would like to thank Gérard Sagon and Ludovic Bello-Gurlet for their help with the Raman spectrometer and André Crétot for teaching me the art of glass blowing.

Thank you to the team of the Centre of Materials Science and Engineering of the University of Edinburgh for creating interesting discussion and for offering their help and advice all along this project.

I wish to thank Sarah Fearn (Imperial College) for introducing me to SIMS and for her help throughout this research and John Craven (University of Edinburgh) for his patience and his extended help with this instrument (Swiss chocolate provided). I would like to thank Nicola Meller (University of Edinburgh) for her help with the XRD, Peter Hill (University of Edinburgh) for helping with the electron microprobe, Lorraine Gibson (Strathclyde University) for undertaking the pollutants analyses, and Robert Brill and Stephen Koob (The Corning Museum of Glass) for introducing us to their museum and providing samples for this research. In addition I wish to thank Jacques Chevalier (French Embassy) for his optimism and his help with the administration of this new shared PhD.

I am grateful to the EPSRC, the University of Edinburgh, the Ministère des Affaires Étrangères, Stevenson Trust and the National Museums of Scotland for funding and to the British country for giving me a chance.

Enfin, je souhaiterais remercier mes parents, et mon frère Gilles pour avoir toujours été derrière moi pour m’aider et me soutenir et remercier Hans de tout cœur pour m’avoir prêté ses ailes.

*‘Avant que vous ne viviez, la vie, elle, n’est rien,  
mais c’est à vous de lui donner un sens’*

J.-P. Sartre  
L’existentialisme est un humanisme

## SUMMARY

### **The role of organic pollutants in the alteration of historic soda silicate glasses**

The stability of glass is linked to its composition and the atmosphere controls its alteration. The organic pollutants emitted by wooden showcases play a role in the alteration of historic glasses. This study examines the effects of acetic acid, formic acid and formaldehyde on objects from the National Museums of Scotland and on replica glasses aged artificially, all with a soda silicate composition. Composition was determined by electron microprobe and analytical decomposition of the Raman spectra was used to establish correlations between glass structure and composition. This allowed interpretation of the structural variations between bulk and altered glass. The structure of the glasses altered by pollutants is characteristic of an alteration by selective leaching, with transformation of the silicates linked to alkali into silanols, which subsequently underwent condensation reactions to form a more polymerised structure. The SIMS concentration profiles of glass aged in artificial and real atmospheres were used to follow the alteration evolution as a function of time, humidity and pollutant concentration. The water film formed by the humidity at the surface and its acidity control the alteration by leaching of alkali and hydration of the glass. Formaldehyde does not act on the leaching reaction while acids accelerate and amplify it. In mixed polluted atmosphere, formates compounds always predominate in the film even at low formic acid concentration. The humidity and temperature fluctuations in museums maintain the leaching reaction. Knowledge of the harmful effect of organic acid pollutants in the alteration of soda silicate glasses will help improve their conservation.

**Keywords:** soda silicate glass, alteration, museum, sodium formate, stability, Raman, SIMS.

## RESUME

### **Le rôle des polluants organiques dans l'altération des verres sodiques historiques**

La stabilité d'un verre est liée à sa composition et l'environnement contrôle son altération. Pour les verres historiques, les polluants organiques émis par les vitrines en bois interviennent dans leur altération. Ce travail étudie les mécanismes d'altération des acides acétique et formique et du formaldéhyde sur des objets de musée et des verres vieilliss artificiellement, de composition sodique. Après détermination de la composition par microsonde électronique, la décomposition des spectres Raman a servi à établir des corrélations entre composition et structure des verres, et à interpréter les variations de structure entre verre sain et altéré. La structure des objets altérés par les polluants est caractéristique d'une altération par lixiviation, où seuls les silicates liés aux alcalins sont transformés en silanols, qui polymérisent par la suite. Les profils de concentrations SIMS de verres vieilliss en atmosphères artificielles et réelles ont permis de suivre l'altération en fonction du temps, l'humidité et la concentration en polluants. Le film d'eau formé à la surface par l'humidité et son acidité contrôlent l'altération par lixiviation des alcalins et hydratation du verre. Le formaldéhyde n'agit pas sur la réaction de lixiviation tandis que les acides l'accélèrent et l'amplifient. Quelque soient les proportions des polluants, les composés formates prédominent dans les produits cristallins, même en faible concentration d'acide formique. L'humidité et la température fluctuante des musées entretiennent la réaction de lixiviation. L'évidence du rôle néfaste des polluants organiques acides dans l'altération des verres sodiques permettra d'améliorer leur conservation.

**Mots-clés:** verre sodique, altération, musée, formate de sodium, stabilité, Raman, SIMS.

# TABLE OF CONTENTS

<b>DECLARATION .....</b>	<b>2</b>
<b>ACKNOWLEDGMENTS .....</b>	<b>3</b>
<b>SUMMARY – RESUME .....</b>	<b>6</b>
<b>TABLE OF CONTENTS .....</b>	<b>7</b>
<b>GENERAL INTRODUCTION .....</b>	<b>11</b>
<b>I- STATE OF THE ART .....</b>	<b>13</b>
<b>I- 1. Introduction to glass .....</b>	<b>14</b>
I- 1.1 Technology of ancient glasses .....	14
I- 1.2 The structure of silicate glasses .....	18
<b>I- 2. Alteration of glasses .....</b>	<b>23</b>
I- 2.1 Influence of the composition .....	23
I- 2.2 Alteration mechanisms .....	25
I- 2.3 Glass surface reactivity .....	30
I- 2.4 Factors influencing the alteration process and kinetics .....	31
<b>I- 3. Alteration of historic glasses from the NMS collections .....</b>	<b>35</b>
I- 3.1 Identification of the problem .....	35
I- 3.2 Elemental composition .....	36
I- 3.3 Crystalline corrosion products .....	36
I- 3.4 Environmental conditions .....	37
I- 3.5 Artificial ageing experiments .....	39
I- 3.6 Conclusions from the scientific study .....	40
<b>I- 4. Volatile organic pollutants .....</b>	<b>41</b>
<b>I- 5. Summary and research strategy .....</b>	<b>43</b>
<b>I- 6. References .....</b>	<b>45</b>

<b>II-</b>	<b>EXPERIMENTAL AND INSTRUMENTAL .....</b>	<b>53</b>
<b>II- 1</b>	<b>Introduction .....</b>	<b>54</b>
<b>II- 2</b>	<b>Materials and samples .....</b>	<b>56</b>
II- 2.1	Museum objects .....	56
II- 2.2	Replica glasses .....	58
<b>II- 3</b>	<b>Ageing experiments .....</b>	<b>60</b>
II- 3.1	Ambient ageing experiments.....	60
II- 3.2	Accelerated ageing experiments.....	65
<b>II- 4</b>	<b>Analytical techniques.....</b>	<b>67</b>
II- 4.1	Raman spectroscopy .....	67
II- 4.2	Secondary ion mass spectrometry (SIMS) .....	73
II- 4.3	Electron probe microanalysis (EPMA) .....	78
II- 4.4	Scanning electron microscopy-energy dispersive spectrometry (SEM-EDS) .....	79
II- 4.5	Light microcopy .....	80
II- 4.6	X-Ray Diffraction (XRD) .....	81
<b>II- 5</b>	<b>References.....</b>	<b>82</b>
<b>III.</b>	<b>THE CRYSTALLINE DEPOSITS ON GLASSES .....</b>	<b>84</b>
<b>III.1.</b>	<b>Introduction.....</b>	<b>85</b>
<b>III.2.</b>	<b>Introduction to sodium formates .....</b>	<b>86</b>
<b>III.3.</b>	<b>Museum objects.....</b>	<b>87</b>
<b>III.4.</b>	<b>Artificial experiments .....</b>	<b>90</b>
III- 1.1	Accelerated ageing experiments.....	90
III- 1.2	Ambient ageing experiments.....	91
<b>III.5.</b>	<b>Sodium formate heating.....</b>	<b>93</b>
<b>III.6.</b>	<b>Conclusion .....</b>	<b>95</b>
<b>III.7.</b>	<b>References.....</b>	<b>96</b>

<b>IV.</b>	<b>THE CHEMICAL STRUCTURE OF SODA SILICATE GLASSES ...</b>	<b>97</b>
IV- 1.	<b>Introduction</b> .....	<b>98</b>
IV- 2.	<b>Application of Raman spectroscopy to glass</b> .....	<b>99</b>
IV- 3.	<b>Influence of the composition on the glass structure</b> .....	<b>100</b>
IV- 3.1	Stability and composition .....	101
IV- 3.2	Raman spectra and composition.....	104
IV- 3.3	Decomposition model.....	108
IV- 3.4	Composition correlations with Raman spectra.....	110
IV- 4.	<b>Structure modification with alteration</b> .....	<b>115</b>
IV- 4.1	Museum objects .....	116
IV- 4.2	Artificial accelerated ageing experiments .....	125
IV- 5.	<b>Non-destructive analyses of objects</b> .....	<b>142</b>
IV- 5.1	Determination of the degree of alteration.....	142
IV- 5.2	Depth profiling analyses .....	144
IV- 6.	<b>Conclusion on the structure of soda silicate glass</b> .....	<b>146</b>
IV- 7.	<b>References</b> .....	<b>149</b>
<b>V.</b>	<b>MECHANISMS AND KINETICS OF THE ALTERATION .....</b>	<b>152</b>
V- 1.	<b>Introduction</b> .....	<b>153</b>
V- 2.	<b>Data treatment</b> .....	<b>155</b>
V- 2.1	Interference correction .....	155
V- 2.2	Sputter rate and depth quantification .....	155
V- 2.3	Ion yield and elemental profile quantification .....	157
V- 2.4	Quantitative measurement of the alteration .....	159
V- 3.	<b>Results</b> .....	<b>161</b>
V- 3.1	Reliability of the SIMS measurements .....	161
V- 3.2	Effect of CO <sub>2</sub> .....	164
V- 3.3	Effect of RH and organic pollutants .....	168
V- 3.4	Progress of the alteration with time.....	177
V- 4.	<b>Conclusion</b> .....	<b>197</b>
V- 5.	<b>References</b> .....	<b>200</b>

<b>GENERAL CONCLUSION .....</b>	<b>202</b>
<b>APPENDICES.....</b>	<b>205</b>
APPENDIX - I : Cation radii.....	206
APPENDIX - II : Ambient experiments.....	207
APPENDIX - III : Accelerated experiments.....	208
APPENDIX - IV : Crystalline products on glasses .....	209
APPENDIX - V : Publications and conferences.....	210
<b>RESUME DETAILLE EN FRANCAIS.....</b>	<b>212</b>
Introduction .....	213
I. Etat de l'art .....	214
II. Expérimentation et instrumentation .....	216
III. Produits cristallins sur les verres.....	218
IV. La structure des verres sodiques.....	219
V. Mécanismes et cinétique de l'altération .....	222
Conclusion .....	225

## GENERAL INTRODUCTION

Glass is a beautiful material. It forms a large part of our cultural heritage as well as our everyday life; however much remains unknown about its nature and properties. Early science benefited greatly from its development: glass lenses and prisms in optics, chemistry with the transparent glassware, or physics with the creation of thermometers and barometers. In return advances in these sciences have provided an insight into the material itself.

The chemical alteration of glass is a problem that affects its use in a number of fields and this is the reason why the material science of glass has been studied for many decades. It is well recognised that the two main factors responsible for alteration of glass are *water* and the glasses chemical *composition*. The interaction between glass and its environment, and the affects on the alteration processes and on the characteristic and visual appearance of the glass, are subjects of continued investigation.

All ancient and historic glasses are more or less affected by alteration. Within museum collections, this is a particular matter of concern as deterioration results in visual alteration and physical damage to the objects, including development of surface iridescence, formation of crystalline products or liquid droplets (depending on the relative humidity), crizzling, cracking and flaking. In extreme cases, the entire object may disintegrate. Because of this many museums are concerned with the stability of their glass collections and attempt to control variations in relative humidity which clearly affects their conditions. However, detailed knowledge of the chemical processes leading to alteration is required to improve preservation and conservation.

Compared with the simple binary glasses compositions which are generally studied in glass science, historic glasses are complex systems that contain a mixture of elements, each one of which influences differently the structure and so the durability of the glass. In addition, the alteration processes which occur are very different for archaeological glass, stained glass windows or decorative historical glass, due to the different environments to which they have been exposed. The large range of factors involved makes the investigation of ancient/historic glasses a complex subject.

In the National Museums of Scotland (NMS), widespread alteration was observed for part of the historic glass collection of the 19<sup>th</sup>-20<sup>th</sup> centuries. A first scientific study undertaken by the Conservation and Analytical Research department of the NMS on the British collection studied the cause of this alteration. It revealed that organic pollutants, mainly acetic acid, formic acid, and formaldehyde emitted by the wooden cabinets in which objects were stored or displayed, were involved in this alteration. Similar alterations have been reported in other museums; but the exact effect of these pollutants on the alteration of historic glasses has never been investigated or modelled.

This thesis studies *the role of these organic pollutants on the alteration of historic soda silicate glasses*. The first chapter reviews the state of understanding of historic glass alteration, focusing on the aspects developed in the following chapters: the composition and structure of the material; the mechanisms, kinetics and the role the different external factors in the alteration of glass; the alteration of the NMS glass collection; and finally the organic pollutants.

The research strategy and the organisation of the thesis, which was developed following the review of previous work, are introduced at the end of the first chapter.

## **Chapter I.**

# **STATE OF THE ART**

## I- 1. Introduction to glass

### I- 1.1 Technology of ancient glasses

Ancient man-made silicate glasses generally contain a mixture of silica, alkali and lime, obtained from naturally occurring materials. It is thought likely that the first glass was created as a result of chance, when fire, sand and a melting agent such as natron met, and Syria, Mesopotamia or Egypt have been proposed as the birth place of glass around 2500 BC. Although the colour, shape, working process and raw materials evolved through the ages, the composition remained similar, mainly alkali-lime silicate (either soda or potash) and later on lead silicate glasses [1, 2]. The increased sophistication of glass design or the changes in demand and supply favoured changes in the choice of the raw materials, which led to modification of the glass composition [1, 2, 3].

#### I- 1.1.1 *Materials and composition*

The source of the main chemical constituent silica was sand, quartz pebbles and flint, and typically makes up to 50-70 weight % (wt%) of ancient glass. The alkali, soda or potash, were mixed with the silica to reduce the melting temperature. Thus 20 wt% alkali reduced the temperature from 1700 °C to under 1000 °C [3]. The alkali were obtained either from naturally occurring minerals or from ashes formed by burning plant or wood. Soda was predominantly used until about AD 1000. It was provided by lacustrine deposits, such as natron (sodium sesquicarbonate), saltmarsh plants, or seaweed. The use of natron stopped after the 7<sup>th</sup> to 9<sup>th</sup> century, after which only plant ashes were used [1, 4]. The magnesium and potassium oxides content in the glass can inform on the soda source used. When the content of the two oxides is below 1.5 wt%, as in Roman glass, natron was used; however when the content of the two oxides is much greater, as in Bronze Age, Islamic or Venetian glasses, the source used was plant ash [1, 5, 6]. Around AD 1000, potash began to replace soda as a regular source of alkali, possibly as a result of the large demand for window glasses in monuments and buildings in the medieval period. The potash was provided by the wood (mainly beechwood) or fern ashes [1]. Table I- 1 presents examples of composition for glasses from different periods.

Table I- 1: Typical composition of ancient and modern glasses; in addition to those listed, the ancient glasses would have contained also up to 1 wt% FeO and 3 wt% Al<sub>2</sub>O<sub>3</sub> as well as colorants or decolourisers [3].

Wt %	Egyptian 15 <sup>th</sup> cen. BC	Roman 1 <sup>st</sup> cen. AD	European 13 <sup>th</sup> cen. AD	Syrian 14 <sup>th</sup> cen. AD	Modern
SiO <sub>2</sub>	65	68	53	70	73
Na <sub>2</sub> O	20	16	3	12	16
K <sub>2</sub> O	2	0.5	17	2	0.5
CaO	4	8	12	10	5
MgO	4	0.5	7	3	3
Raw materials	Plant ash quartz	Natron sand	Wood ash sand/quartz	Plant ash sand/quartz	Synthetic components

Lime (CaO) was also present in the glass and was probably not added intentionally before and during the Roman period and the Middle Ages. In those times, the lime present in the glass came as an impurity from the sand, which may contain around 7 wt% CaO from shell as in the sand of the Belus river in Syria. From 14<sup>th</sup> century in Europe, CaO was voluntarily added for economical reason, to reduce the ashes consumption. Purification of the ashes sometimes reduced the CaO content as in Venetian or Murano glasses in the 15<sup>th</sup> century [1, 3].

If no metallic oxide were added, as colorant or decolouriser, the glass had a yellow or greenish colour owing to the presence of mostly iron contaminant in the sand. From the middle of the 1<sup>st</sup> century BC, decolouriser components started to be used to neutralise the colorant effect of iron. Antimony was the main decolourant before the Roman period, and then manganese dominated from the 2<sup>nd</sup> century AD [3].

Lead oxide was incorporated in some glass since the second millennium BC, but its use was probably unintentional. In 1675, George Ravenscroft invented the lead crystal glass (or flint) to compete with the transparent Cristallo and Bohemian glass produced in Europe at that period, and reduces the use of plant ashes which had to be imported. Lead crystal glass was made by mixing litharge, saltpetre and flint, and the main component of the glass were SiO<sub>2</sub>, PbO, K<sub>2</sub>O, with up to 30 wt% lead oxide [1].

### I- 1.1.2 Manufacturing process

The mixture of components was generally heated around 1000 °C so the ingredient slowly melted and reacted. Scraps of glass of a similar composition were sometimes added to the mixture to act as a nucleus around which the new glass was formed. Depending on the viscosity of the glass, which varies with the composition of the glass and heating temperature, the glass could be worked and given a wide range of shapes. The glass formed was cooled slowly in an annealing oven to relieve stresses created during the manufacture [1].

The first glasses were not translucent but opaque because of the incomplete fusion and the presence of varied impurities in the materials used. They were produced by trailing molten glass onto cores made of clay, which was removed after the glass had cooled and hardened [3]. The blowing of glass was invented between 50-40 BC along the decoloration methods, and was a revolution for the technology of glass [1]. The glassblowing technique, which consisted of blowing through a metal tube (blowpipe) to produce a bubble into the molten glass, spread rapidly, particularly throughout the Roman world (Figure I- 1).



Figure I- 1: Still life with glassware, painted plaster, 1<sup>st</sup> Century AD, Herculaneum (photograph taken by the author at the exhibition 'Le verre dans l'Empire romain' Paris, 2006)

From the blowing technique, two processes were developed to make flat transparent glass around the 4<sup>th</sup> century and used, while being improved, up to the 19<sup>th</sup> century [2]:

- **Crown glass:** made by blowing the glass to form a "crown" or hollow globe. This was then flattened by reheating and spinning out the bowl-shaped piece of glass into a flat disk by centrifugal force, up to 1.5 to 1.8 meters in diameter (Figure I- 2).
- **Cylinder glass:** made by blowing a cylinder, then cutting, opening, and gently flattening the glass while it was still hot and pliable.

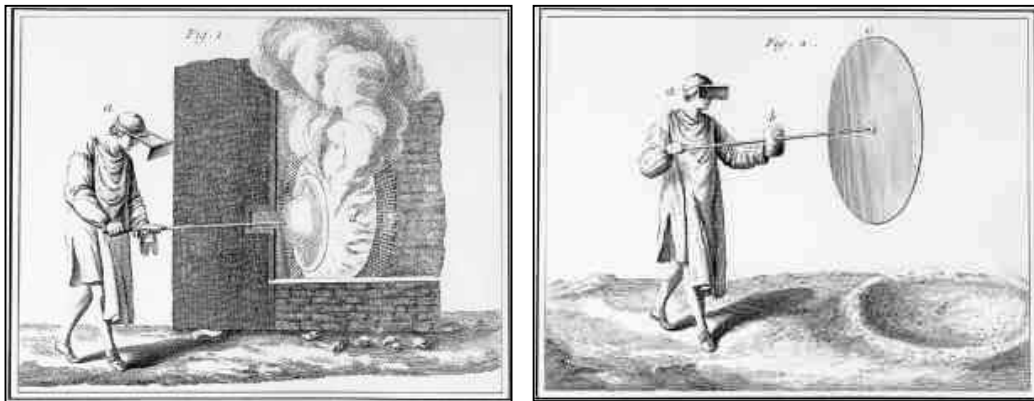


Figure I- 2: Crown glass fabrication from Diderot's Encyclopedia

The availability of flat glass, made by either process across the world, favoured the development of stained glass windows (from 10-11<sup>th</sup> century), mirrors (15<sup>th</sup> century) and the use of more and more clear glass windows in buildings (16<sup>th</sup> century). Nowadays, the main flat glass used is the float glass, invented in 1952 by A. Pilkington and made by pouring the molten glass onto a bath of molten tin.

## I- 1.2 The structure of silicate glasses

### I- 1.2.1 Basic concepts – $\text{SiO}_2$

Silicate glass displays short-range order with the arrangement of atoms into  $\text{SiO}_4$  tetrahedra, but no order at the medium- and long-range. These  $\text{SiO}_4$  units form the backbone of silicate glass, for this reason Si is termed **former** ion. The disorder present in glass is because of the non-crystalline nature of the material induced by the making process. If a liquid is cooled fast enough to prevent crystallisation, the thermodynamic equilibrium cannot be maintained and the viscosity increases up to the point where the 'liquid is frozen' and the glass is formed [7, 8, 9, 10].

In each silicate unit, a silicon charged positively is surrounded by 4 oxygens charged negatively inducing the formation of covalent Si-O bonds with a partially ionic character. In order to satisfy the electrostatic repulsion of Si atoms, the silicate tetrahedra are linked by their corners, thus sharing only one oxygen. The oxygens connecting two silicate tetrahedra are called **bridging oxygens (BOs)** (Figure I- 3). The silicate tetrahedra are organised into rings, which constitute a structure medium-range order. In pure silica, the silicate tetrahedra  $\text{SiO}_4$  are polymerised into a three dimensional network where all oxygens are bridging, and mostly 6-, 4- and 3- members rings are present [10].

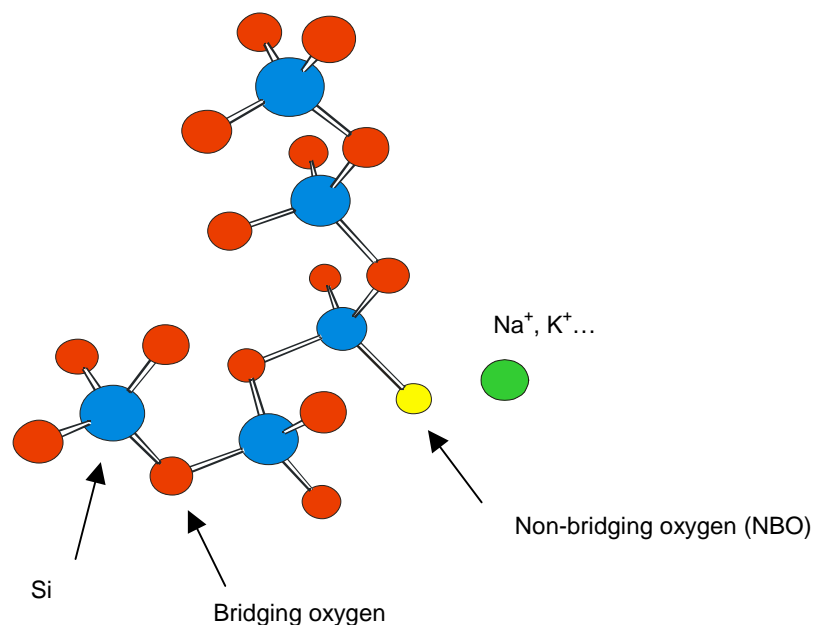


Figure I- 3: Schematic representation of the structure of alkali silicate glasses (L.Bellot-Gurlet, LADIR)

### I- 1.2.2 *The role and effect of the cations*

Cations such as alkali or alkaline-earth metal ions are generally added to a glass to modify its properties, for this reason they are named **modifiers**. In practical terms, the addition of alkali ions (sodium or potassium) lower the temperature needed to melt components and improves the workability of the glass by decreasing the viscosity. Alkaline-earth (calcium, magnesium and barium), and/or aluminium ions also decrease the viscosity, but to a lesser extent, and their main role is to stabilise the glass against alteration, hence are termed **stabilisers**. Lead is added to increase the refractive index of the glass, which then has a greater density and becomes easier to work [9]. Lead cation can be present both as a modifier and as a former, like silicon, with its importance as former increasing with the percentage of lead. The colour of the glass is generally related to the presence and ionic state of small amounts of colorant ions, such as copper, iron, or manganese, and/or decolourisers, such as manganese, arsenic or antimony [11].

Incorporating modifier cations into the glass structure induces a depolymerisation of the silicate network, by breaking the Si-O connectivity, and creates an ionic bond between the oxygen and the cation, which is weaker than the Si-O bond. The oxygens coordinated to cations in the silicate structure are called **non-bridging oxygens (NBOs)** (Figure I- 3) [11]. There are also weaker interactions between the cations and the BOs [12]. The different bonding energy between NBO-cation and Si-O alters the oxygen electronic structure, and this effect is evidenced and used in vibrational and X-ray photoelectron (XPS) spectroscopies [10, 12, 13]. The type of cations introduced affects the NBO-cation and the Si-O (BO and NBO) bonds length and strength, the cation coordination number (which is higher than that for former cations) and the Si-O-Si bond angle, therefore modifying the glass structure [10, 13]. The radii of the cations present in silicate glasses is given as a function of charge and coordination number in **appendix I**.

For alkaline-earth elements, the network connectivity is partially maintained by the link established by the doubly charge cation between the two NBOs created [8], which might account for the stabilising role of alkaline-earth cations compared to alkali cations. In mixed alkali silicate glasses, the substitution of one alkali by another leads to significant non-linear changes in the physical properties of the glasses. The physical origin of this effect, known as the **mixed-alkali effect**, is not currently understood [13]. In the structure, Si may potentially be replaced by other cations that have a similar ionic radius and electric charge of about 4.

Thus cations such as  $\text{Al}^{3+}$  or  $\text{Fe}^{3+}$ , which could substitute  $\text{Si}^{4+}$ , would take the role of network former. In that situation, alkali and alkaline-earth metal ions have a dual structural role, first as network modifier associated with NBOs, and secondly as charge-compensating ions for cations in tetrahedral coordination. For  $\text{Si}^{4+}$ , the most prevalent substitution is  $\text{Al}^{3+}$  [10].

The degree of polymerisation, which directly affects the physical properties of glasses, is given by the average number of NBOs per tetrahedrally coordinated cation, represented by NBO/Si in silicate glasses. However, this parameter does not take into account the nature of the former or modifier cations [10].

The notation  $\text{Q}^n$ , where n is the number of bridging oxygens, which varies from 0 to 4 for  $\text{SiO}_4$ , is used to distinguish between the different tetrahedral species in the network:  $\text{Q}^3$  corresponds to silicate species with one NBO,  $\text{Q}^2$  to silicate species with two NBOs and  $\text{Q}^4$  to silicate species with no NBO (Figure I- 4) [14, 15]. This  $\text{Q}^n$  model is used as a basis for the interpretation of the Raman spectroscopy and NMR data of glasses. By their charge and radius, the cation type and concentration affect the Q distribution, influencing the charge balance conservation, stoichiometry and the electrostatic forces in the glass structure. For alkali silicate glasses, in particular, the NBO distribution per silicon decreases in the order  $\text{Li} > \text{Na} > \text{K}$  [13].

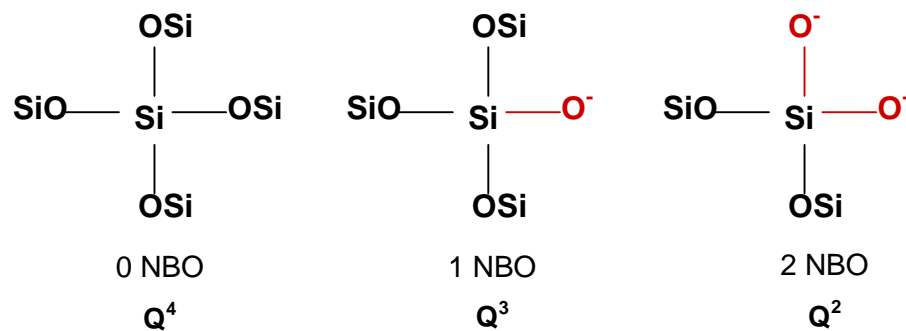


Figure I- 4: Schematic representation of silicate species  $\text{Q}^4$ ,  $\text{Q}^3$  and  $\text{Q}^2$

Moreover, in glass containing mixed cations, there exists an ordering which is governed by the charge and ionic radii of the cations [12]. Alkali and alkaline-earth cations are ordered differently among the different NBOs. The more electronegative the metal cation, the stronger is its tendency to form bonds with NBO in the least polymerised  $\text{Q}^n$  species. Thus alkali cations are preferentially bonded to NBO from  $\text{Q}^3$  units, while alkaline-earth cations

are preferentially bonded to NBO from  $Q^2$  units [10]. In soda-lime silicate glasses the prevalence of Na-Ca pairs has been demonstrated and explained by the similarity of the two cations radii [12]. The disorder and the different effects induced by the cations create a distribution of bond strengths and angles in the structure, which results in a distribution of vibrational frequencies and thus a broadening of bands in Raman spectra.

### I- 1.2.3 The structural models

With the progress of analytical techniques and increasing knowledge in glass science, the understanding of the medium- and long-range structure of glasses evolved. Lebedev in 1921 first suggested that glass was made up of disordered arrangement of very small crystals whose structure is similar to the crystalline form [16].

Later the **Continuous Random Network (CRN)** model was proposed by Zachariasen in 1932 and confirmed experimentally by Warren [17, 18, 19]. This widely accepted model considers that the structure of glasses is close to the structure of the crystal, as they share the same basic structural elements ( $SiO_4$  units in silicate). However, they differ by their lack or symmetry and periodicity caused by slight atomic displacements inducing random variation of bonding angles and length (Figure I- 5). In this model random distribution of the cations was considered and the notion of bridging and non-bridging oxygens was introduced.

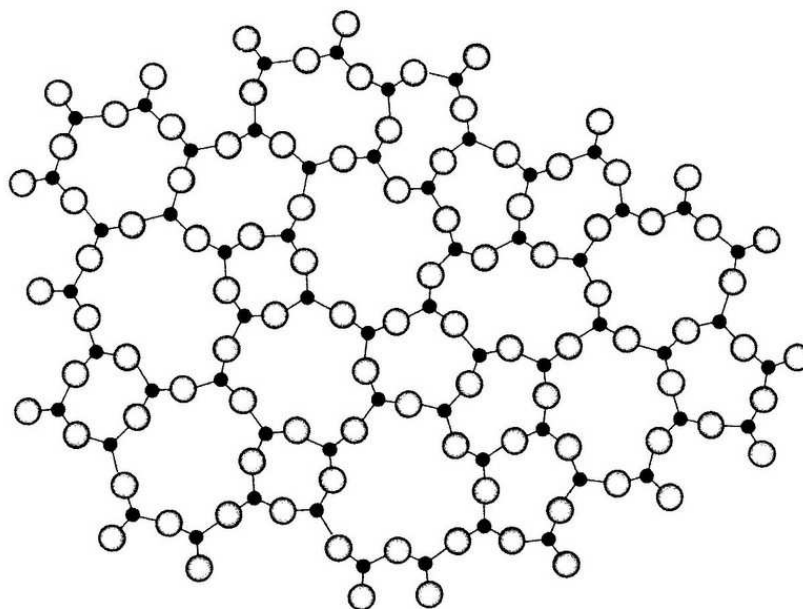


Figure I- 5: Two-dimensional glass network of a silicate glass (after Zachariasen [13]). Dark circles: Si atoms; light circles: O atoms [9].

Greaves modified the previous model to explain the experimental results on alkali silicate glasses which could not be applied to the CRN model. Based on EXAFS (Extended X-ray Absorption Fine Structure) measurements, he studied the local structure of sodium silicate glasses and introduced the notion of percolation channels occupied by modifying metals in the silicate network [20, 21]. These channels would weave between the network parts of the structure, facilitating the displacement of cations in the structure (Figure I- 6). This new model, called the **Modified Random Network (MRN)** is the most widely accepted model at the present time.

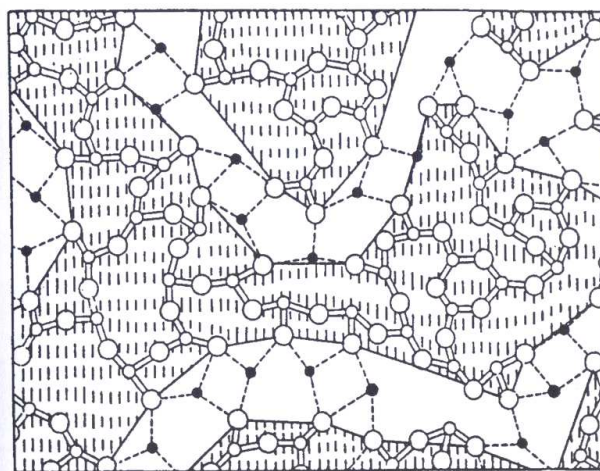


Figure I- 6: Modified Random Network (MRN) model for a silicate glass [16]. Open circles: glass network; filled circles: modifiers.

## I- 2. Alteration of glasses

Water and the glass composition are the two major factors responsible for the alteration of glasses. The effect of water was reported by Lavoisier in 1770 [22]; while the influence of glass composition was noted in 1760 by the director of the 'Manufacture Royale' in France. He observed that the use of modifier cations of a highest purity induced a decrease in quality and concluded that the presence of lime, present in large quantity in ashes, stopped the glass from corroding [2].

Fields as varied as the glass industry [23, 24], biomedical research [25, 26], geology [27, 28, 29], material science [30, 31, 32] museum science [1, 33, 34, 35] and the nuclear waste industry [36, 37] are concerned by the question of the alteration of glass. In the industry in particular, minute modification or irregularities in the glass surface, affect subsequent treatments, such as deposition of a film to modify the transmission properties of the glass.

### I- 2.1 Influence of the composition

It is generally admitted that glasses with high levels of alkali, above 20 wt% (~13.5 at%), and low levels of calcium, below 4 wt% (~2.3 at%), are the most prone to degradation [29, 33, 38, 39]. Alteration of glasses, ancient or otherwise, is linked to their chemical composition in two main ways: the structure of the network, which depends on the composition, and their coordination strength of cations to the structure.

The first compositional factor determining the tendency of a glass to deteriorate is the silica content. Because silica is the former cation of the network, its content determines to the number of NBOs in the structure and therefore the degree of polymerisation of the glass. The presence of NBOs in the structure enhances the susceptibility of silicate glass to alteration primarily as they create a more 'open' silicate network [8, 40]. It has been noted that alteration increases rapidly for silica content below the 66 mol% (~22 at%), point at which every silicate has 1 NBO [41]. In addition, the mobility of the ions is linked to the structure of the glasses and the presence of connected conduction pathways, both of which are influenced by the type and size of the cations present in the structure [20, 42]. Greaves

suggests that these percolation channels are the most likely routes for alkali diffusion, ion-exchange and water diffusion as well as crack propagation [20].

The different modifier cations do not react with water in the same way. In general, the glass becomes more reactive as the charge-to-ionic radius ratio of the cation decreases (see **appendix I**). Thus, **alkali** ions are the first affected by the alteration as they are the less strongly coordinated and therefore the most mobile cations. Ions with larger radius have weaker bonds with the NBO and have smaller (larger negative) free energy of hydration, hence they are most likely to be extracted from the matrix. Consequently, lithium glass is more resistant than soda glass, which is slightly more resistant than potash glass [9, 29]. However, in a glass containing mixed alkali the diffusion of the alkali in minor concentration is always smaller than for the alkali in major concentration, no matter the size of the cation [8]. This phenomenon associated with the mixed alkali effect means that a glass containing mixed sodium to potassium cations has lower corrosion rate than a glass containing only sodium ions, in equivalent alkali content [43].

In parallel, the addition of **alkaline-earth** ions to soda glasses greatly enhances the corrosion resistance when compared to a simple sodium silicate glass. This is explained by the stronger bond formed between the ions and the NBOs, and possibly to the fact that the doubly charged cations establish a connexion between NBOs, blocking the alkali migration [42, 44, 45]. In mixed alkali / alkaline-earth silicate glass, it was noted that the sodium mobility increases as the alkaline-earth ion size decreases [42, 44, 46, 47]. Thus,  $\text{Na}^+$  is more mobile in a glass containing  $\text{Mg}^{2+}$  than it is in a glass containing  $\text{Ca}^{2+}$  in identical proportion. This was explained by the different polarisation effect induced by the cation on the NBO. The cation  $\text{Mg}^{2+}$  polarises the NBO more than  $\text{Ca}^{2+}$ , thus the attraction force between the NBO and  $\text{Na}^+$  is reduced and  $\text{Na}^+$  mobility increase [8]. Moreover, the Na-Ca pairing may also be responsible for the reduced Na mobility [12]. In general, alkaline-earth cations are not affected by the alteration, however at high concentration (>10-15 mol% for CaO) in the glass, the alkaline-earth are extracted at the same levels as the alkali [48]. This may be related to the high depolymerisation of the structure induced rather than a concentration effect. Finally, it has been reported that the precipitation of alkaline-earth silicate at the glass surface may act as a barrier for further hydrolysis [8].

Aluminium ions improve the durability considerably because they can immobilise alkali ions which acts as charge compensating ions. Similarly ferric oxide could improve durability

by immobilising alkali ions. Thus glass coloured yellow by ferric ions would be more durable than the corresponding blue glass containing ferrous ions [49].

Finally, the durability of glass is influenced by its manufacturing process ; it appears that durability can be improved slightly by the repeated re-heating of the glass in the 'glory hole' (furnace), this producing a fire-finished surface which is depleted in alkali and forms a protective layer at the surface of alkali silicate glasses [49].

## I- 2.2 Alteration mechanisms

The alteration caused by the atmosphere, rather than solution, is generally called weathering. Its effect on the glass has been far less studied, although it has been mentioned that a humid atmosphere can induce more severe degradation on silicate glass than liquid water, since there is no solution to carry away the species (degradation products) sitting on the surface [49, 50, 51]. However, the alteration process of the glass in the atmosphere is expected to be similar to that in solution, where two alternative reactions exist, the relative proportions controlled by the pH of the solution [23, 29, 49, 51, 52, 53, 53]. Thus, when a glass is exposed to water, a **selective leaching** reaction takes place with the removal of mostly alkali metal ions from the glass structure and the entering of hydrogen bearing species from the water. As long as the pH remains between 1 and 9, the leaching reaction is enhanced. Through the leaching reaction a solution of NaOH, which is highly alkaline, builds up at the surface of the glass and triggers the second stage of the alteration. Above pH 9, the leaching process is slowed down and **congruent dissolution** of the silicate network is enhanced [23, 25, 29, 40, 53, 54, 55, 56].

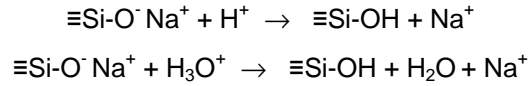
### I- 2.2.1 *Selective leaching*

The leaching reaction in solution is characterised by [53, 29, 52, 57] :

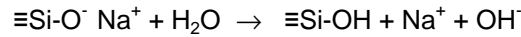
- A reaction rate largely independent of pH from 1 to 9
- The migration of mostly univalent cations (alkali)
- Low levels of alkali retained in the altered glass (to promote the ion-exchange ?)
- The formation of a **leached layer** (de-alkalised), which is silica rich and hydrated
- The altered layer may act as a protective barrier against further attack

During leaching three types of reaction occur simultaneously, each one influencing the others, and all resulting in an hydration of the glass [30, 40, 58]:

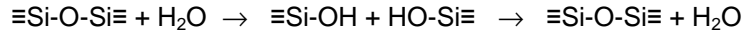
- 1) *Ion-exchange*: when cations, such as alkali ions, are replaced by  $H^+$  or  $H_3O^+$



- 2) *Hydration*: when molecular water enters the glass as an intact solvent



- 3) *Hydrolysis*: when water breaks Si-O-Si bonds to form silanols



#### **Interdiffusion / ion-exchange:**

The penetration in the glass by H-bearing species is only possible if there is diffusion of alkali out of the glass in a way such that the electric neutrality is conserved at each point [59]. The high mobility of  $Na^+$  ions, the existence of a concentration gradient and the presence of positive ions such as  $H^+$  or  $H_3O^+$ , result in the diffusion of  $Na^+$  out of the glass as it is replaced by  $H^+$  or  $H_3O^+$  by formation of a silanol.

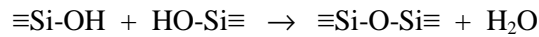
The nature of the species from the water exchanging with the alkali ions remains under discussions [58, 60, 61, 62, 63]. While an H/Na ratio around 1 would support an exchange with  $H^+$ , a ratio around 3 would instead support an exchange with  $H_3O^+$ . The interpretations based on this ratio do not agree because experimental data display a ratio varying between under 1 to over 3. Scholze mentions that the H/Na ratio depends on the glass composition and thus more H would be expected in glass with larger cations [58]. For examples  $K^+$  and  $H_3O^+$  ions have similar radius with ~140 pm and it was suggested that hydronium ions could replace potassium ions in the structure of potash silicate glass [59]. It is currently believed that the experimental differences are caused by the rearrangement of the structure and the rapid drying of the hydrated layer (by exposure to ambient air or high vacuum) with a removal of the water [9, 64]. Therefore, it appears that an exchange with hydronium ions is more likely.

**Diffusion of molecular water [60]:**

The water molecules can diffuse into the glass in two different ways, either as an intact solvent through void spaces between oxygens in the structure or through hydrolysis and condensation reaction of the silicate network. The rate of molecular diffusion is controlled by steric effects, determined by the size of the silicate rings and the cations filling and blocking the voids. The diffusing H<sub>2</sub>O molecules are immobilized at the sodium NBO's sites resulting in the formation of silanol groups. Thus, the sodium ions are freed and can, together with hydroxyl co-ions, diffuse towards the surface.

**Network rearrangement**

The formation of silanols is followed by a rearrangement of the silicate network which occurs by condensation of the silanols, resulting in the formation of molecular water [40, 58, 64]. This reaction implies that the leaching reaction is not reversible.

**Kinetics of the leaching reaction**

In all three situations, water reacts with the silicate network (either with BOs or NBOs) to create hydroxyl ions that migrate in the glass while leaching out the alkali ions so that the electrical neutrality is maintained. The **kinetics** of the leaching reaction is controlled by a diffusion process as indicated by the S-shape profile observed in SIMS measurements of the extraction of alkali as a function of depth (see chapter V). Therefore the amount of alkali leached is proportional to the square root of time and the reaction process is governed by the Fick law [60, 65]. Therefore the amount of alkali leached (Q) from the glass with time (t) follows the relation [66]:

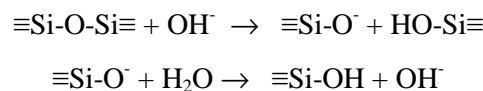
$$Q = 2C_o \sqrt{\frac{Dt}{\pi}}$$

where C<sub>o</sub> corresponds to the initial alkali concentration and D the diffusion coefficient

After a time, the leaching reaction slows down because of the presence of the leached layer through which the ions must diffuse and because the bonds created between NBOs and H species are stronger than between NBOs and Na cations [9, 49]. Moreover, at higher pH the NBO are increasingly occupied by alkali ions causing the slow down of the Na<sup>+</sup> ions exchange and transport. At long times a steady state is reached so the thickness of the leached layer is constant. In some unstable soda silicate glass however, the formation of cracks in the leached layer causes a linear progress of the alteration with time, presumably because water continues to reach the bulk glass directly [30, 67].

### 1- 2.2.2 Dissolution of the silicate network

The dissolution of the silicate network, also called corrosion, corresponds to the breakdown of the siloxane bonds at the interface between the glass and solution. The dissolution is said to be congruent because all constituents of the glass are present in the altered layer in the same proportion as they exist in the glass. The silica breakdown predominates in alkaline solution, and its rate increases with pH above 9, because OH<sup>-</sup> species catalyse a nucleophilic attack of the siloxane sites. Since the OH<sup>-</sup> concentration is kept constant through the equation reaction below, the amount of glass hydrolysed is linear with time and is only limited by the solubility in water of the hydrated silicate species formed [9].



After dissolution, a **gel layer** made of hydrated silicate species is formed at the surface. At pH 10, HSiO<sub>3</sub><sup>-</sup> is predominant and at pH 12 both HSiO<sub>3</sub><sup>-</sup> & SiO<sub>3</sub><sup>2-</sup> are present. After condensation of the gel, an amorphous, hydrated and porous material forms. A leached layer is present between the gel/amorphous material and the unaltered glass [29, 37, 52, 53].

Dissolution of the silicate matrix also occurs at pH below 9, but at a much slower rate that is negligible compared to the leaching reaction [9]. In that situation silicic acid (H<sub>4</sub>SiO<sub>4</sub>) is formed according to the equation:



As a result of both alteration process, the glass surface is made of a stack of different layers: the bulk glass, non affected by the alteration, the leached layer (de-alkalinised) and the gel layer, containing crystalline deposits and amorphous materials, which is sometimes separated into two separate layers [8]. A schematic description summarises the different steps of the alteration on the glass in Figure I- 7.

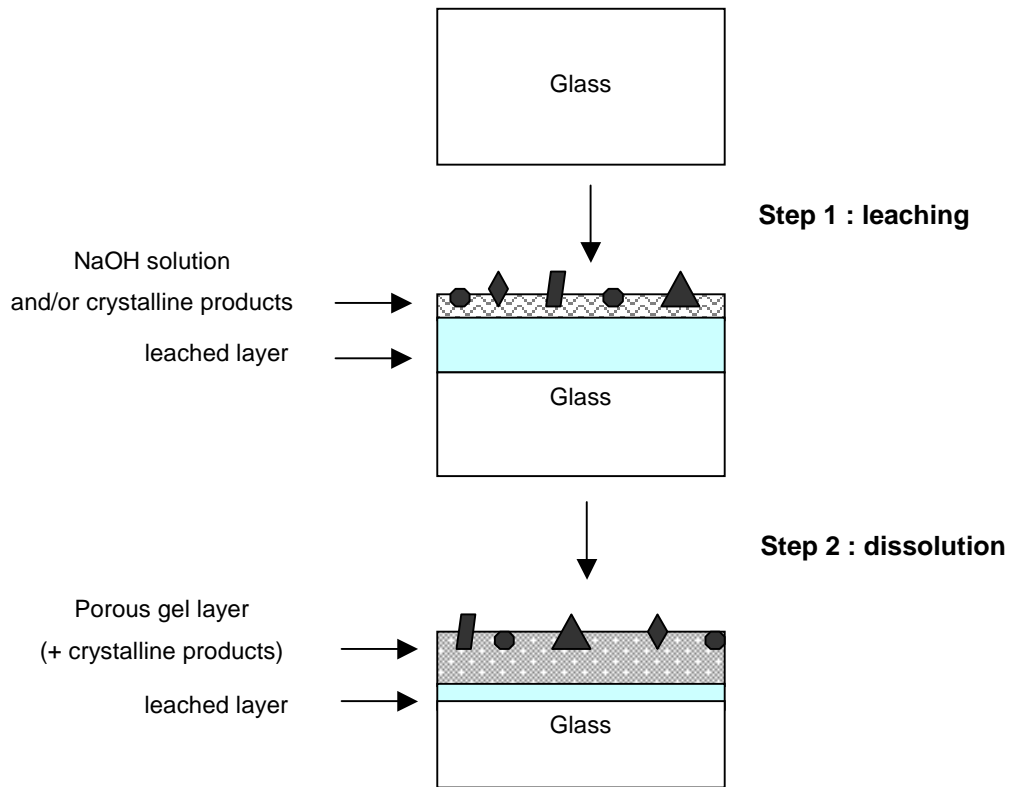
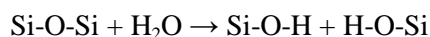


Figure I- 7: Morphological evolution during the alteration of a soda silicate glass with water.

### I- 2.3 Glass surface reactivity

During cooling, the siloxane bondings Si-O-Si present at the extreme surface of the glass react with water molecules present in the surrounding atmosphere to create silanol groups with the dissociation of water as in the following the reaction:



Due to the high energy of adsorption of water on siloxane ( $\sim 80$  KJ/mol), the primitive surface of the glass is rapidly covered by a large number of silanols sites [68, 69, 70]. Subsequently water molecules are adsorbed at the glass surface without dissociation by forming hydrogen bonds with the silanols. Thus, a glass exposed to the atmosphere is rapidly covered with one or several layers of adsorbed water, in which some organic molecules can also be present [68, 71]. The amount of water layers adsorbed on different glass surface is a function of the relative humidity of the atmosphere (Figure I- 8) [72, 73].

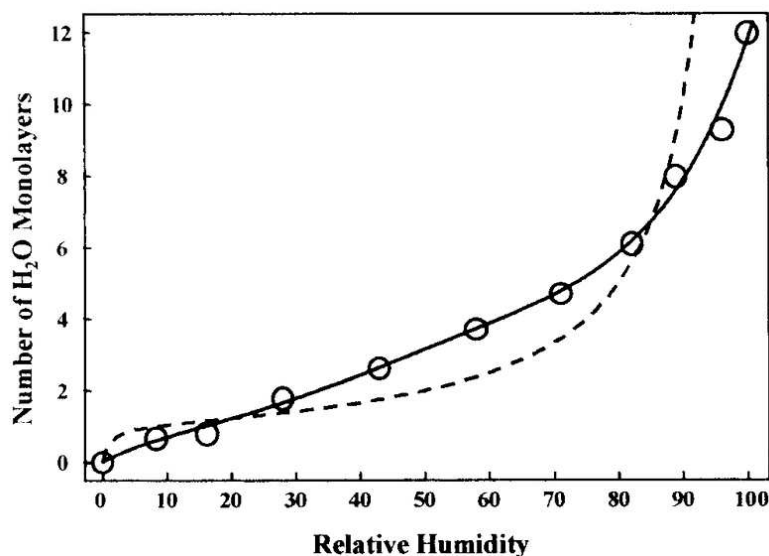


Figure I- 8: Number of monolayers of adsorbed H<sub>2</sub>O on glass as a function of relative humidity. Solid line: fit of the data and the dotted line shows a BET isotherm for multilayer adsorption from Saliba [68].

The surface density of one monolayer of water is  $1 \times 10^{15}$  molecule  $\text{cm}^{-2}$ , based on an area per water molecule of  $10 \text{ \AA}^2$  [72]. The first few layers interact strongly with the silica surface, and at RH below 50 %, the water coverage is thought to form clusters on the surface [72]. However, at higher RH the water uptake is sensitive to the pre-treatment of the surface,

with less water if the glass has been cleaned [73]. Sumner's measurements indicated that water adsorbs even to hydrophobic materials present at the glass surface and showed that the presence of micropores on a glass surface, created by the leaching of the alkali ions, provided the major sites for water uptake [73].

The addition of cations to the silicate structure induces the formation of permanent dipoles at the glass surface (as  $\text{Si-O}^-\text{Na}^+$ ). These sites modify the reactivity of the glass surface compared to pure silica. Thus silicate glasses are able to attract molecules charged or polar molecules (permanent dipoles) close to the surface, or can create induced dipoles in apolar molecules, which will undergo electrostatic attractions. Therefore, there exist physiosorption interactions on the glass surface which involve Van der Waals interactions with polar or polarisable molecules. This explains the contamination of glass surface with volatiles hydrocarbons [68, 74]. Moreover, silanol groups and siloxanes tend to form hydrogen bonds, which are stronger than the Van der Waals interactions, with numerous compounds such as water, alcohols, ester, amine, carboxylic acids, or amino-acids... The adsorption of these molecules is accentuated when the concentrations in alkali and alkaline-earth ions in the glass are high.

## I- 2.4 Factors influencing the alteration process and kinetics

### I- 2.4.1 Alteration in static or dynamic condition

In **dynamic** conditions, as in ventilated environments or by exposure to rain, the solution at the surface of the glass is removed, therefore reducing the rate of the alteration. In **static** condition however, the water sits on the glass and the concentration of NaOH builds up, enhancing the progression of the alteration.

### I- 2.4.2 Surface area to volume ratio, SA/V

The ratio of the surface area to the volume of solution in contact with this surface, **SA/V** has a great impact on the rate at which the pH increases [43, 56].

- If a large volume of water is in contact with a given glass surface (SA/V low), the concentration  $\text{OH}^-$  formed via the leaching process, remains low due to dilution and it takes a long time before the pH 9 at the surface is reached.

- However, if the volume of water is small, as in atmospheric alteration with thin film of water spread over the surface (SA/V high), the OH<sup>-</sup> concentration and so the pH increases rapidly to the critical value.

#### *I- 2.4.3 Relative humidity, RH*

The **Relative Humidity, or RH**, is the ratio of the amount of water vapour in the air at a specific temperature to the maximum amount that the air could hold at that temperature. It is expressed as  $100 \times P/P_0$ , where P is the pressure of the water vapour in the air and P<sub>0</sub> is the equilibrium vapour pressure of water at the same temperature.

The **dew point**, is related to the RH, and corresponds to the temperature to which the air must be cooled, at constant pressure, for the water vapour to become saturated (100 % RH) and condense, so produce dew.

As mentioned earlier, water is the principal factor of alteration, whether it be in the liquid or gas state. When a glass is exposed to air, even at low relative humidity (RH), a thin film of adsorbed water is formed at the surface following the mechanisms outlined above. An increase in the environmental RH results in an increase of the amount of adsorbed water, causing an acceleration of the alteration process [54, 75, 76].

#### *I- 2.4.4 Temperature*

The **temperature** is important from two points of views:

- It increases the kinetics of the chemical reactions, so both stage of the alteration process are accelerated. For example, an increase by 10 °C, doubles the speed of the leaching reaction [77]. Moreover the solubility of silica increases significantly at higher temperatures and pressures [54].
- Since the relative humidity is closely linked (inversely) to the temperature, if the temperature drops suddenly below the dew point, condensation of atmospheric water forms on surface, accelerating the alteration.

#### *1- 2.4.5 Environmental pollutant*

In general the alteration of glass is associated with the formation of crystalline products at its surface. These products are formed by reaction of the cations extracted from the glass and present in solution at the glass surface with the gas-phase **pollutants** in the surrounding environment. Carbonates and sulfates generally represent most of the crystalline products formed at the glass surface due to the reaction with CO<sub>2</sub> and SO<sub>2</sub> from the atmosphere [38, 75, 76, 78]. It is believed that sulfates are secondary reaction products formed by reaction of carbonates with SO<sub>2</sub> [48, 49]. Atmospheric pollutants are dominated by elevated levels of nitrogen compounds (NO<sub>x</sub>, HNO<sub>3</sub>...), mainly from vehicles emission, as well as ozone which may also affect the glass alteration [48].

In the presence of enough water, these pollutants are transformed into their respective acid, which accelerates the leaching of alkali from the glass. Many other pollutants can interact with the ions extracted from the glass, particularly organic pollutants which are presented in details later in this chapter. Acidic pollutants are expected to accelerate the alteration as they enhance the leaching reaction [24, 79]. Acids influence the alteration depending on their strength and their ability to create stable complex with the cations [24, 79, 80].

#### *1- 2.4.6 Particles*

Studies on the role of **particles** or solid pollutants are limited, and their effect on the alteration process is not well determined [81]. Atmospheric particles have different origins: biogenic, terrigenous, marine, anthropogenic. In the case of glass exposed outdoors in an urban area the anthropogenic particles (sulphate and microsoots) are predominant [82, 83, 84]. In museums, the major source of particulate pollutants is the dust induced by visitors, which can affect objects when showcases are not very well sealed. In the case of unstable glass, Munier suggested that particles act as nuclei for condensation and facilitate the crystallisation at the surface [84].

The crystalline products formed at the glass surface through the alteration reaction play a similar role, as these are generally hygroscopic and facilitate the condensation and the retention of water at the surface. In order to keep them crystalline, the recommended RH in

the range 35-40 % currently applied for the storage of unstable glass in museums was defined by considering the stability ranges of sodium or potassium carbonate [38, 78].

#### *1- 2.4.7 Combination of factors*

All the factors presented above play an important role in the alteration of glasses stored in environment where the RH and temperature are not controlled. For example, when industry glass sheets are packed in a warehouse, a confined environment where air circulation is limited is created [56]. If the temperature drops suddenly below the dew point, condensation appears at the glass surface, initiating the leaching process. Due to the small amount of water, the SA/V is high, consequently the OH<sup>-</sup> concentration rapidly builds up and reaches the critical pH of 9, when the silicate dissolution starts. Any increase in the temperature accelerates further the rate of leaching. It was noted that the use of wood flour, which is a source of organic pollutants, as a dust between lights of flat glass during shipment caused an increase of the alteration and its use for the packing during storage of industrial glass was ruled out [85].

In museums, glasses having thick hydrated layers sometimes appear unaltered and retain their shiny surface up to the point they are dried by heating (eg from a spot light in a display) or by a low RH. In such situation crizzling develops, from dimensional changes due to the different thermal expansion coefficients of the layers and the glass, causing a diminution of the transparency by the presence of very fine surface crazing. For this reason, Brill concluded that ancient (altered) glass should not be exposed to dry atmospheres and that storing the glasses in the range 40-55 % RH using equilibrated silica gel would be safe [86].

### I- 3. Alteration of historic glasses from the NMS collections

#### I- 3.1 Identification of the problem

A survey of the glass collection of the National Museums of Scotland (NMS) carried out in 1996 showed deterioration in proportion higher than expected of the 19<sup>th</sup> to 20<sup>th</sup> century British, Islamic and Asian glass collections [87]. In the case of the British collection, 19 % of the objects were unstable and showed visible signs of deterioration: 80 % of the unstable objects had white crystalline surface deposits or were weeping/slippery (depending on relative humidity at the time of examination), 15 % were crizzled with very fine networks of fractures and 5 % had surface flaking (Figure I- 9).

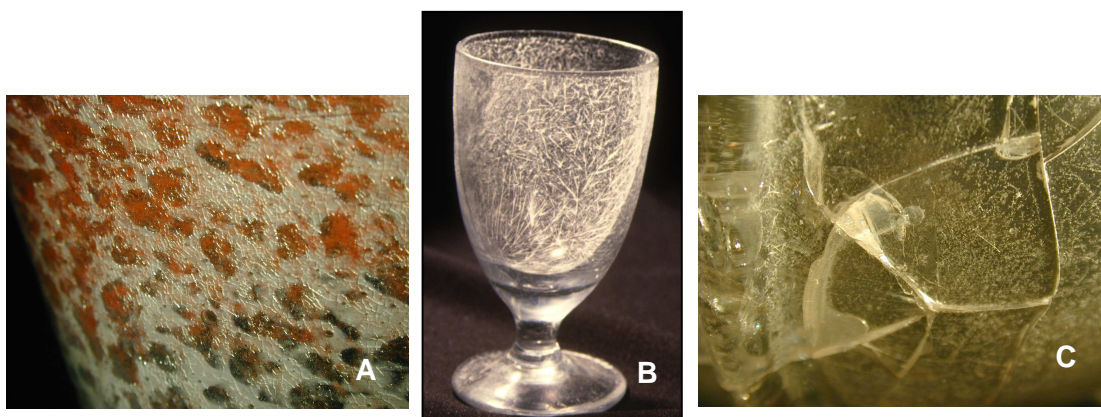


Figure I- 9: Photograph displaying the different signs of deterioration: (A) crizzling, (B) crystalline deposits, (C) cracking (NMS copyright).

A first scientific study was carried in the Conservation and Analytical Research department of the NMS and investigated the causes of this alteration. This study concentrated on the British collection, and examined the compositional difference between stable (showing no sign of alteration) and unstable (altered) glasses, identifying the crystalline corrosion products, and measuring the environment [88, 89]. The results are summarised below.

### I- 3.2 Elemental composition

The composition of the glass was analysed using X-ray fluorescence and electron microprobe (EPMA).

Two general compositional groups were distinguished for the **stable** glasses:

- Group 1: high levels of potassium (9-11 wt%  $K_2O$ ) and lead (34-35 wt%  $PbO$ ) and low levels of sodium (<2 wt%  $Na_2O$ ).
- Group 2: high levels of both calcium and potassium (11 wt%  $CaO$  and 13 wt%  $K_2O$ ) low levels of sodium (1 wt%  $Na_2O$ ).

In contrast, the majority of the **deteriorating (unstable)** artefacts had high levels of sodium with moderate to low levels of calcium and potassium. For example, samples of glass from 19 unstable clear press-moulded glasses had 18-19 wt%  $Na_2O$  and 4-6 wt%  $CaO$ . Two severely deteriorated glass decanters had a composition with 4-7 wt%  $PbO$ , 4-5 wt%  $K_2O$ , 13-14 wt%  $Na_2O$  and <0.5 wt%  $CaO$ . The low content or absence of calcium accounted for their instability.

### I- 3.3 Crystalline corrosion products

Deposits taken from 108 British glass artefacts during their conservation treatment were analysed by ion chromatography (ions quantification) and Raman spectroscopy (molecular identification).

The samples were generally composed of a heterogeneous mixture of crystals with varied size and morphology, including small round, needle-like crystals, large flat angular crystals and liquid droplets (Figure I- 10). Raman microscopy and Ion chromatography (IC) showed that the crystalline products were dominated by sodium formates, mainly small round crystals or larger flat angular crystals of sodium formate anhydrous II. The fine needle-shape crystals were identified as sodium formate phase I' (Figure I- 10).

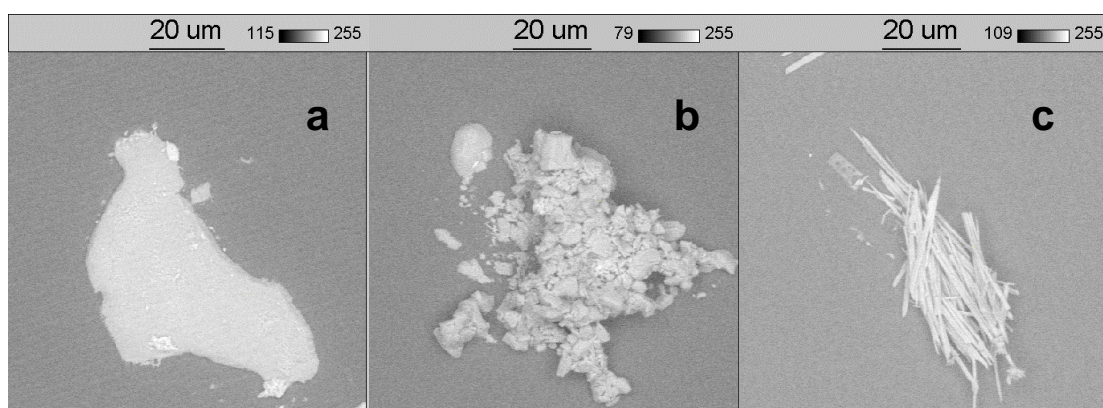


Figure I- 10: SEM image of the different crystal shapes for sodium formate (a) large flat crystal, (b) small round crystals, (c) needle-shape crystals [89].

The presence of the phase I' was unexpected and could not be explained as this metastable phase is known to form after the cooling of the high temperature form, phase I, itself formed by heating at 250 °C [90, 91, 92]. In addition minor sodium sulphate decahydrate and sodium calcium formate were identified as possible secondary alteration products of sodium formate. Only traces of acetate compounds were detected by IC, but were not unambiguously identified by Raman spectroscopy. Finally, SEM-EDS suggested the presence, at minor levels, of sodium and potassium chloride crystals. The origin of the chloride may be due to the fact that the storage site was close to the coast.

Sodium formate has previously been identified as corrosion product on glass and it was suggested that the formaldehyde, emitted from the chipboard shelves in the storage cupboards, was responsible for its formation [93, 94, 95].

### I- 3.4 Environmental conditions

#### I- 3.4.1 Humidity and Temperature

The majority of the unstable glass artefacts were stored at Leith Customs House (LCH) prior to 1999, after which they were moved to a more suitable store at Granton following the conservation survey. The original store at LCH suffers from fluctuating RH and temperature, with RH levels between:

- 20-40 % in the winter months
- 40-65 % in the summer and autumn months.

The temperature showed a variation of 12-25 °C.

Some unstable glass artefacts are also on display in the gallery of the Royal Museum of Scotland (RMS) (Figure I- 11), where the RH reached values as low as 15-20 % during the winter and as high as 60-65 % during the summer, with a temperature of 17-31 °C.



Figure I- 11: Showcase displaying Chinese glasses in the Royal Museum of Scotland

These environmental conditions are extremely unsuitable for unstable glass since the cyclical deliquescence and crystallisation accelerates the rate of deterioration of the glass surface. In contrast, the new store at Granton is controlled to give a RH of 35-40 %, as recommended for unstable glass, and a temperature of 16-22 °C.

#### *I- 3.4.2 Pollutants*

Pollution monitoring was undertaken on several occasions in the three sites mentioned. Levels of acetic acid, formic acid and formaldehyde were measured using diffusion tubes [96, 97] placed inside the case or cupboard and in the gallery or store room. After exposure the pollutants absorbed by the reagents in the tubes were analysed by ion chromatography or high performance chromatography. The mean values for the concentration of acetic and formic acids and formaldehyde determined for each location are shown in Table I- 2.

Table I- 2: Carbonyl pollutant concentrations in case, gallery and storage area [88, 89].

Site	Acetic acid $\mu\text{g m}^{-3}$	Formic acid $\mu\text{g m}^{-3}$	Formaldehyde $\mu\text{g m}^{-3}$
<b>LCH cases 1998</b>			<b>858 ± 39</b>
LCH room 1998			118 ± 12
<b>LCH cases Sep 2002</b>	<b>1193 ±19</b>	<b>366 ±18</b>	<b>280 ± 10</b>
LCH room Sep 2002	614 ±41	220 ±11	113 ± 12
<b>RMS cases Sep 2002</b>	<b>1829 ±21</b>	<b>520 ±18</b>	<b>34 ± 23</b>
RMS gallery Sep 2002	481 ±18	100 ±34	< 12
<b>RMS cases Nov 2002</b>	<b>2019 ±85</b>	<b>443 ±14</b>	<b>133 ± 12</b>
RMS gallery Nov 2002	246 ±38	73 ±16	< 12
Granton cases Sep 2002	329 ±41	82 ±18	< 12
Granton area Sep 2002	248 ±18	168 ±7	< 12
Granton cases Nov 2002	204 ±39	62 ±16	< 12
Granton area Nov 2002	345 ±38	83 ±15	16 ± 14

LCH: Leith Custom House; RMS: Royal Museum of Scotland.

The results indicated that the cases at the RMS and in LCH have major levels of acetic acid, and high levels of formic acid and formaldehyde, which exceed those in the environment of the gallery or store room. This suggested that the pollutant gases were generated within the cases or cupboards by materials such as wood products, adhesives and paints.

The presence of formate salts was thus attributed to the reaction of formic acid or formaldehyde with the unstable glass. The lack of significant levels of acetate salts in the corrosion products from the objects was surprising given the high levels of acetic acid vapour measured. The possible transformation of acetate into carbonate by reaction with carbon dioxide was ruled out since no carbonates were detected in the corrosion products.

### I- 3.5 Artificial ageing experiments

To improve understanding of the deterioration processes, experiments were set up to simulate corrosion of glass artefacts exposed to organic gases. Ageing experiments were set up in desiccators to create atmospheres with vapours of acetic acid, formic acid and/or formaldehyde at 100 % RH. Higher pollutant concentrations than those observed in the storage cases were used to accelerate the process. Once the atmospheres were established, a

piece of a British decanter, with a high-soda low-lead and -potassium composition, was placed at the bottom of each desiccator and exposed for 5 months.

The simulation experiments have shown that sodium formate forms in atmospheres containing formic acid, while sodium acetate is expected to form in acetic acid atmospheres. In the presence of formaldehyde, an unidentified formate with dendritic shape was formed.

### **I- 3.6 Conclusions from the scientific study**

This preliminary scientific study demonstrated that the widespread alteration observed on part of the NMS glass collection was the result of the combination of factors: an unstable glass composition, a fluctuating humidity and high concentration of organic pollutants. The pollutants influenced the formation of crystalline sodium formate at the glass surface. Although acetic acid was predominant and is expected to form acetates by reaction with glass at high humidity, no acetates were identified. This suggested that a competing effect occurred between the different pollutants.

The approved RH for the storage of unstable glass is often defined by considering the stability ranges of sodium or potassium carbonate [38, 78]. However these phases were not identified in this case, and the deliquescent point of sodium formate which is at 51-52 %RH [98] should be considered instead. During the original survey in 1996 the salts on the glass objects appeared to deliquesce at around 50-55 % RH at room temperature, which is consistent with the deliquescence range of sodium formate.

The average relative humidity in the RMS gallery and the LCH store fluctuated regularly with < 50 % RH measured in the winter, and > 50 % RH measured in the summer. This suggests that the sodium formate followed a cycle of crystallisation and deliquescence between the winter and the summer months.

## I- 4. Volatile organic pollutants

Most of the research concerning pollutants in the environment and particularly acids focused on strong inorganic acids such as sulfuric, nitric acids originating from sulfur dioxide and oxides of nitrogen. However, organic compounds which are more common in the atmosphere than inorganic species have only scarcely been examined [81, 99]. Formic and acetic acids are the most abundant of these organic compounds and may contribute significantly to the free acidity of rain in the world [99]. The atmospheric sources of these acids are still very uncertain but likely to include anthropogenic sources such as vehicular emissions, natural sources like ants, plants, soil, emission from biomass burning and oxidation of precursor compounds in the gas phase. An interesting route was described by Otha for the formation of formic acid in nature which involved the reaction of CO<sub>2</sub> with silicate rocks in the presence of water and light, possibly catalysed by metal ions [100].

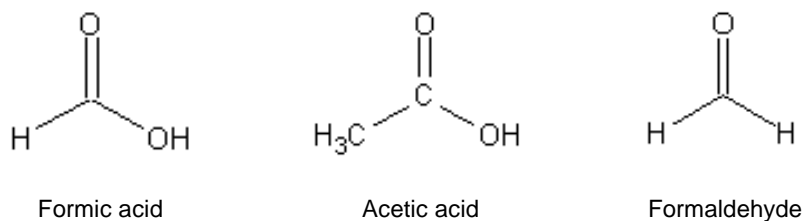
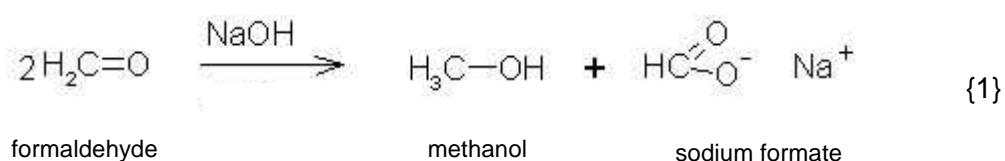


Figure I- 12: Chemical structure of formic acid, acetic acid and formaldehyde.

The deterioration caused by indoor volatile organic pollutants, especially acetic acid, formic acid and formaldehyde is a major problem in museums (Figure I- 12). A large range of inorganic materials is affected by these pollutants; this includes metal objects made of copper and/or lead [101, 102, 103], shells [104], eggs, limestone, ceramics [105, 106, 107] and glass and enamels [93, 108]. The most common sources of these pollutants in museums are the materials used to fabricate the showcases or storage cabinets, mainly wood and wood-products for the organic acids and glues and resins (including resin in medium density fibreboard, MDF) for the formaldehyde [109, 110, 111, 112, 113]. However, paints, adhesives, varnishes or fabric may also contribute. Because the objects are generally displayed in tightly sealed cases where the air exchange rate is low, the ventilation is restricted, pollutant vapours accumulate and their concentration increases, inducing an increase of the deterioration.

The best way to limit the presence of pollutant generating materials within the cases is to carefully select and test all the materials. The accelerated corrosion test is a simple method that is widely used by museums nowadays to assess the corrosiveness of materials during the showcases design process [114].

The route of damage for aldehydes is far from clear and may require oxidation. The oxidation of formaldehyde into formic acid in air is very slow, although the oxidation process is accelerated in the presence of metal or oxidising agents such as peroxide and ozone [115]. The second possible reaction taking place in the presence of formaldehyde is the Cannizzaro reaction {1} [93]:



In this situation formaldehyde does not interact with the glass, but solely with the alteration products NaOH formed through the leaching reaction induced by water.

It is clear from the analysis of the deterioration on the NMS glass collection that acetic and formic acid do not react equally. It has been reported that in the presence of formic acid, the action of acetic acid on lead was inhibited [103]. In rain water, the formate/acetate ratio is higher than the ratio of the corresponding acids in the gas phase. It was suggested that the relative amounts of these acids in rain were controlled by the relative solubilities of both acids (formic acid pKa= 3.75 and acetic acid pKa= 4.75) [99]. Moreover, the estimated dry deposition velocities of formic and acetic acids to dew water indicated that formic acid was incorporated to the liquid phase faster than acetic acid [116]. In the presence of thin film of water on materials, like on the NMS glass artefacts, the solution may reach a saturation point for the dissolved species. If formic acid is incorporated faster, the water film may be saturated in formic acid before acetic acid could be incorporated. This hypothesis may explain why only formate compounds were formed on the NMS glass artefacts although acetic acid vapours were predominant.

## I- 5. Summary and research strategy

The preliminary study undertaken on the British glass collection of the NMS clearly showed that organic pollutants play a role in the alteration of glass. With these pollutants white crystalline deposits of mainly formate compounds are formed at the surface of the glass, which implies that the glass has reacted with its polluted environment. However, the effect of these pollutants on the glass structure itself is unknown. The few studies reporting similar alteration affirm that the formaldehyde vapours within the organic pollutants are responsible of the formate salts formation, without justification, and without considering the role of acids expected to have a larger effect.

Because no *in-depth* research has ever been undertaken on the role of organic pollutants on the alteration of unstable glasses, it was not possible to give any further conclusion concerning the alteration of the NMS glass collections. Moreover, the situation encountered in NMS is not unique and many museums, aware or not, are affected by the same problem. For this reason, it is necessary to get a better understanding of the alteration of glass in the presence these pollutants to develop better conservation treatment and preventive conservation measures.

The aim of this research is to investigate **the role of organic pollutants on the alteration of unstable glass** compared to a non-polluted environment. The research concentrates on the alteration of soda silicate glasses, with an unstable composition, and examines the role of formic acid, acetic acid and formaldehyde pollutants. The research focuses mainly on the modification of the chemical structure, the mechanisms of the reactions involved and the kinetics of the alteration. It is based on the examination of glass objects from the NMS collections, and replica glasses aged in real or artificial environments. Two main analytical techniques were chosen for this investigation: Raman spectroscopy and Secondary Ion Mass Spectrometry (SIMS).

This investigation is presented into four chapter organised as follows:

In the next chapter, *chapter II*, the materials studied, the experimental procedure and the different analytical techniques applied are introduced.

A short chapter, *chapter III*, is devoted to the examination of the crystalline deposits, in order to complement the information obtained from the structure analyses, and to assist in the determination of the reaction mechanisms. Museum glass objects and artificially aged glasses are examined and compared.

The modification of the chemical structure of soda silicate glass with alteration is dealt in *chapter IV*, based mostly on the analyses provided by Raman spectroscopy. The ability of the analytical technique to determine the stability of a soda silicate glass, as well as to examine altered glasses *in-situ* and non-destructively (both extremely important to the study of museum material), is assessed in this chapter.

The mechanisms and kinetics of the alteration are presented in *chapter V*, based on the SIMS depth profiles obtained from replica soda glasses exposed to real and artificial ambient atmospheres.

Finally the conclusion summarises the main information gained from this research and discusses its relevance to the study and preservation of historic material and indicates future perspectives.

## I- 6. References

- 1 Newton R. and Davison S., *Conservation of Glass*, Butterworths, London (1989).
- 2 Richet P., *L'âge du Verre*, Découvertes Gallimard Techniques 399, Gallimard, Evreux (2000)
- 3 Freestone I., Looking into glass, *Science and the Past*, Bowman S., The British Museum Press, London (1991) 37.
- 4 Shortland A., Schachner L., Freestone I., and Tite M., Natron as a flux in the early vitreous materials industry: sources, beginnings and reasons for decline, *J. Archeol. Sci.* **33** (2006) 521.
- 5 Sayre E.V., and Smith R.W., Compositional categories of ancient glass, *Science* **33** (1961) 1824.
- 6 Henderson J., *The science and archaeology of materials. An investigation of inorganic materials*, Routledge, London (2000).
- 7 Perez J., *Matériaux non cristallins et science du désordre*, Presses Polytechniques et universitaires Romandes, Lausanne (2001).
- 8 Barton J., and Guillemet C., *Le Verre, Science et Technologie*, collection Science des Matériaux, EDP Science, Paris (2005).
- 9 Doremus R.H., *Glass Science*. Second Edition, John Wiley & Sons, New York (1994).
- 10 Mysen B.O., and Richet P., *Silicate glasses and melts: Properties and structure*, Developments in Geochemistry 10, Elsevier, Amsterdam (2005).
- 11 Scholze H., *Le Verre: Nature, structure et propriétés*, Institut du verre, Paris (1980).
- 12 Lee S.K., and Stebbins J., Nature of cation mixing and ordering in Na-Ca silicate glasses and melts, *J. Phys. Chem. B.* **107** (2003) 3141.
- 13 Henderson G.S., The structure of silicate melts: A glass perspective, *Can. Mineral.* **43** (2005) 1921.
- 14 Mysen B.O., and Frantz J.D., Silicate melts at magmatic temperatures: *in-situ* structure determination to 1651°C and effect of temperature and bulk composition on the mixing behavior of structural units, *Contrib. Mineral. Petrol.* **117** (1994) 1.

- 15 Matson D.W., Sharma S.K., and Philpotts J.A., The structure of high-silica alkali-silicate glasses. A Raman spectroscopic investigation, *J. Non-Cryst. Solids*. **58** (1983) 323.
- 16 Lebedev A.A., Polymorphism and annealing of glass, *Trans. Opt. Inst. Petrograd* **2** (1921) 1.
- 17 Zachariassen W.H., The atomic arrangement in glass, *J. Am. Chem. Soc.* **54** (1932) 3841.
- 18 Warren B.E., X-ray determination of the structure of glass, *J. Am. Ceram. Soc.* **17** (1934) 249.
- 19 Warren B.E., and Bischof J., Fourier analysis of X-ray patterns of soda-silica glass, *J. Am. Ceram. Soc.* **21** (1938) 259.
- 20 Greaves G.N., EXAFS and the structure of glass, *J. Non-Cryst. Solids*. **71** (1985) 203.
- 21 Greaves G.N., EXAFS for studying corrosion of glass surfaces, *J. Non-Cryst. Solids*. **120** (1990) 108.
- 22 Lavoisier A.L., Sur la nature de l'eau et sur les expériences par lesquelles on a prétendu prouver la possibilité de son changement en terre, *Mémoires de l'Académie des sciences* (1770) 28. (<http://histsciences.univ-paris1.fr/i-corpus/lavoisier/book-detail.php?bookId=2>)
- 23 Clark D.E., Pantano C.G., and Hench L.L., *Corrosion of Glass*, Books for industry and the glass industry, New York (1979).
- 24 Hellmod P., and Sass H., La corrosion de l'émail par les acides organiques, *Galvano-organo-traitements de surface*. **650** (1994) 866.
- 25 Pernot F., Zarzycki J., Baldet P., Bonnel F., and Rabischong P., In vivo corrosion of sodium silicate glasses, *J. Biomed. Mater. Res.* **19** (1985) 293.
- 26 Elgayar I., Aliev A.E., Boccaccini A.R., and Hill R.G., Structural analysis of bioactive glasses, *J. Non-Cryst. Solids*. **351** (2005) 173.
- 27 Mysen B.O., Virgo D., Harrison W.J., and Scarfe C.M., Solubility mechanisms of H<sub>2</sub>O in silicate melts at high pressures and temperatures: a Raman spectroscopic study, *Am. Mineral.* **65** (1980) 900.
- 28 Techmer K.S., and Rädlein E., TEM and AFM studies on the alteration of natural glasses, *Proceedings of ICG 18<sup>th</sup> conference*, San Francisco, American Ceramic Society, Westerville, Ohio (1998) CD-Rom.
- 29 Douglas R.W., and El-Shamy T.M.M., Reactions of glasses with aqueous solutions, *J. Am. Ceram. Soc.* **1** (1967) 1.

- 30 Bunker B.C., Arnold G.W., and Beauchamp E.K., Mechanisms for alkali leaching in mixed-Na-K-silicate glasses, *J. Non-Cryst. Solids*. **58** (1983) 295.
- 31 Bunker B.C., Arnold G.W., Day D.E., and Bray P.J., The effect of molecular structure on borosilicate glass leaching, *J. Non-Cryst. Solids*. **87** (1986) 226.
- 32 Exarhos G.J., and Conaway W.E., Raman study of glass water interactions, *J. Non-Cryst. Solids*. **55** (1983) 445.
- 33 Ryan J.L., McPhail D.S., Rogers P.S., and Oakley V.L., Glass deterioration in the museum environment: a study of the mechanisms of decay using secondary ion mass spectrometry, *ICOM-CC triennial meeting (11<sup>th</sup>)*, Edinburgh, James & James, London (1996) 839.
- 34 Brill R.H., Hanson B., and Fenn P.M., Some miscellaneous thoughts on crizzling, *Proceedings of ICG 18<sup>th</sup> conference*. San Francisco, American Ceramic Society, Westerville, Ohio (1998) CD-Rom.
- 35 Römich H., Aerts A., Janssens K., and Adams F., Simulation of corrosion phenomena of glass objects on model glasses, *Proceedings of ICG 18<sup>th</sup> conference*. San Francisco (1998) CD-Rom
- 36 Raman S.V., Analysis of the hydrated zone in nuclear waste glass forms by electron microprobe, Raman spectroscopy and diffusion models, *Phys. Chem. Glasses*. **1** (2001) 27.
- 37 Rebiscoul D., Van der Lee A., Rieutord F., Ne F., Spalla O., El-Mansouri A., Frugier P., Ayrat A., and Gin S., Morphological evolution of alteration layers formed during nuclear glass alteration: new evidence of a gel as a diffusion barrier, *J. Nucl. Mater.* **326** (2004) 9.
- 38 Brill R.H., Crizzling – a problem in glass conservation, Conservation in Archaeology and the Applied Arts, *preprints of the contributions to the Stockholm congress*, International Institute for Conservation of Historic and Artistic Works, London (1975) 121.
- 39 Werner A.E.A., Problems in the conservation of glass, *Annales du 1<sup>er</sup> Congrès International d'Etude Historique du Verre*, Secretariat general permanent des 'Journées Internationales du Verre', Liege **1** (1958) 189.
- 40 Bunker B.C., Molecular mechanisms for corrosion of silica and silicate glasses, *J. Non-Cryst. Solids*. **179** (1994) 300.
- 41 El-Shamy T. M., The chemical durability of K<sub>2</sub>O-CaO-MgO-SiO<sub>2</sub> glasses, *Phys. Chem. Glasses*. **14** (1973) 1.
- 42 Roling B., and Ingram M.D., Determination of divalent cation mobilities in glass by dynamic mechanical thermal analysis (DMTA): evidence for cation coupling effects, *Solid State Ionics*. **105** (1998) 47.

- 43 Hench L.L., and Clark D.E., Physical chemistry of glass surfaces, *J. Non-Cryst. Solids*. **28** (1978) 83.
- 44 Karlsson C., Zanghellini E., Swenson J., Roling B., Bowron D.T., and Börjesson L., Structure of alkali alkaline-earth silicate glasses from neutron diffraction and vibrational spectroscopy, *Phys. Rev. B*. **72** (2005) 064206.
- 45 Boksay Z., Bouquet G., and Dobos S., Diffusion processes in the surface layer of glass, *Phys. Chem. Glasses*. **4** (1967) 140.
- 46 Natrup F., Bracht H., Martiny C., and Roling S.M.B., Diffusion of calcium and barium in alkali alkaline-earth silicate glasses, *Phys. Chem. Chem. Phys.* **4** (2002) 3225.
- 47 Martiny C., Murugavel S., Roling B., Natrup F., Bracht H., and Ingram M.D., Mobilities of divalent ions in glass, *Glass Technol.* **43C** (2002) 309.
- 48 Melcher M., and Schreiner M., Leaching studies on naturally weathered potash-lime-silica glasses, *J. Non-Cryst. Solids*. **352** (2006) 368.
- 49 Newton R.G., The durability of glass – a review, *Glass Technol.* **26** (1985) 21.
- 50 Bange K., Anderson O., Rauch F., Lehuédé P., Rädlein E., Tadokoro N., Mawwoldi P., Rigato V., Matsumoto K., and Farnworth M., Multi-method characterization of soda-lime glass corrosion. Part 2. Corrosion in humidity. *Glass Sci. Technol.* **1** (2002) 20.
- 51 Youssefi A., and Paul A., Résistance chimique de quelques verres du système Na<sub>2</sub>O-CaO-SiO<sub>2</sub>, *Verres Réfract.* **5** (1978) 663.
- 52 Das C.R., and Douglas R.W., Studies on the reaction between water and glass. Part 3, *Phys. Chem. Glasses*. **5** (1967) 178.
- 53 El-Shamy T.M., and Pantano C.G., Decomposition of silicate glasses in alkaline solutions, *Nature*. **266** (1977) 704.
- 54 Ryan J.L., The atmospheric deterioration of glass: Studies of decay mechanisms and conservation techniques, *PhD thesis*. University of London (1996).
- 55 Fearn S., McPhail D., and Oakley V., Room temperature corrosion of museum glass: an investigation using low-energy SIMS, *App. Surf. Sci.* **231-232** (2004) 510.
- 56 Duffer P., How glass reacts with water and causes surface corrosion, *Glass Digest*. Sept (1994) 76.
- 57 Boksay Z., Bouquet G., and Dobos S., The kinetics of the formation of leached layers on glass surfaces, *Phys. Chem. Glasses*. **2** (1968) 69.
- 58 Scholze H., Glass-water interactions, *J. Non-Cryst. Solids*. **102** (1988) 1.

- 59 Doremus R.H., Interdiffusion of hydrogen and alkali ions in a glass surface, *J. Non-Cryst. Solids*. **19** (1975) 137.
- 60 Smets B.M.J., and Lommen T.P.A., The leaching of sodium containing glasses: ion exchange or diffusion of molecular water, *J. Phys. Paris. colloque C9, supplément to n° 12*, **13** (1982) 649.
- 61 Lanford W., Davis K., Lamarche P., Laursen T., Groleau R., and Doremus R., Hydration of soda-lime glass, *J. Non-Cryst. Solids*. **33** (1979) 249.
- 62 Tsong I., Houser C., White W., Winterberg A., Miller P., and Moak C., Evidence for inter-diffusion of hydronium and alkali ions in leached glasses, *Appl. Phys. Lett.* **39** (1981) 669.
- 63 Cummings K., Lanford W.A., and Feldmann M., Weathering of glass in moist and polluted air, *Nucl. Instrum. Meth. B*. **136-138** (1998) 858.
- 64 Koenderink G.H., Brzesowsky R.H., and Balkenende A.R., Effect of the initial stages of leaching on the surface of alkaline earth sodium silicate glasses, *J. Non-Cryst. Solids*. **262** (2000) 80.
- 65 Smets B.M.J., and Lommen T.P.A., SIMS and XPS investigation of the leaching of glasses, *Verres Réfract.* **1** (1981) 84.
- 66 Zarzycki J., *Le verre et l'état vitreux*, Masson, Paris (1982).
- 67 Bunker B.C., Tallant D.R., Headley T.J., Turner G.L., and Kirkpatrick R.J., The structure of leached sodium borosilicate glass, *Phys. Chem. Glasses*. **3** (1988) 106.
- 68 Chartier P., La surface du verre: bases scientifique pour la recherche industrielle, *Verre*. **3** (1997) 5.
- 69 Birch W., and Carre A., Le nettoyage du verre: Interaction surface/tensioactif, *Verre*. **3** (1997) 29.
- 70 Jupille J., La surface du verre: structure et physico-chimie, *C. R. Acad. Sci. Paris. T. 2, Série IV* (2001) 303.
- 71 Duffer P., How glass reacts with water and causes surface corrosion, *Glass Industry*. April. (1995) 22.
- 72 Saliba N.A., Yang H., and Finlayson-Pitts B.J., Reaction of gaseous nitric oxide with nitric acid on silica surfaces in the presence of water at room temperature, *J. Phys. Chem. A*. **105** (2001) 10339.
- 73 Sumner A.L., Menke E.J., Dubowski Y., Newberg J.T., Penner R.M., Hemminger J.C., Wingen L.M., Brauers T., and Finlayson-Pitts B.J., The nature of water on surfaces of laboratory systems and implications for heterogeneous chemistry in the troposphere, *Phys. Chem. Chem. Phys.* **6** (2004) 604.

- 74 Geotti-Bianchini F., and Preo M., Analysis of polyethylene-based cold end coating on glass containers with contact angle and IR spectroscopy, *Glastech. Ber. Glass Sci. Technol.* **11** (1999) 341.
- 75 Böhm T., The influence of temperature, relative humidity and SO<sub>2</sub>-concentration on weathering of glass, *Proceedings of 5<sup>th</sup> ESG conference*. Prague (1999) CD-Rom.
- 76 Römich H., and Böhm T., Deterioration of glass by atmospheric attack, *CEEES Climatic and Atmospheric Effects on Materials and Equipment.* **2** (1999) 187.
- 77 Verita M., Deterioration mechanisms of ancient soda-lime silica mosaic tesserae, *Proceeding of ICG 18<sup>th</sup> Congress on Glass*, San Francisco, American Ceramic Society, Westerville, Ohio (1998) CD-Rom.
- 78 Tichane R.M., Initial stages of the weathering process on a soda-lime glass surface, *Glass Technol.* **1** (1966) 26.
- 79 Gin S., Godon N., Mestre J.P., and Vernaz E.Y., Experimental investigation of aqueous corrosion of R7T7 nuclear glass at 90°C in the presence of organic species, *Appl. Geochem.* **9** (1994) 255.
- 80 Chaulet D., Bouquillon A., Thomassin J.H., and Le Coustumer P., Mobility or immobility of lead during glass surface alteration in different environments, *Riv. Staz. Sper. Vetro Conference.* **6** (2000) 131.
- 81 Lombardo T., Mécanismes d'altération du verre calco-sodique en atmosphère urbaine polluée, *PhD thesis*. Paris XII University (2002).
- 82 Chabas A., and Lefevre R.-A., Behaviour of soda-lime glass in polluted atmosphere : a case study in Paris, *Riv. Staz. Sper. Vetro Conference.* **6** (2000) 135.
- 83 Chabas A., and Lefevre R.-A., Soiling of soda-lime glass in polluted atmosphere of Paris, *Glass technol.* **43C** (2002) 79.
- 84 Munier I., Lefevre R.-A., Geotti-Bianchini F., and Verita M., Weathering of low-durability glass and air pollution, *Proceedings of 5<sup>th</sup> ESG conference*. Prague (1999) 114.
- 85 Bishop F.L., and Mowrey F.W., Deterioration of the surface of sheet glass, *Ceramic Bulletin.* **1** (1952) 13.
- 86 Brill R.H., The use of equilibrated silica gel for the protection of glass with incipient crizzling, *J. Glass Stud.* **20** (1978)100.
- 87 Cobo del Arco B., Survey of the National Museums of Scotland glass collection, *The Conservation of Glass and Ceramics: Research, Practice and Training*, Tennent N.H. James & James, London (1999) 229.
- 88 Eremin K., Cobo del Arco B., Robinet L., and Gibson L.T., Conservation and analysis of deteriorating 19<sup>th</sup> and 20<sup>th</sup> Century British Glass, *Annales du 16<sup>ème</sup>*

- Congrès International d'Etude Historique du Verre*. London, AIHV, Nottingham (2005) 380.
- 89 Robinet L., Eremin K., Cobo del Arco B., and Gibson L.T., A Raman spectroscopic study of pollution-induced glass deterioration, *J. Raman Spectrosc.* **8/9** (2004) 662.
- 90 Heyns A.M., Van Niekerk O.T., Richter P.W., and Range K.J., The polymorphism of alkali metal formates - Part I. A Raman study of the II-I transition in NaHCOO, *J. Phys. Chem. Solids.* **10** (1988) 1133.
- 91 Heyns A.M., and Range K.J., The polymorphism of alkali metal formates - Part II. A Raman spectroscopic study of the kinetics of the I-II phase transition in NaHCOO, *Mat. Res. Bull.* **26** (1991) 589.
- 92 Heyns A.M., The effect of pressure on the Raman spectra of solids. III. Sodium formate, NaHCOO, *J. Chem. Phys.* **7** (1986) 3610.
- 93 Schmidt S., Na-Formiatbildung auf Glasoberflächen-Untersuchungen an historischen Objekten, *Berliner Beiträge zur Archäometrie.* **11** (1992) 137.
- 94 Nockert M., and Wadsten T., Storage of archaeological textile finds in sealed boxes, *Stud. Conserv.* **1** (1978) 38.
- 95 Schermer M., Glass lantern slides: deterioration and conservation, *ICOM-CC triennial meeting (14<sup>th</sup>)*, The Hague, James & James, London (2005) 154.
- 96 Gibson L.T., and Brokerhof A., A passive tube-type sampler for the determination of formaldehyde vapours in museum enclosures, *Stud. Conserv.* **4** (2001) 289.
- 97 Gibson L.T., Cooksey B.G., Littlejohn D., and Tennent N.H., A diffusion tube sampler for the determination of acetic acid and formic acid vapours in museum cabinets, *Ana. Chim. Acta.* **341** (1997) 11.
- 98 Peng C., and Chan C.K., The water cycles of water-soluble organic salts of atmospheric importance, *Atmos. Environ.* **35** (2000) 1183.
- 99 Khare P., Kumar N., Kumari K.M., and Srivastava S.S., Atmospheric formic and acetic acids - An overview, *Rev. Geophys.* **2** (1999) 227.
- 100 Otha K., Ogawa H., and Mizuno T., Abiological formation of formic acid on rocks in nature, *Appl. Geochem.* **15** (2000) 91.
- 101 Tennent N.H., Tate J., and Cannon L., The corrosion of lead artifacts in wooden storage cabinets, *Scottish Society for Conservation and Restoration.* **4** (1993) 8.
- 102 Tennent N.H., *Images for Posterity: The Conservation of Coins and Medals*, in Scharloo M. and Tijmann I., Leiden (1993) 44-58.
- 103 Tétréault J., Cano E., van Bommel M., Scott D., Dennis M., Barthés-Labrousse M. L., and Robbiola L., Corrosion of copper and lead by formaldehyde, formic and acetic acid vapours, *Stud. Conserv.* **4** (2003) 237.

- 104 Grzywacz C.M., and Tennent N.H., Pollution monitoring in storage and display cabinets: carbonyl pollutant levels in relation to artifact deterioration, *Preventive Conservation, Practice, Theory and Research*, The International Institute for Conservation of Historic and Artistic Works, Roy A. and Smith P., London (1994) 164.
- 105 Gibson L.T., Analytical studies of the degradation of calcareous artefacts in museum environments, *PhD thesis*. The University of Strathclyde, Glasgow (1995).
- 106 Gibson L.T., Cooksey B.G., Littlejohn D., and Tennent N.H., Investigation of the composition of a unique efflorescence on calcareous museum artifacts, *Anal. Chim. Acta.* **337**, 3 (1997) 253.
- 107 Gibson L.T., Cooksey B.G., Littlejohn D., and Tennent N.H., Characterisation of an unusual crystalline efflorescence on an Egyptian limestone relief, *Anal. Chim. Acta.* **337**, 2 (1997) 151.
- 108 Müller W., Adam K., Kruschke D., Köcher C., Jann O., Wilke O., Brödner D., and Schneider U., Deterioration of historic art enamels by indoor pollution, *Proceedings of ICG 18<sup>th</sup> conference*, San Francisco, American Ceramic Society, Westerville, Ohio (1998) CD-Rom.
- 109 Thickett D., Sealing methods for timber composites. Further work: ambient temperature corrosion tests, Report no. 1998/4, British Museum. *Department of Conservation* (1998).
- 110 Arni P.C., Cochrane G.C., and Gray J.D., Emission of corrosive vapours by wood. I. Survey of acid-release properties of certain freshly felled hardwoods and softwoods., *J. Appl. Chem.* **15** (1965) 305.
- 111 Arni P.C., Cochrane G.C., and Gray J.D., Emission of corrosive vapours by wood. II. Analysis of vapours emitted by certain freshly felled hardwoods and softwoods by gas chromatography and spectrophotometry, *J. Appl. Chem.* **15** (1965) 463.
- 112 Greathouse G.A., *Deterioration of Materials, Causes and Preventive Techniques*, Chapman and Hall Ed. London (1954).
- 113 Farmer R.H., *Chemistry in the Utilization of Wood*, Pergamon Press, Oxford (1967).
- 114 Robinet L., and Thickett D., A new methodology for accelerated corrosion testing, *Stud. Conserv.* **4** (2003) 263.
- 115 Raychaudhuri M. R., and Brimblecombe P., Formaldehyde oxidation and lead corrosion, *Stud. Conserv.* **4** (2000) 226.
- 116 Sanhueza E., Santana M., and Hermoso M., Gas-phase and aqueous-phase formic and acetic-acids at a tropical cloud forest site, *Atmos. Environ. A.* **26** (1992) 1421.

## **Chapter II.**

# **EXPERIMENTAL AND INSTRUMENTAL**

## II- 1. Introduction

The extensive glass collection of the National Museums of Scotland (NMS) was used as the basis for this investigation, concentrating on the 19<sup>th</sup> and 20<sup>th</sup> century British, Chinese and Islamic glasses (Figure II- 1). The objects were used to examine different questions, for this reason different types of samples were obtained and are presented in this chapter according to these questions. In parallel, replica glasses with a composition similar to the NMS glass objects were used to examine the effect of different parameters on their alteration through ageing experiments. By examining the effect of organic pollutant on glass in the museum atmosphere, this research extends the work of Ryan and Fearn on the atmospheric deterioration of unstable glassware in museum, where they concentrated on the effect of relative humidity [1, 2, 3]. In their study they used a replica glass with a high-soda low-lime composition (RG1), similar to the unstable glasses in the NMS [1, 2]. For this reason, we chose to work with the same replica glass, which was supplied to us by Fearn. Two additional glass replicas, also with a historic composition, were used for comparison.

The ageing experiments were undertaken either in ambient or in accelerated conditions to examine different aspects. Ambient experiments (both in real and artificial conditions) were carried out to assess the effect of the different parameters on the atmospheric alteration of glass. Accelerated experiments, with high temperature and RH, were applied to obtain altered layers with a sufficient thickness in a reasonable time (several weeks), for the structural analyses.

Because Raman spectroscopy has the interesting ability to analyse materials non-destructively and the Raman spectra of glasses have been widely studied, this technique was chosen to examine the modification of the chemical structure in this research. Both modifications with the composition and the alteration based on objects and replica glasses aged in accelerated conditions were examined. In addition Raman spectroscopy was used also to characterise the crystalline products formed at the glass surface. Because SIMS is a highly sensitive technique perfectly suited to examine the first stage of the atmospheric alteration under ambient conditions [1, 2, 3, 4], it was used in the depth profiling mode to follow the alteration on replica glass aged in ambient conditions to determine the mechanisms and kinetics of the alteration. Additional analytical techniques, presented in this chapter, were used to complement the results from Raman spectroscopy and SIMS.



Figure II- 1: Selected objects from the NMS British, Islamic and Asian glass collection (NMS copyright).

## II- 2. Materials and samples

### II- 2.1 Museum objects

#### *II- 2.1.1 Study of the link composition-stability-Raman spectra*

In order to correlate the stability of glass with Raman spectral data and the composition measured by electron microprobe, small glass samples were required (~0.5 mm). The glass fragments were removed from broken edges, chips or at the pontil mark (left after rod was detached) at the bases of artefacts using scalpel, tweezers and a diamond pen. Both stable and unstable glasses were sampled, however the objects judged visually too fragile or intact, could not be sampled. The stability of a glass was assessed by the museum conservator from visual and microscopic observation. In this classification, glasses which displayed crystalline or liquid alteration products at their surfaces were considered unstable. The glasses sampled include ten 19-20<sup>th</sup> century British glasses (museum reference starting with 'Hmen' or 'unreg'), 40 Islamic glasses (museum reference starting with 'A.') from the 19-20<sup>th</sup> century, one 18<sup>th</sup> century Venetian glass (1956.1233) and one Napoleonic glass (1998.492).

#### *II- 2.1.2 Study of the glass structure modification with alteration*

Two objects from the NMS collections were chosen to examine the modification of the chemical structure following the alteration by the museum atmosphere (Figure II- 2):

- A British glass decanter (unregistered) dating from the late 19<sup>th</sup> to early 20<sup>th</sup> century,
- An Islamic bottle (A.1893.61) attributed to 19<sup>th</sup> century Iran.

The two objects were chosen because their base composition is similar as both are silicate glasses with major soda but differs in the stabiliser cation content. Both objects have deteriorated over several decades as a result of storage in wooden cabinets emitting high levels of organic pollutants.



Figure II- 2: NMS glass objects (left) British decanter; (right) Islamic bottle (NMS copyright).

Moreover the British decanter was de-accessioned and fragments could be cut and used for analyses and experiments. This same decanter was examined and used in the series of ageing experiments during the first scientific investigation carried out at the NMS. In the case of the Islamic bottle a fragment naturally broken from the bottom of the artefact was used for the analyses.

Two additional glass artefacts from the NMS collections showing signs of alteration were also examined as application examples: a British necklace made of glass beads (H.1992.392) and an Islamic glazed ceramic (A.1886.568). The use of non-destructive analyses was required on both objects. Because the objects had detached fragments available before the conservation treatment was undertaken, these fragments could be taken away and analysed non-destructively by Raman spectroscopy and controlled pressure SEM.

### *II- 2.1.3 Characterisation of the crystalline products*

Crystalline products formed in the museum environment were examined on objects from the NMS collections, mostly Chinese and Islamic glasses. In addition crystalline products from glass objects in the Corning Museum of Glass (Corning, USA) were sampled during a visit to the research laboratory in April 2004. The crystalline products were sampled using a tungsten needle or a scalpel and stored between two glass slides.

## II- 2.2 Replica glasses

Three different soda silicate glass replicas, two with an unstable composition and one stable composition, were used for the ageing experiments. Replica glasses used in research for artificial ageing experiments are generally made in laboratories, using chemically pure components and inert containers, controlled melting conditions, to be finally cast into flat plate. Through this process, most of the effects induced by the ancient manufacturing techniques are lost resulting in a glass that obviously differs from ancient glasses. In order to replicate a glass as close to the ancient objects as possible, the replica used in this study are based on ancient composition and are blown and worked by a glass blower.

As mentioned earlier, the main glass used was the replica **RG1**, from the batch fabricated by Fearn for her experiments [2, 3]. RG1 is a replica of the composition of an original Venetian glass artefact from the Victoria & Albert Museum [1]. It was made on 9<sup>th</sup> June 2003 by Ian Hankey who melted the glass components at 1200°C and blew the glass into circular flat plates as in crown glass making (see chapter I). The finished material was not perfectly flat owing to the manufacturing process; however it was possible to get reasonably flat glass fragments with a thickness between 1-2 mm from the band at the edge of the disk. A flat and smooth surface is important for SIMS analyses to ensure stability of the beam. The glass disks were stored at ambient temperature and low RH using dry silica gel.



Two other replica glasses **RRo** and **RRn** were used for comparison in some experiments. RRo is an unstable glass originally used to replicate a Roman glass vessel. However its composition did not correspond to the Roman composition as magnesium was used instead of calcium causing instability of the glass and the formation of white crystalline products at its surface (Figure II- 3). On the contrary, the RRn glass had the stable composition typical of Roman glasses. Both glasses were blown into the shape of a Roman glass bottle (Figure II- 3).

Figure II- 3: RRo replica glass.

The composition of all three soda silicate glasses measured by EPMA is presented in Table II- 1, both in weight percent (wt%) and atomic percent (at%). EPMA gave compositions in atomic percent and the weight percent values were calculated on the basis of the equivalent oxides. For manganese and iron the oxidation state was assumed to be +2 in all glasses. Although composition is usually given in mass percent, the research showed that the use of composition in atomic percent was mandatory to interpret structural modification by Raman spectrometry and establish correlations. Consequently all composition will be presented in at% in the rest of the study.

Table II- 1: Elemental composition of the replica glasses measured by EPMA; Top in atomic % (at%); Bottom/italic in weight % (wt%).

<b>At%</b>	<b>Si</b>	<b>Al</b>	<b>Na</b>	<b>K</b>	<b>Ca</b>	<b>Mg</b>	<b>Ba</b>	<b>Pb</b>	<b>Cu</b>	<b>Mn</b>	<b>Fe</b>	<b>O</b>
<b>Wt%</b>	<b>SiO<sub>2</sub></b>	<b>Al<sub>2</sub>O<sub>3</sub></b>	<b>Na<sub>2</sub>O</b>	<b>K<sub>2</sub>O</b>	<b>CaO</b>	<b>MgO</b>	<b>BaO</b>	<b>PbO</b>	<b>CuO</b>	<b>MnO</b>	<b>FeO</b>	
<b>RG1</b>	24.64	0.29	12.22	1.44	1.52	0.60	0.00	0.00	0.01	0.17	0.12	58.98
	<i>71.80</i>	<i>1.19</i>	<i>18.36</i>	<i>3.29</i>	<i>2.75</i>	<i>0.78</i>	<i>0.02</i>	<i>0.01</i>	<i>0.03</i>	<i>0.39</i>	<i>0.29</i>	-
<b>RRo</b>	22.51	0.45	13.56	1.68	0.51	3.23	0.00	0.00	0.11	0.01	0.38	57.55
	<i>67.04</i>	<i>1.89</i>	<i>20.83</i>	<i>3.93</i>	<i>0.94</i>	<i>4.30</i>	<i>0.02</i>	<i>0.02</i>	<i>0.29</i>	<i>0.03</i>	<i>0.90</i>	-
<b>RRn</b>	22.88	0.57	12.60	0.58	3.48	1.24	0.01	0.00	0.00	0.01	0.32	58.29
	<i>67.47</i>	<i>2.39</i>	<i>19.16</i>	<i>1.34</i>	<i>6.39</i>	<i>1.64</i>	<i>0.03</i>	<i>0.02</i>	<i>0.01</i>	<i>0.03</i>	<i>0.76</i>	

The replica glasses as well as six modern glass samples having similar compositions were examined as part of the investigation aimed to link the Raman spectral data to the glass composition and stability. The modern samples include 3 Corning reference glasses A, B and D, a fragment of float glass (FG), a reference named 'CL127' and a modern lead crystal glass named 'flute'.

## II- 3. Ageing experiments

### II- 3.1 Ambient ageing experiments

#### II- 3.1.1 Artificial environment

Considering the numerous factors involved in the atmospheric alteration of glass, artificial ageing experiments replicating the museum atmosphere were set up to determine the role of the different factors involved. All ageing experiments were undertaken in static conditions, typical of the storage and display of museum objects, and were set up in 2 L glass desiccators with a controlled environment. The effect of the following parameters on the alteration of glasses was examined within different series of experiments: the RH, type of organic pollutants, pollutant concentration, time, and the presence of CO<sub>2</sub> with light.

The decision to use only glass-made materials for the experiments was taken after contamination problems were encountered when using plastics (such as polystyrene) or zinc metal disk in the presence of the high humidity and/or pollutants. The temperature was regulated at 19 °C ± 0.5 °C by the laboratory air conditioning system and Artsorb® (Fuji Silysia Chemical Ltd) was used to control the RH at ± 1 %. The temperature and RH were monitored continuously in the reference desiccators using a humbug® data logger (Hanwell Ltd) telemetry system. Artsorb is a moisture-sensitive silica material which adsorbs and desorbs moisture in order to offset changes in relative humidity. Compared with the conventional silica gel, Artsorb has a greater capacity for moisture and desorption and is used successfully in museums worldwide. Artsorb was preferred over saturated salt solutions to control the humidity after contamination problems were encountered during the first scientific investigation at the NMS.

Glass fragments were cut to size of approximately 10 × 10 mm using a diamond wheel and a pair of pliers. Prior to the experiments, the desiccators and the glass fragments were cleaned using distilled water followed by ethanol and dried with wipe tissues. The glass fragments were placed on the bottom of an upturned beaker (Figure II- 1). When the glasses were sampled the face exposed to the atmosphere, and which was subsequently analysed, was scratched using a diamond pen. When the glass fragments could not be analysed by SIMS on the day, they were placed in a glass vial stored in the fridge at low RH with silica gel.

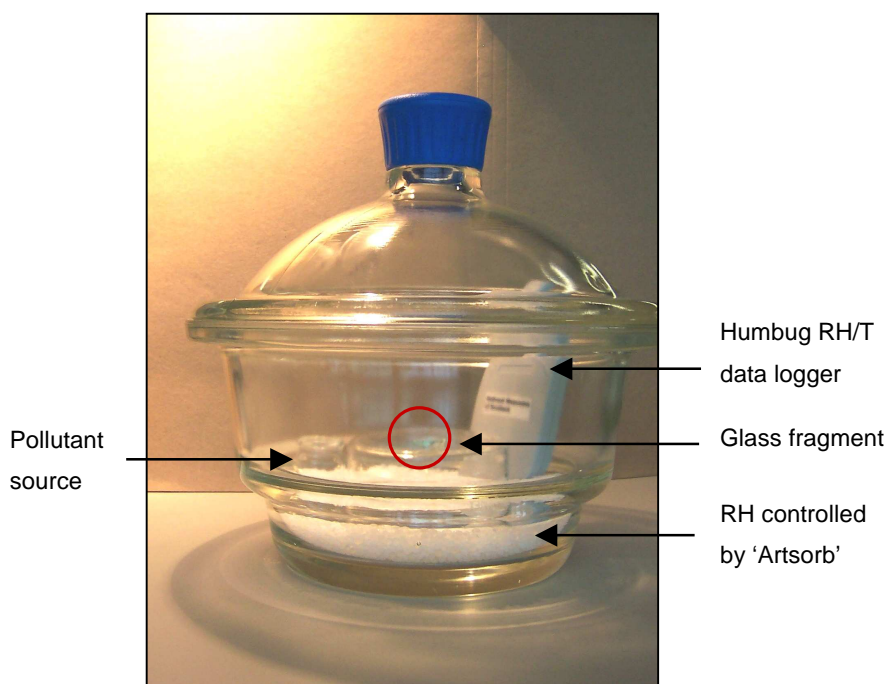


Figure II- 4: Ambient artificial ageing set up

#### Series 1: Effect of CO<sub>2</sub>

The possible formation of formic acid from the reaction of silicate glass in the presence of CO<sub>2</sub>, water and light was examined. In that case, fragments of RG1 glass were exposed to 100 % RH for 6 weeks in atmospheres containing saturated CO<sub>2</sub>, ambient air or saturated N<sub>2</sub>, in the presence of daylight or in the dark. The high humidity atmosphere was created by placing a 10 mL glass vial filled with distilled water, and the saturated CO<sub>2</sub> atmosphere was obtained by evaporating dry ice in the desiccators.

#### Series 2: Effect of RH and organic pollutants

Fragments of RG1 and RRn replica glasses were exposed for 6 weeks to either 50 µL formic acid, 50 µL acetic acid or saturated N<sub>2</sub> atmospheres kept at 40 %, 50 % or 60 % RH, as well as a mixed atmosphere with 50 µL formic acid + 100 µL acetic acid kept at 50 % or 60 % RH. The different humidities were obtained using Artsorb pellet pre-conditioned at the different RH. A summary of the experiment is presented in a table in **Appendix II**. In addition, a fragment of RG1 glass was exposed to 100 % RH for 4 months at ambient temperature in glass desiccators by Sarah Fearn at the Department of Materials, Imperial College.

### Series 3: Progress of the alteration with time

In order to determine the effect of the pollutants on the alteration kinetics, glass fragments were exposed to polluted and non-polluted atmospheres over 13 months and examined at regular intervals during this period.

Fragments of RG1 glass were exposed to polluted atmospheres with either formic acid or formaldehyde. A volume of 50  $\mu\text{L}$  concentrated solution of the volatile pollutants was introduced within a glass vial at the bottom of the desiccators. Assuming that all the liquid pollutant rapidly passed in the gas-phase, it was possible to calculate the gas-pollutant concentration, which was 30.5  $\mu\text{g m}^{-3}$  for formic acid and 27  $\mu\text{g m}^{-3}$  for formaldehyde at the start of the experiment. Ambient air (laboratory air) and saturated  $\text{N}_2$  were used as non-polluted atmospheres for comparison. All environments were fixed at 48 % RH and 19°C for the duration of the experiment. For each pollutant, a series of 10 desiccators were set up with 3 glass fragments in each. In contrast, only one desiccator was set up for the ambient air or  $\text{N}_2$  atmospheres, with 30 glass fragment in each. The reason for using separate desiccators for each time period in the case of polluted atmospheres was to avoid disturbing the atmosphere when opening the desiccators to collect the glasses. The opening of the ‘ambient air’ desiccators did not appear to affect the atmosphere inside since the RH and temperature, measured precisely by the humbug sensor in this desiccator were unaffected. However, the pollutants present at low levels in the air were renewed each time, which is taken into consideration for the interpretation of the results. The desiccator containing  $\text{N}_2$  was refilled after each opening.

The glass fragments were taken out approximately every 4 weeks in the first 7 months, then at larger time intervals in the following 6 months. At least one sample was kept undisturbed for the SIMS analyses, while the others were examined with other analytical instruments.

Independently, another series of RG1 glass were exposed to the same atmospheres but for shorter duration of 4 days, 1, 2, and 3 weeks. An additional sample was exposed for 18h in the formic acid atmosphere.

These experiments are summarised in a table in **Appendix II**.

### II- 3.1.2 Real environment

In parallel to the artificial experiments set up in desiccators, a series of RG1 glass fragments were exposed to the polluted atmosphere of two storage cupboards in the NMS for 13 months. As mentioned by the preliminary study, the environmental conditions (RH/temperature) of the NMS fluctuated greatly between the winter and summer months. By setting up the experiment for just over a year, the glass could be exposed to the complete fluctuation cycle. Cupboard 29 in cellar 3 and cupboard B1-7 in cellar 12 (referred later on only as cellars 3 and 12) were selected as they emitted high concentration of pollutants which caused alteration to the glass and glazed ceramic artefacts stored in them. The pollutant concentrations were measured by Lorraine Gibson (University of Strathclyde) using the diffusion tube method [5, 6]. The measurements obtained for formic acid, acetic acid and formaldehyde in the two cupboards and in the rooms are presented in Table II- 2.

Table II- 2: Pollutant concentrations in cupboard and in the room of cellar 3 and 12 of the NMS.

	Acetic acid ( $\mu\text{g m}^{-3}$ )	Formic acid ( $\mu\text{g m}^{-3}$ )	Formaldehyde ( $\mu\text{g m}^{-3}$ )
Cellar 3 - room	$310 \pm 9$	$40 \pm 10$	$104 \pm 1$
Cellar 3 – cupboard 29	$2827 \pm 35$	$416 \pm 16$	$957 \pm 6$
Cellar 12 - room	$40 \pm 10$	$< 40$	$7 \pm 1$
Cellar 12 – cupboard B1-7	$1722 \pm 22$	$189 \pm 15$	$258 \pm 2$

Detection limits for acetic acid:  $27 \mu\text{g m}^{-3}$ ; formic acid:  $40 \mu\text{g m}^{-3}$ ; formaldehyde:  $\mu\text{g m}^{-3}$ .

RG1 glass cut into  $10 \times 10$  mm fragments, and cleaned as for the artificial experiments, were placed next to the objects in the tray in cellar 3 (Figure II- 5) or on the shelf in cellar 12 (Figure II- 6). Enough glass pieces were introduced so that three fragments could be sampled each time. At least one sample was kept undisturbed for the SIMS analyses, while the others were examined with other analytical instruments.

The temperature and RH within the cellars were monitored via the NMS environmental telemetry system. A glass fragment was taken out approximately every 4 weeks in the first 7 months, then at larger time intervals in the following 6 months. Independently, a series of RG1 glass were exposed to the same atmospheres but for duration of 1, 2, and 3 weeks. The samples were marked and stored as in the artificial experiments.



Figure II- 5: Glass fragments set up in cellar 3.



Figure II- 6: Glass fragments set up in cellar 12.

### II- 3.2 Accelerated ageing experiments

The glass replica RG1, RRo and RRn were aged following the accelerated corrosion method used in museums to assess the corrosiveness of materials [7], with a glass fragment (size around  $30 \times 8$  mm) inserted into the silicon stopper instead of a metal coupon (Figure II- 7). The glass was suspended by the stopper into a 50 mL glass tube which was sealed with the stopper. A small glass tube (around 1 mL) filled with distilled water was placed in the bottom of the tube to generate a saturated humid atmosphere.

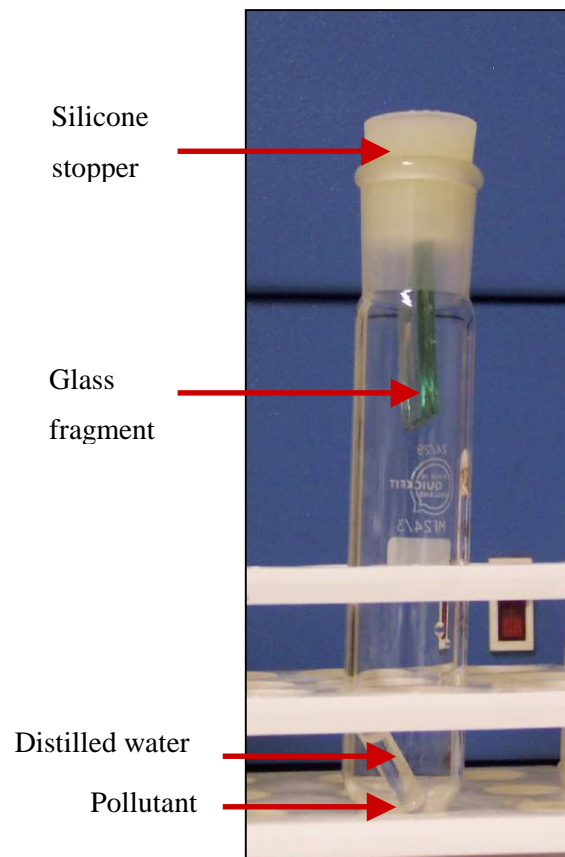


Figure II- 7: Glass accelerated ageing set up.

In order to examine the structural modification induced by different atmospheres, the RG1 glass was exposed either to a polluted or a non-polluted atmosphere at high humidity. To do so, the atmosphere in the tube was either left as it was (humid/non-polluted) or saturated by a pollutant source: either formic acid, acetic acid, formaldehyde or wood (humid/polluted). The amount introduced was approximately 0.1 mL concentrated pollutant solution or 2 g of MDF wood. The tubes were placed in an oven at 60 °C for durations between 1 to 4 weeks or at 50 °C for 3 months. At the end of the experiment, water remained in the tube, confirming the RH had been maintained at 100 % throughout. The pH of the liquid solution present at the surface of the glass was measured with pH paper. After ageing, half of the glass fragments were stored in ambient atmosphere and the other half was dried in silica gel at 60 °C for up to 1 week. One experiment undertaken in the humid/non-polluted atmosphere, using only 0.5 mL water, was left in the oven until the water was completely consumed (approximately 8 weeks).

For comparison a series of RRo and RRn glasses were exposed to polluted and non-polluted atmosphere at 100 % RH for durations between 6 and 8 weeks using this test.

The experiments are summarised in the table in **Annexe III**.

A notation giving the type of glass, atmosphere of exposure and the duration will be used through this study. Thus, RG1FAw2 will correspond to the ageing of the replica glass RG1 in formic acid vapour and 100 % RH for 2 weeks while RRoH<sub>2</sub>Om3 will correspond to the ageing of the replica glass RRo in 100 % RH and non polluted atmosphere for 3 months.

## II- 4. Analytical techniques

### II- 4.1 Raman spectroscopy

#### II- 4.1.1 Theory

Raman spectroscopy relies on the scattered radiation with modified wavelengths, the **Raman scattering**, produced after interaction of a monochromatic radiation with a molecule. The modification of the wavelength is associated with the vibrational energy levels of molecules.

When an intense monochromatic light, usually from a laser in the visible range, interacts with a molecular system, the vibrational energy levels generally reach a virtual state (Figure II- 8). When the molecular system returns to stable state photons are scattered. The major part of the photons are elastically scattered (Rayleigh scattering), which means that the emitted photons have the same wavelength as the absorbing photons. A very small fraction ( $\sim 1/10^7$ ) of the incident photons are inelastically scattered (Raman scattering), which means that the energy/wavelength of the incident and scattered photons are different. Two types of Raman scattering are produced: the Stokes and the anti-Stokes (Figure II- 8). Both processes provide the same information; however Stokes scattering are stronger, since at room temperature the population state of a molecule is principally in its ground vibrational state [8].

The amount of energy change of a photon is characteristic of the nature of each vibration, involving one or several bonds, and is independent of the wavelength of the laser used. However, not all vibrations are observable with Raman spectroscopy, since the necessary rule for the Raman transition to be active is that a change in the *polarisability* of the molecule is created by the interaction, which corresponds to a deformation of the electron cloud. The amount of the polarisability of the bond determines the intensity and frequency of the Raman shift.

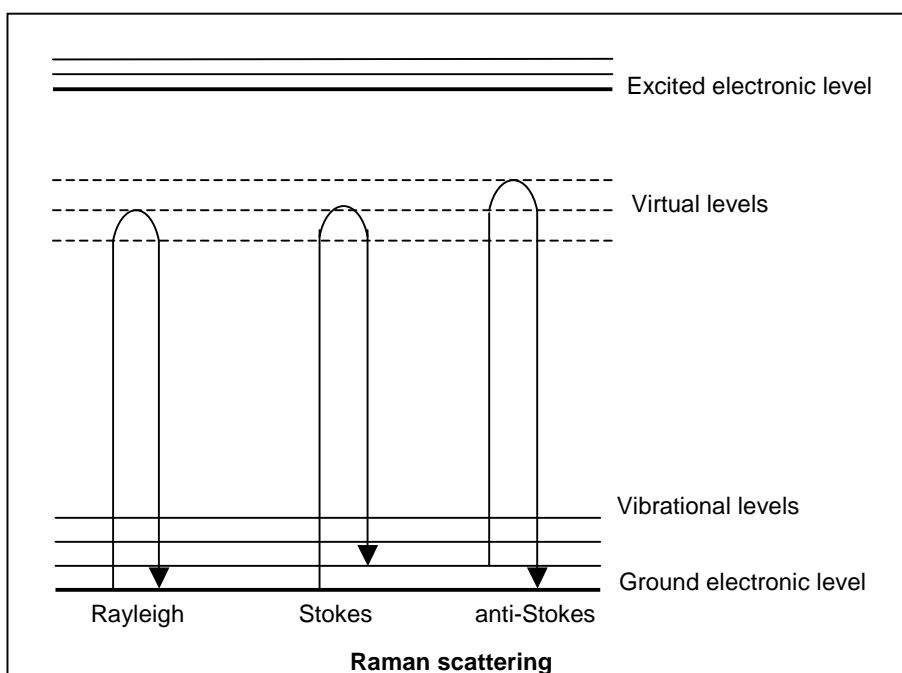


Figure II- 8: Diagram of the photon relaxation after interaction with molecule.

The interaction and the different scattering can be explained by the classical model [8]. The light is an electromagnetic radiation of frequency  $\nu_0$  and amplitude  $E_0$  written as:

$$\vec{E} = \vec{E}_0 \cos(2\pi \nu_0 t) \quad \{\text{II.1}\}$$

The effect of the electric field on a molecule is to polarise the electron distribution, thus inducing a dipole moment given by:

$$\vec{P} = \alpha \vec{E} = \alpha \vec{E}_0 \cos(2\pi \nu_0 t) \quad \{\text{II.2}\}$$

where  $\alpha$  is the polarisability of the molecule and corresponds to a tensor.

A molecule vibrates at a frequency  $\nu_v$  and its internuclear distance from the equilibrium is given by:

$$q = q_0 \cos(2\pi \nu_v t) \quad \{\text{II.3}\}$$

where  $q_0$  is the amplitude of vibration.

The polarisability  $\alpha$  can be developed as:

$$\alpha = \alpha_0 + \left( \frac{d\alpha}{dq} \right)_0 q + \dots \quad \{\text{II.4}\}$$

where  $\alpha_0$  is the polarisability of the molecule at the equilibrium and  $(d\alpha/dq)_0$  is the polarisability change with the internuclear distance from the equilibrium. The higher terms from the development of  $\alpha$  are neglected for small atomic displacements.

During the vibration, the variation of the polarisability of the molecule is:

$$\alpha = \alpha_0 + \left( \frac{d\alpha}{dq} \right)_0 q_0 \cos(2\pi \nu_v t) \quad \{\text{II.5}\}$$

Therefore, the induced dipole moment varies according to:

$$\vec{P} = \alpha_0 \vec{E}_0 \cos(2\pi \nu_0 t) + \left( \frac{d\alpha}{dq} \right)_0 q_0 \cos(2\pi \nu_v t) \vec{E}_0 \cos(2\pi \nu_0 t) \quad \{\text{II.6}\}$$

$$\vec{P} = \alpha_0 \vec{E}_0 \cos(2\pi \nu_0 t) + \left( \frac{d\alpha}{dq} \right)_0 \frac{q_0}{2} \vec{E}_0 \{ \cos[2\pi(\nu_0 - \nu_v)t] + \cos[2\pi(\nu_0 + \nu_v)t] \} \quad \{\text{II.7}\}$$

This classical description indicates that the interaction of the electromagnetic radiation of frequency  $\nu_0$  with the molecular system creates an induced dipole with 3 frequencies terms:  $\nu_0$ , corresponding to the Rayleigh radiation,  $\nu_0 - \nu_v$  corresponding to the Stokes Raman scattering and  $\nu_0 + \nu_v$  corresponding to the anti-stokes Raman scattering.

Experimentally, the Raman spectrum displays bands associated with the frequency change  $\nu_v$  for each vibration. The frequency values are divided by the speed of light and the Raman frequencies appear as wavenumbers given in  $\text{cm}^{-1}$ , which is defined by:

$$\bar{\nu}_v = \frac{\nu_v}{c} = \frac{1}{\lambda_v} \quad \{\text{II.8}\}$$

The vibrational frequencies depend on the atomic masses, the molecular geometry and the interatomic forces in the molecule. From the molecular geometry of the molecule and based on the group theory it is possible to classify the molecular vibrations observed in the Raman spectrum. Although the vibrations of individual bonds are tightly coupled and affected by their environment, it is possible to identify frequencies characteristic of chemical groups, which can be used to interpret the vibrational spectra. Thus, the relative intensity of the Raman bands and their frequencies can provide structural information.

In crystalline solids, the molecules have fixed orientations therefore their Raman spectra display sharp bands and are dependent on the overall orientation of the molecules relative to the direction of irradiation. For this reason the bands intensities in the spectra of single-

crystals may vary with orientation. For non-crystalline solids however, the Raman spectra are associated with the vibration of the species in the short-range, but the distribution of bonding forces within the tetrahedra and the variation of the inter-tetrahedral angles cause the broadening and overlapping of the bands. Nevertheless, it is possible to gain qualitative structural information on glass from the knowledge of the characteristic vibration of the short-range species (like silicate tetrahedra in silicate glasses). A description of the Raman spectrum of silicate glasses is given at the beginning of Chapter IV.

#### II- 4.1.2 Instrumentation

Fifty years ago, Raman spectroscopy was undertaken using an iron arc as an exciting source, and, interestingly, glass plates to collect the scattered radiation (Figure II- 9). Due to the low intensity of the exciting source and the weakness of the Raman scattering, the acquisition time needed was a few hours for each material analysed.

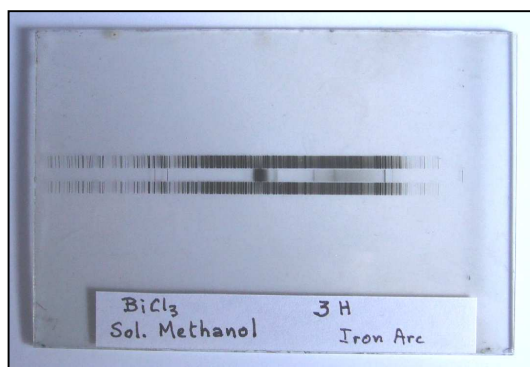


Figure II- 9: Raman spectrum of  $\text{BiCl}_3$  in methanol solution collected for 3 hours using an iron arc exciting source, done in 1948 (plate provided by M. Delhay, LASIR-CNRS, Lille).

The use of lasers as the exciting source provided a very intense and monochromatic source of energy, which increased the intensity of the scattered radiation, nowadays visualised on a computer, and greatly reduced the acquisition time.

A microscope focuses the laser on the sample and collects the scattered light. In order to observe the Raman scattering, the Rayleigh line is cut out generally using a notch filter, which eliminate signal generally below  $100 \text{ cm}^{-1}$ . After going through a confocal hole (detailed below), the Raman scattering is dispersed by a grating and detected by a charged coupled device (CCD).

The technique known as ‘confocal microscopy’ allows probing discrete Z-planes and analysing well defined volume in a heterogeneous material. The principle of this technique, graphically shown in Figure II- 10, is based on the application of a diaphragm (confocal pinhole) to reject out of focus radiation originating from different Z-planes from reaching the detector. The size of the volume can be varied by changing both the opening of the confocal diaphragm and the couple magnification/numerical aperture of the objective [8, 9]. However the volume analysed may be influenced by the nature of the material traversed, especially when the refractive index of the different materials are very different [10].

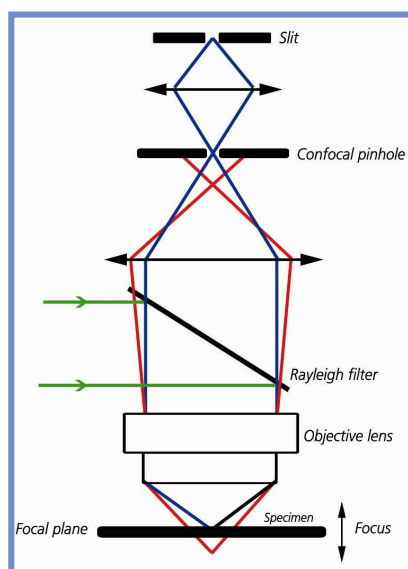


Figure II- 10: Schematic description of the confocal system (provided by Jobin-Yvon Horiba).

### II- 4.1.3 Experimental conditions

#### Glass

Raman spectra of the glasses were recorded on a LabRam Infinity micro-spectrometer (Jobin-Yvon-Horiba, Longjumeau, France) at the Laboratoire de Dynamique Interactions et Réactivité-CNRS (LADIR-CNRS), equipped with a Peltier-cooled CCD. The 532 nm line of a doubled diode laser was used as the exciting radiation and the power of illumination at the sample surface ranged between 5 and 9 mW. The backscattered light was collected through the  $\times 100$  objective of an Olympus microscope. Preliminary tests using different laser sources showed that the green laser at 532 nm was best suited for the analysis of glasses as it provided a reasonable window size ( $1450 \text{ cm}^{-1}$ ) and a low fluorescence background

compared to red (633 nm) and blue (488 nm) lasers. Glasses (except altered glasses) were analysed directly under the microscope without preparation using a confocal hole ranging between 100 and 200  $\mu\text{m}$ .

The Raman spectra of glasses aged naturally and artificially in an acidic environment were recorded from the broken section (not mounted) with a confocal hole of 100  $\mu\text{m}$ . In the case of the glasses aged in purely humid environment, the altered layer was very thin and gave a very weak Raman signal compared to the bulk glass. Hence, these altered glass flakes were scraped from the surface and analysed independently. In that situation, a confocal hole of 200  $\mu\text{m}$  was used. For all glasses, the spectra were recorded between 150 and 1650  $\text{cm}^{-1}$  for the silicate structure on both altered and unaltered areas, and between 2900 and 3900  $\text{cm}^{-1}$  for the O-H vibration on the altered area only. The spectral resolution was 2-3  $\text{cm}^{-1}$ . Because of the influence of the fluorescence, a baseline correction was undertaken by subtraction of a segment baseline by Labspec software with the number of segment reduced to a minimum and placed at about the same position for each spectrum. The corrected Raman spectra were curve fitted with Gaussian functions using Origin microcal software.

The confocal microscopy technique was assessed on the British decanter to examine the structure of the glass at different depths and thus discriminate *in-situ* and non-destructively measurements from the bulk and the altered layer. The method consisted of focusing manually the laser spot at the different depths by moving the platform stage. The displacement was calibrated using transparent materials of known thickness. The depth resolution on the measurements is 1  $\mu\text{m}$ . The analysed volume was varied by changing the diameter of the confocal hole with a  $\times 100$  objective. The dimension of the volume analysed based on the diameter at the waist and along the vertical axis are given for the confocal hole studied in Table II- 3.

Table II- 3: Spot dimensions as a function of the confocal hole with a x100 objective (supplied by Jobin Yvon Horiba).

Hole size ( $\mu\text{m}$ )	Spot diameter at the waist ( $\mu\text{m}$ )	Spot diameter along the vertical axis ( $\mu\text{m}$ )
25	1.1	2.5
50	2.3	3
100	3	5
200	9	6

### Crystalline products

Raman spectra of the crystalline products were recorded either on the LabRam Infinity micro-spectrometer at the LADIR-CNRS laboratory using the 532 nm line of a doubled diode laser or the LabRam 300 at the University of Edinburgh using a He-Ne laser operating at 633 nm. The analysis of the crystals was carried out directly on the aged glass or on a glass slide for object samples. On both instruments, the power of illumination at the sample surface ranged between 0.5 and 9 mW. The backscattered light was collected through the  $\times 100$  objective of an Olympus microscope. The spectra were recorded between 120 and  $4000\text{ cm}^{-1}$ .

## II- 4.2 Secondary ion mass spectrometry (SIMS)

### II- 4.2.1 Principle

The principle of SIMS relies on the bombardment of a solid surface in vacuum by a *primary ions* beam, which is focused, mass-filtered, and has energy between 250 eV to 30 keV. The kinetic energy supplied to the solid by the impact induces a series of atomic collision, known as the collision cascade, in which some of the atomic bonds are broken liberating atomic or molecular species into the vacuum (Figure II- 11). This sputtering process is poorly understood and no quantitative model currently exists that can accurately predict the secondary ionisation process.

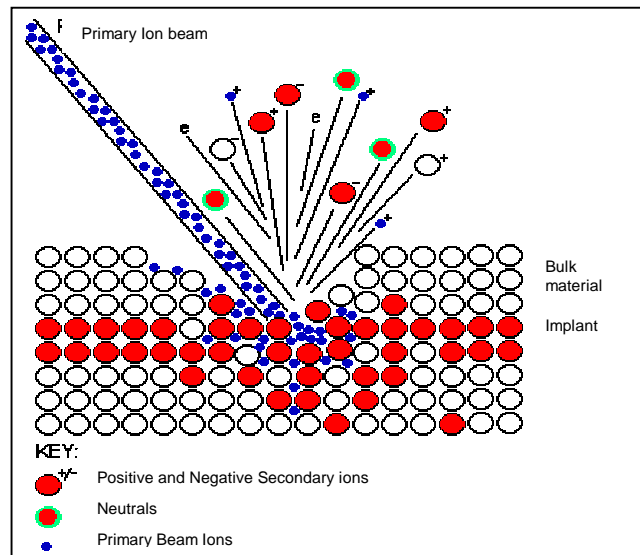


Figure II- 11: Bombardment of solid surface by primary ion beam (supplied by S. Fearn, Imperial College).

A small proportion of the sputtered species are ionised and are called the *secondary ions*. These ions are analysed by a mass spectrometer which separate them as a function of their mass/charge ratio  $m/q$  [11, 12, 13]. The magnitude of the magnetic field required to deflect the ion species is given by the equation:

$$\frac{m}{q} = \frac{B^2}{2V} r^2 \quad \{\text{II.9}\}$$

with  $m/q$  = mass to charge ratio (Kg/C)

$B$  = strength of the magnetic field (Wb/m<sup>2</sup>)

$V$  = the ion accelerating voltage (V)

$r$  = the radius of curvature of the magnetic field (m)

Two different SIMS techniques are distinguished:

- *Static SIMS*: used for the analysis of molecular species (organic and inorganic) and atomic composition at the surface. Low-energy and low primary beam densities are used so that the material sputtered is exceedingly small, with surface mono-layers lasting hours or days.
- *Dynamic SIMS*: follows the modification of the elemental composition as a function of depth, providing a compositional profile. In that case high-energy and high primary beam densities are applied to analyse volume of a 100 to 1000  $\mu\text{m}^3$ .



right level for the analysis and allowed charge evacuation by contact between the metal holder and the gold layer. Because the replica glasses RG1 were not perfectly flat owing to their manufacturing process, a silver metallic paint was added at the point of contact between the glass surface and the holder to reduce charging. The holder with samples were placed in a first chamber kept at  $10^{-6}$  torr, allowing the removal of adsorbed water and complete the evaporation of the paint solvent, before being introduced in the main chamber kept at  $10^{-8}$ - $10^{-9}$  torr for analysis.

### Instrumental conditions

Samples were sputter depth profiled using an  $O^-$  primary beam of 60 nA, from a duoplasmatron, and accelerated on to the sample surface with a net impact energy of 10 keV. Secondary ions of H, Na, Al, Si, K, Mg and Ca were collected and detected with an electron multiplier, operating in pulse counting mode. The isotopes of the selected elements were counted for 5 s. The beam was positioned in the centre of the sample to avoid magnetic field distortion produced by the metal holder on the edges. The beam was rastered over an area that was generally 60 % of  $250 \times 250 \mu\text{m}$ . In order to avoid contribution from a non-uniform crater (edge and bottom), the secondary ions analysed were collected from only a small area within the rastered area using a gate on the detector which size was fixed for all the analyses. The size of the gate was  $79 \times 69$  pixels within a rastered area of  $256 \times 256$  pixels. The sputter rate, and so the depth resolution of the measurements can be modified by changing the percentage of the zone rastered. Thus by increasing the size of the area, slower sputter rates were gained, but the analysed area was modified. The area of analysis  $A$  is calculated by:

$$A = \left(\frac{79}{256}\right) \times \left(\frac{69}{256}\right) \times (250 \times 250) \times p \quad \{\text{II.10}\}$$

where  $p$  is the percentage of the rastered area (0-1).

When  $p$  was equal to 0.6 (60 %), the area of analysis was  $3119 \mu\text{m}^2$  and the sputter rate varied between 10 and 15 nm.

**Depth determination**

At the end of the measurement, the height of the crater produced by sputtering craters was measured using a stylus profilometer. After treatment of the raw data obtained from the SIMS, elemental concentration could be plotted as a function of time. The raw data treatment and quantification method used is developed in the result chapter V. The reliability of the measurements is also assessed and presented in chapter V.

**Imperial College instrument**

The University of Edinburgh SIMS instrument was compared to the low-energy SIMS instrument at Imperial College using the series of RG1 glasses aged in artificial conditions for 1, 2 and 3 weeks. The measurements at Imperial College were undertaken by Sarah Fearn using an Atomika quadrupole SIMS tool equipped with a floating low energy primary ion gun. A nitrogen beam at 500 eV and normal incidence was used to perform the analyses, with a current of 90 nA and a scan size of 375  $\mu\text{m}$ . Charge compensation was obtained using an electron energy of 70 eV. SIMS crater depths were measured using a Zygo white light optical interferometer [2, 3].

**Water content analyses**

The water content could be determined by SIMS on glass having an altered layer with a minimum thickness of 10  $\mu\text{m}$ . The measurements were carried out by John Craven (School of GeoSciences, University of Edinburgh) from the Geology department of the University of Edinburgh on the British decanter glass, and the replica glass RG1 aged in atmospheres humid/non-polluted (RG1H<sub>2</sub>Ow4), and humid/wood (RG1woodw4). The SIMS analyses were undertaken on the cross section of the samples prepared for the electron microprobe analyses (see electron microprobe section), but coated with a gold layer. A rastered primary beam of 60 nA, O<sup>-</sup> was accelerated on to the sample surface with a net impact energy of ~14 kV. High energy (120 eV  $\pm$  25 eV) secondary ions sputtered from the sample were detected with an electron multiplier operating in pulse counting mode. The isotopes hydrogen and silicon were counted for 5 s and 2 s respectively. In order to obtain quantitative information standards of internal granitic compositions were used with a water content that ranged from 2.1 to 5.6 wt % H<sub>2</sub>O.

When the water content could not be measured, it was estimated for the altered glass composition assuming the silicon content before and after leaching remained constant and the deficit in the total ion content of the altered glass was mostly H.

## II- 4.3 Electron probe microanalysis (EPMA)

### II- 4.3.1 Principle

Electron probe micro-analysis (EPMA) is a fully qualitative and quantitative method for elemental analysis of micron-sized volumes at the surface of materials, with sensitivity at the level of ppm. It is the most precise and accurate micro-analysis technique available and all elements from beryllium to uranium can be analyzed. In EPMA a micro-volume of a sample is bombarded with a focused electron beam (typical energy= 5-30 keV) and the X-ray photons thereby induced and emitted by the various elemental species were collected. Because the wavelengths of these X-rays are characteristic of the emitting species, the sample composition can be easily identified by recording WDS spectra (Wavelength Dispersive Spectroscopy). By comparing the intensities of these lines with those emitted from standards (of known composition) it is possible to determine the concentrations of the elements to accuracy around  $\pm 1$  %. Wavelength discriminating X-ray detectors are the most quantitative because their signal-to-noise ratio is high and they have excellent wavelength resolution. The high signal-to-noise also implies higher sensitivity to minor and trace elements. Disadvantages are that X-ray measurement is time consuming, and since the elements of interest have to be tuned, this implies they need be first anticipated [14, 15, 16].

### II- 4.3.2 Experimental conditions

The electron microprobe was used to obtain the accurate composition of the glasses from which a fragment could be taken and mounted into a cross section. Glass samples from museum objects and replica glasses artificially aged were mounted in epoxy resin and polished to a finish of 0.25  $\mu\text{m}$ . The analyses were carried out by Katherine Eremin (NMS) on two WDS electron microprobe systems at the University of Edinburgh:

- Initially a Cameca Camebax Microbeam - 1985 with three crystal spectrometers at 20 kV and 9 nA with the Cameca ZAF correction procedure
- Subsequently a Cameca SX100 microprobe with five crystal spectrometers at 20 kV and 4 nA.

A rastered beam was used for a spot size of 8-10  $\mu\text{m}$  to prevent volatilisation and loss of alkali during analysis. For each sample, a minimum of 12 analyses was taken in different spots and the results averaged. Samples were analysed for up to 23 elements commonly

found in historic glasses. Mineral standards were used for instrument calibration, and glass standards were analysed and compared to the unknowns.

## II- 4.4 Scanning electron microscopy - energy dispersive spectrometry (SEM-EDS)

### II- 4.4.1 Principle

Scanning electron microscope is very similar to electron microprobe, but it is designed primarily for imaging rather than analysis. A compositional contrasted image is obtained from the secondary and backscattered electrons produced after scanning an electron beam on the sample surface. SEM has the advantage to offer high spatial resolution images (~5 nm) with large depth of field. It is generally fitted with an energy dispersive spectrometer (EDS), which provides easy and rapid compositional information derived from the emitted X-rays. The approximate penetration depth of the beam is ~ 1  $\mu$ m. The drawbacks of this detector are the relatively poor spectral resolution and low signal-to-noise, which results in many spectral interferences and poor sensitivity (relative to WDS) [15, 16]. The compositional information given by EPMA and SEM-EDS are compared for the three replica glasses in Table II- 4. The results indicate that SEM-EDS measurements tend to underestimate the concentration of sodium, calcium and magnesium probably because of the migration of these cations under the beam.

Table II- 4: Comparison of the elemental composition measured by EPMA and SEM-EDS.

At%		Si	Al	Na	K	Ca	Mg	Cu	Mn	Fe	O
RG1	EPMA	24.64	0.29	12.22	1.44	1.52	0.60	0.01	0.17	0.12	58.98
	SEM	25.9	0.4	9.8	1.6	1.2	0.3	-	0.1	0.1	60.5
RRo	EPMA	22.51	0.45	13.56	1.68	0.51	3.23	0.11	0.01	0.38	57.55
	SEM	22.2	0.8	11.7	1.5	0.3	1.9	0.4	-	0.3	60.8
RRn	EPMA	22.88	0.57	12.60	0.58	3.48	1.24	-	0.01	0.32	58.29
	SEM	23.5	1.3	10.7	0.6	2.0	0.6	-	-	0.2	61.0

#### ***II- 4.4.2 Experimental conditions***

The scanning electron microscope was used mostly to obtain high resolution images of the altered glass surface or sections. By working in controlled pressure mode it was possible to image the glass without surface coating or high vacuum causing dehydration of the glass. Ryan experienced dehydration of the altered layer while working under high vacuum, resulting in strong cracking of the layer [1]. Since the presence of cracks and their pattern is one of the characteristic of the alteration, it is important that this information is conserved and not created or influenced by external factors. Approximate elemental compositions were obtained by an EDS detector on materials which could not be examined by EPMA (because a sample could not be taken or limited access to the technique). To reduce alkali migration induced by the electron beam, a low energy beam rastered over a large area was used.

The samples were either mounted on an aluminium stub and maintained by an aluminium foil or attached to a carbon tape. Cross sections mounted in resin for EPMA were also examined. The analyses were undertaken on a CamScan MX 2500 SEM combined with a Noran Vantage analytical system at the NMS. An accelerating voltage of 15 kV was used for the electron beam and the samples were kept at pressure of 15 Pa in the controlled pressure mode.

#### **II- 4.5 Light microscopy**

The visual appearance of the glass surface after ageing was recorded with a light microscope. This observation was particularly important to relate the present work to the museum objects through the characteristic surface morphologies. Moreover it was complementary to SIMS analyses to examine the evolution of the alteration with time and determine the mechanisms of these alterations.

The surfaces of the glass samples were examined with a Zeiss light microscope Axioskop 2 at the University of Edinburgh. Reflected light and in few occasion dark field was used.

## II- 4.6 X-Ray Diffraction (XRD)

### II- 4.6.1 Principle

X-ray diffraction is used to determine the structure of molecule, mostly crystals with atoms are organised in repeating planes. These planes can act as reflecting surface for X-rays as a result of the interaction of X-ray radiation with the electrons in the atoms. When the distances between the atoms are of the same magnitude as the wavelength of the X-rays, constructive and destructive interferences occur. This result in the diffraction of X-rays emitted at characteristic angles based on the planes between the atoms organised in crystalline structures. The diffraction pattern is characteristic of a crystal and provides information on the positions of each atom in the unit cell, and therefore in the molecule [17, 18]. The relationship between wavelength, atomic spacing ( $d$ ) and angle is defined by the Bragg Equation:

$$n\lambda = 2d \sin\theta \quad \{\text{II.11}\}$$

with  $\theta$ : angle between the incident and refracted beam

$\lambda$ : wavelength of the incident beam (X-ray)

$d$ : spacing between planes (Å)

The identification of a compound is made by comparison with sets of  $d$ -spacing of the diffraction pattern obtained from standard compounds.

### II- 4.6.2 Experimental conditions

XRD using a heating stage was applied to a solid of sodium formate to examine the different phases formed at high temperature and after cooling. The measurements were undertaken on a Bruker AXS D8 diffractometer at the University of Edinburgh equipped with an Anton Parr TTK450 heating stage. The diffractometer was set up in Bragg-Brentano parafocussing geometry with a monochromated beam. The X-rays were generated by a copper K-alpha 1. The sample was finely ground and presented as a flat pressed powder to be heated in air. Six scans were taken from 5 to approximately  $69^\circ 2\theta$  with a step size of 0.014  $\theta$ - $2\theta$  and a count time per step of 0.1s. The scans were taken at the following temperatures: 28, 127, 237, 247, 63 at a rate of 0.5  $^\circ\text{C/s}$  and at 28  $^\circ\text{C}$  after melting the compound above 260  $^\circ\text{C}$ . The powder patterns were identified based on the published  $d$ -spacing data.

## II- 5. References

- 1 Ryan J.L., The atmospheric deterioration of Glass: Studies of decay mechanisms and conservation techniques, *PhD thesis*. University of London (1996).
- 2 Fearn S., McPhail D., and Oakley V., Room temperature corrosion of museum glass: an investigation using low-energy SIMS, *App. Surf. Sci.* **231-232** (2004) 510.
- 3 Fearn S., McPhail D., and Oakley V., Moisture attack on museum glass measured by SIMS, *Phys. Chem. Glasses.* **5** (2005) 505.
- 4 Lombardo T., Mécanismes d'altération du verre calco-sodique en atmosphère urbaine polluée, *PhD thesis*. Paris XII University (2002).
- 5 Gibson L.T., Cooksey B.G., Littlejohn D., and Tennent N.H., A diffusion tube sampler for the determination of acetic acid and formic acid vapours in museum cabinets, *Ana. Chim. Acta.* **341** (1997) 11.
- 6 Gibson L T, and Brokerhof A., A passive tube-type sampler for the determination of formaldehyde vapours in museum enclosures, *Stud. Conserv.* **4** (2001) 289.
- 7 Robinet L., and Thickett D., A new methodology for accelerated corrosion testing, *Stud. Conserv.* **4** (2003) 263.
- 8 Turrell G., and Corset J., *Raman microscopy, Developments and applications*, Academic Press, London (1996).
- 9 Lenain B.P., Analytical Raman spectroscopy: a new generation of instruments, *Analysis.* **1** (2000) 11.
- 10 Bruneel J. L., Lassegues J. C., and Sourisseau C., In-depth analyses by confocal Raman microspectrometry: experimental features and modeling of the refraction effects, *J. Raman Spectrosc.* **10** (2002) 815.
- 11 Grimblot J., La spectroscopie de mass d'ions secondaires: SIMS, *L'analyse de surface des solides par spectroscopies électroniques et ioniques*, Masson, Paris (1995).
- 12 Craven J., Secondary Ion Mass Spectrometry (SIMS), unpublished manual, School of Geosciences, The University of Edinburgh, undated.
- 13 Dowsett M., and Adriaens A., The role of SIMS in cultural heritage studies, *Nucl. Instrum. Meth. B* **226** (2004) 38.
- 14 [http://www.cameca.fr/html/epma\\_technique.html](http://www.cameca.fr/html/epma_technique.html)
- 15 Reed S.J.B., *Electron microprobe analysis and scanning electron microscopy in geology*, Cambridge University Press, Cambridge (1996).
- 16 Goldstein J.I., Newbury D.E., Echlin P., Joy D.C., Romig A.D., Lyman C.E., Fiori C., and Lifshin E., *Scanning electron microscopy and X-ray microanalysis. A text for*

*biologists, materials scientists and geologists*, second edition, Plenum Press, New York and London (1992).

- 17 Woolfson M.M., *An introduction to X-ray crystallography*, Cambridge university press, London (1970).
- 18 [http://www.rigakumsc.com/xrd/about\\_tech.html](http://www.rigakumsc.com/xrd/about_tech.html)

## **Chapter III.**

# **THE CRYSTALLINE DEPOSITS ON GLASSES**

### III- 1. Introduction

In the scientific study undertaken by the Conservation and Analytical Research department of the NMS (see chapter I), the alteration of the glass objects was investigated mostly through examination of the crystalline deposits formed at their surfaces [1]. Although the aim of the present study was to investigate the modification of the glass structure itself, the crystalline deposits were examined in parallel to assist in the interpretation of the mechanisms.

The aim of this brief chapter is to compare the crystalline deposits formed on museum objects with those formed in ambient and accelerated ageing experiments. Because the first study only examined British glasses, more analyses of the deposits were undertaken to explore whether similar alterations were observed for British, Islamic and Chinese glasses in the NMS collection. Islamic glazed ceramics from the NMS collections are stored in the same cabinets as the deteriorating glass objects and also display signs of alteration. The alteration of glazed ceramics is more dramatic since the glaze is attacked from the side exposed to the air and the side in contact with the porous ceramic body. This allows circulation of water vapour and pollutants. As a result, crystalline products, formed at the interface between the glaze and the ceramic as well as the surface, cause cracking and flaking of the glaze. Analyses of the crystalline products formed on two glazed ceramics are presented.

Objects from the Corning Museum of Glass also displayed white crystalline deposits whilst being stored in wooden cabinets and fluctuating environmental conditions. Samples of the deposits were analysed as part of this research and these results are presented.

This chapter describes the products identified in the different ageing atmospheres. Further analyses of crystalline products are presented in chapter V together with examination of the alteration progress using the SIMS technique.

### III- 2. Introduction to sodium formates

The most common and stable phase at ambient conditions is anhydrous sodium formate ( $\text{NaHCO}_2$ ), known as phase II. Two hydrated phases can be formed from saturated solution of sodium formate: sodium formate dihydrate, stable between 18 and 25 °C, and sodium formate trihydrate stable below 18 °C [2]. Under high pressure two polymorphs of the anhydrous sodium formate are formed: the phase III between 11 and 23 kbar and phase IV above 23 kbar [3]; as well as another sodium formate dihydrate phase [4]. Different polymorphs of the anhydrous sodium formate are formed on heating. When the ambient phase II is heated, it undergoes a transition to a high temperature phase, called phase I, at about 250 °C. Upon cooling phase I, an intermediate phase, phase I', is formed and after an induction period of approximately 10-12 hours it slowly retransforms into the original phase II at room temperature [5, 6, 7]. Masuda et al. noted that the re-transformation phase I'-II scarcely occurs if the sample is kept under vacuum but is accelerated in humid air [7].

The Raman spectra of formates exhibit characteristic peaks in the 1350-1390  $\text{cm}^{-1}$  region corresponding to the C-O symmetric stretching mode and the C-H bending modes; in the 2780-2850  $\text{cm}^{-1}$  region, associated with C-H stretching modes; and in the 770  $\text{cm}^{-1}$  region, corresponding to O-C-O bending vibrations [3].

The first study highlighted the presence of different phases of sodium formate in the crystalline deposits based on the comparison of their Raman spectra with the spectra of reference compounds or in the literature [1]. Sodium formate phase II was the main phase in the deposits, but another phase whose Raman spectrum was similar to that of phase I' measured by Heyns was identified for needle-shape crystals [5]. Because the high temperature required for its formation could not have been experienced by the objects, if the phase I' is present, another explanation for its formation must exist at ambient condition. In addition a new formate compound of sodium and calcium in an approximate Na:Ca ratio of 6:1 was identified in few samples [1]. The positions of the peaks in the Raman spectra and their intensities are given for sodium formate phase II and I' and the sodium calcium formate in **Appendix IV**.

### III- 3. Museum objects

The deposits observed at the surface of the glass objects were generally small white crystals, sometimes having a needle or dendritic morphology (Figure III- 1). Analysis by Raman spectroscopy showed that formate compounds were the major component of all the samples found on the NMS glasses, with mostly sodium formate phase II,  $\text{NaHCOO II}$  (Table III- 1). The sodium formate phase I',  $\text{NaHCOO I'}$ , and sodium calcium formate, sometimes present, could be associated with the needle and dendritic crystal morphologies. In the sample taken from the British biscuit barrel (HMEN 190) an organic compound, possibly a polymer was identified along the formate crystals. This polymer was possibly applied during a conservation treatment and may have played a role in the deterioration of the glass object. Although it was an isolated case and organic pollutants are the main source responsible for the formation of these formate compounds, it was a reminder that conservation products can participate in the alteration.

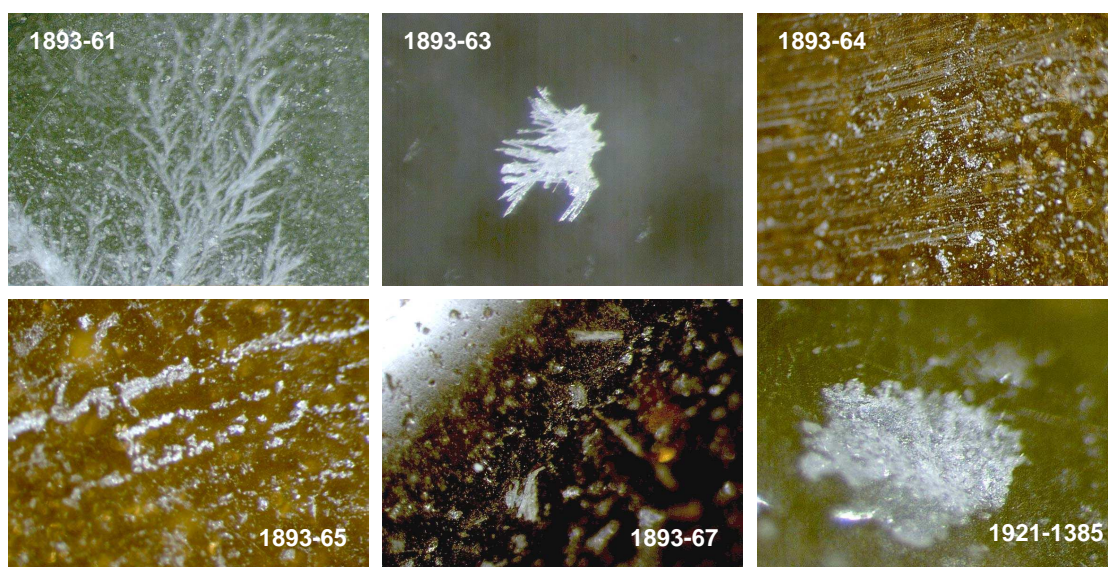


Figure III- 1: Crystalline products at the surface of Islamic glass objects from the NMS (field of view approximately 5 mm).

Table III- 1: Surface deposits identification from objects of the NMS and Corning Museum of Glass collections by Raman spectroscopy.

<b>Objects</b>	<b>Reference</b>	<b>Deposit morphology</b>	<b>Identification</b>
<b><i>Islamic glasses</i></b>			
Bottle clear	A.1893.61	White dendrite crystals	NaHCOO II, NaHCOO I', NaCH <sub>3</sub> COO, (Na,Ca) HCOO
Bottle brown	A.1893.63	White needle crystals	NaHCOO II + acetate?
Bottle brown	A.1893.64	White crystals	NaHCOO II
Bottle brown	A.1893.65	White crystals	NaHCOO II
Bottle light green	A.1893.66	White crystals	NaHCOO II
Bowl brown	A.1893.67	White crystals	NaHCOO II
Bottle brown	A.1921.1385	White crystals	NaHCOO II
Glazed ceramic	A.1886.573	White needles	(Na, Ca) HCOO
Glazed ceramic	A.1886.580	White needles	(Na, Ca) HCOO
<b><i>Chinese glasses</i></b>			
Red bowl	A.1921.1159	Liquid droplets	KHCOO ? + KSO <sub>4</sub>
Blue bowl	A.1948.75	White spots	NaHCOO II + NaSO <sub>4</sub>
Dark blue vase	A.1921.1149A	White spots	NaHCOO II
Blue bottle	no reference	White crystals	NaHCOO II
<b><i>British glasses</i></b>			
British biscuit barrel	HMEN 190	Translucent material	Polymer? + NaHCOO II
		White crystals	(Na, Ca) HCOO
	HMEN 98	White crystals	(Na, Ca) HCOO
	HMEN 215.36	White crystals	NaHCOO II
	HMEN 215.52	White crystals	NaHCOO II
	HMEN 215.191	White crystals	NaHCOO II
	HMEN 215.243	White crystals	NaHCOO II
Decanter	Unregistered	White crystals	NaHCOO II
Glass necklace	H.1992.392	White crystals	NaHCOO II
<b><i>Corning Museum glasses</i></b>			
Paper weight	no reference	Dendrite crystals	Unknown formate Y
Chinese tube clear	no reference	White needle crystals	NaHCOO II
Engraved bowl clear	RR11701	White dendrite	NaHCOO II + acetate ?
Daguerrotype	8R3	Sticky spider crystals	Formate ?
Purple glass	71.6.25	White crystals	NaHCOO II + NaSO <sub>4</sub> anhydrous

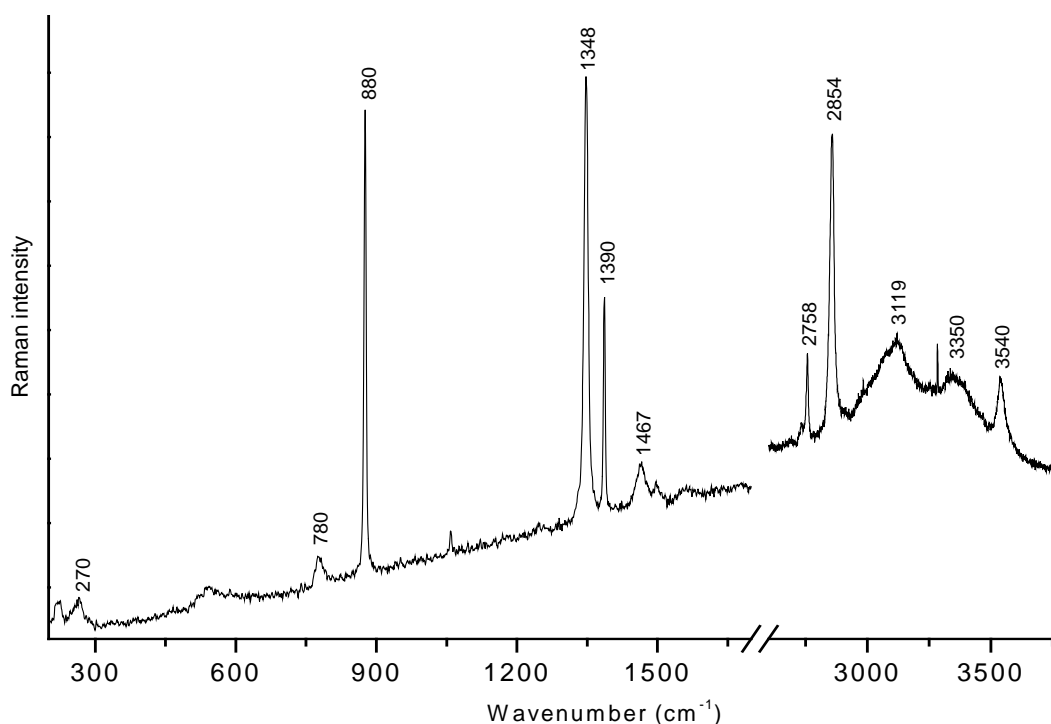


Figure III- 2: Raman spectrum of an unknown formate Y from the Corning paper weight object.

Formate compounds were also characterised in all the samples taken on the Corning glass objects. A new unidentified phase was observed in the deposit from one of the Corning objects, and its Raman spectrum is given in Figure III- 2. This new compound was identified as a new formate phase based on the characteristic positions of the peaks associated with C-H and C-O vibrations, and it was called here *formate Y*. The presence of a mixture of compounds can not be excluded. Moreover the Raman spectrum showed that this new formate is a hydrated phase owing to the presence of peaks above 3100 cm<sup>-1</sup>, associated with the stretching vibrations of O-H, and the sharper peak at 3540 cm<sup>-1</sup> suggested that it contains a hydroxide group. The intense peak at 880 cm<sup>-1</sup> is striking; however its associated vibration could not be identified. Acetate and sulfate of generally sodium were also identified as minor phases in the sampled deposits from both museums. The peak positions in the Raman spectra of all the formate and acetate compounds characterised are given in **Appendix IV**. These results are consistent with the results obtained during the first investigation and confirm that all the unstable glasses as well as the glazed ceramics in the NMS collection were affected by the organic pollutants.

### III- 4. Artificial experiments

#### III- 1.1 Accelerated ageing experiments

After ageing the RG1 glass under accelerated conditions, the surface of the glass was generally covered with liquid droplets. After exposure to the ambient environment, this liquid deposit dried and crystallised (Figure III- 3).

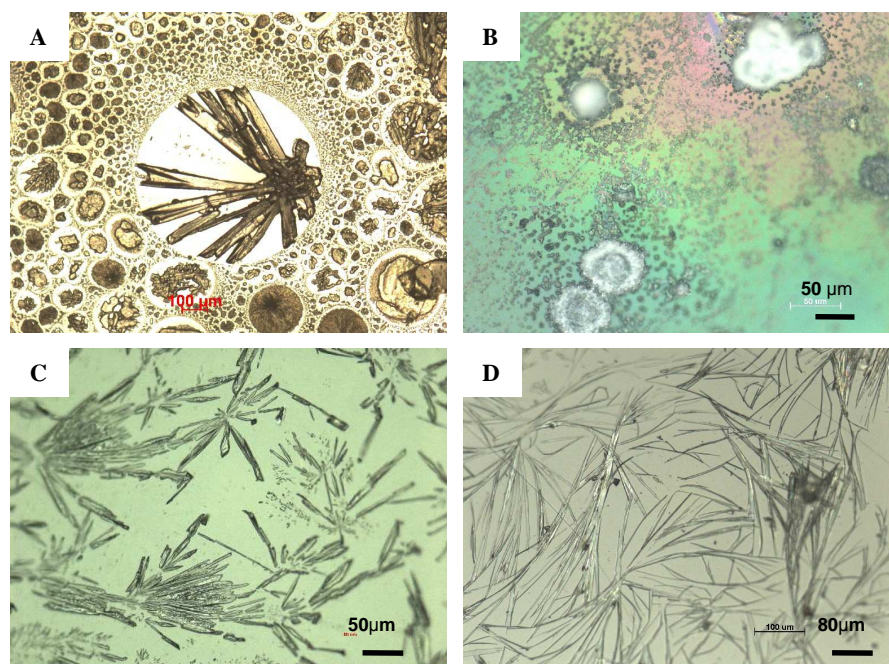


Figure III- 3: Image of RG1 glass surface after exposure to (A) formic acid, (B) formaldehyde, (C) acetic acid, (D) wood under 4 weeks accelerated ageing conditions and dried.

The Raman analyses of the crystals indicated that formic acid atmospheres induced the formation of sodium formate phase II and I'. The morphology of the crystals differed between the two phases with flat (hexagonal) crystals for the phase II and needle crystals for the phase I' (Figure III- 4). When the glass was exposed to formaldehyde vapour, crystals of sodium carbonate, sodium sulfate and sodium formate I' formed in isolated locations. The presence of acetic acid induced the formation of crystals of sodium acetate trihydrate. Finally when the soda silicate glass was exposed to the vapour emitted by a fragment of wood, both sodium acetate trihydrate and sodium formate phase II were formed.

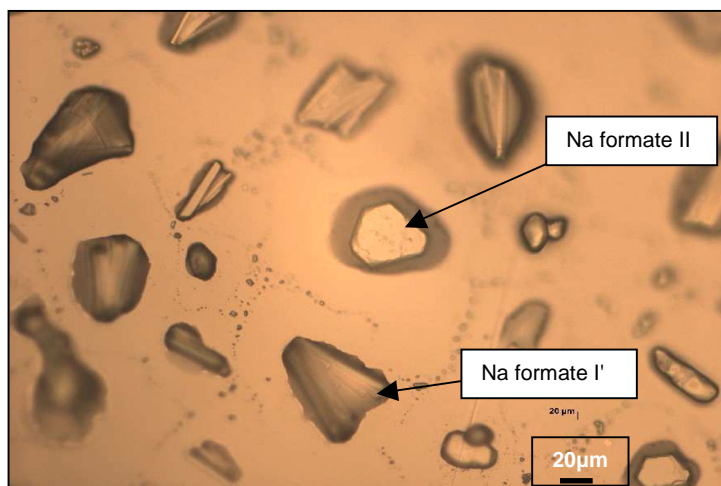


Figure III- 4: RG1 glass exposed to formic acid, 100 % RH, 60 °C, 4 weeks.

### III- 1.2 Ambient ageing experiments

In the ambient ageing experiments, the effect of single and mixed pollutants and the museum pollutants from the cabinets on the RG1 glass were examined. The crystals formed in single polluted atmosphere were similar to those found during the accelerated ageing experiments. However, discrepancies were observed in the mixed polluted atmospheres. Under an atmosphere of formic acid, flat crystals, filaments and needle-like crystals were formed (Figure III- 5). The flat crystals were identified as sodium formate II whilst needles were identified as sodium formate I'. The filaments often contained two phases, sodium formate I' and an unknown phase which Raman spectrum resembles that of *formate Y* observed earlier in the Corning paper weight object. The filaments were generally concentrated around the edges of the glass and appeared to transform into the needle crystals with time. The Raman spectra of the different phases are compared in Figure III- 6. In the formaldehyde atmosphere, it was necessary to expose the glass for a much longer period (~ 4 months) before crystals formed. The crystals which have a dendritic morphology were identified as sodium formate phase I'.

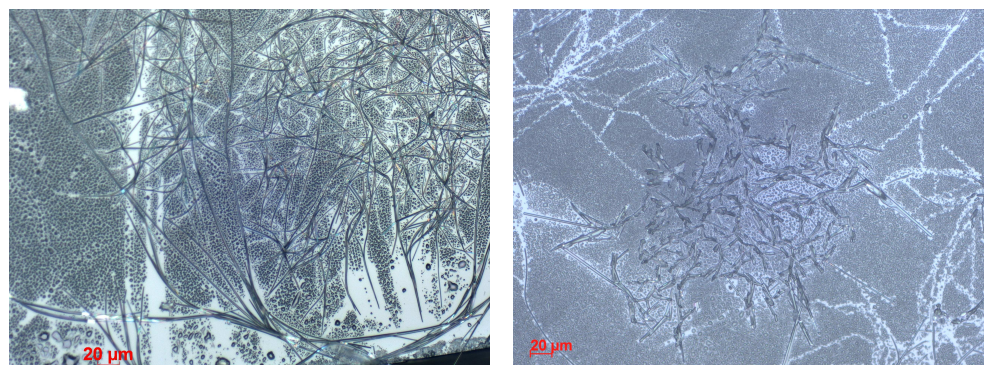


Figure III- 5: RG1 glass exposed to formic acid vapour, 48 % RH, 19 °C; (left) filament crystals, (right) needle crystals.

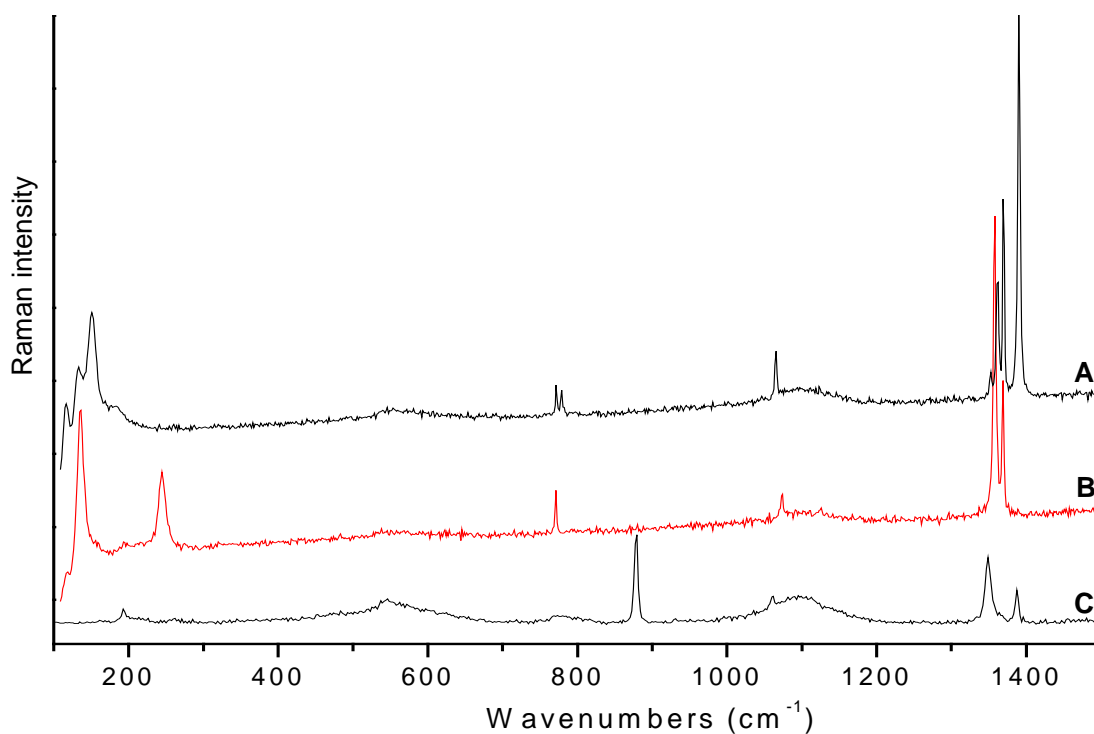


Figure III- 6: Raman spectra of sodium formate crystals formed on RG1 glass exposed to formic acid 48 % RH, 19 °C ; (A) phase I', (B) phase II, (C) formate Y.

When the glass was exposed to atmosphere of acetic acid, needle crystals of sodium acetate anhydrate were formed instead of the trihydrate phase found in highly humid atmosphere. However when the glasses were exposed to an atmosphere containing both acids, with more acetic than formic acid, or to the polluted cabinets atmosphere, only sodium formate phase II (major) and phase I' (minor) were formed. It was generally observed that sodium formate I' was present on glass exposed to RH below the deliquescence point of sodium formate (~52 %), while sodium formate II dominated on the glass exposed to RH over that point.

### III- 5. Sodium formate heating

In order to confirm the presence of sodium formate phase I' in the object deposit samples, the experiment undertaken by Heyns was repeated in the present study. A sample of sodium formate (phase II) was heated directly on the heating stage of an XRD instrument and the powder pattern was collected at different temperatures. The XRD analyses confirmed that a transformation occurred at high temperature, which was observed at 237 °C in this case (Figure III- 7). The powder pattern recorded at 237 °C and 247 °C correspond to phase I of sodium formate by reference to Masuda measurements [7]. The powder pattern obtained upon cooling indicates that a different phase was formed, the Raman spectrum (Figure III- 8) of which matched the spectrum of sodium formate phase I' recorded by Heyns [5, 6]. The same phase was obtained when molten sodium formate was rapidly cooled. The Raman spectrum of this phase matched the spectrum obtained on the museum objects (Figure III- 8), and strongly suggests that sodium formate phase I' is present on museum objects. However in both spectra, the presence of peaks at 135 and 245  $\text{cm}^{-1}$  indicates that some sodium formate phase II is also present.

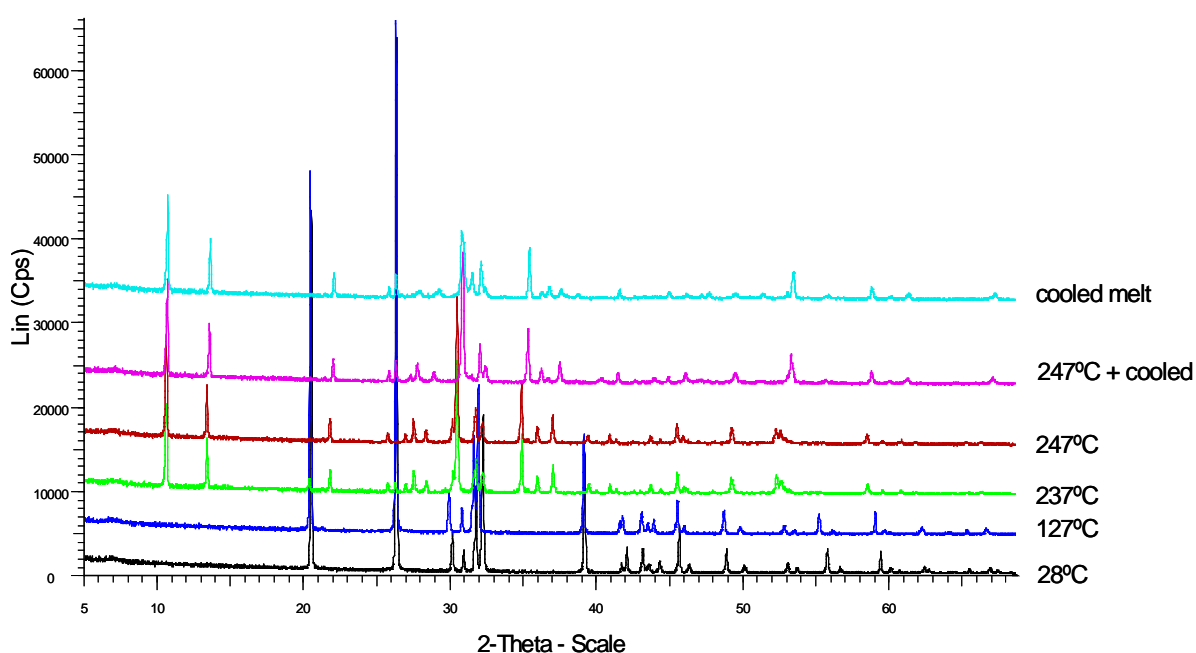


Figure III- 7: Powder pattern of sodium formate at increasing temperature and after cooling.

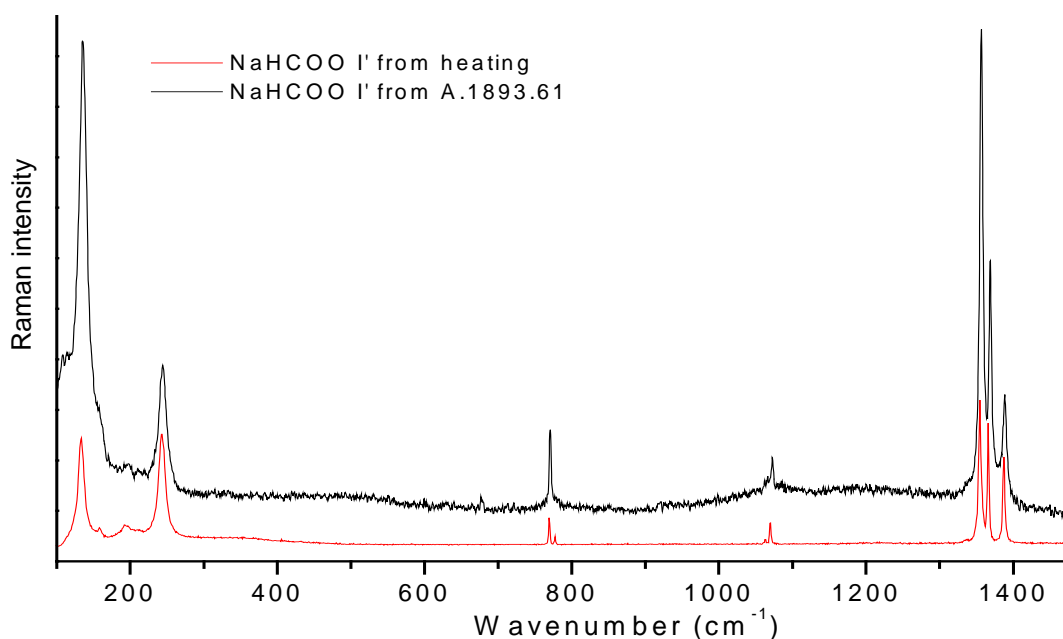


Figure III- 8: Raman spectra of sodium formate phase I' from heating and from museum object.

The sodium formate phase I', formed through this experiment, re-transformed back to the more stable phase II after several hours as observed by Heyns and Masuda [5, 6, 7]. Clearly the sodium formate phase I' on the museum objects has not experienced this temperature regime and has been formed in a different way at much lower temperature. The interconversion of metastable phases is often promoted by the presence of small amounts of seeds crystallites. It is therefore possible that in the heating experiment small quantities of the more stable phase II, evidenced from the Raman spectra, either persisted or were produced on cooling. Over time those acted as nucleation sites, and the humidity as a solvent, for conversion of phase I' to phase II. In the museum objects, phase I' has been formed under kinetic control by crystallisation from solution at much lower temperature. This results in regions of phase I' and phase II (Figure III- 4), but in the absence of solvent (H<sub>2</sub>O) these are isolated in space, thereby preventing interconversion of phase I' to phase II. Further support to this hypothesis comes from the observation that exposure to high RH causes dissolution of the sodium formates, and when the droplets are dried only phase II is observed. Consequently, the interconversion is mediated by the solvent, water, provided by the relative humidity.

### III- 6. Conclusion

This brief chapter confirmed that the alteration caused by organic pollutants emitted by the showcases and storage cabinets affects all unstable glasses in the NMS collection. The NMS is not the only museum concerned with this problem, which supports the need for this research. In both the NMS and the Corning Museum of Glass, formates were the major compounds present in the alteration products, indicating that formic acid and/or formaldehyde react predominantly with the glass. The presence of sodium formate phase I' in the objects deposits was confirmed and it was determined that its interconversion into sodium formate II is controlled by the relative humidity.

The crystals formed in the artificial atmospheres are consistent with the crystalline deposits present on the museum objects. The discrepancies observed between the accelerated and ambient ageing experiments for the mixed polluted atmospheres suggest that the competitiveness factor between the pollutants is affected by the increased temperature and/or RH conditions.

### III- 7. References

- 1 Robinet L., Eremin K., Cobo del Arco B., and Gibson L.T., A Raman spectroscopic study of pollution-induced glass deterioration, *J. Raman Spectrosc.* **8/9** (2004) 662.
- 2 Muller K., Range K.J., and Heyns A.M., Die Kristallstruktur von Natriumformiat-Dihydrat,  $\text{NaHCO}_2 \cdot 2\text{H}_2\text{O}$ , *Zeitschrift fuer Naturforschung, B: Chemical Sciences.* **9** (1994) 1179.
- 3 Heyns A.M., The effect of pressure on the Raman spectra of solids. III. Sodium formate,  $\text{NaHCOO}$ , *J. Chem. Phys.* **7** (1986) 3610.
- 4 Allan D.R., Marshall W.G., and C.R. Pulham, High-pressure studies of sodium formate dihydrate, unpublished results.
- 5 Heyns A.M., Van Niekerk O.T., Richter P.W., and Range K.J., The polymorphism of alkali metal formates-Part I. A Raman study of the II-I transition in  $\text{NaHCOO}$ , *J. Phys. Chem. Solids.* **10** (1988) 1133.
- 6 Heyns A M, and Range K.J., The polymorphism of alkali metal formates - Part II. A Raman spectroscopic study of the kinetics of the I'-II phase transition in  $\text{NaHCOO}$ , *Mat. Res. Bull.* **26** (1991) 589.
- 7 Masuda Y., Hashimoto K., and Ito Y., The thermal phase transformations of lithium, sodium and potassium formates, *Thermochim. Acta.* **163** (1990) 271.

## **Chapter IV.**

# **THE CHEMICAL STRUCTURE OF SODA SILICATE GLASSES**

## IV- 1. Introduction

The different techniques currently applied to examine the spatial distribution of atoms in glass are based on different types of interaction and provide different information. X-ray and neutron diffraction techniques give information about interatomic distances and bond angles. X-ray absorption techniques, such as EXAFS (X-ray Absorption Fine Structure) or XANES (X-ray Absorption Near Edge Structure), provide information on the coordination of each atom, while X-ray photo-electron spectroscopy (XPS) distinguishes BOs and NBOs in the structure. Solid state NMR provides information on the local coordination geometry of some elements in the structure such as  $^{29}\text{Si}$  or  $^{23}\text{Na}$ , while Raman and infrared spectroscopy inform about the concentration of non-bridging oxygens (associated with metal ions or as silanol groups), water and the discrete silicate ring.

For applications within a museum, Raman spectroscopy and FTIR are the most interesting techniques as they can be applied *in situ* and non-destructively to objects. The confocal system of the micro-Raman spectrometer allows *in-depth* measurements of transparent materials, suggesting that the bulk and the altered glass can both be analysed directly without contact. Moreover, glasses have been extensively studied by Raman spectroscopy and a lot of information is available concerning the interpretation of Raman data to glasses. For this reasons, we chose to use Raman spectroscopy for the examination of the glass structure in this investigation.

Raman spectroscopy was applied in this research for two purposes. First, we wished to assess the ability of the technique in distinguishing stable and unstable glass, based on objects from the NMS collections. Then, we examined the effect of the atmosphere on structural modifications of soda silicate glasses. This study was based on altered objects from the NMS collections, and replica glass aged in accelerated conditions. Accelerated ageing conditions were needed to obtain altered layers thick enough for Raman analyses in a reasonable time. The study concentrates solely on the structural modifications, characteristic of the alteration process, and does not consider the kinetics of the alteration which is affected by the elevated temperature. The kinetics is dealt in the next chapter based on glass samples aged under ambient conditions.

## IV- 2. Application of Raman spectroscopy to glass

Raman spectra of glasses generally display broad peaks owing to the distribution of local environments in the structure of these materials. The peaks in the spectra are associated with the vibration of the partially covalent bonds, essentially Si-O bonding in silicate glasses, and the structure of the silicate tetrahedra. The vibrational spectra reflect the degree of polymerisation of the glass, and the type of silicate species  $Q^n$ , influenced by their environment (surrounding cations).

The assignments of the vibrational components of the vitreous silica gave a basis for the interpretation of Raman spectra of glasses (Figure IV- 1). The three main regions and their assignments are as follow [1]:

- $430\text{ cm}^{-1}$ : Symmetric motion of the bridged oxygens in the plane bisecting the Si-O-Si bonds, with little associated silicon displacement (bending vibration).
- $800\text{ cm}^{-1}$ : Motion of silicon against its tetrahedral oxygen cage.
- $1060\text{-}1200\text{ cm}^{-1}$ : Bond stretching motions of oxygen relative to silicon, involving both silicon and oxygen displacements.

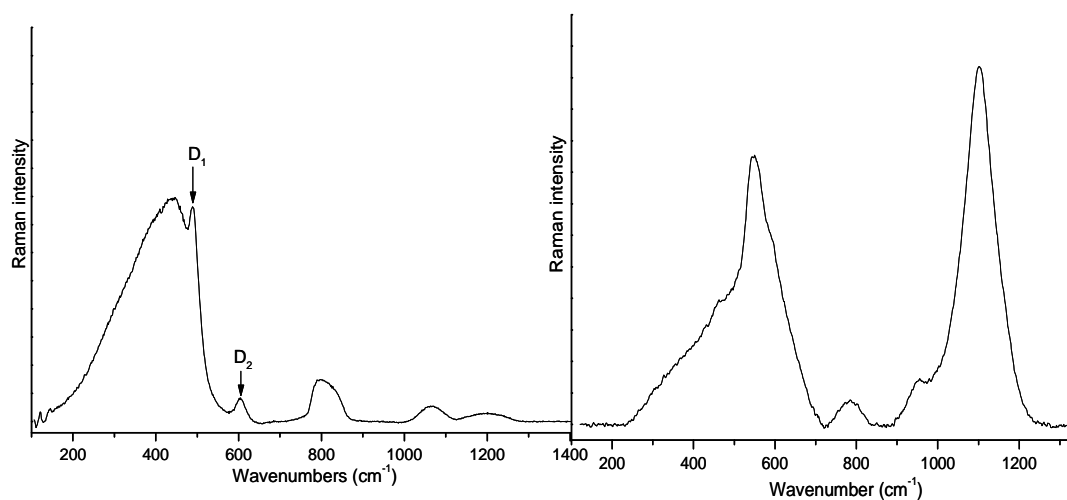


Figure IV- 1: Raman spectra of vitreous silica (left) and a soda silicate glass (right).

In addition, the spectrum of vitreous silica exhibits two narrow bands  $D_1$  and  $D_2$  at 490 and 607  $\text{cm}^{-1}$ , which are assigned respectively to silicate rings containing four and three silicon atoms (Figure IV- 2) [2, 3, 4, 5].

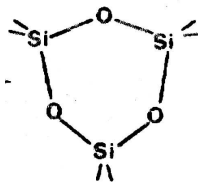


Figure IV- 2: Three-fold silicate ring giving  $D_2$  band.

The non-bridging oxygens (NBOs) created by the introduction of cations in the silicate structure greatly modify the structure and hence the Raman spectrum (Figure IV- 1). With a lower degree of polymerisation of the structure, the region between 900 and 1300  $\text{cm}^{-1}$  is more developed owing to the stretching vibration of species containing NBOs [6, 7, 8, 10]. Thus, in the spectra of alkali silicate glasses, the region between 300 and 600  $\text{cm}^{-1}$  is mostly associated with bending vibrations of the polymerised structure and the region between 900 and 1300  $\text{cm}^{-1}$  is associated with stretching vibrations of mostly depolymerised silicate species. The bands at 1100-1050, 1000-950, 900 and 850  $\text{cm}^{-1}$  are attributed respectively to the vibration of the species  $Q^3$ ,  $Q^2$ ,  $Q^1$  and  $Q^0$  (presented in chapter I) [6, 7, 8].

### IV- 3. Influence of the composition on the glass structure

It is important for museums to be able to distinguish between stable and unstable glasses, so particular care can be applied to the most sensitive objects. The literature as well as the examination of the NMS British glass collection (see chapter I) clearly showed that the degree of stability of the glass was directly linked to the composition. Since sampling of the glass objects is often difficult or impossible, we investigated the ability of Raman spectroscopy, which can be applied *in-situ* and non-destructively, to distinguish between stable and unstable glasses.

### IV- 3.1 Stability and composition

The composition of 61 glass samples taken mostly from NMS objects and a few modern glasses was measured by EPMA. Although, the concentrations of 23 elements commonly present in historic glass were measured by electron microprobe, the elements present at trace level (<0.01 at%) were assumed to have little effect on the structure and therefore were not considered in this study. Consequently, only 12 elements are examined and presented. The composition of the unstable glasses is presented in Table IV- 1 and the stable glasses in Table IV- 2.

Table IV- 1: Elemental composition (at%) of the unstable glasses measured by electron microprobe;  $X_a$ ,  $X_1$  and  $X_3$  calculation (see text).

At%	Si	Al	Na	K	Ca	Mg	Ba	Pb	Cu	Mn	Fe	O	$X_a$	$X_1$	$X_3$
<b>Alkali-Ca glass</b>															
Unreg 5	24.35	0.04	13.10	0.05	3.41	0.09	0.01	0.00	0.00	0.04	0.02	58.90	0.11	0.17	0.84
HMEN 209.401	24.67	0.03	12.40	0.07	3.46	0.07	0.00	0.00	0.00	0.04	0.02	59.23	0.11	0.17	0.80
HMEN 209.429	24.88	0.04	12.57	0.06	3.04	0.06	0.01	0.01	0.00	0.03	0.02	59.29	0.11	0.16	0.77
HMEN 98	24.46	0.03	12.92	0.03	3.43	0.05	0.02	0.00	0.00	0.04	0.02	59.00	0.11	0.17	0.82
HMEN 209.507	25.18	0.06	12.84	0.02	2.35	0.06	0.00	0.02	0.00	0.04	0.03	59.39	0.11	0.15	0.72
HMEN 215.45	26.35	0.15	11.35	0.03	1.64	0.03	0.00	0.00	0.00	0.07	0.02	60.37	0.09	0.13	0.58
A.1893.61	21.77	0.29	15.25	0.08	3.73	0.63	0.00	0.00	0.01	0.87	0.24	57.12	0.13	0.24	1.25
A.1893.63	22.51	0.32	15.06	0.12	3.35	0.62	0.01	0.01	0.02	0.21	0.24	57.54	0.13	0.22	1.11
A.1893.64	23.32	0.36	14.67	0.13	2.52	0.60	0.00	0.00	0.02	0.05	0.27	58.05	0.13	0.20	0.98
A.1893.65	23.56	0.37	14.42	0.14	2.34	0.59	0.01	0.00	0.03	0.06	0.24	58.23	0.13	0.19	0.94
A.1893.66	22.01	0.31	14.89	0.10	3.69	0.56	0.01	0.00	0.01	0.83	0.25	57.33	0.13	0.23	1.21
A.1893.67	22.52	0.32	15.20	0.11	3.27	0.62	0.00	0.01	0.04	0.18	0.24	57.51	0.13	0.22	1.11
A.1890.1372	21.58	0.28	13.51	1.63	2.39	2.54	0.02	0.01	0.01	0.67	0.28	57.07	0.13	0.24	1.29
A.1921.1385	23.03	0.28	14.63	0.26	2.69	0.91	0.00	0.00	0.03	0.10	0.20	57.86	0.13	0.20	1.03
A.1958.147	22.20	0.40	14.21	1.57	2.31	1.65	0.02	0.01	0.02	0.03	0.32	57.26	0.14	0.22	1.16
RG <sub>1</sub>	24.64	0.29	12.22	1.44	1.52	0.60	0.00	0.00	0.01	0.17	0.12	58.98	0.12	0.16	0.79
RRo	22.51	0.45	13.56	1.68	0.51	3.23	0.00	0.00	0.11	0.01	0.38	57.55	0.13	0.22	1.11
<b>Alkali-Pb glass</b>															
Unreg decanter	26.12	0.10	10.16	2.22	0.35	0.03	0.00	0.96	0.00	0.04	0.03	59.99	0.10	0.13	0.59
Unreg 3	26.64	0.08	9.72	2.07	0.28	0.02	0.00	0.70	0.00	0.06	0.05	60.39	0.10	0.12	0.53

The elemental analyses presented in Tables IV- 1 and IV- 2 show the presence of three main compositional groups among the 61 glasses examined, based on the main modifier in the glass: alkali silicate (54), calcium silicate (3) or lead silicate glasses (4). The majority of the glasses studied are alkali silicate, mainly soda-rich, with low-lime and a few with low-lead contents.

Table IV- 2: Elemental composition (at %) of the stable glasses measured by electron microprobe;  $X_a$ ,  $X_1$  and  $X_3$  calculation (see text); (Corning D has 0.67 at% phosphorus).

At %	Si	Al	Na	K	Ca	Mg	Ba	Pb	Cu	Mn	Fe	O	$X_a$	$X_1$	$X_3$
<b>Alkali-Ca glass</b>															
A.1890.360	20.74	0.59	11.55	1.09	4.88	2.82	0.01	0.03	0.13	0.34	0.48	57.36	0.11	0.28	1.53
A.1890.363	21.25	0.51	12.24	0.82	4.29	2.25	0.01	0.01	0.03	0.44	0.68	57.49	0.11	0.26	1.41
A.1890.366	20.90	0.37	13.06	1.45	3.92	2.84	0.00	0.00	0.00	0.21	0.32	56.92	0.13	0.27	1.45
A.1890.373	20.63	0.41	13.74	1.30	4.25	2.52	0.01	0.00	0.01	0.07	0.41	56.66	0.13	0.27	1.49
A.1890.375	21.77	0.25	13.69	1.43	2.85	2.32	0.01	0.00	0.01	0.23	0.26	57.17	0.13	0.24	1.25
A.1893.59	24.02	0.26	12.02	1.33	1.67	0.52	0.00	0.08	0.95	0.07	0.33	58.74	0.11	0.18	0.89
A.1895.266	23.91	0.42	10.51	1.58	3.67	0.26	0.01	0.10	0.01	0.30	0.19	59.04	0.10	0.19	0.94
A.1895.268	21.72	0.93	7.90	4.38	4.00	2.78	0.01	0.00	0.01	0.13	0.11	58.02	0.11	0.25	1.34
A.1895.271	21.17	0.45	12.81	1.02	4.29	2.26	0.01	0.01	0.02	0.35	0.36	57.24	0.12	0.26	1.41
A.1895.272	21.48	0.55	12.55	0.71	4.06	2.58	0.01	0.00	0.01	0.11	0.38	57.56	0.12	0.25	1.36
A.1895.284	22.73	0.62	11.43	0.31	4.86	0.53	0.01	0.00	0.03	0.21	0.69	58.58	0.10	0.22	1.16
A.1896.349	20.97	0.22	9.87	0.66	7.07	3.11	0.01	0.01	0.00	0.01	0.16	57.91	0.09	0.28	1.52
A.1906.441	20.92	0.61	14.27	1.59	3.28	2.08	0.01	0.00	0.00	0.03	0.54	56.65	0.14	0.26	1.41
A.1921.1371	22.47	0.21	12.39	1.27	2.90	2.39	0.01	0.01	0.02	0.24	0.23	57.87	0.12	0.22	1.15
A.1921.1373	20.88	0.43	13.90	0.87	3.64	2.64	0.01	0.01	0.03	0.40	0.32	56.85	0.13	0.27	1.45
A.1921.1374	22.22	0.31	13.15	1.29	2.71	2.04	0.01	0.01	0.02	0.23	0.43	57.58	0.13	0.23	1.18
A.1921.1375	20.82	0.58	11.44	1.18	4.28	2.48	0.04	0.03	0.03	1.23	0.48	57.40	0.11	0.27	1.51
A.1921.1376	20.61	0.43	13.90	1.00	3.62	2.80	0.02	0.01	0.02	0.44	0.47	56.69	0.13	0.27	1.50
A.1921.1377	21.35	0.10	10.71	0.77	5.50	3.35	0.01	0.00	0.00	0.34	0.04	57.83	0.10	0.26	1.42
A.1921.1378	20.86	0.46	13.89	1.21	3.78	2.60	0.01	0.00	0.01	0.06	0.36	56.77	0.13	0.27	1.44
A.1921.1379	23.14	0.20	10.76	2.76	3.66	0.36	0.01	0.45	0.00	0.26	0.17	58.24	0.12	0.21	1.03
A.1921.1380	21.55	0.33	13.60	1.28	3.21	2.54	0.01	0.00	0.01	0.08	0.25	57.14	0.13	0.25	1.30
A.1921.1381	22.09	0.41	11.05	1.93	3.47	2.72	0.00	0.00	0.01	0.03	0.38	57.90	0.11	0.24	1.24
A.1924.456	21.02	0.33	14.08	0.90	3.13	2.40	0.02	0.00	0.01	1.01	0.25	56.85	0.13	0.26	1.41
A.1929.88	21.63	0.47	11.32	1.81	3.99	2.60	0.01	0.00	0.01	0.05	0.45	57.65	0.11	0.25	1.33
A.1948.73	22.73	0.27	6.30	3.09	5.28	1.94	0.03	0.41	0.00	0.59	0.27	59.08	0.08	0.23	1.20
A.1959.74	21.87	0.41	10.58	1.12	4.75	2.79	0.01	0.00	0.01	0.11	0.24	58.11	0.10	0.25	1.31
A.1975.145	22.57	0.25	9.29	0.86	5.48	2.52	0.01	0.01	0.01	0.02	0.19	58.81	0.09	0.23	1.21
Corning B	21.45	1.03	12.09	0.45	4.85	0.82	0.02	0.07	1.12	0.11	0.14	57.85	0.11	0.26	1.39
Corning A	23.23	0.22	10.01	1.30	2.90	2.08	0.00	0.01	0.49	0.47	0.45	58.84	0.10	0.21	1.07
float glass	24.10	0.26	7.86	0.30	4.54	2.83	0.00	0.00	0.00	0.00	0.04	60.07	0.07	0.20	0.99
CL127	24.18	0.45	8.89	0.46	3.58	2.56	0.00	0.00	0.00	0.00	0.01	59.86	0.08	0.19	0.95
RRn	22.88	0.57	12.60	0.58	3.48	1.24	0.01	0.00	0.00	0.01	0.32	58.29	0.11	0.21	1.09
A.1888.89	26.04	0.15	1.08	6.92	4.48	0.11	0.01	0.00	0.00	0.10	0.06	61.06	0.07	0.15	0.69
1956.1233	25.11	0.14	0.47	7.55	4.92	1.09	0.00	0.00	0.01	0.08	0.04	60.58	0.07	0.17	0.83
<b>Calcium glass</b>															
A.1895.270	21.73	0.41	0.13	2.27	13.27	1.41	0.02	0.00	0.00	0.17	0.21	60.37			
A.1920.268	21.34	0.60	5.34	1.58	6.94	4.54	0.01	0.04	0.00	0.05	0.47	59.09			
Corning D	19.86	1.31	0.95	5.35	8.73	3.18	0.07	0.04	0.16	0.26	0.22	59.19			
<b>Lead glass</b>															
1998.492	26.12	0.04	0.47	5.41	0.04	0.01	0.01	6.24	0.02	0.02	0.02	61.60			
Flute	25.57	0.04	0.48	8.52	0.01	0.01	0.38	4.44	0.00	0.01	0.02	60.54			
HMEN 209.359	25.28	0.12	0.37	6.76	0.01	0.02	0.00	6.48	0.00	0.03	0.04	60.89			
HMEN 209.347	26.11	0.05	0.16	5.33	0.04	0.03	0.00	6.55	0.00	0.01	0.03	61.70			

All the glasses correspond to a trisilicate or disilicate composition. The lead silicate and calcium silicate glasses are all stable. In fact, all the unstable glasses belong to the alkali silicate group, generally having a high alkali and a low stabiliser contents ( $x_{Al} + x_{Ca} + x_{Mg} + x_{Ba}$  generally below 5 at%).

A general method based on the composition was sought to identify the stability of the glass. The best result was obtained by simply plotting the total alkali charge ( $X_a$ ) against the total non-Si cation charge ( $X_1$ ) for the alkali group with:

$$X_1 = [3x_{Al} + x_{Na} + x_K + 2(x_{Ca} + x_{Mg} + x_{Ba} + x_{Cu} + x_{Pb} + x_{Mn} + x_{Fe})] / (2x_O) \quad \{IV.1\}$$

$$\text{and } X_a = (x_{Na} + x_K) / 2x_O, \quad \{IV.2\}$$

with  $x_i$  corresponding to the atomic concentration (at%) of the element  $i$ .  $X_1$  and  $X_a$  calculation are given in Table IV- 1 and Table IV- 2. The graph presented in Figure IV- 3 displays a separate clustering between the stable and unstable glasses.

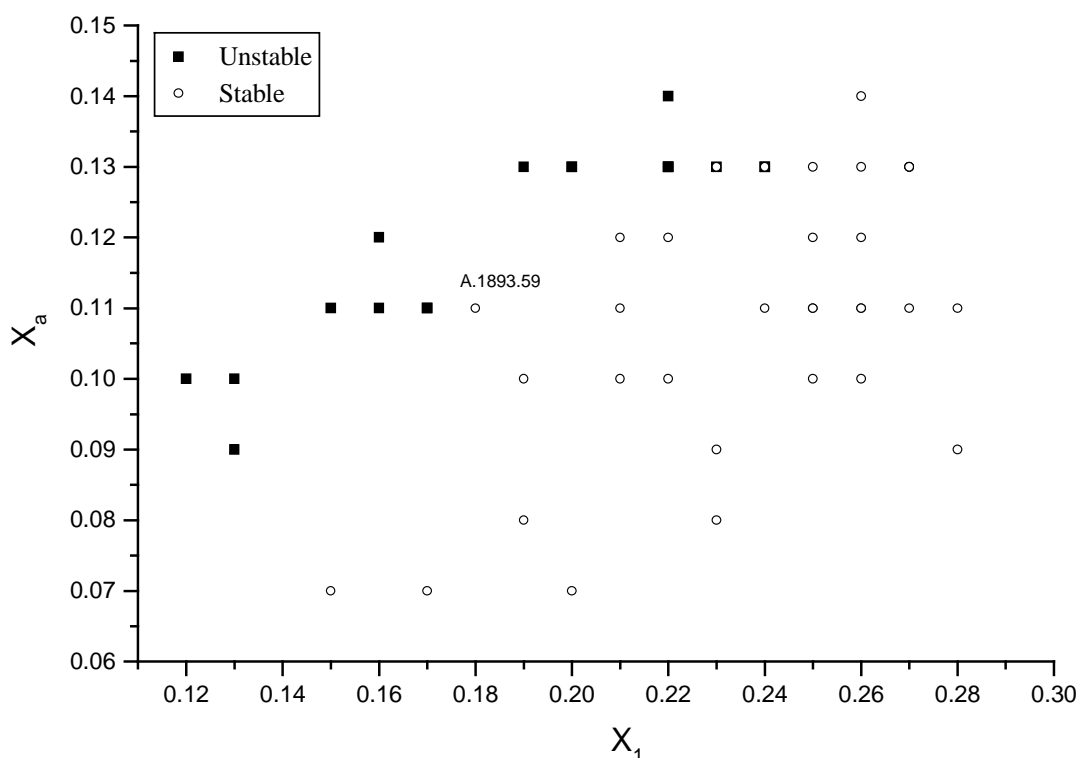


Figure IV- 3: Plot of the Na+K charge  $X_a = (x_{Na} + x_K) / 2x_O$  against the total non-Si cation charge  $X_1 = [3x_{Al} + x_{Na} + x_K + 2(x_{Ca} + x_{Mg} + x_{Ba} + x_{Cu} + x_{Pb} + x_{Mn} + x_{Fe})] / (2x_O)$

Although Mn and Fe can have different oxidation states in a glass, we choose to fix the oxidation state of these two elements at +2 in all this study for simplification, on the basis that these elements were present in very low concentrations. However, such simplification may not be suitable if higher concentrations of these elements are present in the glass. We note from the graph (Figure IV- 1) that we have an intermediate region of composition where the glass can be either stable or unstable. This is the case of A.1893.59 which does not display obvious signs of instability although its composition resembles an unstable glass. If a line is drawn between the two clusters in the graph, we see that in general, the unstable compositions lie close to or above the line  $X_a = 0.148 X_1 + 0.059$ , while all stable compositions lie well below this line. Consequently, in order to determine the stability of an alkali glass using this graph, we need to obtain the components  $X_a$  and  $X_1$ .

### **IV- 3.2 Raman spectra and composition**

Simply on the basis of their profile, the spectra of the glasses can be separated into three families, which correspond to the groups identified from the composition. This indicates that from the Raman spectra we can already separate alkali silicate glasses, which have a mixed stability, from the calcium and lead silicate glasses which are stable (Figure IV- 4). Within each group the differences in the spectra are less marked. Because the aim of this investigation is to assess the ability of Raman spectroscopy in distinguishing stable and unstable glass, from now on we will concentrate solely on the alkali silicate glass group that displays the mixed stability.

The Raman spectra of the alkali silicate glasses, that have a disilicate or trisilicate composition, is similar to the profile of the Raman spectra of binary alkali trisilicate and disilicate glasses [9, 10]. This composition implies the existence of three different types of silicate species joined into sheets:  $Q^3$  in major concentrations and  $Q^2$  and  $Q^4$  in minor concentration [10,11, 12].

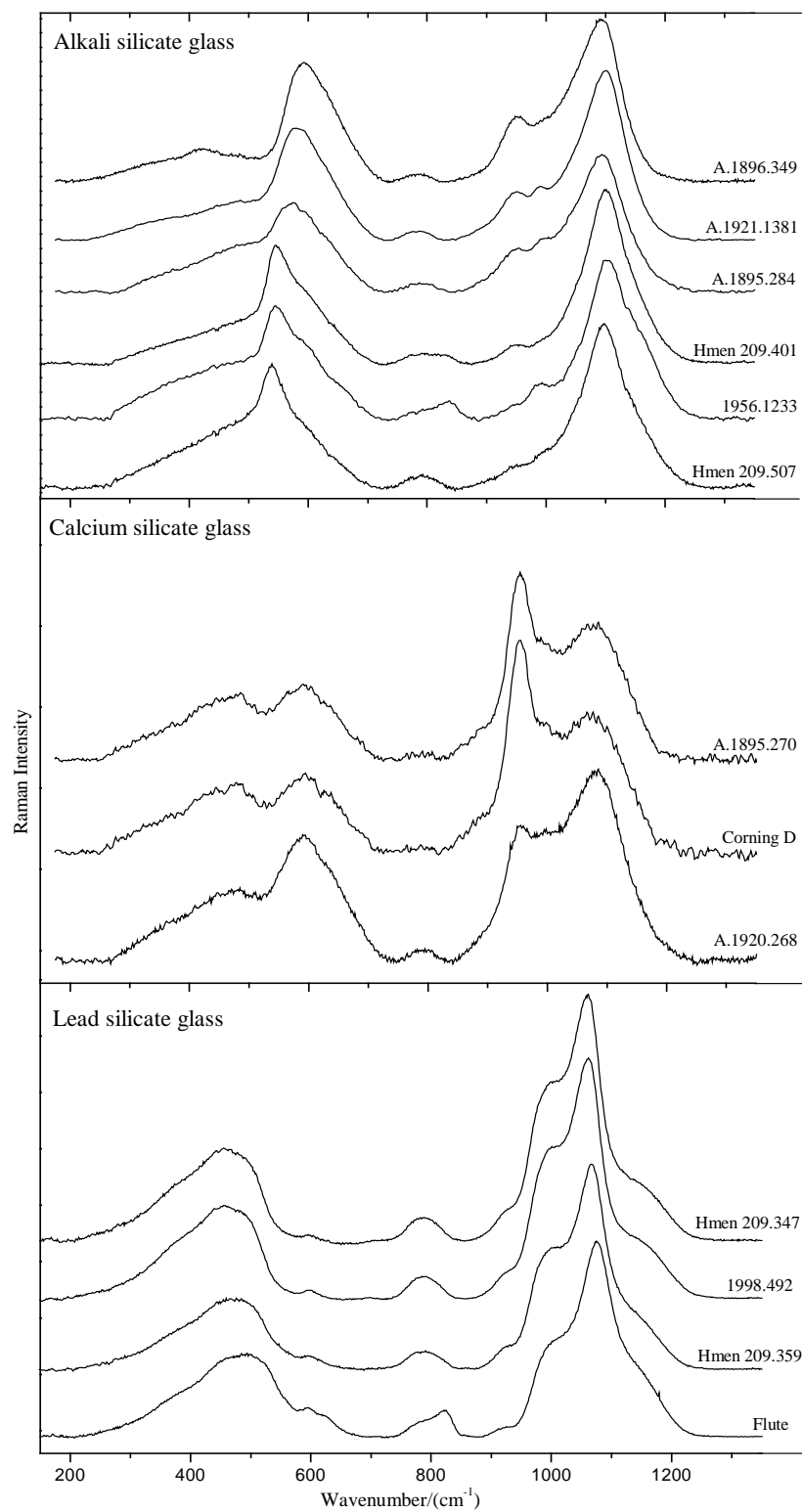


Figure IV- 4: Raman spectra of the different compositional groups: alkali silicate, calcium silicate, and lead silicate glasses.

In the Raman spectra (Figure IV- 4), the peak around  $1100\text{ cm}^{-1}$ , particularly intense in alkali silicate glass spectra, is associated with the symmetric Si-O stretching vibration of the major  $Q^3$  species [8, 10, 13]. The less intense band in the region  $900\text{-}1000\text{ cm}^{-1}$  is associated with the Si-O stretching vibration of  $Q^2$  species [10, 13]. The enhancement of peaks in this region is correlated with the increase in calcium content [14], as in calcium silicate glasses (Figure IV- 4). Fully polymerised silicates  $Q^4$ , corresponding to vitreous silica regions, display a weak Si-O stretching vibration around  $1150\text{ cm}^{-1}$ , superimposed onto the Si-O stretching vibration of a different type of  $Q^3$ , and Si-O-Si bending vibration bands between  $300\text{ and }500\text{ cm}^{-1}$  [10, 13, 14]. The peaks between  $500\text{-}700\text{ cm}^{-1}$ , in the spectra of soda silicate glasses, are assigned to Si-O-Si bending vibrations in depolymerised species, with the possible association of peaks near  $550\text{ cm}^{-1}$  with  $Q^3$  species and peaks near  $600\text{ cm}^{-1}$  with  $Q^2$  species [8, 13, 15].

If we look for the characteristic features induced by the presence of different elements, we note that the spectra of alkali silicate glass containing around 1 at% copper or lead present a relatively sharp band at  $988\text{ cm}^{-1}$ , as in Unreg decanter and A.1893.59 shown in Figure IV- 5 and Corning B glass (not shown). The sharpness of the band may indicate that copper and lead ions occupy well-defined coordination sites in the structure, in contrast to the other ions. Moreover, the similar ion charge and electronegativity of the two ions (see Appendix I) may explain their similar effect on the silicate structure.

The distinction between the spectra of potash-lime (1956.1233) and soda-lime glasses appears more difficult (Figure IV- 4). The distinction is even more difficult between the stable soda-lime (RRn) and the unstable soda-magnesium (RRo) glasses presented in Figure IV- 6. The first reason for this is that sodium and potassium, both alkali ions, are chemically very similar, as are the stabilisers calcium and magnesium. Although in the spectra of pure binary glasses, distinct differences, induced by the different alkali metal ions, can be observed [9, 7, 10], these differences cannot be distinguished easily in the case of more complex glasses. Ancient and historic glasses have complex compositions with many different cations present at varied concentration, each cation having an effect on the silicate structure and consequently on the Raman spectrum. All these effects are superimposed in the Raman spectra making interpretation more difficult. In order to investigate if Raman spectroscopy has the ability to distinguish between stable and unstable alkali glasses, a detailed analysis of the spectra, examining the different vibrational components is required.

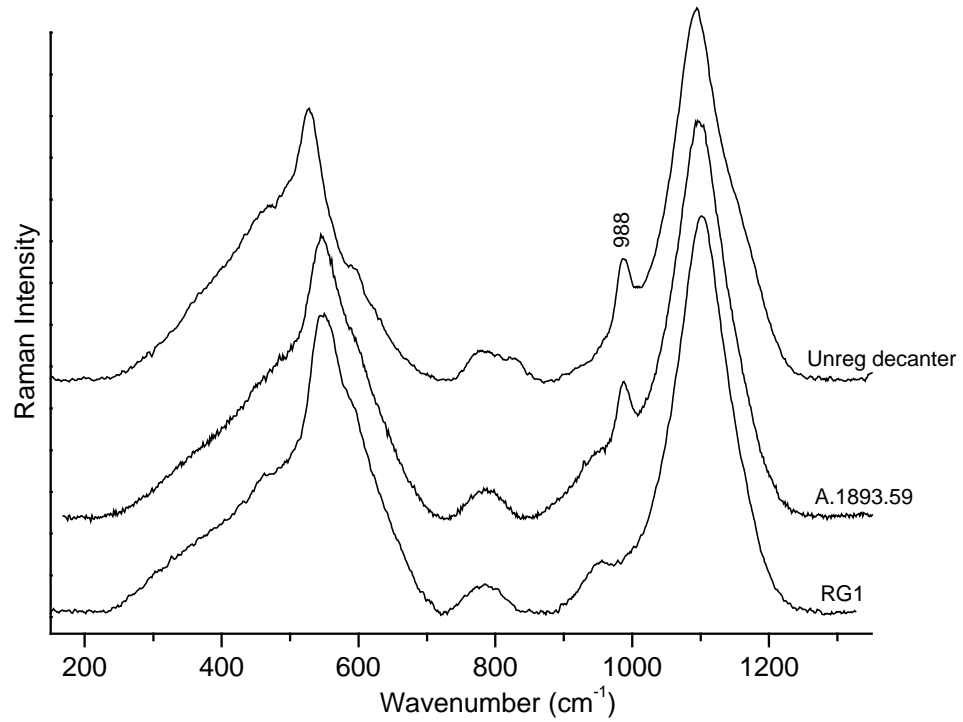


Figure IV- 5: Raman spectra of high-soda glass with low-lead (Unreg decanter), low-copper (A.1893.59) and low-calcium (RG1).

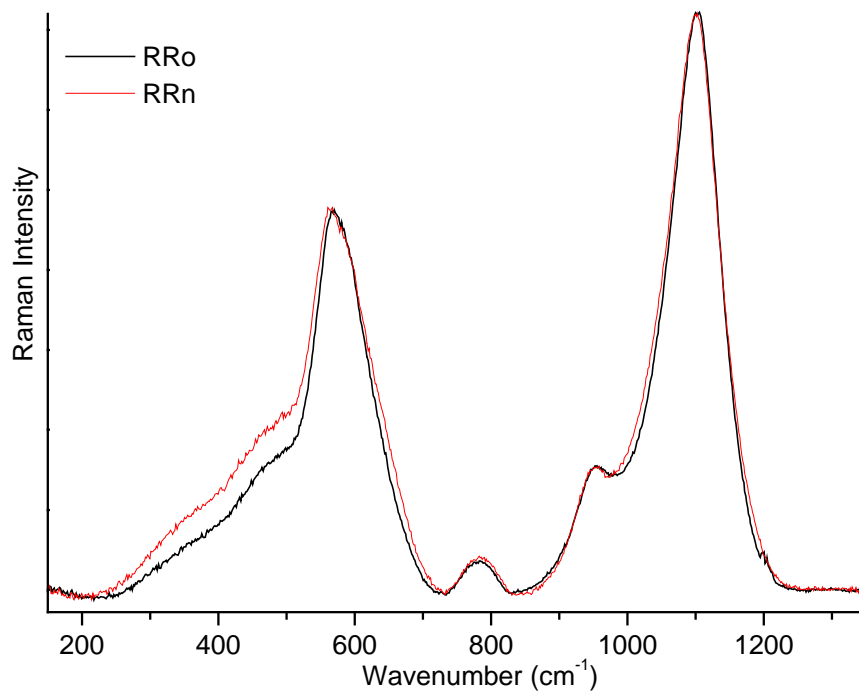


Figure IV- 6: Raman spectra of stable soda-lime (RRn) and unstable soda-magnesium (RRo) silicate glasses.

### IV- 3.3 Decomposition model

Since any variation in composition results in a variation in the Q species distribution, we decomposed the Raman spectra into their different vibrational components in order to examine these variations. It was obvious from the decomposition of the numerous spectra that each silicate species was not associated with only a single band but sometimes with two or three. This effect is probably linked to different ordering of the modifier cations around the silicate species.

The decomposition was undertaken into two stages. In the first stage, the Raman spectra between 150 and 1350  $\text{cm}^{-1}$  of all the alkali silicate glasses were decomposed independently to provide the best fit with the minimum number of components. The components obtained were then compared and a set of components appearing in all decompositions was identified. All spectra were then decomposed again, this time, applying the same set of bands (13 in total) to all the spectra. The frequency and width was fixed for bands in the stretching region (see Table IV- 3) in which very little frequency shift was visible with the change in composition. In contrast, the frequency and width of the bands in the bending region are very sensitive to the compositional variation. In particular, the position of the band between 400 and 600  $\text{cm}^{-1}$  is influenced by the average angle of Si-O-Si. Matson indicated that a shift towards higher frequency of the band is associated with a decrease of the Si-O-Si angle [6, 10, 16].

The decomposition model established for alkali silicate glass spectra is presented in Table IV- 3. The components in brackets were applied but disappeared due to their weak intensity and/or superposition with adjacent components. Two examples of spectra decomposition are presented in Figure IV- 7. The fit obtained for the high frequency region presents the same bands as those used by Mysen for alkali silicate glasses [8], with the difference of two additional components at 895-910 and 990  $\text{cm}^{-1}$ , assigned to the Si-O stretching of Q<sup>2</sup> species.

Table IV- 3: Decomposition model for alkali silicate glasses; underlined= values fixed; in bracket= components that sometimes vanished due to band superposition;  $\delta$ = bending;  $\nu$ = stretching.

Frequency ( $\text{cm}^{-1}$ )	Bandwidth ( $\text{cm}^{-1}$ )	Assignment suggested
330-380	-	$\delta$ Si-O-Si $Q^4$
460-500	-	$\delta$ Si-O-Si $Q^4$
540-590 ( $B_{550}$ )	-	$\delta$ Si-O-Si depolymerised
580-640	-	$\delta$ Si-O-Si depolymerised
(640-690)	-	
770-800	-	Si motion in tetrahedral oxygen cage
(800-830)	-	
(895-910)	-	$\nu$ Si-O $Q^2$
<u>950</u>	<u>50</u>	$\nu$ Si-O $Q^2$
<u>990</u>	<u>33</u>	$\nu$ Si-O $Q^2$
<u>1040</u>	<u>70</u>	
1100	<u>65</u>	$\nu$ Si-O $Q^3$
<u>1150</u>	-	$\nu$ Si-O $Q^4$ + $\nu$ Si-O $Q^3$

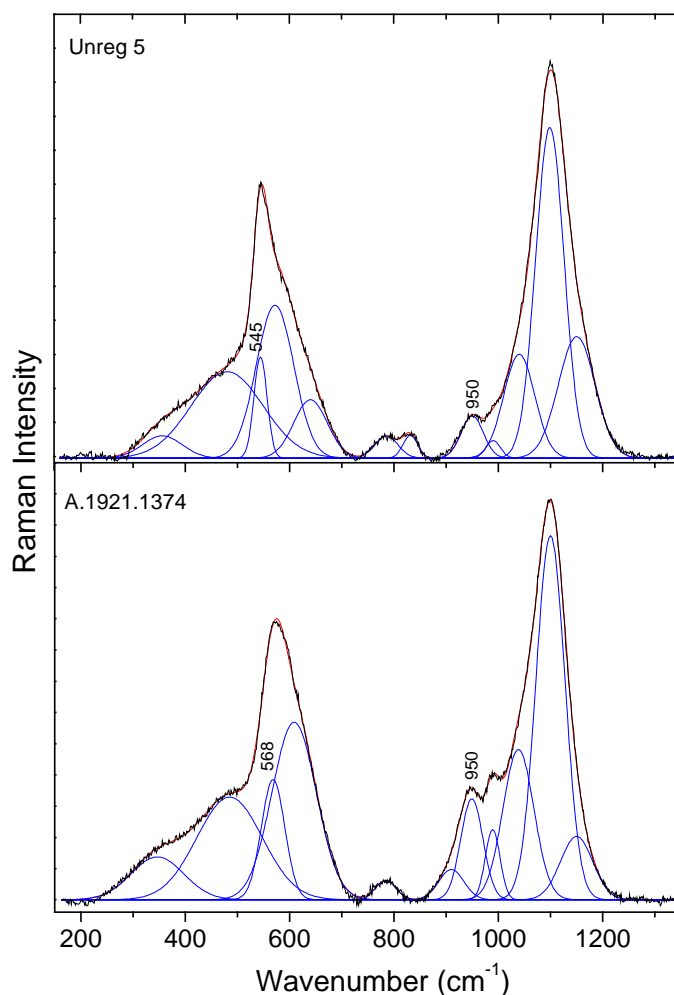


Figure IV- 7: Spectral decomposition of alkali silicate glasses based on model in Table IV- 3.

#### IV- 3.4 Composition correlations with Raman spectra

Our results show that two significant correlations can be established between the spectral components and the composition. The first correlation concerns the component around  $550\text{ cm}^{-1}$ , here named  $B_{550}$ . The results indicate that the position of this narrow band is directly linked to the  $\text{SiO}_2$  content of the glass and consequently the total amount of charge from the modifier cations in the structure. As the number of cations increases, the band shifts towards higher frequencies. This shift, which corresponds to a decrease in the average Si-O-Si angle, correlates with the increased steric effect produced by the cations. This phenomenon was previously observed with the increase of the alkali content in binary alkali silicate glasses [7, 10]. Matson noted that the type of alkali cation present determined the magnitude of the frequency shift, with smaller cations producing larger effects [10]. We show, for historic glasses, that a correlation can be established between the position of  $B_{550}$  and the  $\text{SiO}_2$  content (Figure IV- 8).

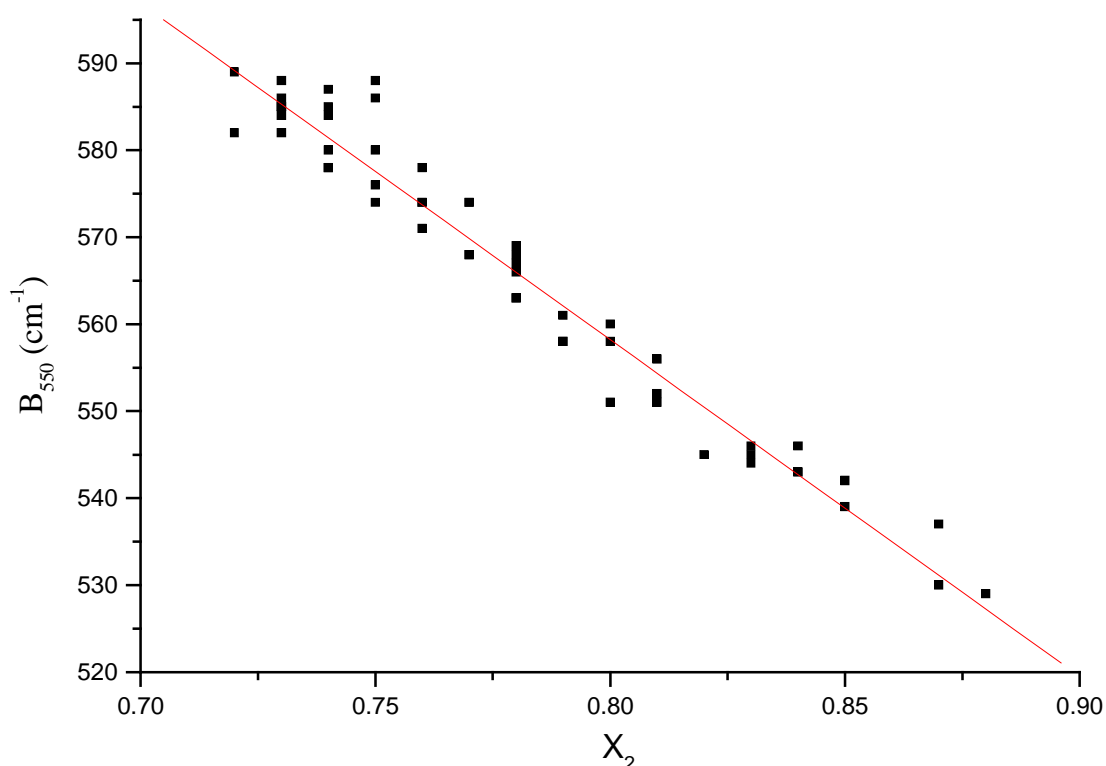


Figure IV- 8: Correlation between frequency of  $B_{550}$  ( $\text{cm}^{-1}$ ) and  $\text{SiO}_2$  content  $X_2 = 2x_{\text{Si}} / x_{\text{O}}$ .

The  $\text{SiO}_2$  content is calculated by  $X_2 = 2x_{\text{Si}}/x_{\text{O}}$ . Consequently, when  $X_2 = 1$ , the structure corresponds to pure silica,  $\text{SiO}_2$ . The band shift is directly correlated to the total non-Si cation charge ( $X_1$ ) defined as  $X_1 = 1 - 2x_{\text{Si}}/x_{\text{O}}$ . The data in the graph (Figure IV- 8) have been fitted to a regression equation below with  $B_{550}$  in  $\text{cm}^{-1}$ :

$$B_{550} = -387 X_2 + 868 \quad (R^2 = 0.978) \quad \text{\{IV.3\}}$$

From this, we can see by extrapolation that in pure silica, when  $X_2 = 1$ , the band should appear at  $B_{550} = 481 \text{ cm}^{-1}$ . Since the position of  $B_{550}$  is directly correlated to the  $\text{SiO}_2$  content, it is then linked to the degree of polymerisation (or depolymerisation) of alkali silicate glass. Previous studies have employed the  $A_{500}/A_{1000}$  area ratio to compare the degree of polymerisation of glass [17]. The  $A_{500}/A_{1000}$  method is valuable for comparison of glasses with very different compositions often belonging to different compositional group. However, this method is not applicable to compare objects that belong to the same compositional group and show only small compositional differences, as in the present study. Consequently, the method based on the position of  $B_{550}$  is more accurate for determination and comparison of the degree of polymerisation within a group of alkali silicate glasses. It would be interesting to investigate if this method can be extended to other types of silicate glasses. Although the degree of polymerisation has an influence on the stability of the glass, the type of cation influencing the degree of depolymerisation is the determining factor. Thus, the ability of Raman spectroscopy to determine the ratio alkali content: stabiliser content is investigated.

A second correlation was established between the  $950 \text{ cm}^{-1}$  component and the total charge associated with cations coordinated to silicate with 2 NBOs ( $Q^2$ ). We noticed that by using the ratio of the areas of the bands at  $950$  and  $1040 \text{ cm}^{-1}$  we could follow the intensity change of the  $950 \text{ cm}^{-1}$  component with elemental composition. The assignment of the band at  $1040 \text{ cm}^{-1}$  is still controversial and is currently assigned to the stretching vibration of bridging Si-O bonds in silicate species that are not fully polymerised [8]. Figure IV- 9 displays the area ratio of the bands  $A_{950}/A_{1040}$  as a function of the total cation charge per silicon ( $X_3$  calculation given in Table IV- 1 and Table IV- 2):

$$X_3 = [3x_{\text{Al}} + x_{\text{Na}} + x_{\text{K}} + 2(x_{\text{Ca}} + x_{\text{Mg}} + x_{\text{Ba}} + x_{\text{Cu}} + x_{\text{Pb}} + x_{\text{Mn}} + x_{\text{Fe}})]/x_{\text{Si}} \quad \text{\{IV.4\}}$$

The regression equation obtained for this correlation is:

$$A_{950}/A_{1040} = 0.43 X_3 - 0.03 \quad (R^2 = 0.953) \quad \text{\{IV.5\}}$$

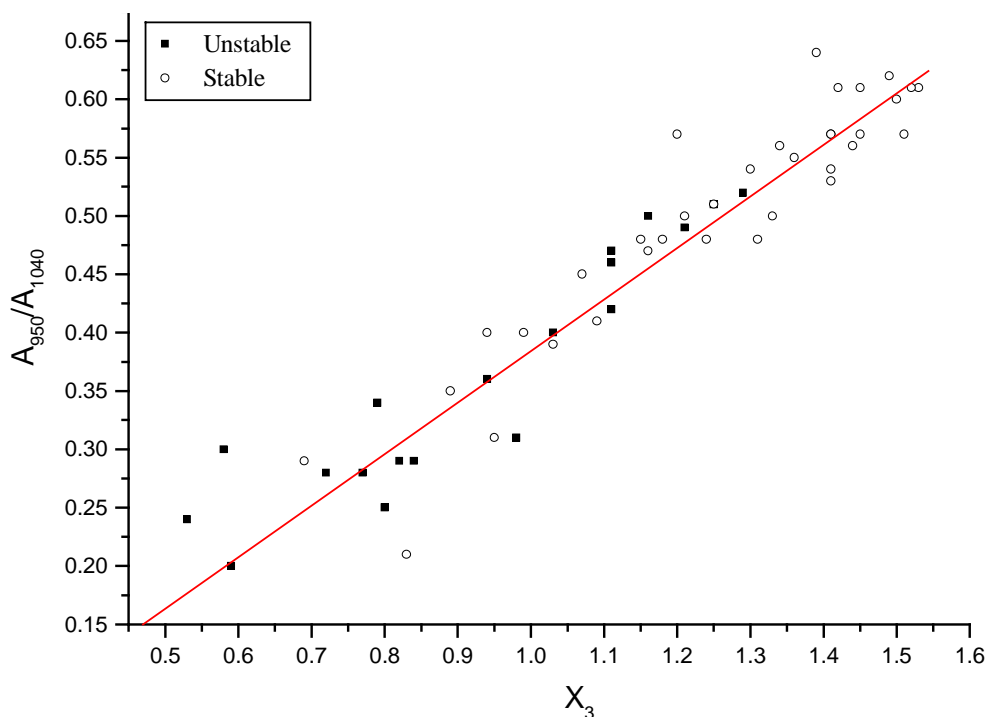


Figure IV- 9: Correlation between  $A_{950}/A_{1040}$  and the total cation charge per silicon  $X_3 = [3X_{Al} + X_{Na} + X_K + 2(X_{Ca} + X_{Mg} + X_{Ba} + X_{Cu} + X_{Pb} + X_{Mn} + X_{Fe})]/X_{Si}$

No marked separation between the unstable and stable glasses was visible. Both correlations {IV.3} and {IV.5} were remarkably strong and showed that these features of the Raman spectra are controlled by the total non-Si cation charge. Such high correlations were not found when plotting the Raman component with specific elements or families of elements. Both equations showed that the intensity of the band, or magnitude of the shift, is mainly influenced by the content of doubly and triply charged cations, i.e. the stabilisers. However, the alkali content still has an impact on the intensity of this band due to their high content in the glass. Consequently, it did not appear possible to extract the values  $X_a$  and  $X_1$  from the Raman bands in order to establish the stability of the glass using Figure IV- 3.

We found, however, that another feature in the Raman spectra may provide a valuable diagnostic tool for assessing stability. It is based on the observation that stabilisers favour the formation of  $Q^2$  species. In this method, we examined the proportion of  $Q^2$  species in the silicate species based on the stretching region, and compared it to the proportion of charge from the stabiliser cations in the total charge from the cations. In that case, all cations except silicon and alkalis were considered as stabilisers. We then plotted  $(A_{900} + A_{950} + A_{990})/(A_{900-1150})$ , called  $\nu Q^2/stretch$  for simplification, against  $(X_1 - X_a)/X_1$  (Figure IV- 10).

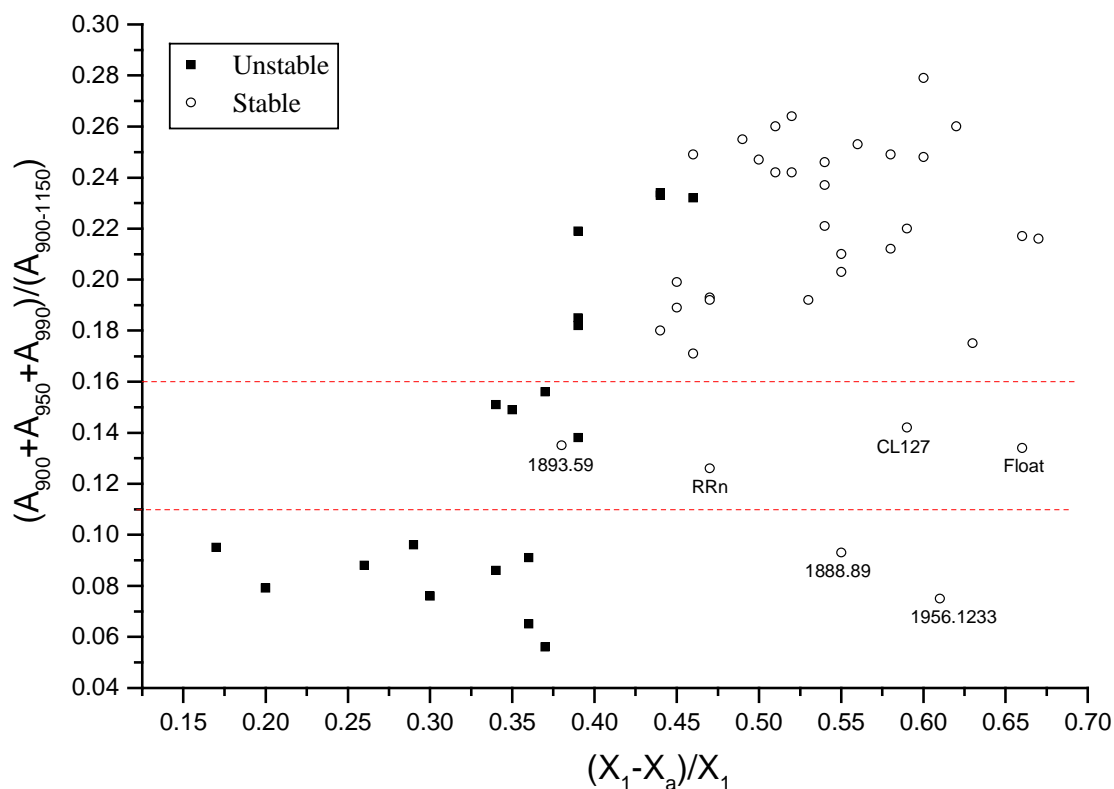


Figure IV- 10: Plot of the area ratio  $\nu Q^2/stretch$  region  $(A_{900}+A_{950}+A_{990})/(A_{900-1150})$  as a function of stabiliser charge content to the total cations charge  $(X_1-X_a)/X_1$ .

The graph shows a clear clustering between unstable and stable glasses as a function of the composition ratio, with almost all unstable glasses located below  $(X_1-X_a)/X_1 < 0.4$ . However the aim of this study is to investigate if Raman spectroscopy has the ability to make this distinction. The separation as a function of the Raman parameters is not complete, but the unstable glasses are generally gathered in the low  $\nu Q^2/stretch$  region. We note that a few stable glasses are present in the low  $\nu Q^2/stretch$  region. Among them are the two potash silicate glasses (1888.89 and 1956.1233), which indicates that potassium induces less  $Q^2$  species than sodium ions, as expected. Two modern stable glasses (Float glass and CL127) are also present in this region due to their low alkali content. Finally, two glasses (1893.59 and RRn), recorded as stable, but with elemental compositions resembling the unstable glasses, are situated in this region. This may indicate that although no visible sign of alteration were observed, these two glasses have an unstable composition and may show sign of decay at a later stage. The few unstable glass present in the high  $\nu Q^2/stretch$  region belong to the intermediate region of composition, described before, where the glass can be either stable or unstable.

Although, the method should be tested further on a larger set of composition, the present results suggest that soda silicate glass with  $\nu Q^2/stretch < 0.11$  are very unstable and glasses with  $0.11 < \nu Q^2/stretch < 0.16$  are likely to be unstable (Figure IV- 10). Currently it is not possible to predict the stability of a glass with a composition in the intermediate region. However, this method will allow museums to identify easily the very unstable, hence most sensitive, soda silicate glass objects so that these can be cared for specially. We expect that a similar method could be designed for potash silicate glasses.

## IV- 4. Structure modification with alteration

There have been a few studies that applied Raman spectroscopy to examine the effect of either solution leaching or hydration on the structure of simple binary or ternary glass compositions [3, 18, 19, 20, 21, 22, 23, 24, 25, 26, 27, 28, 29]. All showed important changes between the altered and the original glass spectra in the region between  $450\text{ cm}^{-1}$  and  $1100\text{ cm}^{-1}$ . By combining Raman spectroscopy and solid state  $^{29}\text{Si}$  NMR, Bunker noted that the leaching of alkali silicate and borosilicate glasses causes the decrease or disappearance of the depolymerised structure coordinated to the metal cations (disappearance of NBO sites) and the formation of silanols and molecular water in the structure [19]. The two techniques also revealed that polymerisation of the silanols in the hydrosilicate structure created new Si-O-Si linkages and, in the case of an acid leachant, four-fold silicate rings ( $D_1$ ) [12, 20, 19, 30]. In the case of hydration of sodium silicate glass, where water is introduced without removal of any element, the Raman spectra display a shift of the major bands [23]. These shifts were attributed to a decrease in the average Si-O-Si angle accompanied by a decrease in the average polymerisation of the silicate unit of the structure [23].

Compared with simple binary glasses, historic glasses are complex systems, containing a mixture of cations to modify the properties of the glass. As explained in chapter I, the alteration process, and so the altered layer, are influenced by the composition both of the glass and of the solution.

In this part of the chapter, micro-Raman spectroscopy supported by EPMA and SEM-EDS is used to examine the impact of organic pollutants on the structure of soda silicate glass in the following ways;

- (i) through the examination of two historic glass objects from the NMS collections, stored over several decades in the wooden cabinets;
- (ii) from replica glass aged in accelerated conditions.
- (iii) Finally, non-destructively determination by Raman spectroscopy and SEM-EDS of the cause of the alteration is assessed on two NMS objects.

## IV- 4.1 Museum objects

### IV- 4.1.1 British decanter

The British glass decanter (unregistered) was heavily cracked as shown by optical microscopy images (Figure IV- 11) and SEM images of a cross section and the surface of the glass (Figure IV- 12). The surface was no longer smooth as scales were detached from the surface leading to the occurrence of iridescence and sometimes flaking. The crystalline products present under the altered glass (Figure IV- 11B) might be partly responsible for this effect. In the SEM image of the cross section, the altered layer corresponds to the dark grey region and has a thickness of about 37  $\mu\text{m}$  (Figure IV- 12A). We noted from the cross section the formation of cracks parallel to the surface far into the bulk glass ( $\sim 80\mu\text{m}$ ).

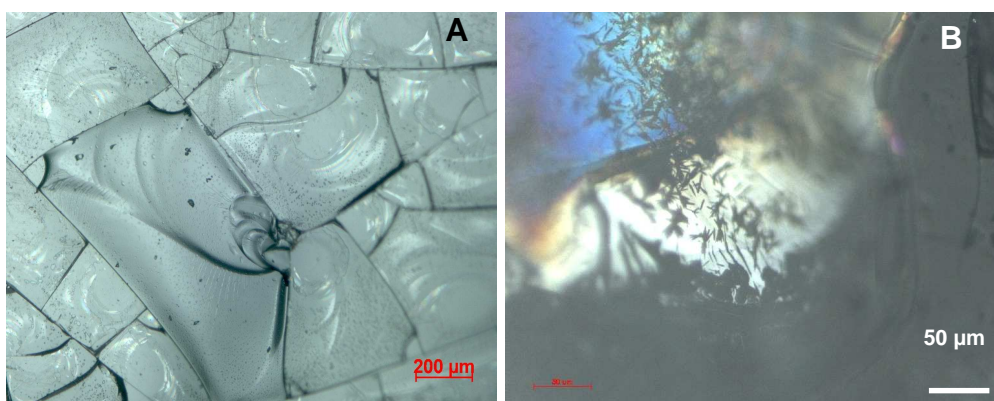


Figure IV- 11: Light microscopy image of the decanter surface (A) and underneath the surface (B).

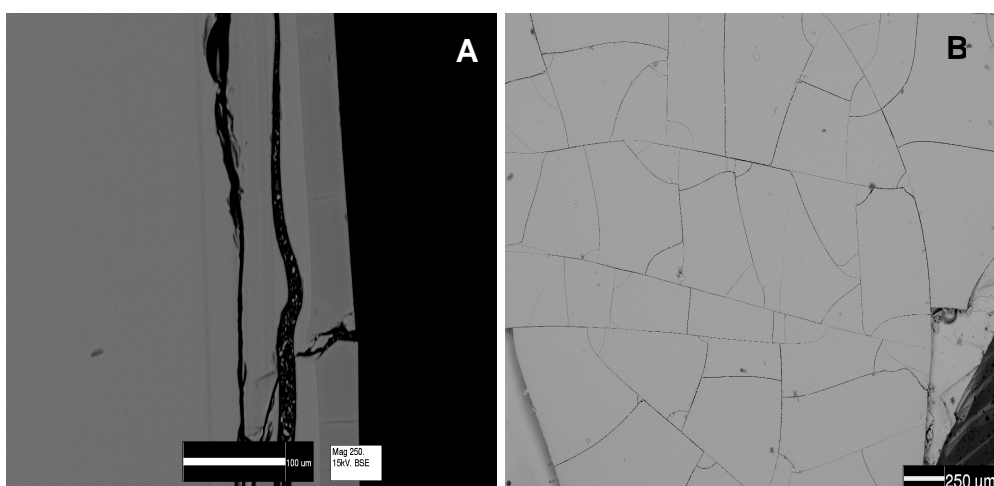


Figure IV- 12: SEM images of the decanter glass: cross section (A) and surface (B).

Table IV- 4: Elemental composition (at%) of altered and bulk regions of the decanter glass measured by EPMA. H content of the altered region measured by SIMS ( $\pm 1.5$  at%).

At %	Si	Al	Na	K	Ca	Mg	Pb	Mn	Fe	O	H
bulk	26.12	0.10	10.16	2.22	0.35	0.03	0.96	0.04	0.03	59.99	-
altered	24.07	0.08	1.01	0.88	0.32	0.02	0.94	0.08	0.04	57.93	14.63

The bulk glass of the decanter has a high-soda silicate composition with minor amounts of potassium and lead (Table IV- 4). The composition of the altered layer indicated almost complete depletion of the sodium and potassium within this layer (from 10.16 to 1.01 at% of Na and 2.22 to 0.88 at% of K) and the presence of high concentration of hydrogen species. However, the lead and calcium contents remained constant ( $\sim 0.95$  at% Pb and  $\sim 0.35$  at% Ca) suggesting that these ions have not been leached. Consequently, these results indicated that selective leaching of alkali cations has taken place.

The comparison of the Raman spectra of the bulk and altered region of the decanter (Figure IV- 13) indicated that significant modification of the structure has occurred. Interestingly, the spectrum of the altered layer is close to that of vitreous silica  $\text{SiO}_2$  (Figure IV- 13) which suggested that the structure became more polymerised on alteration. Bunker made similar observations for binary soda silicate glass [19]. However, compared to vitreous silica, the spectrum of the altered layer has additional bands in the region near  $1000 \text{ cm}^{-1}$ .

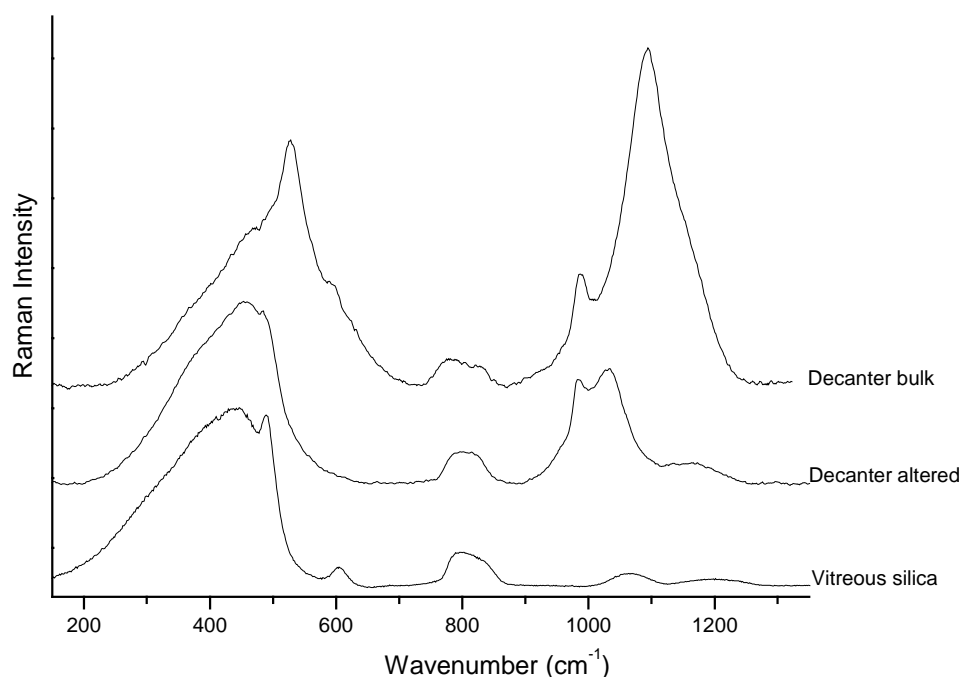


Figure IV- 13: Comparison of the Raman spectra of the British decanter glass, bulk and altered, and of vitreous silica.

These bands, and in particular the sharp band around  $990\text{ cm}^{-1}$ , were present in the original glass spectra and from the first part of this investigation were thought to be associated with the presence of lead. This hypothesis was supported by the elemental analyses, which indicated that lead ions remained in the altered glass structure. Consequently, lead ions and the silicate species to which these are coordinated (giving the sharp band around  $990\text{ cm}^{-1}$ ) were not affected by alteration and so retain their place in the structure.

Comparison of the vibrational components of the altered and bulk glass spectra, obtained through curve-fitting, indicated almost complete disappearance of the components at  $529$ ,  $573$  and  $1092\text{ cm}^{-1}$  and a significant decrease of the component at  $1150\text{ cm}^{-1}$  (Figure IV- 14, Table IV- 5). The component at  $1092\text{ cm}^{-1}$  is associated with the Si-O stretching vibration of  $Q^3$  species, which dominated in the alkali glasses studied [8, 10]. The bands at  $529\text{ cm}^{-1}$  and at  $573\text{ cm}^{-1}$  were assigned to the Si-O-Si bending vibrations in depolymerised species, mainly  $Q^3$ . As described in the first part of this investigation, the position of these bands is influenced by the Si-O-Si average angle and the cation content of the glass. The disappearance or decrease of the depolymerised species, mostly  $Q^3$  species, was directly associated with the leaching of alkali ions out of the structure.

In the case of a leaching reaction, silanol species were created to compensate for the removal of sodium in the structure. In the high frequency range ( $3000$ - $3700\text{ cm}^{-1}$ ), the spectrum of the altered glass displayed a broad band assigned to the stretching of O-H species (Figure IV- 15), which was absent in the bulk glass spectrum. The best curve-fit for the band was obtained using 7 Gaussian components, two more bands than was used by Holtz for the curve-fitting of hydrated silicates [29]. These components were associated with the vibration of OH in molecular water ( $3000$  to  $3450$ - $3550\text{ cm}^{-1}$ ) and hydroxyl groups such as silanols ( $3450$ - $3550$  to  $3700\text{ cm}^{-1}$ ) [23, 27, 29]. Hydrogen bonding with these species induced a broadening and shift of the bands towards lower frequency in this region [23, 31]. The sharp component observed at  $3598\text{ cm}^{-1}$  was assigned to a different type of SiO-H hydroxyl group present in hydrous glass with high water content [23].

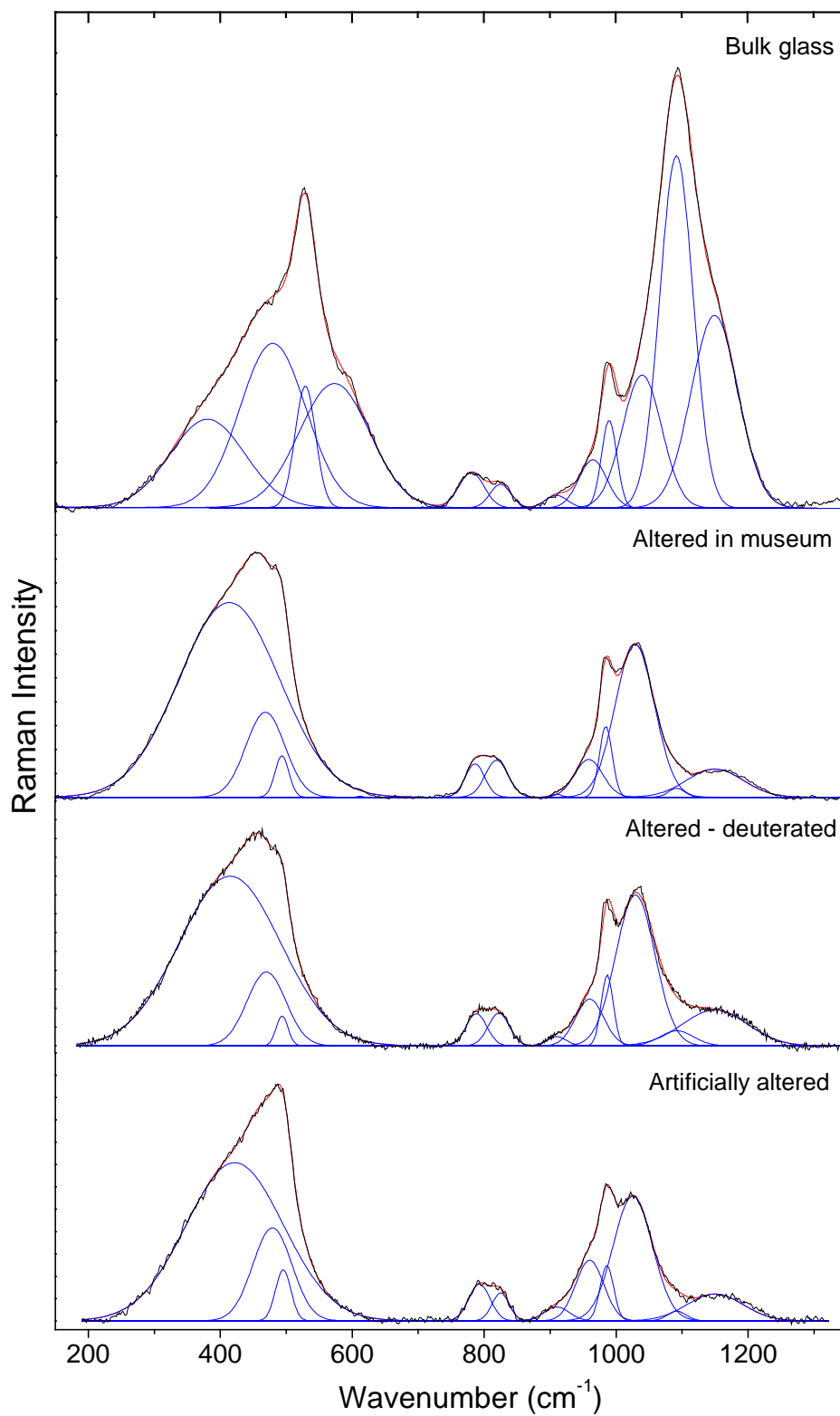
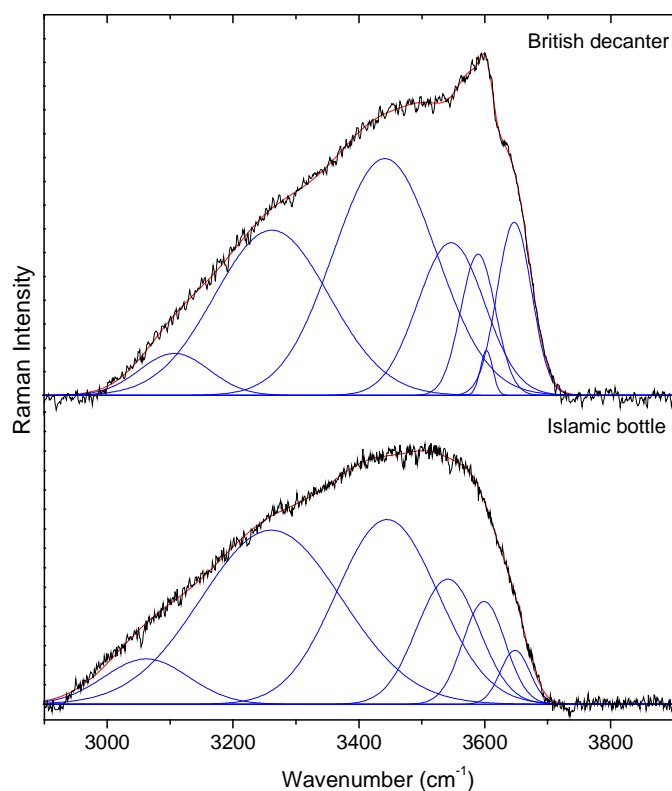


Figure IV- 14: Raman spectra of the British decanter and their decomposition: bulk, altered in museum, altered in museum and deuterated, and altered artificially.

Table IV- 5: Frequencies of the components of the Raman spectra ( $\text{cm}^{-1}$ ) from the British decanter glass: bulk, altered in museum, altered in museum + deuterated and altered artificially.

Bulk	Altered museum	Altered artificial	Altered deuterated	Assignment suggested
381	414	422	415	$\delta$ Si-O-Si polymerised
480	469	479	470	$\delta$ Si-O-Si polymerised
-	494	495	494	D <sub>1</sub> rings
529	-	-	-	$\delta$ Si-O-Si depolymerised
573	-	-	-	$\delta$ Si-O-Si depolymerised
781	786	793	788	Si motion in tetrahedral oxygen cage
825	819	825	822	
910	910	910	910	$\nu$ Si-O Q <sup>2</sup>
965	959	960	960	$\nu$ Si-O Q <sup>2</sup> & ( $\nu$ Si-OD)
990	985	986	987	$\nu$ Si-O Q <sup>2</sup> & ( $\nu$ Si-OH)
-	1029	1025	1029	
1040	-	-	-	$\nu$ Si-O
1092	1092	1092	1092	$\nu$ Si-O Q <sup>3</sup>
1150	1192	1150	1150	$\nu$ Si-O Q <sup>4</sup> + $\nu$ Si-O Q <sup>3</sup>

Figure IV- 15: Raman spectra of the 3000-3800  $\text{cm}^{-1}$  region and their decomposition from the altered British decanter and altered Islamic bottle glasses.

The stretching vibration of silanol expected at  $970\text{ cm}^{-1}$  in the Raman spectrum was superposed on the silicate stretching bands in this region. In order to verify the presence of silanols in the structure, the altered glass was deuterated. The transformation of Si-OH species into Si-OD was expected to induce a frequency shift from  $970$  to  $950\text{ cm}^{-1}$  in the Raman spectrum [26]. The spectrum of the deuterated decanter glass was almost identical to the spectrum of the museum-altered glass (Figure IV- 14), which suggested that only low concentration of silanols were present in the glass. The absence of large concentration of silanols, expected from the extensive leaching reaction, suggested that the rearrangement by condensation of the silanols had taken place [12, 19]. The increase in intensity near the  $300\text{-}500\text{ cm}^{-1}$  region, associated with the bending vibration of Si-O-Si, confirmed that new Si-O-Si bonds formed by condensation of the silanol species. As a result, molecular water was formed in the structure, as seen in the high frequency region of the spectrum. The presence of the sharp peak at  $494\text{ cm}^{-1}$  in the spectrum indicated formation by polymerisation of the four-fold silicate  $D_1$  rings normally observed in vitreous silica, but no three-fold  $D_2$  rings were seen. The spectrum of high-water content silica glass had a similar structure, with the presence of  $D_1$  but no  $D_2$  rings [23]. The modifications that occurred to the structure of the British decanter glass recall those observed by Bunker for sodium borosilicate glass leached in an acidic solution [19]. This similarity suggests that organic acids in the environment, which induced the formation of an acidic rather than alkaline solution on the glass surface, are responsible for the structural change of the decanter glass.

During the scientific study undertaken at the NMS one unaltered section of the decanter glass was exposed to a humid and acid-polluted atmosphere (formic acid) at ambient temperature for 5 months. The altered layer formed through this experiment, referred to as 'artificially altered' layer, extended to around  $14\text{ }\mu\text{m}$ . The Raman spectra of the glass altered in the museum environment and artificially were very similar (Figure IV- 14), supporting the role of organic acid pollutants in the modification of the glass structure. The slight difference observed between the two spectra was due to a higher silanol content ( $970\text{ cm}^{-1}$  band) and lower Si-O-Si ( $300\text{-}500\text{ cm}^{-1}$  region) in the artificially altered glass. The condensation reaction was hence more extensive in the museum-altered glass than in the artificially altered sample, possibly due to the different timescales of the alteration, the absence of humidity fluctuation in the artificial example or the effect of other pollutants and/or variations in pollutant concentrations in the decanter environment.

Finally, in all the spectra of the altered glasses, the low frequency component of the band near  $800\text{ cm}^{-1}$  was shifted towards higher frequency. Shift in this region was previously correlated to a change in the Si-O-Si angle and in the present case can be associated with an increase of the angle, which is consistent with the cation content decrease [32].

#### IV- 4.1.2 *Islamic bottle*

The Islamic glass bottle (A.1893.61) appeared less damage than the decanter. Microscope examination of the altered glass surface revealed fine widely-spaced cracks, barely visible by eye. The SEM image of the cross section (Figure IV- 16) indicated the presence of an altered layer on the glass surface, which was more extensive on the internal side ( $\sim 19\text{ }\mu\text{m}$ ) than on the external side ( $\sim 5\text{ }\mu\text{m}$ ). The altered layer displayed cracks perpendicular and parallel to the surface, some of which run into the bulk glass, just as in the British decanter glass.

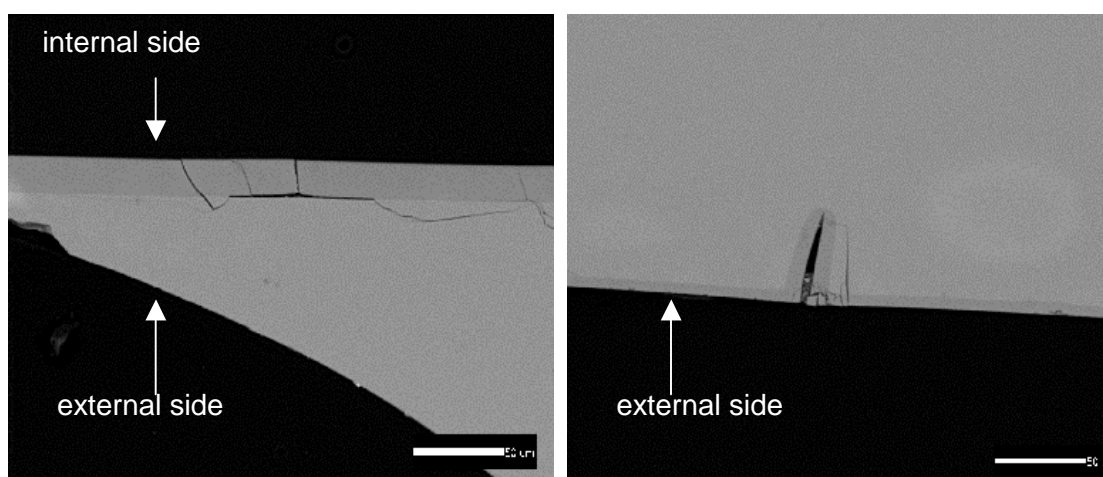


Figure IV- 16: SEM images of the cross-section of the Islamic bottle glass bottle (bar scale represents  $50\text{ }\mu\text{m}$ ).

The bulk glass of the Islamic composition has a soda lime silicate composition (Table IV- 6). The composition of the altered layer indicated that alteration caused almost complete depletion of the sodium within the glass surface (from 15.25 to 1.2 at% Na) with introduction of hydrogen species, and leaving the calcium and other ions undisturbed.

Table IV- 6: Elemental composition (at%) of altered and bulk regions of the Islamic bottle glass measured by EPMA. The H content of the altered region was estimated.

At %	Si	Al	Na	K	Ca	Mg	Mn	Fe	O	H
bulk	21.77	0.29	15.25	0.08	3.73	0.63	0.87	0.24	57.12	-
altered	21.77	0.28	1.20	0.33	3.59	0.56	0.81	0.23	57.05	14.15

Significant modifications were visible in the Raman spectrum of the glass after alteration (Figure IV- 17 , Table IV- 7). Spectral decomposition indicated that the component at  $1100\text{ cm}^{-1}$  decreased with the loss of the  $Q^3$  species. The decrease in the cation content in the structure induced a shift of the  $B_{550}$  component from  $573$  to  $548\text{ cm}^{-1}$ . The bands between  $900$  and  $1000\text{ cm}^{-1}$ , associated with the stretching of  $Q^2$  species, remained essentially unaltered because the calcium ions were retained in the structure. As a result, the component near  $600\text{ cm}^{-1}$ , believed to be linked to the Si-O-Si bending vibrations of  $Q^2$  species, remained intense in the spectrum. The apparent increase of the  $990\text{ cm}^{-1}$  component was due to superposition of a vibrational band at  $970\text{ cm}^{-1}$  associated with silanol species coincident with the  $990\text{ cm}^{-1}$  component. The presence of OH species in the structure was confirmed by the presence of a broad band in the high frequency region  $3000\text{-}3700\text{ cm}^{-1}$  (Figure IV- 15). The decomposition of this band indicated that both water and silanols were present. However, the profile of this high frequency band in the spectrum of the Islamic glass was different from that in the British glass, mainly due to the absence of the sharp band around  $3598\text{ cm}^{-1}$  associated with a different type of SiO-H hydroxyl group (Figure IV- 15). This difference cannot currently be explained. Finally the alteration caused an increase in intensity in the  $300\text{-}500\text{ cm}^{-1}$  region and the creation of a sharp component at  $493\text{ cm}^{-1}$  characteristic of the formation of new Si-O-Si linkages and  $D_1$  rings. In addition, a band was created around  $1075\text{ cm}^{-1}$ , previously attributed to the stretching of Si-O bridging bonds in hydrous glasses [23, 29]. This indicated that polymerisation of the silanols had occurred.

The structure of the altered layer indicated that the Islamic bottle glass underwent selective leaching of alkali ions and the formation of silanols from  $Q^3$  species. These silanol species polymerised to form new Si-O-Si linkages and four-fold silicate  $D_1$  rings. The stabilising cations, mainly calcium, were not affected by the leaching reaction and were retained in their original location in the glass structure, coordinated to  $Q^2$  species. Because the cations remained in the altered structure of the Islamic glass but not in the British glass, the band around  $550\text{ cm}^{-1}$  ( $B_{550}$ ), the wavenumber of which depends on the cation content, was still present in the spectrum of the Islamic glass, although shifted to lower frequency.

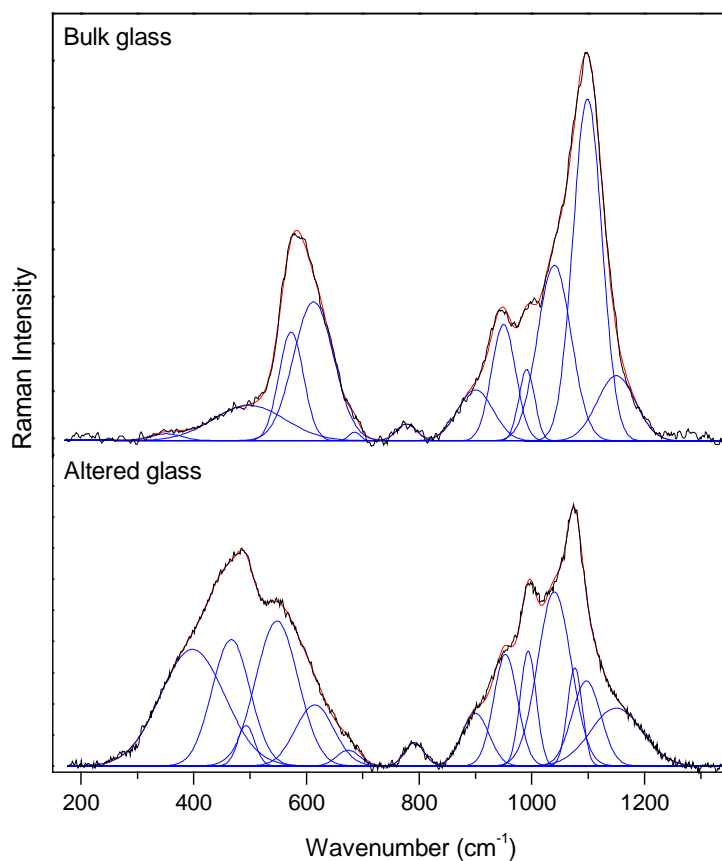


Figure IV- 17: Raman spectra with decomposition of altered and bulk area of the Islamic glass bottle.

Table IV- 7: Frequencies of the components of the Raman spectra ( $\text{cm}^{-1}$ ) of the Islamic glass bottle bulk and altered.

Bulk	Altered	Assignment suggested
352	398	$\delta$ Si-O-Si polymerised
499	467	$\delta$ Si-O-Si polymerised
-	493	$D_1$ rings
573	548	$\delta$ Si-O-Si depolymerised
613	615	$\delta$ Si-O-Si depolymerised
686	674	$\delta$ Si-O-Si depolymerised
778	792	network $\nu$ Si-O-Si
900	900	$\nu$ Si-O $Q^2$
950	954	$\nu$ Si-O $Q^2$
991	994	$\nu$ Si-O $Q^2$ & ( $\nu$ Si-OH)
1040	1040	$\nu$ Si-O
-	1076	$\nu$ Si-O
1099	1097	$\nu$ Si-O $Q^3$
1150	1150	$\nu$ Si-O $Q^4$ + $\nu$ Si-O $Q^3$

## IV- 4.2 Artificial accelerated ageing experiments

The effect of organic pollutants on the structural modification of glass with alteration were investigated and compared to non-polluted atmospheres. Replica glasses were aged in accelerated conditions using the method described in chapter II. The major part of the investigation was undertaken on the RG1 replica, for which the aspects of the experiments were varied, and the RRo glass was only used for comparison on some experiments.

The altered layers formed can be separated into two main structures, which are associated with the two main alteration processes: leaching and dissolution. These processes and the components formed during these processes can be linked directly to the acidity of the atmosphere. The visual and structural characteristics of the alteration are presented according to the type of atmosphere: acidic or non-acidic.

### IV- 4.2.1 Alteration in humid / acid atmosphere

Formic acid, acetic acid, and wood vapours, all created an acidic atmosphere which favoured the leaching reaction. The pH of the aqueous condensate formed on the surface was ~2. A leached layer was also produced by formaldehyde, but it was much thinner; ~2  $\mu\text{m}$  compared to ~15  $\mu\text{m}$  in acidic atmospheres. As a result of exposure to acidic atmospheres, the similar visual and structural modifications were created. For this reason we will concentrate mainly on the effect of formic acid.

After ageing in acidic atmospheres, droplets or white crystals formed at the glass surface, depending on the humidity of the environment. Visually the glass remained unchanged, when exposed to the ambient atmosphere after the experiment, since it retained its transparency and displayed only fine widely-spaced cracks (Figure IV- 18 and Figure IV- 19: A, C). However, drying of the hydrated layer using silica gel induced strong mechanical strains, which caused the surface to crack, bend and sometimes flake off, thereby pulling the bulk glass with it (Figure IV- 18 and Figure IV- 19: B, D). The visual appearance of the glass surface after drying resembles that of the British decanter (Figure IV- 11 and Figure IV- 12). We note in both cases the formation of rectangular scales, approximately 200  $\mu\text{m}$  wide, with the corner sometimes broken into a triangular shape with one circular edge; as well as the presence of iridescence caused by the lifting of the scale.

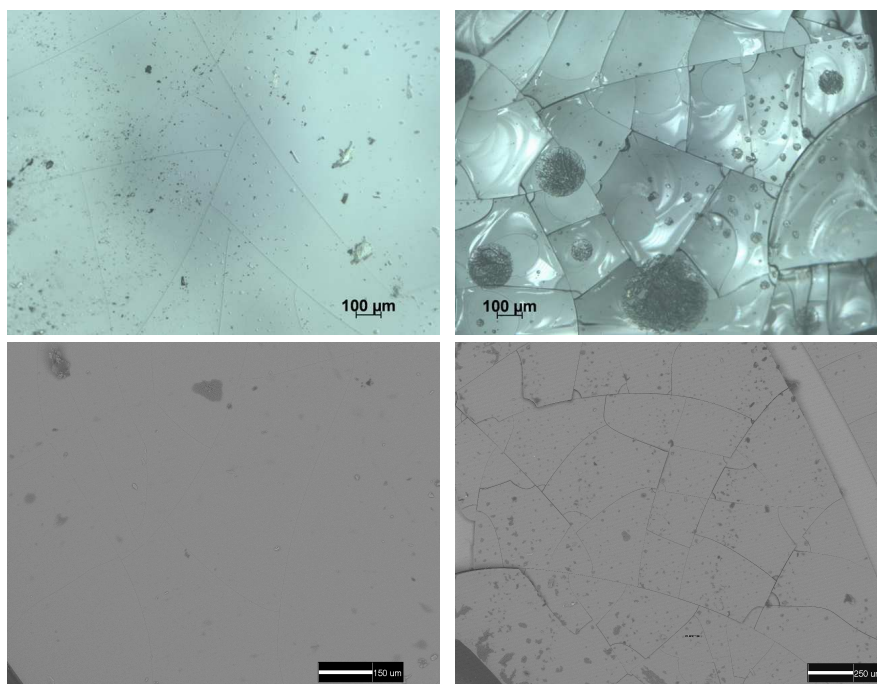


Figure IV- 18: RG1 glass aged in humid / formic acid atmosphere for 3 weeks at 60 °C. Light microscopy image *before* (A), *after drying* (B); SEM image *before* (C), *after drying* (D).

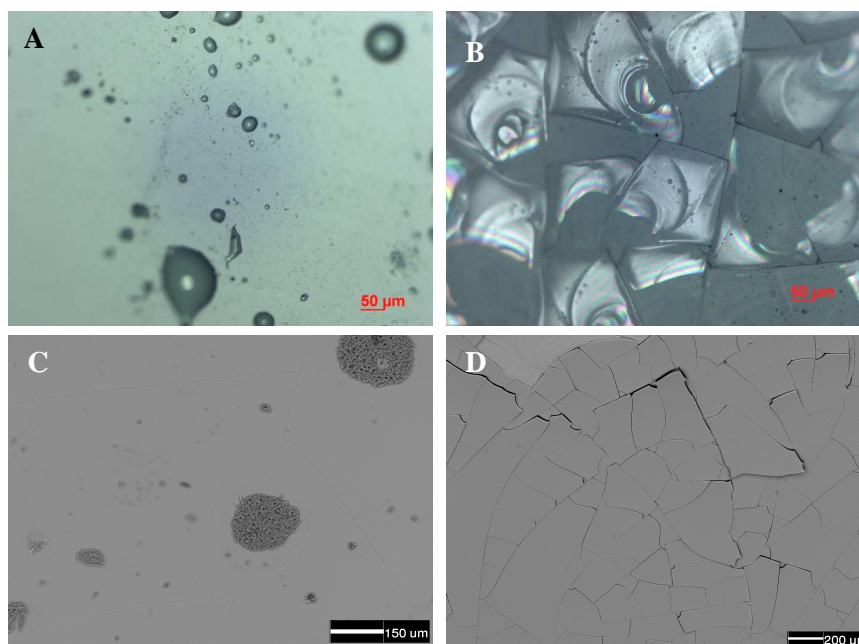


Figure IV- 19: RRo glass aged in humid / formic acid atmosphere for 3 months at 50 °C. Light microscopy image *before* (A), *after drying* (B); SEM image *before* (C), *after drying* (D).

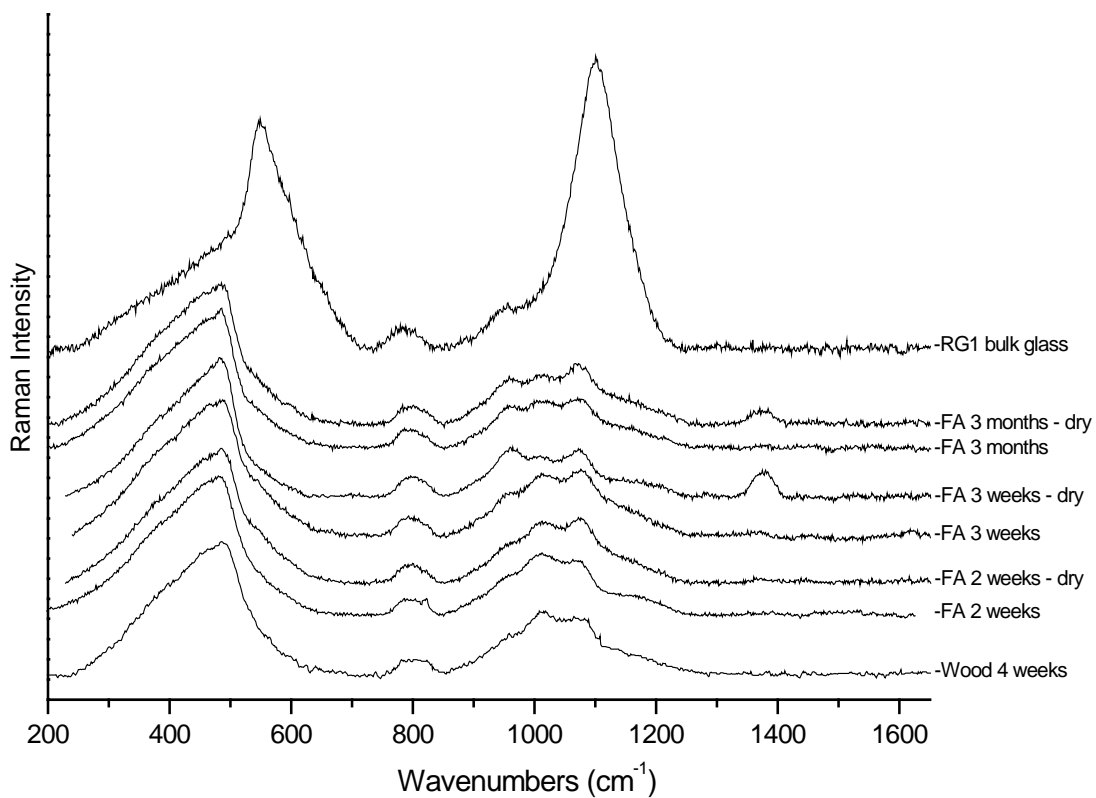


Figure IV- 20: Raman spectra of RG1 glass aged in humid / acidic atmosphere at 60 °C for different durations.

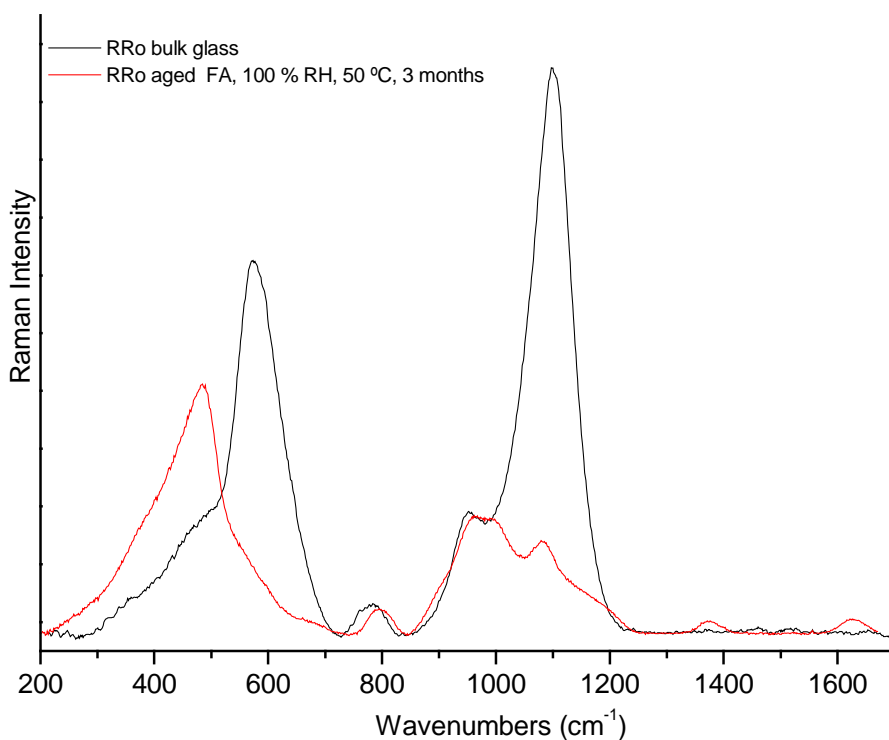


Figure IV- 21: Raman spectra of RRo glass aged 3 months in humid / formic acid atmosphere, at 50 °C

Table IV- 8: Elemental composition of the bulk and altered glass measured by EPMA on the RG1 replica, and by SEM-EDS on the RRo replica. H content estimated, excepted for '\*' measured by SIMS.

	At %	Si	Al	Na	K	Ca	Mg	Mn	Fe	O	H
RG1	Bulk	24.64	0.29	12.22	1.44	1.52	0.60	0.17	0.12	58.98	-
	Woodw4*	25.29	0.30	1.17	0.62	1.57	0.60	0.16	0.11	59.64	10.53
	FAw2	24.64	0.29	1.34	0.70	1.43	0.55	0.15	0.10	58.92	11.87
	H <sub>2</sub> Ow4*	21.96	0.25	7.61	1.15	1.14	0.50	0.12	0.08	56.08	11.11
RRo	Bulk	22.2	0.8	11.7	1.5	0.3	1.9	-	0.3	60.8	-
	FAw6	22.5	1.0	1.7	1.1	0.3	1.8	-	0.3	60.8	10.1
	H <sub>2</sub> Ow6	17.0	0.9	10.3	1.2	0.3	1.3	-	0.2	61.5	7.5

The acidic atmosphere induced similar changes to the Raman spectra and elemental composition of the RG1 and RRo glasses (Figure IV- 20, Figure IV- 21 and Table IV- 8). The compositional data confirm that selective leaching of the alkali metal ions has taken place with the introduction of hydrogen while the polyvalent cations, as Ca<sup>2+</sup>, Mg<sup>2+</sup>, are retained in the structure (Woodw4, FAw2 and FAw6 in Table IV- 8). These compositional data are consistent with the measurements made on the historic glass objects naturally altered in the museum environment. The acidic atmosphere caused almost complete depletion of the alkali ions and the remaining sodium content in the altered layer is around 1-1.5 at%.

The Raman spectra of the RG1 and RRo glass before and after alteration in formic acid were curve-fitted using the decomposition model defined in Table IV- 3 adding new component when necessary (Figure IV- 22 and Figure IV- 23). The different components obtained through the decomposition are presented in Table IV- 9. With the leaching of alkali metal ions, the associated Q<sup>3</sup> species were lost as indicated by the decrease of the components at 1100 cm<sup>-1</sup> and near 550 cm<sup>-1</sup>. However, the Q<sup>2</sup> species mainly coordinated to doubly charged cations are retained as evidenced by the components around 900-1000 cm<sup>-1</sup>. In the meantime two additional components appeared in the stretching region, at 1010 and 1070 cm<sup>-1</sup> in the RG1 glasses and at 1000 and 1080 cm<sup>-1</sup> in the RRo glass. The slight difference in position between the two glasses may indicate that the position of these components is composition dependent. The component at 1070 or 1080 cm<sup>-1</sup>, also observed in the Islamic glass bottle, may correspond to the 1075 cm<sup>-1</sup> peak attributed in hydrous glasses to the stretching of Si-O bridging bonds [23, 29]. The 1010 cm<sup>-1</sup> component probably contains several bands, in particular the band associated with silanols at 970 cm<sup>-1</sup>.

In the low frequency region, the creation of components at 420-450  $\text{cm}^{-1}$  and 490  $\text{cm}^{-1}$ , associated respectively with new Si-O-Si bonds and  $D_1$  rings, proves that the polymerisation of the silanols has occurred in the structure. Finally the two components near 800  $\text{cm}^{-1}$  shifted by about 20  $\text{cm}^{-1}$  towards higher frequency, which is associated with an increase of the Si-O-Si angle, caused by the decrease of the cation content.

By increasing the duration of alteration the thickness of the RG1 altered layer increased, however the structure did not greatly change with time (Figure IV- 20). We note slight differences in the peak ratio in the Si-O stretching region (900-1300  $\text{cm}^{-1}$ ) which suggests some modification in the concentration ratio of the different species in the glass.

The profile of the broad band in the 3000-3800  $\text{cm}^{-1}$  region of the spectrum indicates the presence of molecular water and silanols as well as the 3598  $\text{cm}^{-1}$  band (Figure IV- 24), as for the British decanter glass (Figure IV- 15). The weak peak at 1630  $\text{cm}^{-1}$  associated with the  $\text{H}_2\text{O}$  bending was not visible in the RG1 glass but was observed in the RRo glass (Figure IV- 21) [23]. Drying the altered layer in RG1 glass with silica gel induced a decrease of the broad band in the 3000-3800  $\text{cm}^{-1}$  in the Raman spectrum as well as a modification of the intensity ratio between the components around 1010  $\text{cm}^{-1}$  and 1070  $\text{cm}^{-1}$ . These observations are linked to a decrease in the proportion of OH from water and silanols species show that more bridging bonds are created through further condensation of the silanols. As a result of the removal of molecular water and silanol condensation, strains develop in the glass which cause fractures in the altered and the bulk glass (Figure IV- 18 and Figure IV- 19: B, D).

The presence of a peak near 1400  $\text{cm}^{-1}$  was observed in the Raman spectra of the altered RG1 glass dried in silica gel after alteration (Figure IV- 20), as well as in the altered layer of the RRo glass (Figure IV- 21). This peak corresponds to the deformation vibration of C-H bonds, which is confirmed by the presence of weak bands around 2900  $\text{cm}^{-1}$  in the spectrum of the altered RG1 glass attributed to the C-H stretching modes (Figure IV- 24). This C-H group likely originates from the vibration of formate groups present within the silicate structure. Formate could be present as  $\text{Na}^+\text{HCOO}^-$  in solution and/or as silicon formate species  $\text{Si-OC(=O)H}$ . The formation of silicon formate groups was reported in the study of silica gels formed by the direct reaction between formic acid and tetraethyl orthosilicate, and causing an accelerated gelation by condensation of silicon formate groups with silanols [33, 34]. Thus, if these formate groups are present in the altered glass, they may induce an acceleration of the structure condensation creating new Si-O-Si linkage.

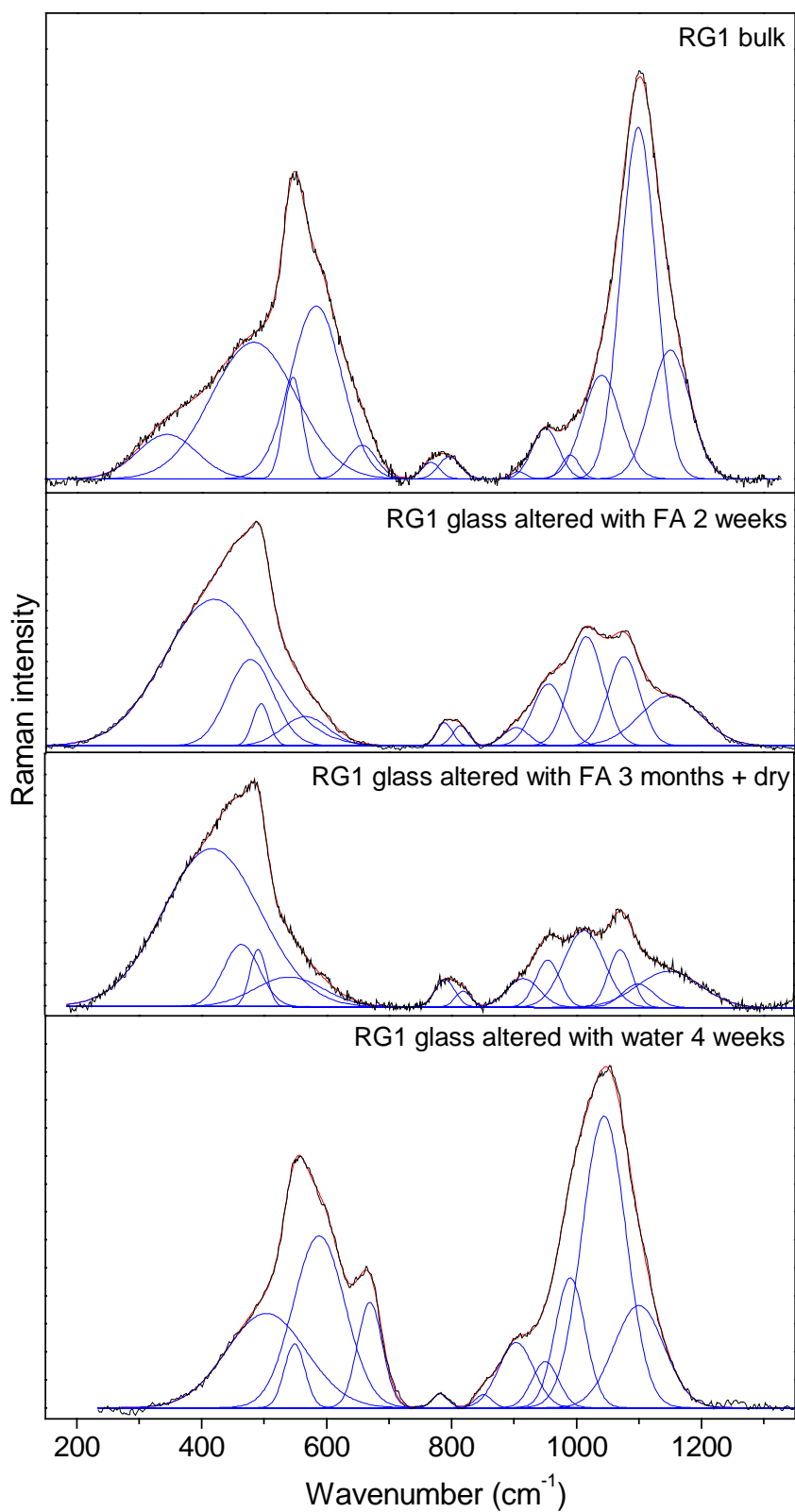


Figure IV- 22: Decomposition of the Raman spectra of RG1 glass before and after alteration in humid/non-acid and humid/acid atmosphere with formic acid (FA).

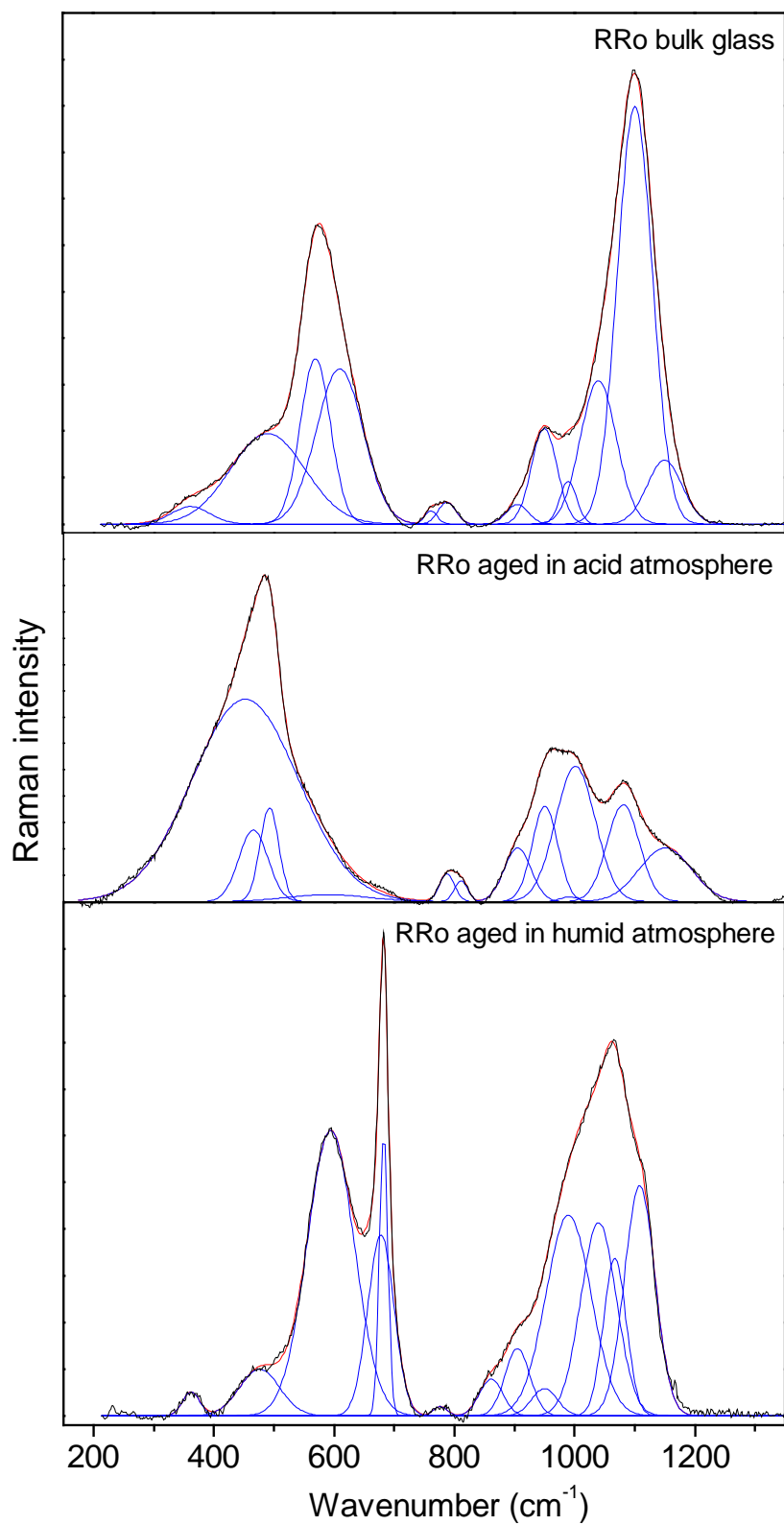


Figure IV- 23: Decomposition of the Raman spectra of RRo glass before and after alteration in humid/non-acid and humid/acid atmosphere with formic acid.

Table IV- 9: Curve-fitted components position ( $\text{cm}^{-1}$ ) from decomposition in Figure IV- 22 and Figure IV- 23. Underlined = parameter fixed;

RG1 glass				RRo glass			Suggested assignments
bulk	FAw2	FAM3	H <sub>2</sub> Ow4	bulk	FAM3	H <sub>2</sub> Ow8	
344				362		362	$\delta$ Si-O-Si Q <sup>4</sup>
	419	417			452		$\delta$ Si-O-Si Q <sup>4</sup>
483	478	465			466	476	$\delta$ Si-O-Si Q <sup>4</sup>
	495	491		491	492		D <sub>1</sub> rings
			503				
546	565	541	549	570			$\delta$ Si-O-Si depolymerised
583			588	610	(590)	594	$\delta$ Si-O-Si depolymerised
656			669			678	$\delta$ Si-O-Si depolymerised
						683	
766	788	791	782	762	787	777	Si motion in oxygen cage
796	814	820		789	810		
			851			861	$\nu$ Si-O Q <sup>1</sup>
907	903	916	903	<u>905</u>	<u>905</u>	<u>905</u>	$\nu$ Si-O Q <sup>2</sup>
<u>950</u>	<u>955</u>	956	<u>950</u>	<u>950</u>	<u>950</u>	<u>950</u>	$\nu$ Si-O Q <sup>2</sup> and ( $\nu$ Si-OH)
<u>990</u>			990	<u>990</u>	<u>990</u>	<u>990</u>	$\nu$ Si-O Q <sup>2</sup> and ( $\nu$ Si-OH)
	1016	1013			1001		
<u>1040</u>			1044	<u>1040</u>		<u>1040</u>	
	1076	1071			1080	1067	
1099	<u>1100</u>	<u>1100</u>	<u>1100</u>	1101		1108	$\nu$ Si-O Q <sup>3</sup>
<u>1150</u>	<u>1150</u>	<u>1150</u>		<u>1150</u>	<u>1150</u>		$\nu$ Si-O Q <sup>4</sup> + $\nu$ Si-O Q <sup>3</sup>

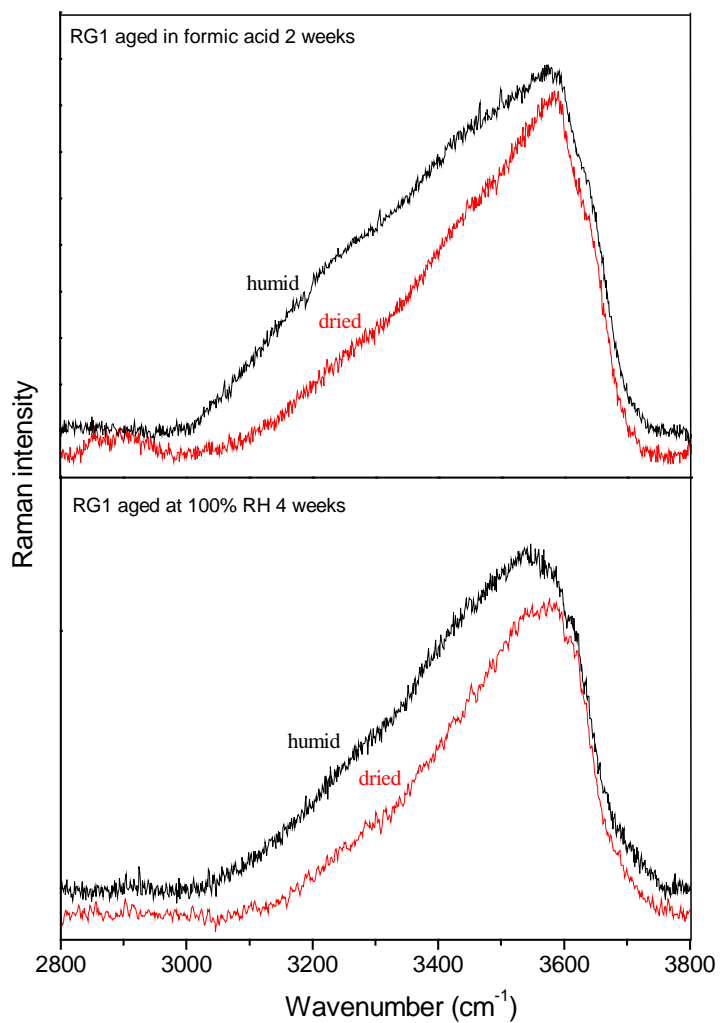


Figure IV- 24: Raman spectra of the 3000-3800 cm<sup>-1</sup> region of the RG1 glass altered in humid/acid (formic acid) and humid/non-acid atmospheres, before and after drying.

#### *IV- 4.2.2 Alteration in humid / non-acid atmosphere*

At the end of the experiment, the pH of the solution present at the surface of the glass was very alkaline with a pH around 12-14, indicating that the dissolution reaction was predominant in the alteration. The surface after exposure to the humid/non-acid atmosphere was visually very different from the one generated by the humid/acid atmosphere (Figure IV- 25, Figure IV- 26, Figure IV- 27 and Figure IV- 28). In this atmosphere, the duration, drying process and interaction with the external air after the experiment greatly influenced the visual aspect of the glass surface.

After one week, iridescences were visible at the surface, due to the presence of a thin surface layer (hundreds of nanometre in thickness) with a different structure to the underlying glass (Figure IV- 25 A-D). With time, the altered layer, known as the gel layer, due to its resemblance to a gel (Figure IV- 26A and Figure IV- 27A), thickened, became opaque and developed a porous structure (Figure IV- 25F). As soon as the humidity or temperature dropped, the altered layer started to dry causing cracks and fractures. The altered layer also curled and eventually peeled off (Figure IV- 25, Figure IV- 28 and Figure IV- 26C). When the gel layer was in contact with the external air, while still wet, the sodium hydroxide solution reacted with the air to form crystalline products at the surface and within the gel, inducing a whitening of the surface. The crystalline products were characterised by Raman spectroscopy generally as sodium carbonates, formates, acetates and/or sulfates. Through this process, intriguing patterns were sometimes formed such as a cracking pattern with rectangular areas of clear material surrounded by crystals of sodium carbonate monohydrate after ageing the RG1 glass 4 weeks at 60 °C (Figure IV- 25 I, J ). In some cases, liquid pockets were trapped under the glass surface (Figure IV- 25G). The liquid pockets probably contained concentrated NaOH solution as sodium carbonate crystallised under the glass on contact with CO<sub>2</sub> in the air. When the glass was dried further in silica gel, the cracking was enhanced and the altered layer flaked off. Similar visual observations were made by Ryan while ageing the RG1 glass at various humidities [35].

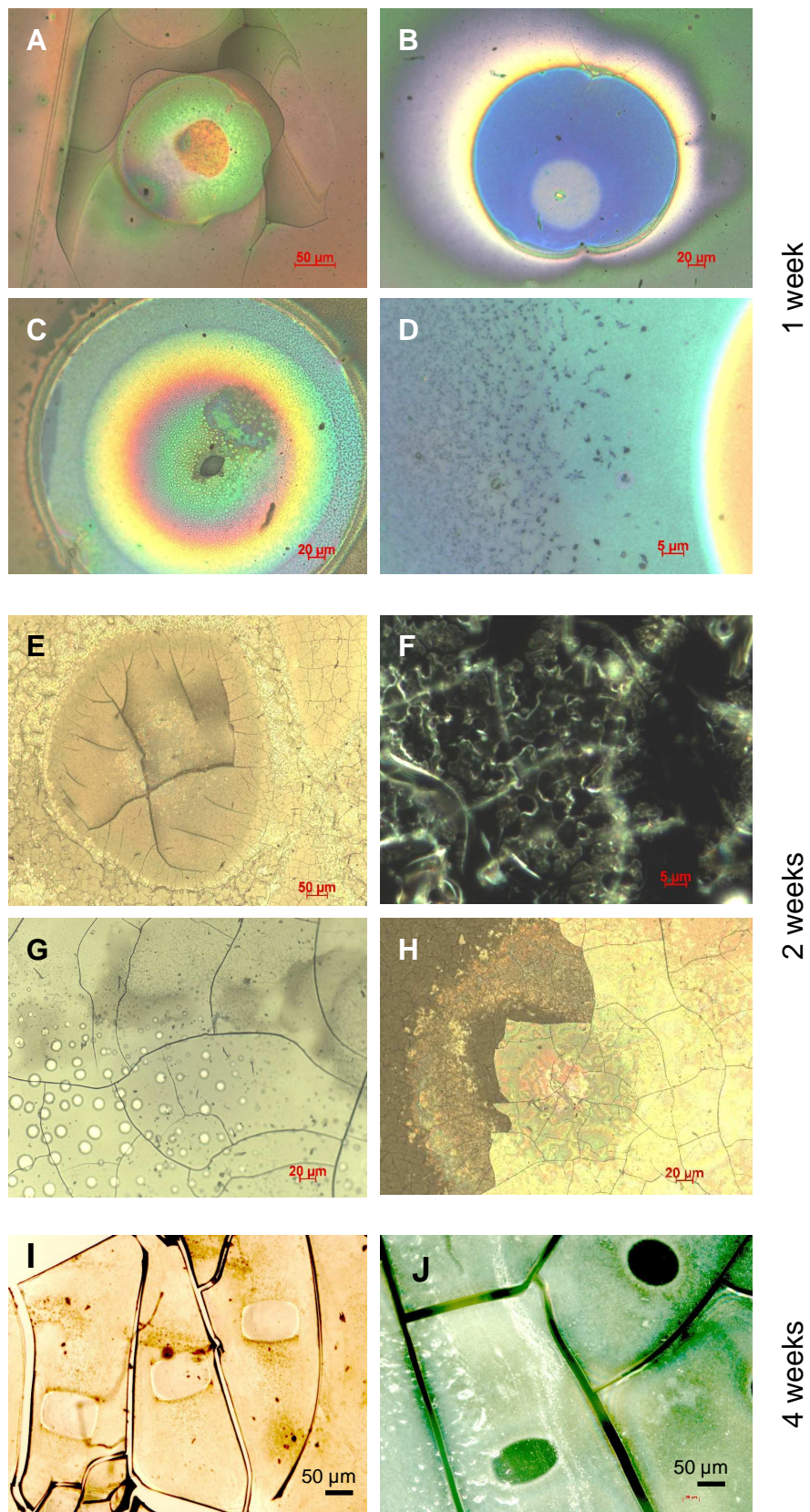


Figure IV- 25: Light microscopy images of the RG1 glass surface after exposure to 100 % RH at 60 °C. All images taken in reflected light except F taken in dark field.

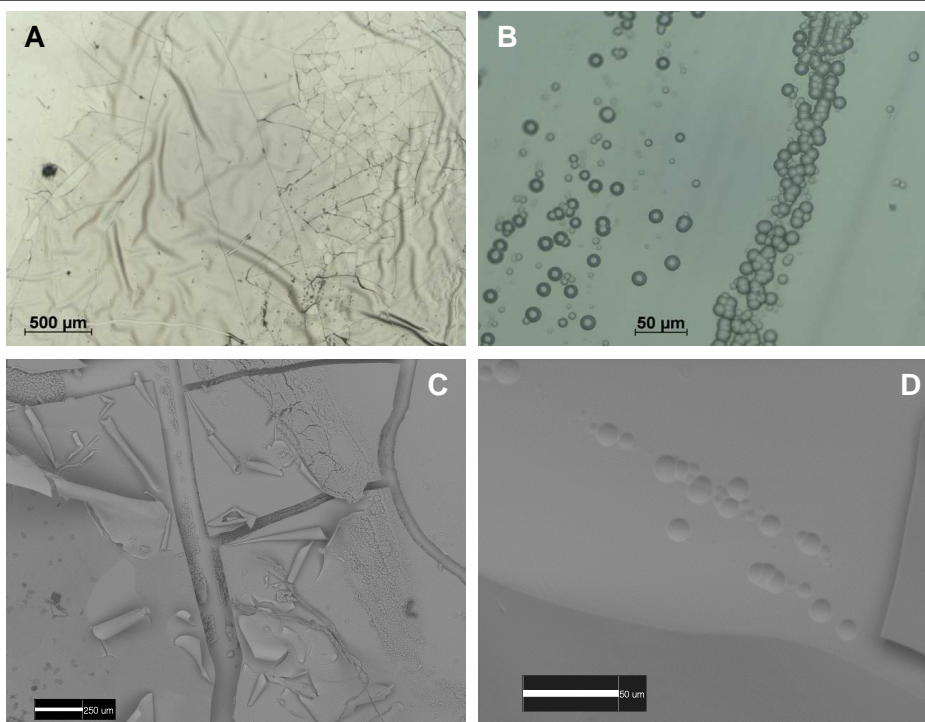


Figure IV- 26: RG1 glass aged 6 weeks at 100 % RH, 60°C and dried before contact with air. Altered layer: (A) *light microscopy image*, (C) *SEM*; Bulk glass (B) *light microscopy images*, (D) *SEM*.

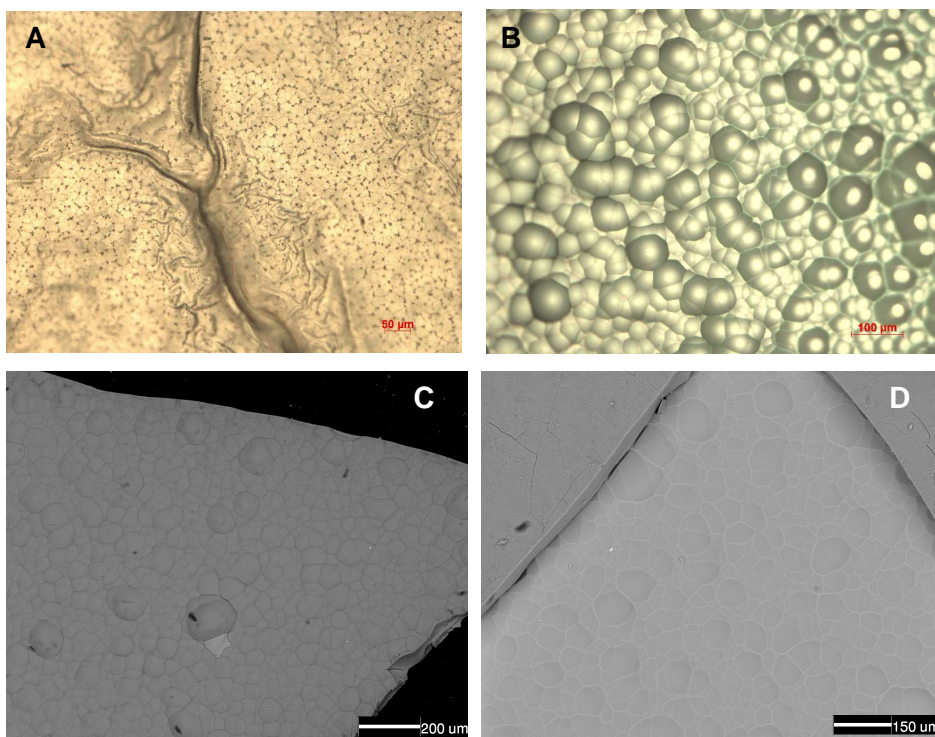


Figure IV- 27: RRo glass aged 8 weeks at 100% RH, 60°C and dried before contact with air. Light microscope: (A) *altered layer surface* (B) *bulk glass surface*, SEM: (C) *back altered layer surface = interface* (D) *surface bulk*.

When the altered layer was dried before coming into contact with the air (while opening the tube), crystallisation did not occur and the gel condensed into a solid and uniform material. This material was compact and opaque in the case of the aged RRo replica (Figure IV- 27A), but in the case of RG1 replica it was transparent and composed of several thin curling and peeling off layers (Figure IV- 28 and Figure IV- 26C). This difference may be linked to the compositional difference between the two glasses. In both situations, a blister pattern formed on the side of the altered layer at the interface with the glass (Figure IV- 26B and Figure IV- 27B, C). The glass displayed a pattern of depressions associated with the negative of these blisters (Figure IV- 26D and Figure IV- 27D). An identical pattern has been described on archaeological glass originating from a shipwreck [36] and on nuclear glass ageing experiments [37] and was possibly present as the marks left on the bulk glass after congruent dissolution of an alkali silicate glass [38]. This parallel suggests that this blister pattern is characteristic of the congruent dissolution of a glass.

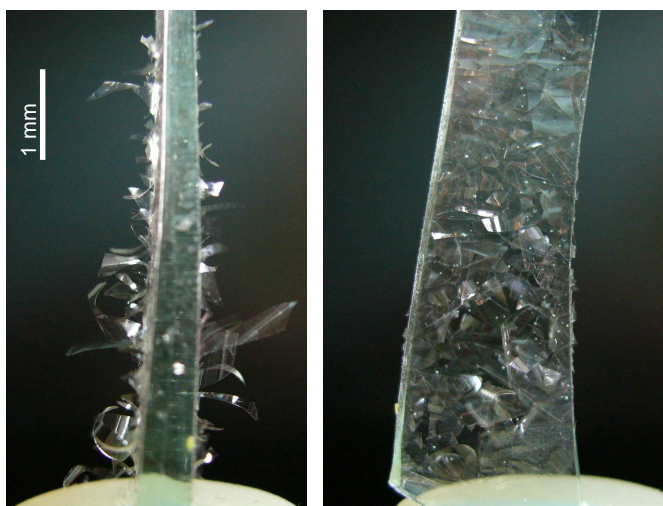


Figure IV- 28: Photograph of the RG1 glass aged 6 weeks at 100 % RH and 60 °C and dried before contact with the external air: profile (left) and face (right).

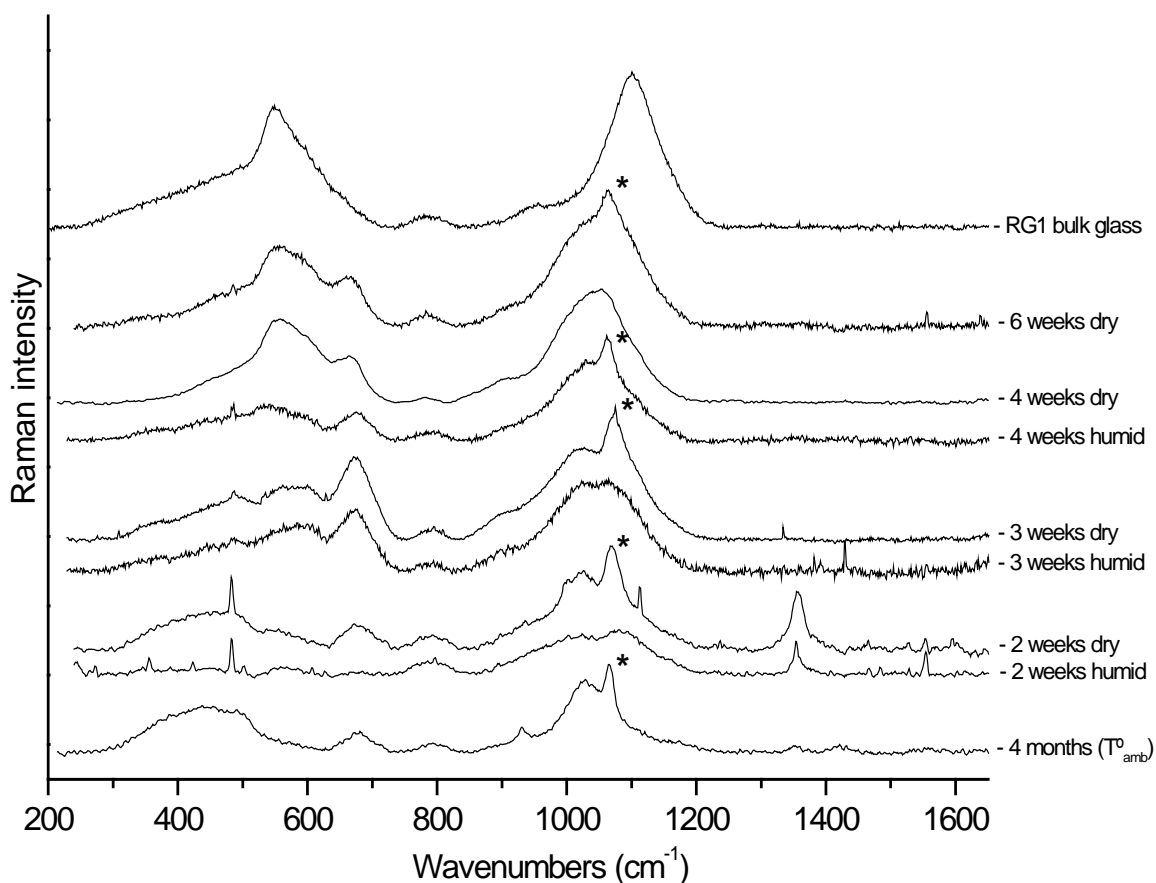


Figure IV- 29: Raman spectra of RG1glass aged at 100 % RH and 60 °C for various duration and RG1glass aged at 100 % RH and ambient temperature ( $T^{\circ}_{amb}$ ) for 4 months. (\* sharp peak associated with the presence of carbonate crystals within the layer).

The application of Raman spectroscopy to the humid gel layer was difficult due to its reactivity with the environment (crystallisation and/or drying). Moreover, the layer was too thin before two weeks exposure to be analysed. The spectra recorded for RG1 glass aged for different duration show an evolution in the structure of the gel layer (Figure IV- 29). After two weeks the intensity of the spectra of the gel is very weak, particularly in the 300-700  $\text{cm}^{-1}$  region which indicates that the Si-O bridging structure was completely broken by the dissolution. The structure of the gel layer formed after two weeks at 60 °C and dried is similar to that formed after 4 months at ambient temperature ( $\sim 20^{\circ}\text{C}$ ), which support that the temperature increase did not modify the structure of the gel layer. The spectrum of the gel layer at this stage resembled the spectra of acid-aged glasses, which have undergone leaching, except for the presence of a new peak near 670  $\text{cm}^{-1}$  (Figure IV- 29).

The sharp peaks such as the one near  $1080\text{ cm}^{-1}$  (marked with \*) or near  $1370\text{ cm}^{-1}$  correspond to crystalline products formed within or on the gel layer and are associated respectively with carbonates and formates. These crystals formed after the NaOH solution present has reacted with the pollutants in the ambient air when opening the tube. With time and as the gel layer dries, the Raman spectra became more intense, particularly in the  $300\text{--}700\text{ cm}^{-1}$  region, indicating that new Si-O-Si bridging bonds were created through polymerisation. The final structure of the RG1 gel layer was that of an amorphous material, but with a structure different from the original glass. Similar structural modifications were induced in the RG1 and RRo glasses after alteration in humid/non-acid atmosphere based on their Raman spectra (Figure IV- 22, Figure IV- 23 and Figure IV- 30).

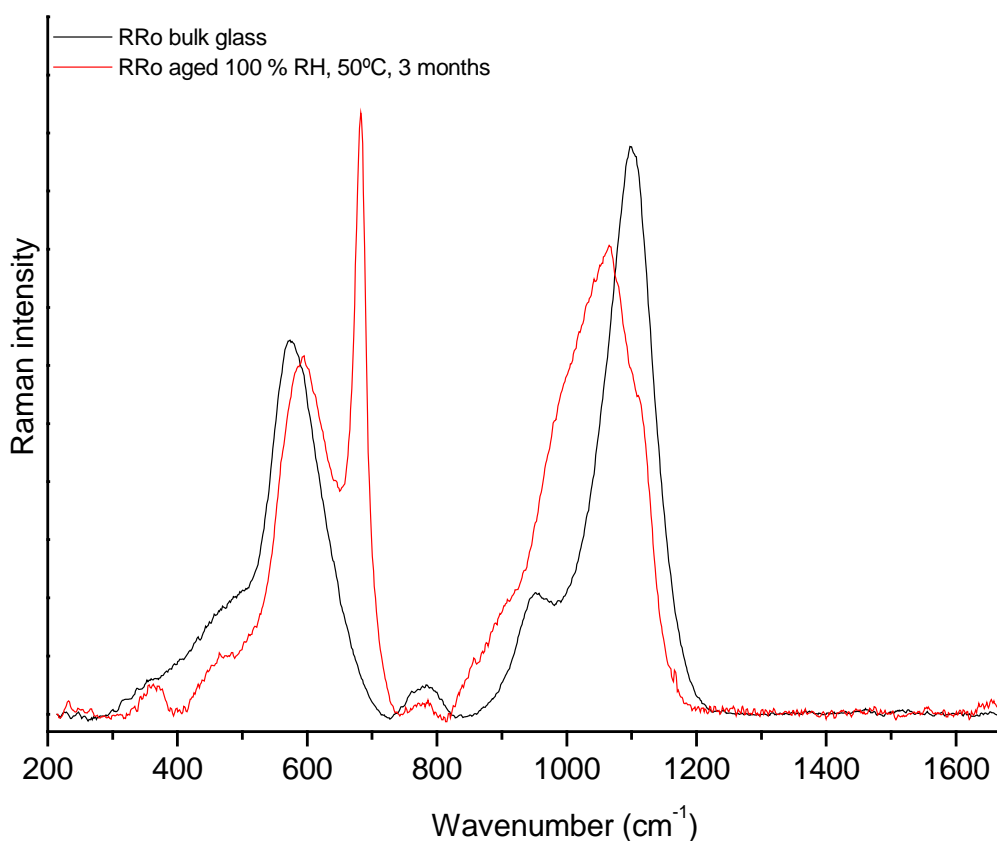


Figure IV- 30: Raman spectra of RRo glass aged 8 weeks at 100 % RH, 60 °C and dried before contact with air.

The elemental composition of the altered layer formed after 4 weeks for RG1 (H<sub>2</sub>Ow4) and 6 weeks for RRo (H<sub>2</sub>Ow6) indicated that all the cations originally present in the bulk glass were incorporated (Table IV- 8), which confirms that the dissolution was congruent. Thus, all the species present in the gel which includes the leached alkali, HSiO<sub>3</sub><sup>-</sup> and SiO<sub>3</sub><sup>2-</sup> species, the cations extracted through dissolution were combined to form the new material. This altered layer did not adhere to the glass underneath, and easily detached and flaked off when it dried. SIMS depth profiling measurements from the glass just under the gel layer from of a RG1 sample exposed 3 weeks to water showed that the surface of the glass was depleted in sodium and hydrated over 1.5 μm (Figure IV- 31). Consequently, the glass possessed at least three regions: the bulk (unaltered glass), an alkali leached region and a new amorphous material created from the condensation of the gel layer. This morphological description as well as the structural modification observed agreed with the results obtained by Ryan for the RG1 glass altered in high humidity and high temperature [35] and the ageing of nuclear glass in water solution [39].

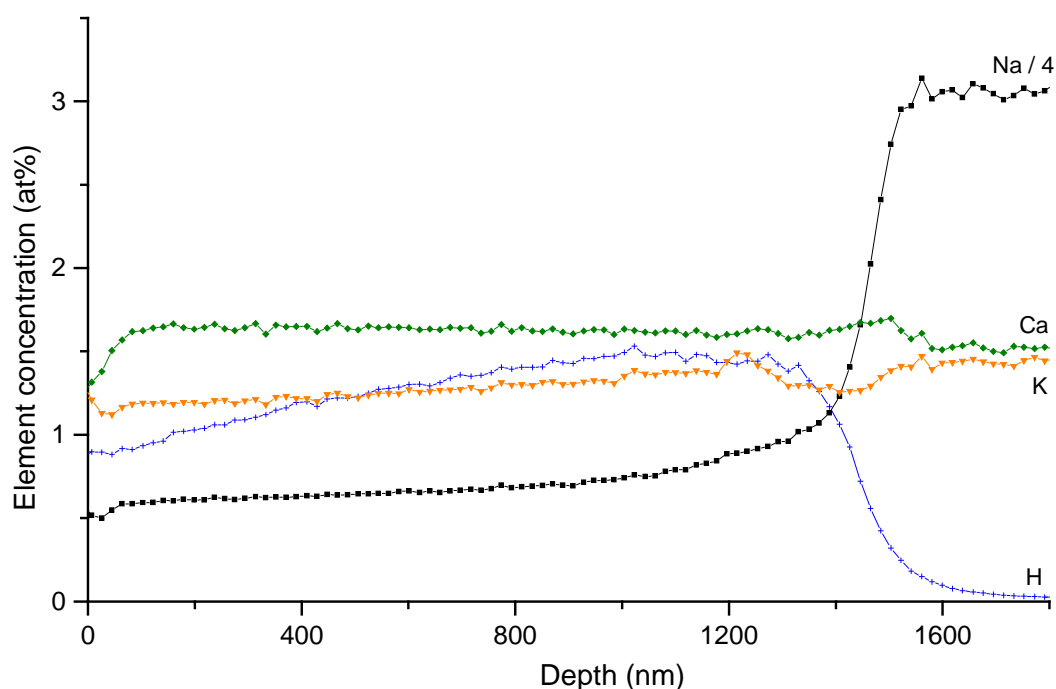


Figure IV- 31: Element SIMS depth profile of glass under gel layer from RG1 glass aged 3 weeks at 100 % RH and 60 °C.

Comparison of the curve-fitting data from the altered layer and the bulk glass spectra gave some information into the new structure (Figure IV- 22, Figure IV- 23 and Table IV- 9). In both RG1 and RRo altered layer spectra, the peak in the stretching region ( $800\text{-}1200\text{ cm}^{-1}$ ) was shifted to lower wavenumbers, which indicated that the structure was more depolymerised than the corresponding bulk glass. The new structure contained mainly  $Q^2$ , rather than  $Q^3$  species. This was consistent with the results obtained by Ryan on the gel layer interpreted as the presence of a metasilicate type of gel [35]. The fitting of the  $300\text{-}700\text{ cm}^{-1}$  region of the Raman spectra indicated the presence of more Si-O-Si within depolymerised species than polymerised ones. We suspect that the strong band present at  $670\text{ cm}^{-1}$  and  $683\text{ cm}^{-1}$  in the spectrum of the altered glass RG1 (Figure IV- 22) and RRo (Figure IV- 23) respectively, are related to the vibration of the same entities. This implies that the band is composition dependent and it probably corresponds to the bending vibration of Si-O-Si in depolymerised units. This band appeared very early in the alteration and seemed characteristic of this type of alteration (Figure IV- 29).

The Raman spectrum of the region  $3000\text{-}3800\text{ cm}^{-1}$  (Figure IV- 24) indicated the presence of silanols and molecular water in the structure. The profile of the band in this region was different from the one observed in the case of acid-altered glass. The  $3300\text{-}3600\text{ cm}^{-1}$  region, associated with the vibration of O-H from silanols, was more intense in the spectra of the glass altered in the humid-only atmosphere. Again we observed a decrease of the bands with drying, mostly in the low wavenumbers region associated with the vibration of O-H from molecular water.

## IV- 5. Non-destructive analyses of objects

### IV- 5.1 Determination of the degree of alteration

A modern glass necklace (H.1992.392) and an Islamic glazed ceramic (A.1886.573) were examined as application examples for non-destructive analyses by Raman spectroscopy and SEM-EDS, to gain information about their composition, stability and assess the state of deterioration.

The surface of both glass retained their shiny and transparent appearance, but it was strongly cracked and scales were lifted with creation of interferences (Figure IV- 32). On both objects the crystalline products were formates, with sodium formate II on the necklace and sodium calcium formate on the Islamic glazed ceramic (Table III-1). The calcium in the deposits on the glazed ceramic may originate from the ceramic body rather than the glaze.

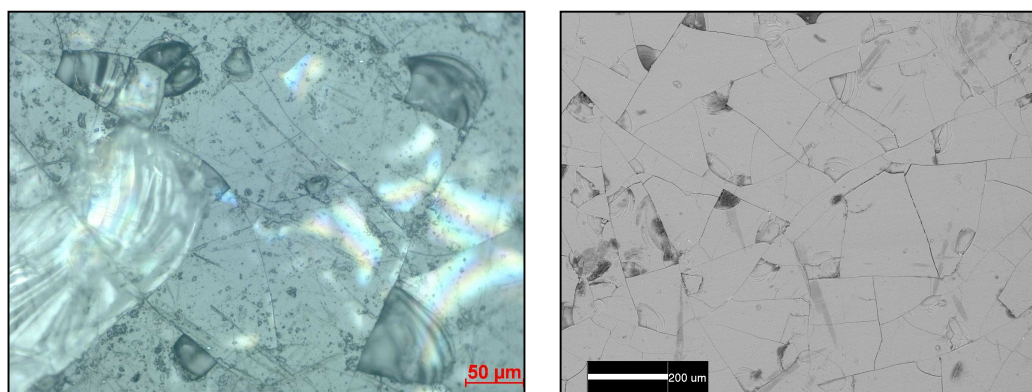


Figure IV- 32: Surface of the glass necklace H.1992.392 by light microscopy (left) and SEM (right).

SEM-EDS analyses indicated that both objects were alkali silicate glasses with the presence of mainly sodium and with low calcium, magnesium and lead. In the case on the necklace we noted the presence of approximately ~2 at% arsenic. Based on the previous results, we can say that in the Raman spectra of the glass the bands near 550 and 1100  $\text{cm}^{-1}$  were associated with the presence of sodium and the sharp peak around 990  $\text{cm}^{-1}$  with the presence of lead (Figure IV- 33 and Figure IV- 34). We suspect the arsenic induced the creation of  $Q^1$  or  $Q^0$  species in the structure, which stretching vibration was responsible of the strong peak at 831  $\text{cm}^{-1}$  in the spectrum. With the alteration, the spectra showed the depletion of the alkali within the altered layer and the conservation of the polyvalent cations.

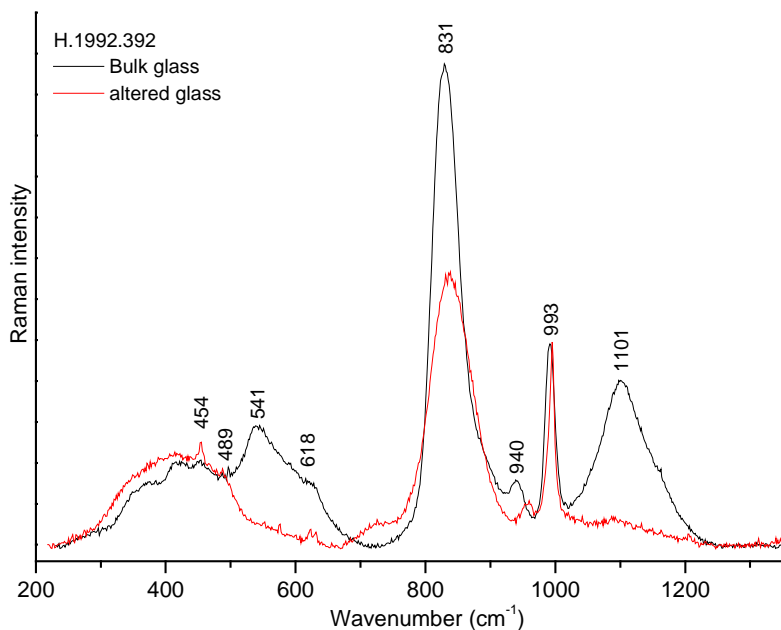


Figure IV- 33: Raman spectra of the bulk and altered glass from glass necklace H.1992.392.

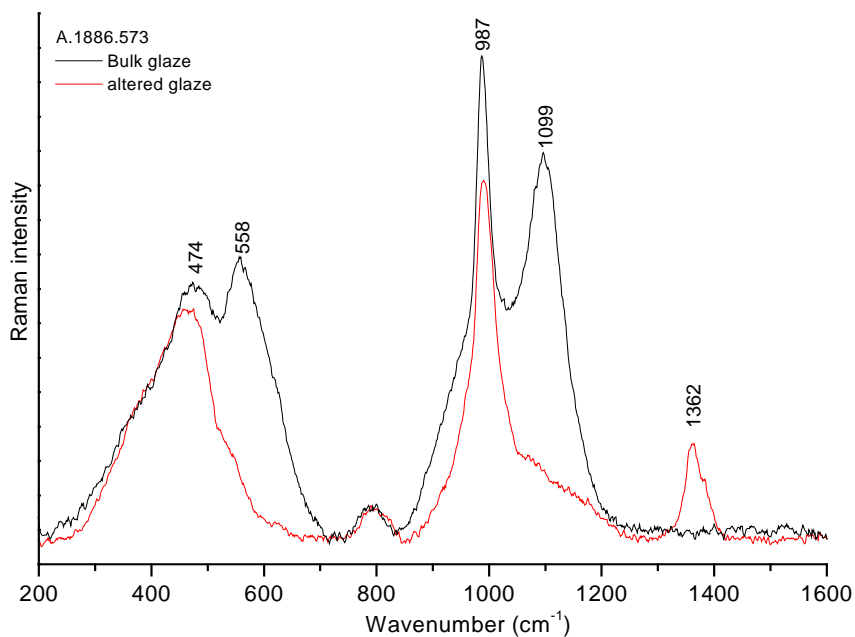


Figure IV- 34: Raman spectra of the bulk and altered glaze from ceramic A.1886.573.

The spectra of the bulk glasses could be decomposed using the model defined for alkali silicate glass, adding component for H.1992.392. The position of the  $B_{550}$  component indicated that the silicon content was relatively high in both glasses with  $X_2=0.84$  for the

glass necklace, and  $X_2=0.81$  for the glazed ceramic obtained based on Figure IV- 8. However the components could not be used to estimate the stability of the glasses based on the  $\nu Q^2/stretch$  area ratio because the lead and arsenic cations induced strong spectral changes as a result of their strong polarising effect on the NBO (**Appendix I**). This effect may account for the increased instability of these glasses, as it reduced the attraction force between  $Na^+$  and NBO, thus increasing the mobility of  $Na^+$ .

The modifications that occurred to the glass necklace and the glaze are characteristic of an alteration by leaching, with the depletion of alkali and the polyvalent cations retained in the structure. The presence of formates at the surface, as well as in the altered layer for the glaze, and the leached structure confirm that organic acids are responsible of this alteration.

## IV- 5.2 Depth profiling analyses

*In-situ* depth profiling Raman analyses using the confocal system were undertaken on the decanter glass. Spectra were recorded from the surface to increasing depths by progressively focusing the beam at known depths. The results obtained from confocal holes 100 and 50  $\mu m$  (corresponding volume of analysis given in Table II- 3) are presented in Figure IV- 35.

The two series showed an evolution of the spectra from the altered structure of the glass to the structure of the bulk glass. As we go in depth, we observed the presence of intermediate spectra between 32 and 36  $\mu m$  in both cases. These spectra are not associated with the presence of an intermediate structure in the glass but are linear combinations of the altered and bulk glass spectra, owing to a diameter of the spot along the vertical axis of 5 and 3  $\mu m$  for the 100 and 50  $\mu m$  confocal holes respectively. The thickness of the alteration layer was defined as the depth at which only the bulk glass structure was measured, which was at 36  $\mu m$  in the case of the 100  $\mu m$  confocal hole and 37.5  $\mu m$  for the 50  $\mu m$  confocal hole, with a precision of  $\pm 1 \mu m$ . These measurements were consistent with the 37  $\mu m$  thickness measured by SEM from a cross section of the glass, which indicated that Raman spectroscopy can be used to estimate non-destructively the depth of alteration on transparent glasses. As expected the measurement was slightly more accurate using the smaller confocal hole, however the use of smaller confocal holes implied the need of longer acquisition times owing to the signal intensity loss, which can be an inconvenient.

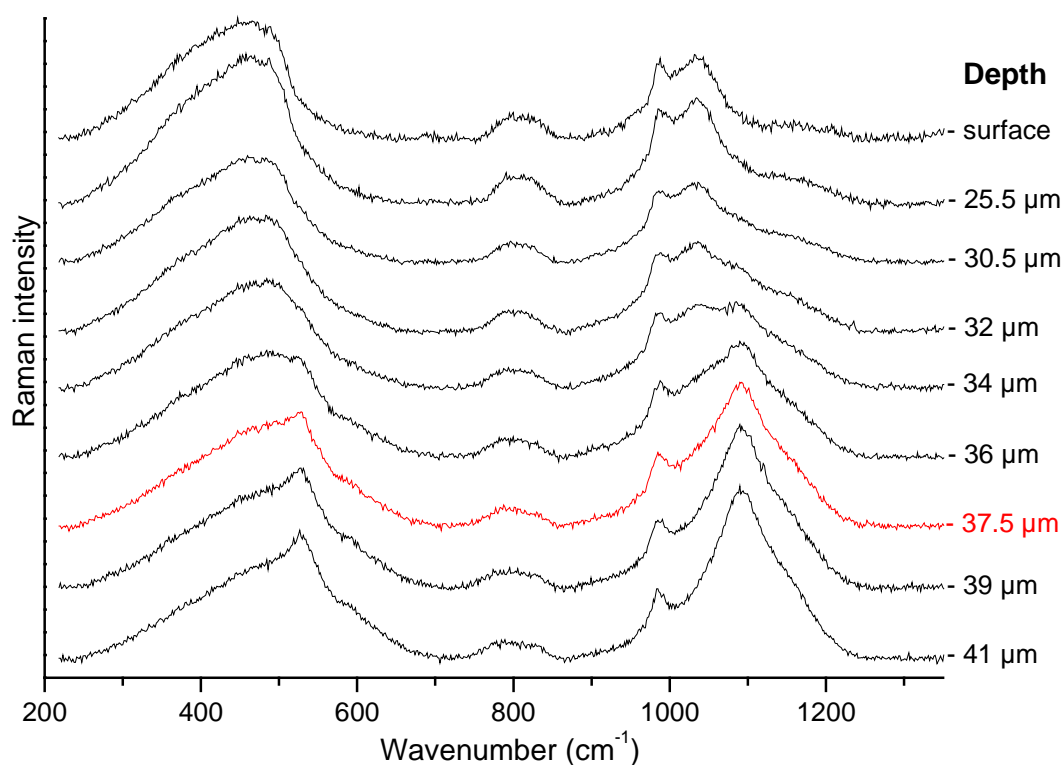
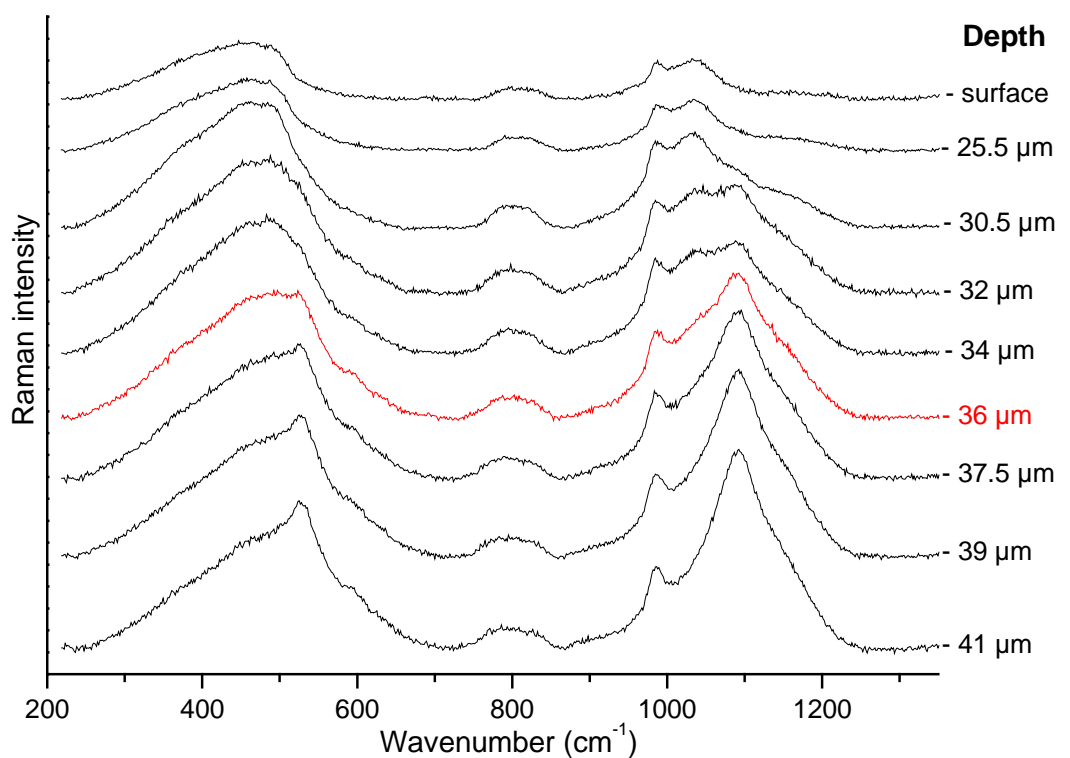


Figure IV- 35: In-situ measurements of the Raman spectra from the British decanter at varied depths for 600s with a x 100 lens and a confocal hole of (top) 100 μm or (bottom) 50 μm.

## IV- 6. Conclusion on the structure of soda silicate glass

The present investigation showed that Raman spectroscopy can provide a guide to the stability of a glass without the need for full compositional information. A first classification can be made without detailed analysis of the spectra between calcium silicate or lead silicate glasses, both of which are stable, and alkali silicate glasses, which have a mixed stability. In the case of alkali silicate glasses, a more detailed analysis is required to gain information on the different vibrational components which are associated with the type and concentration of cations. For this reason we developed a spectral decomposition method for analysing the spectra of these glass and correlations were established from the spectral components obtained. The position of the band at  $550\text{ cm}^{-1}$  was directly correlated to the silica content or the total cation charge, hence to the degree of polymerisation of the glass. This method proved most suitable for comparison of the degree of polymerisation within a similar compositional group, such as alkali silicate glasses. Another correlation was established between the total cation charge and the relative intensity of the band at  $950\text{ cm}^{-1}$ , associated with the vibration of  $Q^2$  species. This correlation indicates that the intensity of this band is mainly influenced by the content of doubly and triply charged cations, i.e. the stabilisers. Finally, a method based on the peak area ratio  $(A_{900}+A_{950}+A_{990})/(A_{900-1150})$  from the Raman spectrum was proposed to determine the stability of soda silicate glass. Although this method should be tested further, this demonstrates that Raman spectroscopy can help museums in assessing, *in-situ* and non-destructively, the general composition of their glass objects and the stability of their soda silicate glasses.

The present investigation confirmed the difference in the alteration process between a purely humid atmosphere, and a humid / acid-polluted atmosphere, showing that each environment generates a characteristic structural changes and visual appearance.

### **Humid acid-polluted atmospheres**

In acidic atmospheres, the leaching reaction is dominant and is maintained and the dissolution of the network is negligible. After alteration in an acidic atmosphere, the glass is visually unchanged although it is heavily hydrated. On dehydration, caused by exposure to very low RH or high temperature, loss of  $\text{H}_2\text{O}$  and condensation of silanols occur. Thus induces large cracks causing significant and irreparable damage to the glass and its visual

appearance. These cracks and fractures can lead to flaking off of the surface and ultimately complete disintegration of the object.

Selective leaching of alkali metal ions results in the disappearance of  $Q^3$  species and the formation of silanol species. These modifications in the glass are characterised by the decrease in intensity of the bands near 550 and 1100  $\text{cm}^{-1}$  in the Raman spectrum. The polyvalent cations in the glass, mostly stabilisers such as calcium, magnesium, or lead, are retained in the structure because they are coordinated much more strongly to the silicate [14, 40, 41]. As a consequence,  $Q^2$  species mainly coordinated to these species remain in the structure. The  $Q^2$  species display vibrational bands in the 900-1000  $\text{cm}^{-1}$  region of the Raman spectra, which appear as two components around 950 and 990  $\text{cm}^{-1}$  when the cation is calcium, or a single sharper component at 990  $\text{cm}^{-1}$  when the cation is lead or copper. To compensate for the loss of monovalent cations,  $\text{H}^+$  or  $\text{H}_3\text{O}^+$  is incorporated leading to the formation of silanols. New bands at 970-1000  $\text{cm}^{-1}$ , 1070-1080  $\text{cm}^{-1}$  and 1630  $\text{cm}^{-1}$  as well as the presence of a broad band in the 3000-3800  $\text{cm}^{-1}$  region in the Raman spectrum seem characteristic of this hydrated layer. In the meantime, the majority of the silanols formed reacts with one another and creates new bridging oxygen with the formation of Si-O-Si linkages as well as four fold  $D_1$  rings and molecular water. The new structure tends towards the structure of hydrated  $\text{SiO}_2$ . Formate groups are sometimes observed within the altered silicate structure, and possibly catalyzes the condensation of silanols as in silica gels [33, 34].

### **Humid non-acid atmosphere**

In humid atmospheres, a leaching reaction takes place at the beginning creating a very alkaline solution at the glass surface. In the absence of acid pollutants to lower the pH of the solution, the critical pH of 9 is rapidly reached and the dissolution reaction dominates the alteration. Because the products of the dissolution are not eliminated, as for the alteration in solution, a gel is created which contains hydrated silicate species  $\text{HSiO}_3^-$  and  $\text{SiO}_3^{2-}$  as well as the cations from the leached and dissolved structure.

After exposure to this humid atmosphere, the visual appearance of a glass is strongly modified and varies depending on the time and exposure conditions. It is mostly associated with a loss of transparency at the surface and the presence of iridescence in the first stage followed by the formation of an opaque layer, which has the characteristic appearance of a gel.

As soon as the gel dries, by a decrease in RH or increase in temperature, it solidifies by condensation of the species in the gel forming a new amorphous material with significant porosity. Crystalline products such as sodium carbonate may form at the surface or within the gel if there is contact with the air before condensation is complete. In the same way, new cations may be incorporated if these are in contact with the gel layer before condensation is complete. This is observed for archaeological glass or stained glasses, which incorporate new cations from the soil or the dust in the atmosphere respectively. Compared to the original glass structure, the structure of the altered layer is highly hydrated and more depolymerised, containing mainly  $Q^2$  species rather than  $Q^3$ . In particular, two modifications can be taken as characteristic marks of a congruent dissolution: the formation of a new band around  $670\text{-}680\text{ cm}^{-1}$  in the Raman spectrum of the altered layer and the formation of a blister pattern at the interface between the altered layer and the bulk glass. After alteration, the modified glass possesses three regions: a new amorphous hydrated material at the surface, a leached region and the bulk glass.

#### **Application to historic glass objects**

The absence of examples from the museum collection did not permit confirmation that the structure of the altered layer produced on the glass aged artificially at  $60\text{ }^\circ\text{C}$  reflects the situation in museums at ambient temperature. Although the production of the surface gel layer is a thermally activated process [35] and such significant and rapid breakdown would not be expected at ambient temperature, we might expect that the structure obtained for the gel layer formed in real conditions is similar to what the structure obtained through this study. Evidence for this comes from the observation that the visual and structural modifications of the NMS objects are similar to those created in acidic atmospheres by accelerated ageing experiments. This result suggests that organic pollutants are responsible for the alteration process and so the structural changes of the altered glass in the NMS objects. Moreover, Raman spectroscopy can be used to determine if a glass was altered by leaching or dissolution and so if it was exposed to an acidic atmosphere or not. Finally, this information, as well as the thickness of the altered layer, can be obtained *in-situ* and non-destructively by Raman spectroscopy.

## IV- 7. References

- 1 McMillan P., and Piriou B., Raman spectroscopic studies of silicate and related glass structure – a review, *B. Mineral.* **106** (1983) 57.
- 2 Galeener F.L., Planar rings in vitreous silica, *J. Non-Cryst. Solids.* **49** (1982) 53.
- 3 Tallant D.R., Bunker B.C., Brinker C.J., and Balfe C.A., Raman spectra of rings in silicate materials, *MRS Symp. Proc.* **73** (1986) 261.
- 4 Pasquarello A., and Car R., Identification of Raman defect lines as signatures of ring structures in vitreous silica, *Phys. Review Letters.* **23** (1998) 5145.
- 5 Nedelec J.M., Bouazaoui M., and Turrell S., Raman spectroscopic investigations of Mn<sup>2+</sup> doping effects on the densification of acid-catalysed silica xerogels, *J. Non-Cryst. Solids.* **243** (1999) 209.
- 6 McMillan P., Structural studies of silicate glasses and melts - applications and limitations of Raman spectroscopy, *Am. Mineral.* **69** (1984) 622.
- 7 Furukawa T., Fox K.E., and White W.B., Raman spectroscopic investigation of the structure of silicate glasses. III. Raman intensities and structural units in sodium silicate glasses, *J. Chem. Phys.* **75** (1981) 3226.
- 8 Mysen B.O., and Frantz J.D., Silicate melts at magmatic temperatures: in-situ structure determination to 1651°C and effect of temperature and bulk composition on the mixing behavior of structural units, *Contrib. Mineral. Petrol.* **117** (1994) 1.
- 9 Brawer S.A., and White W.B., Raman spectroscopic investigation of the structure of silicate glasses. I. The binary silicates, *J. Chem. Phys.* **63**, 6 (1975) 2421.
- 10 Matson D.W., Sharma S.K., and Philpotts J.A., The structure of high-silica alkali-silicate glasses. A Raman spectroscopic investigation, *J. Non-Cryst. Solids.* **58** (1983) 323.
- 11 Zotov N., Effects of composition on the vibrational properties of sodium silicate glasses, *J. Non-Cryst. Solids.* **287** (2001) 231.
- 12 Bunker B.C., Molecular mechanisms for corrosion of silica and silicate glasses, *J. Non-Cryst. Solids.* **179** (1994) 300.
- 13 Xue X, Stebbins J.F., Kanzaki M., Poe B., and McMillan P., Pressure-induced silicon coordination and tetrahedral structural changes in alkali oxide-silica melts up to 12 GPa: NMR, Raman, and infrared spectroscopy, *Am. Mineral.* **76** (1991) 8.
- 14 Karlsson C., Zanghellini E., Swenson J., Roling B., Bowron D.T., and Börjesson L., Structure of alkali alkaline-earth silicate glasses from neutron diffraction and vibrational spectroscopy, *Phys. Rev. B.* **72** (2005) 064206.
- 15 Tan J., Zhao S., Wang W., Davies G., and Mo X., The effect of cooling rate on the structure of sodium silicate glass, *Mater. Sci. Eng. B* **106** (2004) 295.

- 16 Mysen B.O., Virgo D., and Seifert F.A., The structure of silicate melts: implications for chemical and physical properties of natural magma, *Rev. Geophys. Space GE.* **20** (1982) 353.
- 17 Colomban P., Polymerisation degree and Raman identification of ancient glasses used for jewellery, ceramic enamels and mosaics, *J. Non-Cryst. Solids.* **323** (2003) 180.
- 18 Bonnet C., Bouquillon A., Turrell S., Deram V., Mille B., Salomon J., Thomassin J.H., and Fiaud C., Alteration of lead silicate glasses due to leaching in heated acid solutions, *J. Non-Cryst. Solids.* **323** (2003) 214.
- 19 Bunker B.C., Tallant D.R., Headley T.J., Turner G.L., and Kirkpatrick R.J., The structure of leached sodium borosilicate glass, *Phys. Chem. Glasses.* **29**, 3 (1988) 106.
- 20 Exarhos G.J., and Conaway W.E., Raman study of glass, water interactions, *J. Non-Cryst. Solids.* **55** (1983) 445.
- 21 Raman S.V., The effect of mixed modifiers on nuclear waste glass processing, leaching and Raman spectra, *J. Mater. Res.* **1** (1998) 8.
- 22 Ledieu A., Devreux F., Barboux P., Sicard L., and Spalla O., Leaching of borosilicate glasses. I. Experiments, *J. Non-Cryst. Solids.* **343** (2004) 3.
- 23 McMillan P.F., and Remmele R.L., Hydroxyl sites in SiO<sub>2</sub> glass: A note on infrared and Raman spectra, *Am. Mineral.* **71** (1986) 772.
- 24 McMillan P.F., Jakobsson S., Holloway J.R., and Silver L.A., A note on the Raman spectra of water-bearing albite glasses, *Geochim. Cosmochim. Acta.* **47** (1983) 1937.
- 25 Mysen B.O., Virgo D., Harrison W.J., and Scarfe C.M., Solubility mechanisms of H<sub>2</sub>O in silicate melts at high pressures and temperatures: a Raman spectroscopic study, *Am. Mineral.* **65** (1980) 900.
- 26 Stolen R.H., and Walrafen G.E., Water and its relation to broken bond defects in fused silica, *J. Chem. Phys.* **64**, 6 (1976) 2623.
- 27 Mysen B.O., and Virgo D., Volatiles in silicate melts at high pressure and temperature 2. Water in melts along the join NaAlO<sub>2</sub>-SiO<sub>2</sub> and a comparison of solubility mechanisms of water and fluorine, *Chem. Geol.* **57** (1986) 303.
- 28 Pandya N., Muenow D.W., Sharma S.K., and Sherriff B.L., The speciation of water in hydrated alkali silicates glasses, *J. Non-Cryst. Solids.* **176** (1994) 140.
- 29 Holtz F., Beny J.M., Mysen B.O., and Pichavant M., High-temperature Raman spectroscopy of silicate and aluminosilicate hydrous glasses: implications for water speciation, *Chem. Geol.* **128** (1996) 25.
- 30 Scholze H., Glass-water interactions, *J. Non-Cryst. Solids.* **102** (1988) 1.

- 31 Ryskin Y.I., *The infrared spectra of minerals*, Mineralogical Society, Farmer V.C., London (1974) 137.
- 32 Brawer S.A., and White W.B., Raman spectroscopic investigation of the structure of silicate glasses (II). Soda-alkaline earth-alumina ternary and quaternary glasses, *J. Non-Cryst. Solids* **58** (1977) 261.
- 33 Sharp K.G., A two-component, non-aqueous route to silica gel, *J. Sol-Gel Sci. Tech.* **2** (1994) 35.
- 34 Sharp K.G., and Scherer G.W., Interaction of formic acid with the silica gel network, *J. Sol-Gel Sci. Tech.* **8** (1997) 165.
- 35 Ryan J.L., The atmospheric deterioration of Glass: Studies of decay mechanisms and conservation techniques, *PhD thesis*, University of London (1996).
- 36 Dal Bianco B., Bertonecello R., Milanese L., and Barison S., Glasses on the seabed: surface study of chemical corrosion in sunken Roman glasses, *J. Non-Cryst. Solids* **343** (2004) 91.
- 37 Dran J.-C., Petit J.-C., and Brousse C., Mechanism of aqueous dissolution of silicate glasses yielded by fission tracks, *Nature*. **319** (1986) 485.
- 38 Hench L.L., and Clark D.E., Physical chemistry of glass surfaces, *J. Non-Cryst. Solids*. **28** (1978) 83.
- 39 Rebiscoul D., Van der Lee A., Rieutord F., Ne F., Spalla O., El-Mansouri A., Frugier P., Ayral A., and Gin S., Morphological evolution of alteration layers formed during nuclear glass alteration: new evidence of a gel as a diffusion barrier, *J. Nucl. Mater.* **326** (2004) 9.
- 40 Roling B., and Ingram M.D., Determination of divalent cation mobilities in glass by dynamic mechanical thermal analysis (DMTA): evidence for cation coupling effects, *Solid State Ionics*. **105** (1998) 47.
- 41 Boksay Z., Bouquet G., and Dobos S., Diffusion processes in the surface layer of glass, *Phys. Chem. Glasses*. **4** (1967) 140.

## **Chapter V.**

# **MECHANISMS AND KINETICS OF THE ALTERATION**

## V- 1. Introduction

This chapter aim is to establish the mechanisms and kinetics of the alteration of the soda silicate glasses RG1 exposed to organic polluted atmospheres in museums compared to non-polluted atmospheres.

As already mentioned or observed within the previous chapters, alkali ions are preferentially leached out of the glass with alteration in humid atmosphere, with the depth of alkali depletion increasing with time. For this reason, SIMS depth profiling has been increasingly applied to examine the alteration of alkali silicate glass by measuring the alkali concentration depth profile. SIMS profiling was applied in particular by Ryan and Fearn to examine the corrosion of soda silicate glass in museum atmospheres [1, 2, 3]. In the study undertaken by Ryan, the RG1 glass composition was aged at elevated temperature and RH in order to obtain alteration depths that could be measured by SIMS. The problem is that ageing glass at elevated temperature is not an accurate representation of the long-term ageing under ambient conditions. For this reason low energy SIMS was used by Fearn to provide the nanometre depth resolution necessary to follow the first stage of the alteration at room temperature [2, 3]. Figure V- 1 presents the sodium concentration depth profile obtained by Fearn for the RG1 glass aged at 55 % RH for duration between 48 and 96 hours [3].

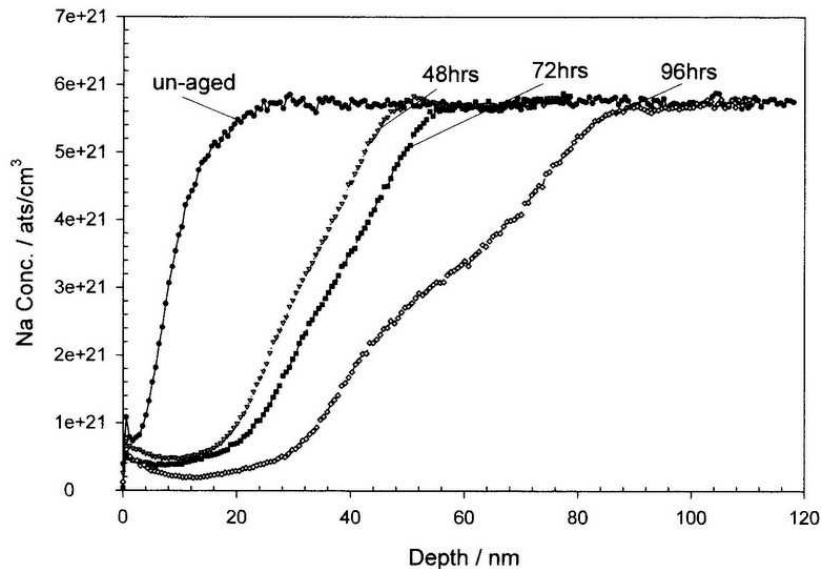


Figure V- 1: Sodium depth profiles for RG1 glasses aged at 55 % RH and room temperature for 48, 72 and 96 hours and compared to the un-aged glass; obtained by Fearn [3].

The SIMS instrument at Imperial College was able to examine the profile of the freshly made RG1 glass (1 day old) used in this research, and showed that even the un-aged blown glass was depleted in sodium at its near surface over approximately 22 nm (Figure V- 1). This loss of sodium is mainly the result of the glass blowing process, whereby volatile elements such as sodium are lost as the glass is repeatedly returned to the glory hole during fabrication [3]. Plates of this RG1 glass were stored under dry nitrogen before use and were given to us approximately 8 months after its fabrication. Although it was not possible to measure the sodium depletion depth just before use in the present experiments, it was estimated that a sodium depleted layer of approximately 40 nm was present based on measurements made by Fearn of the RG1 glass stored for 358 days in dry N<sub>2</sub> (not published).

The depth resolution available on the instrument at Edinburgh University was poorer with approximately 10 nm, similar to the one used by Ryan. In order to obtain glass alterations measurable by SIMS for this research, while ageing under ambient conditions, it was decided to increase the ageing time. Thus, the kinetics of the alteration that was established over a year exposure was more representative of the long-term ageing of glass in museums. Moreover, the ageing of glass in real atmospheres had the advantage of taking into account the effect of the environmental yearly cycle in the alteration process. In addition different parameters expected to affect the alteration are examined through this chapter including: RH, type of organic pollutants, pollutant concentration, time, and the presence of CO<sub>2</sub> with light.

Although the spectral characteristic and morphology of the crystalline products formed on glass will be dealt in a separate chapter (chapter V), the identification of the products formed on the aged glass will be given along with the SIMS results to help in the interpretation and determination of the alteration mechanisms.

A description of the data treatment is detailed in the first part of this chapter and followed by the results from the analyses of the aged glasses. At the beginning of the results chapter a section is devoted to assessing the reliability of the SIMS measurements using data obtained through this investigation.

## V- 2. Data treatment

### V- 2.1 Interference correction

The separation of different ions by the mass spectrometer is based on their mass / charge ratio as described in chapter II. The mass spectrometer is thus tuned to the mass of the isotope of interest ( $^1\text{H}$ ,  $^{23}\text{Na}$ ,  $^{24}\text{Mg}$ ,  $^{27}\text{Al}$ ,  $^{30}\text{Si}$ ,  $^{39}\text{K}$ ,  $^{40}\text{Ca}$ ) and a signal is measured in counts per second (cps), and recorded. The ability of the spectrometer to separate two masses varies with the mass resolution of the instrument. Because some elements have several isotopes and the sputtering process induces the formation of charged molecular species such as oxides, interferences can occur for some selected ions, increasing their signal intensity. Corrections can be applied to the raw intensity signal  $I^{\text{raw}}$  to eliminate the contribution of these interfering species. The corrected intensity signal (in cps) is called here  $I^{\text{cor}}$ . In the case of the analyses undertaken at the University of Edinburgh, corrections were applied to the signal of  $^{24}\text{Mg}$ , for its interference with  $^{48}\text{Ca}$ ,  $^{39}\text{K}$  with  $^{23}\text{Na}^{16}\text{O}$ , and  $^{40}\text{Ca}$  with  $^{40}\text{K}$  and  $^{24}\text{Mg}^{16}\text{O}$ .

### V- 2.2 Sputter rate and depth quantification

The SIMS data are converted to depth by measuring the depth of the crater created by sputtering at the end of the analysis (see chapter II). Knowledge of the sputter rate is important to establish depth quantification. Sputter rate calculations are affected by errors on the depth measurement of the crater, the flatness of the sample, the primary beam focus, but above all the structure of the material analysed, which is known as the 'matrix effect' [4]. The matrix effect modifies the sputter rate with the structure of the matrix sputtered. Previous studies showed that higher sputter rate were obtained for the altered layer compared with the bulk on potash lime glasses leached in acidic solution [4] and on medieval potash silicate glass weathered in atmospheric conditions [5]. Ryan showed however that the sputter rate did not change for the alkali depleted layer but differed for the gel layer compared to the bulk in RG1 glass [1]. This difference is induced by the very different structure of the altered layers. In the present investigation, the leaching reaction was generally the dominant alteration process so mostly alkali depleted layers were created.

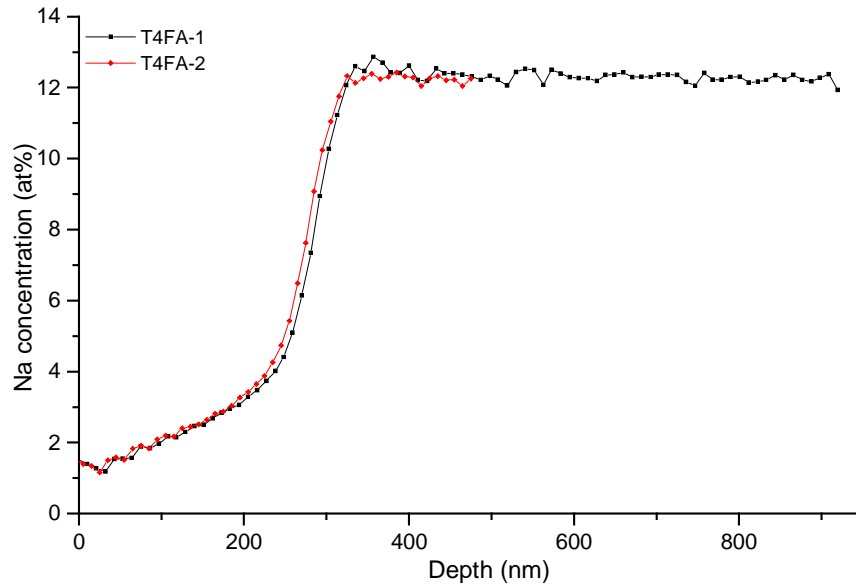


Figure V- 2: Sodium depth profile of T4FA glass: measurements made on two different locations for different collection time.

The measurements in this study show that the sputter rate did not change in the leached layer since it is not affected by the thickness of the altered layer or the proportion altered/bulk measured (Figure V- 2). Consequently, the sputter rate was assumed to be constant during the analysis, and the sputter rate  $S_R$  was calculated by dividing the crater depth directly by the number of cycles, corresponding to the number of sputtered layers, as in equation {V-1}:

$$S_R = \frac{\text{crater depth}}{\text{number of cycle}} \quad \{V-1\}$$

The depth for each measurement was obtained by multiplying the cycle number of each measurement by the sputter rate  $S_R$  and deducting the thickness of the gold layer.

### V- 2.3 Ion yield and elemental profile quantification

The ion yield (IY) is defined as the number of ions detected per atom of a species sputtered from a sample. It depends on the ionisation probability of the element (associated with the electronic configuration), as well as instrumental parameters such as the acceleration potential of the secondary ions, the energy bandpass of the mass spectrometer, the energy and polarity of the secondary ions analysed and the mass resolution of the instrument [6]. For this reason, all ion yields are calculated with reference to an element, which is used as an internal standard to correct the instrumental variation that occurs between samples, such as slight changes in beam size or intensity. The value obtained corresponds to the relative ion yield  $RIY$ . In minerals and glasses, Si is used as the reference, then  $RIY_{Si} = 1$ . The ion yield is often calculated based on materials of known composition, preferably similar to the material studied. Figure V- 3 shows the variations of the  $RIY$  for all the elements between H and U measured predominantly from standard glass SRM610 with the Cameca ims 4f SIMS of the University of Edinburgh under conditions similar to the present study.

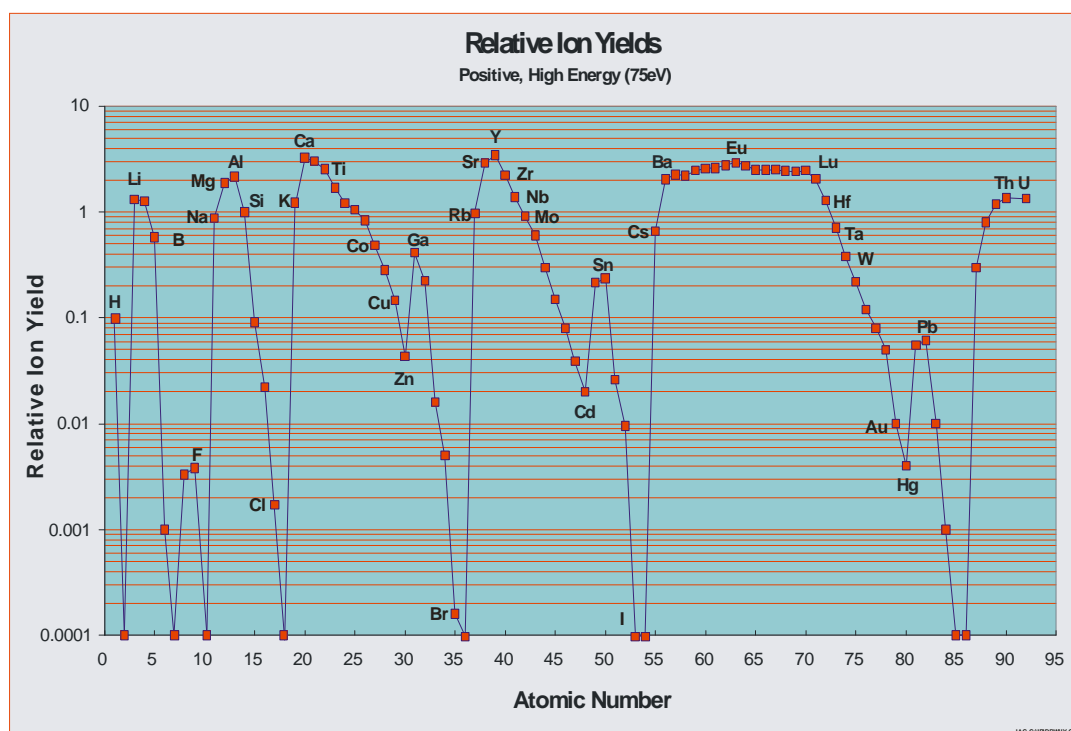


Figure V- 3: Ion yield value for the elements in the periodic table measured on standard glass SRM610 with the Cameca 4f SIMS of the University of Edinburgh [7].

In the present study the RIY of the different elements analysed was determined for each glass sample directly from the region of the bulk glass in the profile, for which the composition was accurately determined by EPMA. This method, which is equivalent to the relative sensitivity factor (RSF) method [4], provides accurate elemental concentration by SIMS and is applicable when the altered layer and the bulk glass have the same major elemental composition (Si and O) [4]. In that case, the intensity  $I^{cor}$  of each element was averaged over the last six measurements in the bulk glass. The calculation of the relative ion yield applied is given in equation {V-2}.

$$RIY_{Na} = \frac{I_{Na}^{cor}}{\left( \frac{I_{Si}^{cor}}{C_{Si}} \right) C_{Na}} \quad \{V-2\}$$

$C_{Si}$  and  $C_{Na}$  correspond to the concentration in at% of these elements in the bulk glass and  $I^{cor}$  the corrected signal intensity (in cps) of the element averaged from the bulk glass region measurements.

To determine the **elemental concentration**, the secondary ions intensity measured for each sputtered layer was converted into concentration using the relative ion yield determined internally and by assuming that the Si content in the glass remained constant throughout the glass after alteration. Thus, the concentration in at% of the element for each measurement was determined according to the equation {V-3}

$$C_{Na} = \frac{I_{Na}^{cor}}{\left( \frac{I_{Si}^{cor}}{C_{Si}} \right) RIY_{Na}} \quad \{V-3\}$$

$C_{Si}$  corresponds to the concentration of Si in at%, which is supposed constant and equal to concentration in the bulk glass, and  $RIY_{Na}$  corresponds to the ion yield of Na determined from equation {V-2}.

## V- 2.4 Quantitative measurement of the alteration

Based on the quantitative determination of the depth and elemental concentration obtained in the previous sections, a concentration/depth profile could be plotted for each element. Because alkalis are preferentially leached and sodium is the main alkali in the glass used in the experiments, the progress of the glass alteration was followed by examining the sodium variation as a function of depth. The sodium concentration depth profile of an altered soda silicate glass has an S-shape characteristic of a diffusion controlled mechanism (Figure V- 4).

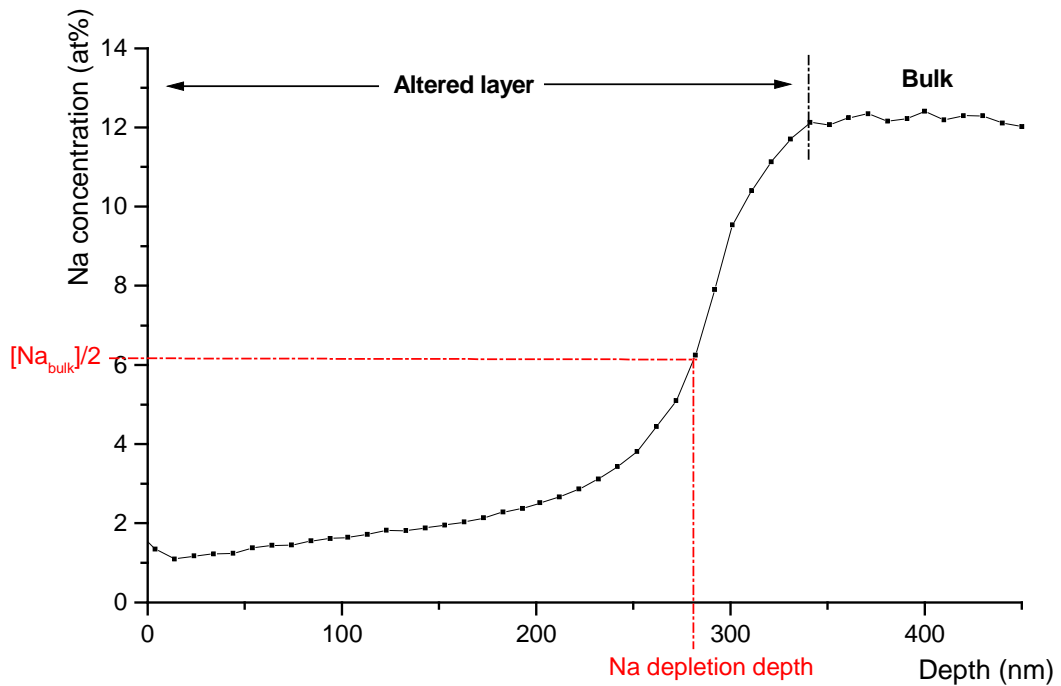


Figure V- 4: Sodium concentration depth profile of a soda silicate altered glass.

This profile can be separated into two regions: the altered layer at the surface generally depleted in alkali; and the bulk glass where the concentration of all elements reaches the bulk glass concentration and stabilises. At the interface of these two regions is an intermediate region where the alkali content increases rapidly. This region corresponds to the reaction front where the ion-exchange takes place [1]. In order to follow the alteration and so determine the kinetics of this alteration, it is necessary to obtain quantitative and comparable measurements of the altered region. The method generally used is based on the measurement

of the alteration depth, considered as the depth at which half of the element content of the bulk is reached (Figure V- 4) [3, 8, 9]. The inconvenience of this method is that it does not take into account the amount of alkali leached within each altered layer, which may be a problem in determining the real effect of the different atmospheres. For this reason, we propose to examine in parallel the amount of atoms leached within the glass surface by calculating for each sputtered layer (each cycle) the amount of atoms lost relative to the bulk, and integrate this result over the entire altered region. The calculation for sodium is given by equation {V-4}:

$$Q = \int_{\text{surface}}^{\text{bulk}} (C_{\text{Na}}^{\text{bulk}} - C_{\text{Na}}) S_{\text{R}} \times D \quad \{\text{V-4}\}$$

with  $Q$ : Total sodium atom depleted per  $\text{nm}^2$  ( $\text{at}/\text{nm}^2$ )

$C_{\text{Na}}^{\text{bulk}}$ : concentration of Na in at% in the bulk

$C_{\text{Na}}$ : concentration of Na in at% in the altered layer for cycle

$S_{\text{R}}$ : sputter rate ( $\text{nm}/\text{number of cycle}$ )

$D$ : atomic density of the glass given as number of atoms per volume ( $\text{ats}/\text{nm}^3$ ), constant for a glass

The atomic density of the glass is not known, however, this parameter being constant for each glass replica, comparison can be made between samples of the same replica.

No quantitative data could be gained from the H profile measurements since there was no internal reference available to determine the corresponding *RIY*. Moreover quantitative measurement at room temperature and under vacuum of hydrogen concentration in altered glass is not reliable as it is influenced by the out gassing of water [10]. Consequently, the H profiles presented in this study are only used to determine the relative variation of this element in the materials as a function of depth.

## V- 3. Results

### V- 3.1 Reliability of the SIMS measurements

#### V- 3.1.1 Size of the analysed area

The area sputtered could be modified by changing the gated signal in order to vary the sputter rate, as described in chapter II. The effect of the sputter rate on the sodium concentration depth profile, modified by changing the analysed area (see section II-4.2.2), is examined for two different altered glasses (Figure V- 5).

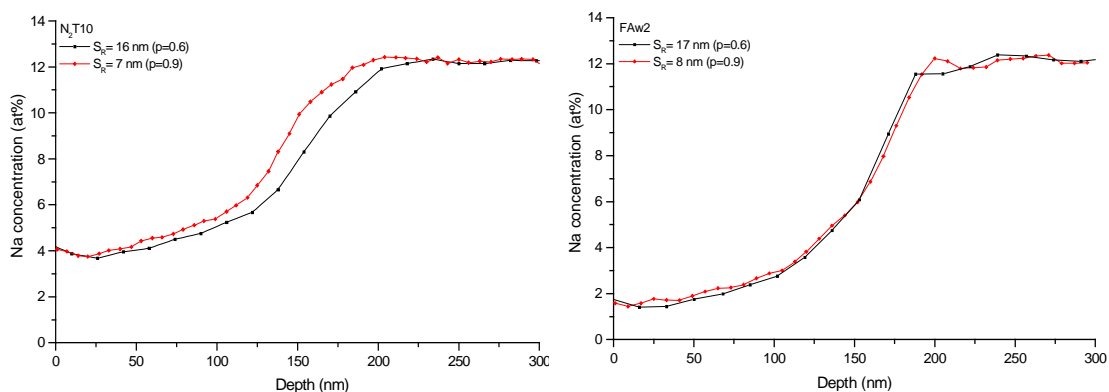


Figure V- 5: Sodium depth profile of N<sub>2</sub>T10 and Faw2 samples analysed at two different sputter rates.

Slower sputter rates provided more detail on the concentration variation and so the profile was slightly different than under faster sputter rates where each measurement was averaged over a larger analysed volume. The use of slower sputter is essential where concentration variations are small; however it implies that more time is required for the analysis of each sample. Because the samples analysed in this study were aged over a long time period and aggressive environments were used, the alteration in the glass was quite extensive and generally very different from one sample to another. For this reason, the size of the analysed area on all samples was fixed (except in the short term experiments over 3 weeks) with  $p=0.6$ , corresponding to sputter rates between 10 and 17 nm/cycle. Although the size of the analysed window was fixed, the sputter rate varied along 18 months use of the SIMS owing to variations in the primary beam density. A slower sputter rate of 7-8 nm/cycle ( $p=0.9$ ) was only used on the RG1 series aged in artificial atmosphere over 3 weeks.

### V- 3.1.2 Different SIMS instrument

The concentration profiles measured on two different instruments were compared based on a series of samples aged in the same experiment. The SIMS instrument at the University of Edinburgh was compared to the low-energy SIMS instrument at Imperial College, which allows nanometre depth resolution in dynamic mode. The differences between the instrument and the analysis conditions are described in section II-4.2.2. The sodium depth profiles measured on the samples aged in formic acid and N<sub>2</sub> atmospheres by both instruments are compared in (Figure V- 6).

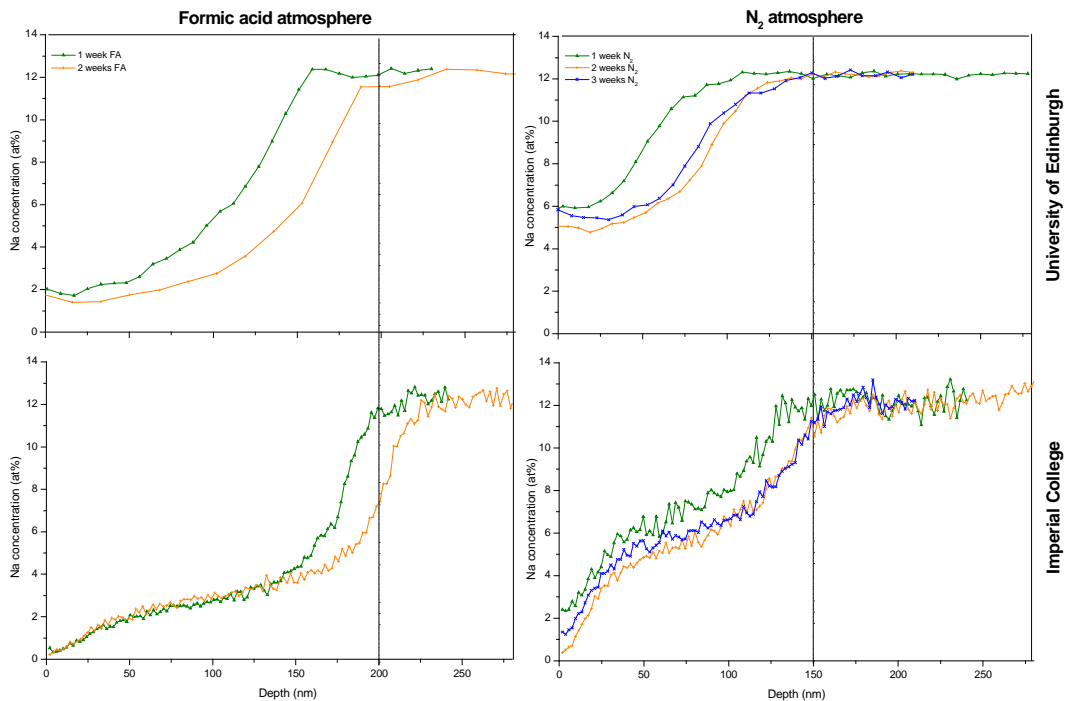


Figure V- 6: Sodium depth profiles evolution of the RG1 glasses exposed to formic acid and N<sub>2</sub> atmospheres between 1 and 3 weeks from the University of Edinburgh or Imperial College SIMS.

The measurements from the two instruments show the same evolution of the profiles and sodium concentration in the altered layer. However, all the profiles from the Imperial College instrument display an almost complete depletion of sodium in the first 20 nm and are shifted by ~40 nm to higher depths compared to the University of Edinburgh instrument. The presence of the gold layer and its contamination effect at the surface of the University of Edinburgh samples may account for that difference. These results indicate that the measurements obtained from the University of Edinburgh instrument are valid but the evolution of the alteration should only be assessed from measurements obtained from a same instrument.

### V- 3.1.3 Sample and instrumental reproducibility

The instrumental reproducibility and the homogeneity of the altered layer were assessed by measuring the sodium depth profile at two different locations on most of the samples. Good reproducibility of the measurements was obtained on all the samples which indicated that the altered layer was homogeneous (Figure V- 7). A good reproducibility was also observed between two separate samples exposed to the same conditions.

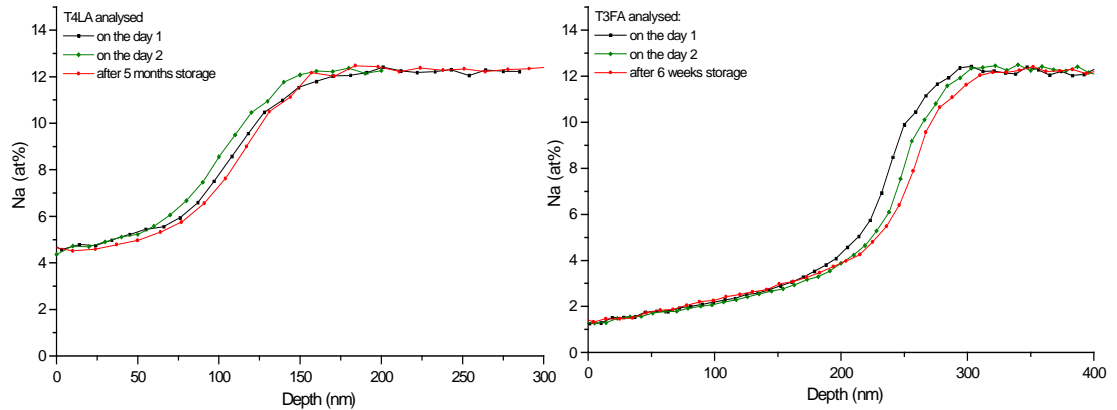


Figure V- 7: Sodium depth profile of T4LA and T3FA glasses analysed in different locations on the day they came out of the experiments and after storage for different durations.

Because all samples could not be analysed on the day they came out of the experiments, these were stored at low RH and temperature to limit further alteration until they could be analysed. Comparison of the measurements taken on the samples on the day they came out of the experiment and after several weeks or months of storage, indicated that storage does not affect the alteration layer (Figure V- 7).

### V- 3.2 Effect of CO<sub>2</sub> (series 1)

The possible formation of formic acid through the interaction of silicate with CO<sub>2</sub>, water and light was investigated by exposing the RG1 glass for 6 weeks to 100% RH and saturated CO<sub>2</sub> atmosphere, either in the light or in the dark. For comparison, glasses were exposed to ambient air or N<sub>2</sub> at 100 % RH. Due to the high humidity, all glass surfaces were covered with liquid at the end of the experiment. The pH of this liquid was 8-9 for glass exposed to pure CO<sub>2</sub>, 9-11 for the glass exposed to ambient air and 10-11 for the glass kept under N<sub>2</sub>. As the solution dried, crystals formed at the surface appearance (Figure V- 8).

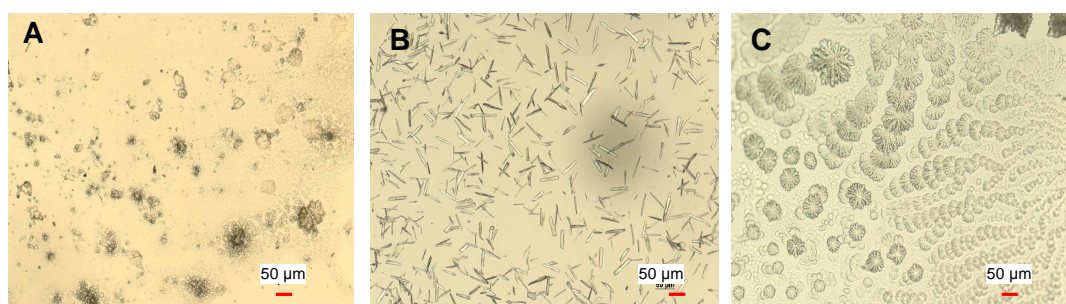


Figure V- 8: Light microscopy images of the RG1 glass surface after exposure to 100 % RH, light and (A) ambient air, (B) N<sub>2</sub>, or (C) saturated CO<sub>2</sub> atmosphere.

The exposure of the RG1 glass to high humidity altered the glass over a thickness ranging between 200 and 600 nm (Figure V- 9 and Figure V- 10). The altered layer was depleted in alkali (Na and K) and highly hydrated as a result of selective leaching. An apparent enrichment in alkaline-earth ions (Ca and Mg) is observed in this region as a result of the loss of the other constituents in the glass. At the interface between the altered and the bulk glass, the potassium profile displays a peak towards lower concentration, which was previously referred to as the ‘K peak’ [1]. A similar peak, less marked, appears in the sodium profile just after reaching the bulk concentration. The presence of this peak is an indication that the ion-exchange reaction is taking place at this reaction front [1].

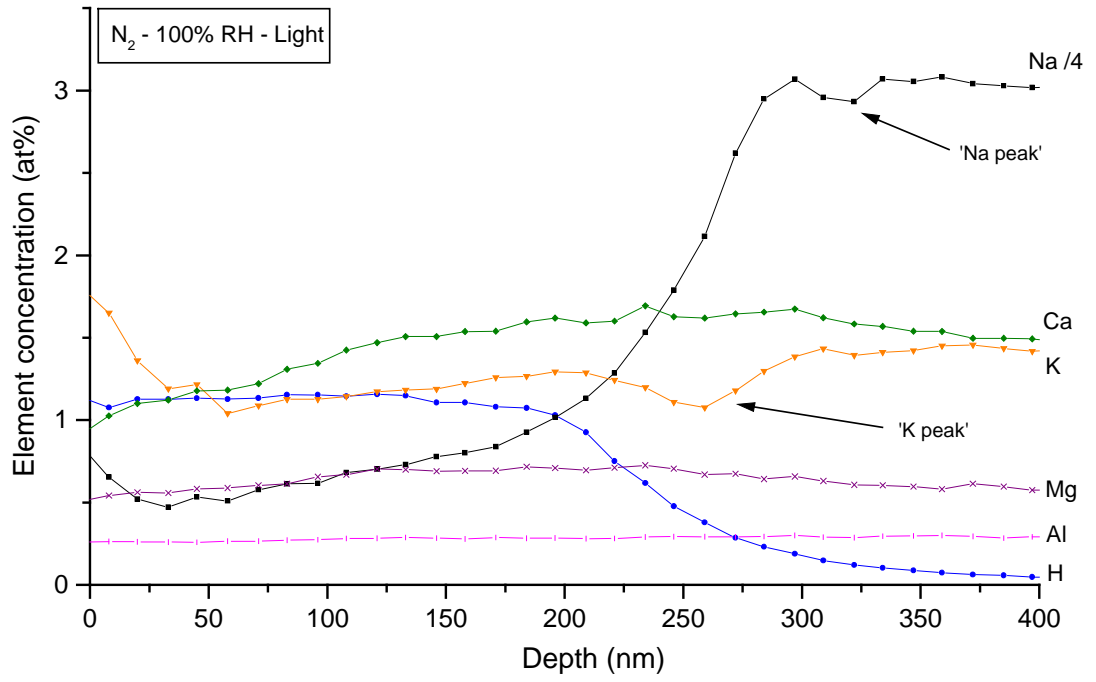


Figure V- 9: Elemental depth profile for RG1 glass exposed to 100% RH and N<sub>2</sub> atmosphere with light.

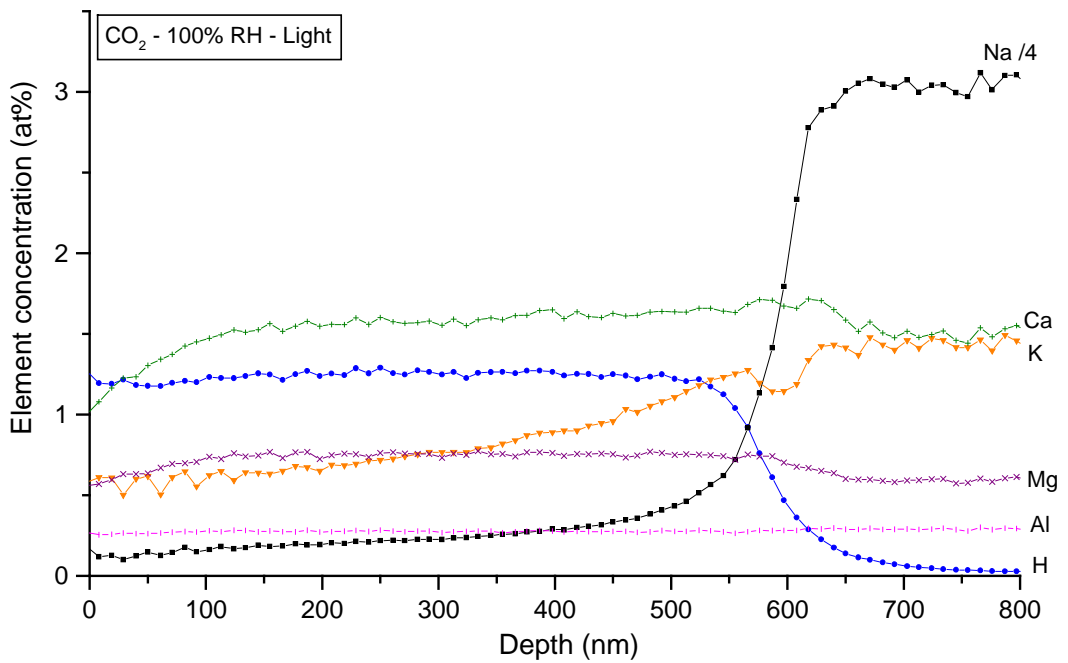


Figure V- 10: Elemental depth profile for RG1 glass exposed to 100% RH and saturated CO<sub>2</sub> atmosphere with light.

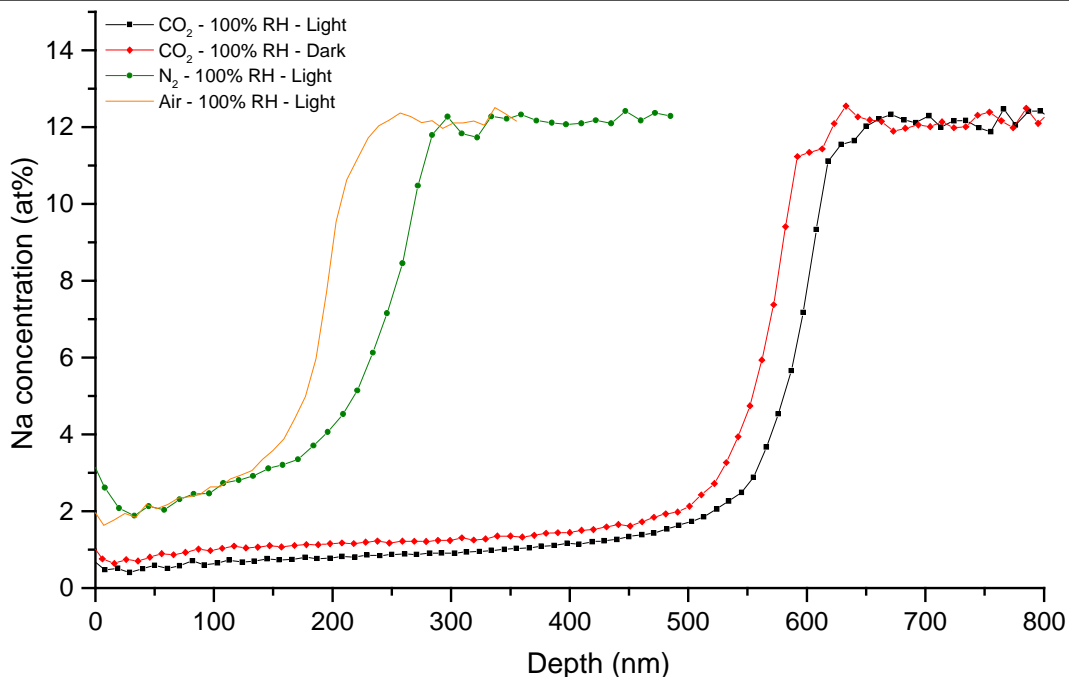
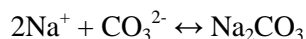
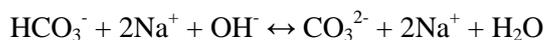


Figure V- 11: Comparison of the sodium depth profiles measured on the RG1 glass exposed to 100% RH with saturated CO<sub>2</sub> with or without light, N<sub>2</sub> and ambient air atmospheres.

The presence of high CO<sub>2</sub> concentration caused greater alkali depletion to the glass compared to the non-polluted atmosphere (Figure V- 9, Figure V- 10 and Figure V- 11). A similar alteration increase with the CO<sub>2</sub> compared to N<sub>2</sub> atmospheres was measured by AFM on lithium, sodium and potassium silicate glasses exposed to RH between 5 and 55 % and ambient temperature [11]. Moreover, the CO<sub>2</sub> atmosphere increased the leaching of alkali in depth as well as within the altered layer. Thus the remaining sodium content in the altered layer is approximately 2 at% for glass exposed to N<sub>2</sub> or ambient air, and around 0.5 at% for glass exposed to high CO<sub>2</sub>. In contrast, the glasses exposed to N<sub>2</sub> show a surface enrichment in alkali. This enrichment, observed by Ryan for RG1 glass aged various RH, was associated with the presence of a gel layer formed after dissolution of the silicate matrix [1]. These results indicate that the different pH of the solution at the surface of the glass induced different reaction and thus different altered layers. In both atmospheres, the water from the humidity caused the leaching of the alkali creating an alkaline film solution at the glass surface. The presence of carbon dioxide, whose solubility is enhanced at greater pH, reduced the pH of the liquid film through the following reactions [11, 12]:



Consequently the dissolution of the network enhanced above pH 9 was avoided and the leaching reaction was enhanced. Moreover, these reactions induced the precipitation of sodium carbonates, which are much more hygroscopic than the glass surface, and caused more water condensation, increasing further the leaching reaction. In contrast, the inert N<sub>2</sub> atmosphere, as well as the low polluted ambient air, favoured the NaOH build up at the glass surface by reaction of the glass and water. Confirmation that NaOH had formed comes from the observation that, on removal from the desiccators, the solution reacted with atmospheric CO<sub>2</sub> to form hydrates of Na<sub>2</sub>CO<sub>3</sub>. The alkaline solution sitting on the glass surface induced dissolution of the silicate matrix and formation of the gel layer. The thickness of the gel layer observed in the SIMS profiles is likely to be underestimated because the gel is expected to be sputtered away at a faster rate due to the very different structure and high porosity of this layer [1].

The presence of light did not have a significant effect on the alteration of glass exposed to high CO<sub>2</sub> atmospheres. The slight difference observed between light and dark experiments most likely results from experimental variation such as a slight temperature difference, expected between light and dark. Furthermore, no formates were identified in the crystalline deposits at the glass surface, but only carbonates in both light and dark experiments. These crystalline deposits, identified by Raman spectroscopy, include sodium carbonate mono- and deca-hydrate and sodium hydrogen carbonate, plus another as yet unidentified hydrated carbonate. These results indicate that the formic acid formation observed with silicate rocks [13] has not occurred with this glass composition.

### V- 3.3 Effect of RH and organic pollutants (series 2)

The present experiment investigated the effect on the RG1 and RRn glasses of different RHs, at 40, 50 and 60 %, and the effect of organic pollutants, mostly acetic and formic acids. As a result of the exposure, crystalline deposits formed at the glass surface whose appearance varied with the atmosphere (Figure V- 12).

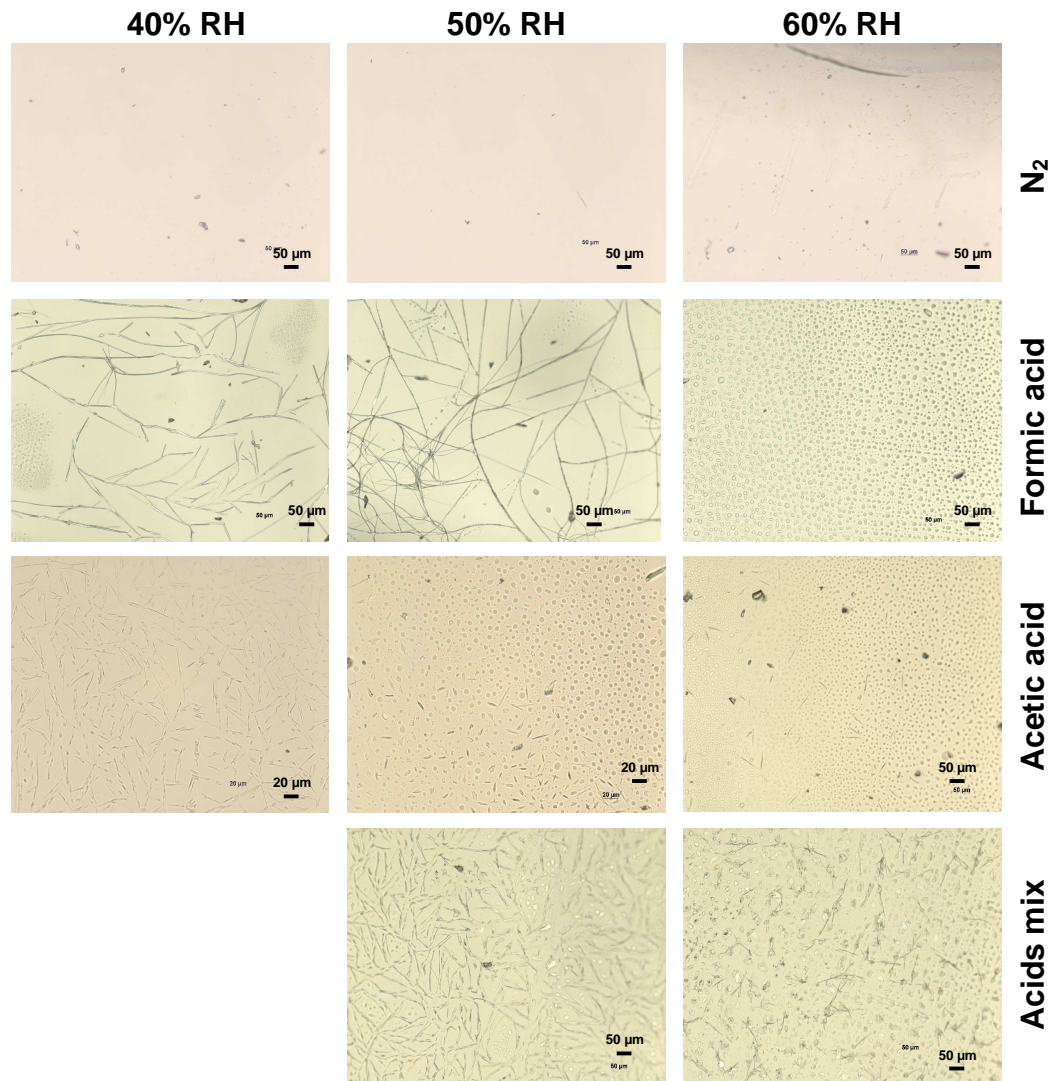


Figure V- 12: Light microscopy images of the RG1 glass surface after exposure to  $N_2$ , acetic and/or formic acids atmospheres at 40, 50 and 60 % RH. (background colours variation are caused by the change in lighting condition of the microscope).

Very few deposits were observed on the glasses exposed to the N<sub>2</sub> atmosphere, except for the presence of a thin dendrite crystal on the edge of the glass exposed at 60 % RH (Figure V- 12), which was too small to be analysed.

In the formic acid atmospheres, the deposits of sodium formates were present as crystals in the form of long filaments or block crystals at 40 and 50 % RH and liquid droplets at 60 % RH. The crystalline products analyses presented in chapter III showed that the block crystals were identified as sodium formate II while the filaments and needles were identified as sodium formate I'. Sodium formate deliquesces between 50 and 52 % RH at 25 °C [14], which explains the presence of droplets on the glass exposed at 60 % RH. When the droplets were dried, sodium formate phase II crystals were formed. These results suggest that the formation process of sodium formate phase I' may be influenced by RH.

When the glass was exposed to pure acetic acid atmospheres, needles of sodium acetate anhydrous were formed, which partly deliquesced at 50 % RH. This is consistent with the known deliquescence point of sodium acetate between 43.5 and 45.2 % at 25 °C [14].

However, when the glasses were exposed to an atmosphere containing both acids, with the concentration of acetic acid being twice that of formic acid, only sodium formate phase II and I' were formed.

The exposure to different acid-polluted and non-polluted atmospheres, at 40, 50 and 60 % RH, modified the glass over a depth ranging from 150 to 250 nm (Figure V- 13 and Figure V- 14). As in the previous experiment, the glass exposed to an acid atmosphere only displayed a leached layer depleted in alkali and highly hydrated with an apparent enrichment in alkali-earth ions (Figure V- 14); while the glass exposed to the N<sub>2</sub> atmosphere displays a smaller leached layer with a gel layer, responsible of the alkali enrichment, at the near surface (Figure V- 13). The K peak at the bulk glass / leached layer interface is only visible in the profile of the glasses exposed to acid atmospheres.

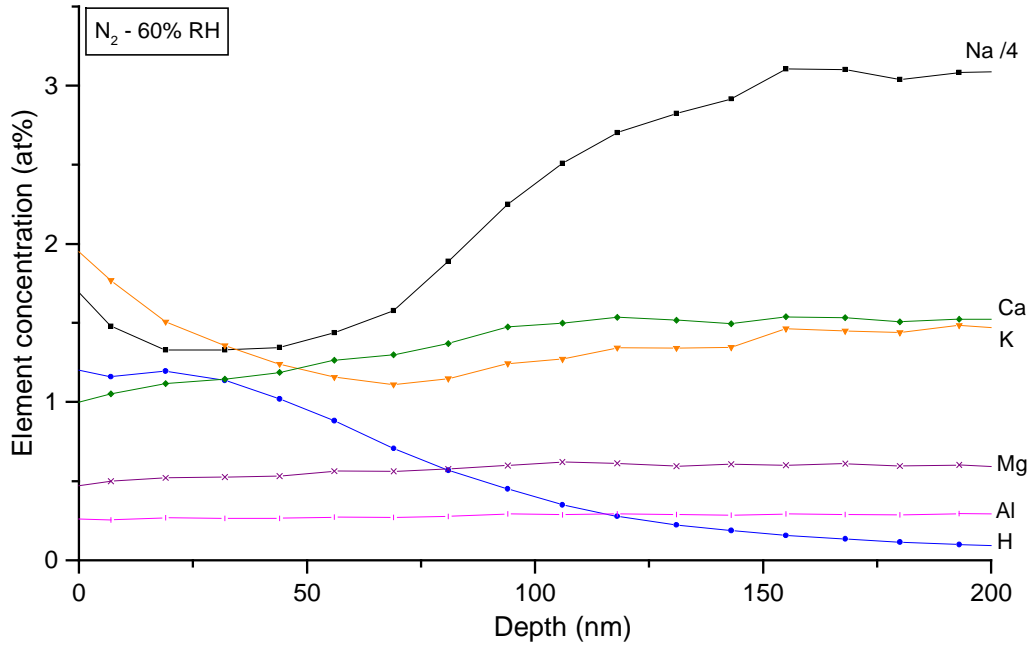


Figure V- 13: Elemental depth profile for RG1 glass exposed to 60 % RH and N<sub>2</sub> atmosphere.

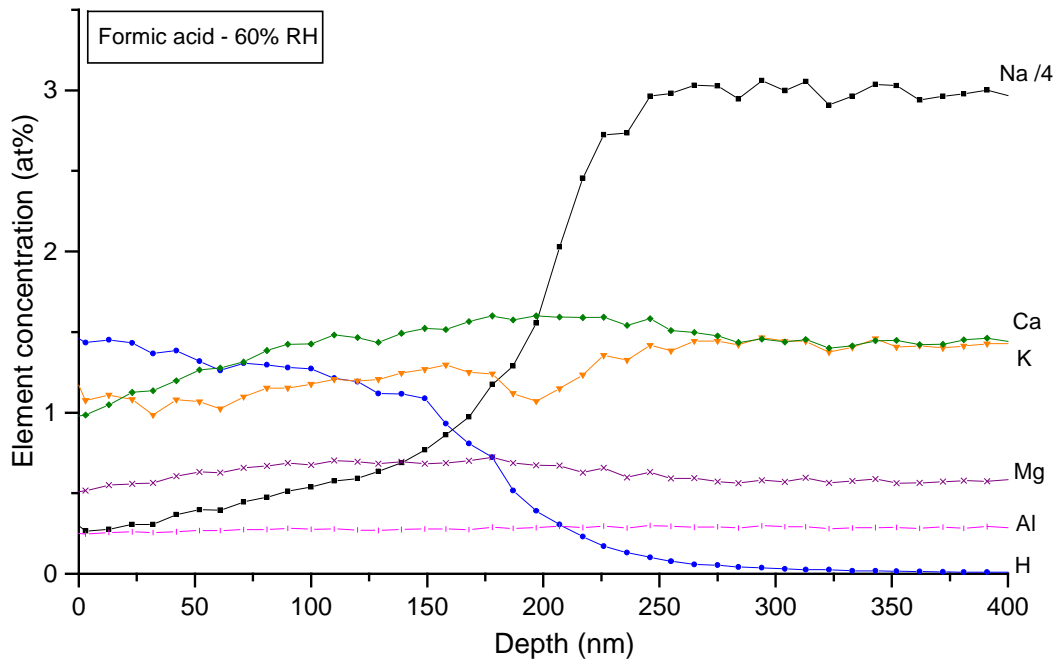


Figure V- 14: Elemental depth profile for RG1 glass exposed to 60 % RH and formic acid atmosphere.

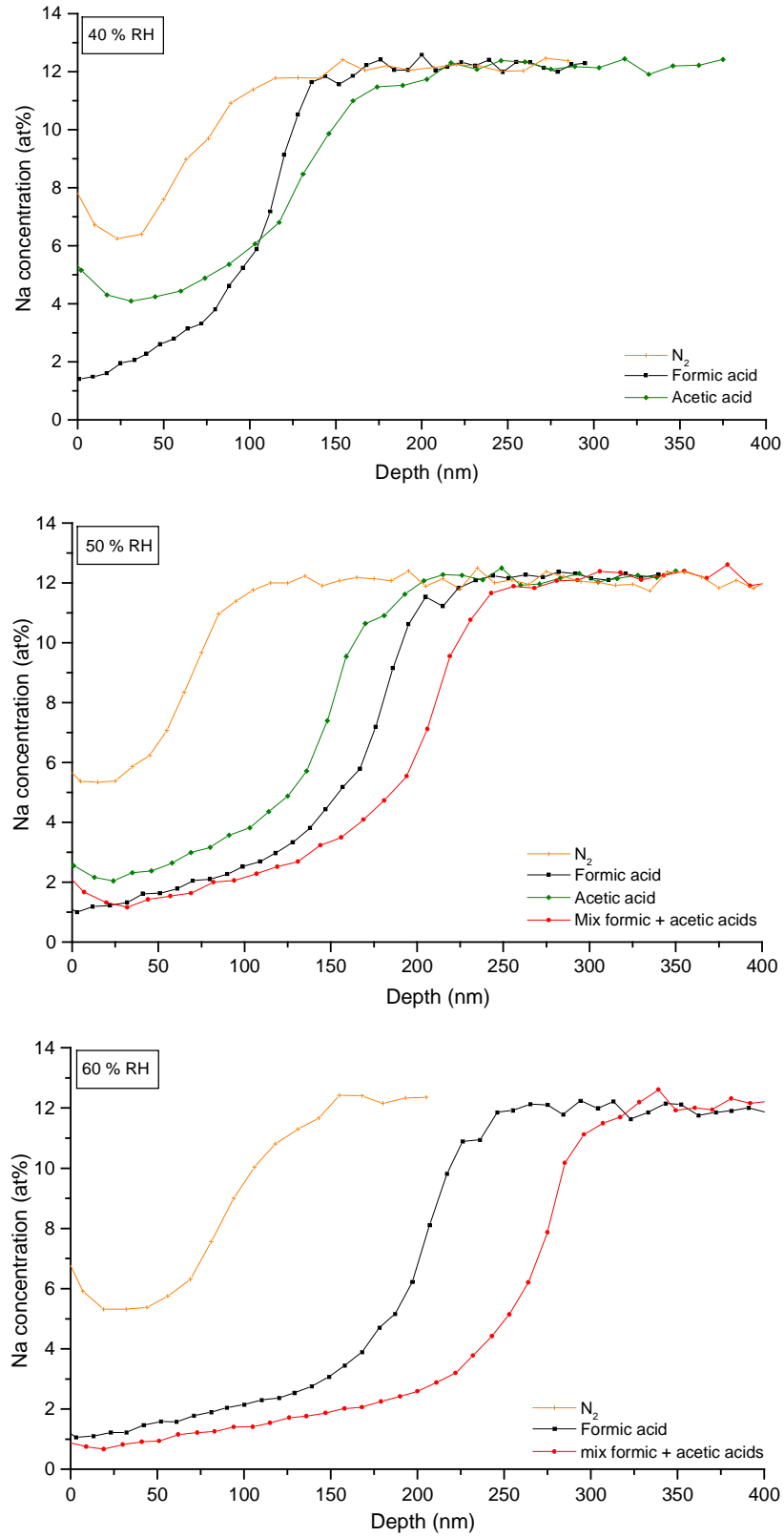


Figure V- 15: Sodium depth profile for RG1 glasses exposed to acid polluted and N<sub>2</sub> atmospheres at 40, 50 and 60 % RH.

In the present experiment, the increase in humidity resulted in an increase in sodium depletion in the glass for all samples (Figure V- 15). For all humidities, the depletion depth was always the smallest in the glass exposed to the N<sub>2</sub> atmosphere. The depletion depth increased substantially in the presence of the acid pollutants. These pollutants increased the acidity of the water film present at the glass surface, enhancing the leaching reaction. Moreover, formic acid causes more alteration than acetic acid, possibly because of the higher acidity of that acid. Despite a pollutant concentration three times higher in the experiment combining the two pollutants, the sodium depletion depth has not increased significantly, particularly for the glass exposed to the lower RH 50 %. A parallel could be made with the research undertaken by Cummings on the atmospheric alteration of glasses. Their research showed that the presence of either SO<sub>2</sub> or NO<sub>2</sub> in the atmosphere increased the alteration, but the presence of both pollutants did not increase the alteration any further [9]. Cummings noted that the hydration rate in the glass increased with increasing SO<sub>2</sub> concentration up to a critical level beyond which no further increase was seen. These results suggest that the water layer film at the glass surface had reached saturation and it is believed that a similar effect occur with organic pollutants. As the RH increase, the critical level of pollutant, corresponding to the saturation, is increased.

Again, the concentration of the sodium remaining in the altered layer was much lower for the glass altered in acid (~1 at%) than in N<sub>2</sub> (~6 at%) atmospheres. Moreover this concentration is affected by the RH of the atmosphere, as it decreases when the RH increases (Figure V- 15). The sodium content in the glass altered in acid atmosphere is consistent with the content measured on the altered historic glass objects in the NMS or the glass aged in accelerated conditions in acidic atmosphere (see chapter IV: Tables IV-4 and IV-6). The potassium content remaining in the altered layer of the glass aged in the acid atmosphere is similar to the sodium content in this layer (Figure V- 14). Considering that potassium cations are more mobile than sodium cations it is surprising that so little potassium ions were leached from the glass. This is associated with the mixed alkali ions effect which implies that in a glass containing mixed alkali, the diffusion of the alkali in minor concentration is always smaller than for the alkali in major concentration, no matter the size of the cation.

The amount of alteration was plotted as a function of the RH for formic acid and N<sub>2</sub> atmospheres based on either the depth of sodium depletion (Figure V- 16) or the total amount of sodium depleted (Figure V- 17). Both graphs show a perfectly linear correlation between the RH and the amount of alteration. The equations of the fitted lines are given in Table V- 1.

Table V- 1: Equations of the lines fitted to correlations graph of the sodium depletion depth (Figure V- 16) or total sodium extracted (Figure V- 17) with RH; with x corresponding to the RH (%) and y the sodium depletion depth (nm) or the total sodium extracted (at/nm<sup>2</sup>).

	Sodium depletion depth		Total sodium extracted	
<b>Formic acid</b>	$y = 7.3 x - 189$	$R^2 = 0.997$	$y = 51.1 x - 856$	$R^2 = 0.981$
<b>N<sub>2</sub></b>	$y = 2.25 x - 67$	$R^2 = 0.999$	$y = 11.5 x - 19$	$R^2 = 0.989$

Similar linear correlation between the alteration progress and the RH was obtained at higher temperatures by Ryan [1] and Cummings [9]. Considering that the number of water layers at the glass surface increases linearly between 10 and 70 % RH [15, 16], the alteration is linearly correlated to the number of water layers at the glass surface. The correlations indicate that the alteration depth is increased by a factor of approximately 3 in the presence of formic acid while the amount of sodium depleted is increased by 4.4. These values may be directly linked to the acid dissociation constant, since formic acid is 4.2 times more dissociated than water. Interestingly, environmental pollution with 5 ppm SO<sub>2</sub> or 1 ppm NO<sub>2</sub> increases the alteration kinetics by 3 compared to ambient air at the same temperature and RH [9]. These results mean that the leaching reaction is controlled by the concentration of H<sup>+</sup> and H<sub>3</sub>O<sup>+</sup> species at the glass surface, provided by water and acid pollutants, and therefore the dissociation constant of the hydrogen species. Any increase in the RH or acidity of the water film induces an increase of the leached layer depth and a decrease of the sodium content remaining in the altered layer.

Both methods used to obtain quantitative measurements of the alteration have their advantages and drawbacks. For example, the method using alteration depths does not take into account the sodium concentration in the altered layer, missing the extent of the leaching reaction that has taken place. The method based on the total sodium depleted improves these aspects however it is affected by the sodium enrichment that can form at the surface of the glass. In the rest of the study, the progress of the alteration will be followed by looking at the sodium depletion depth.

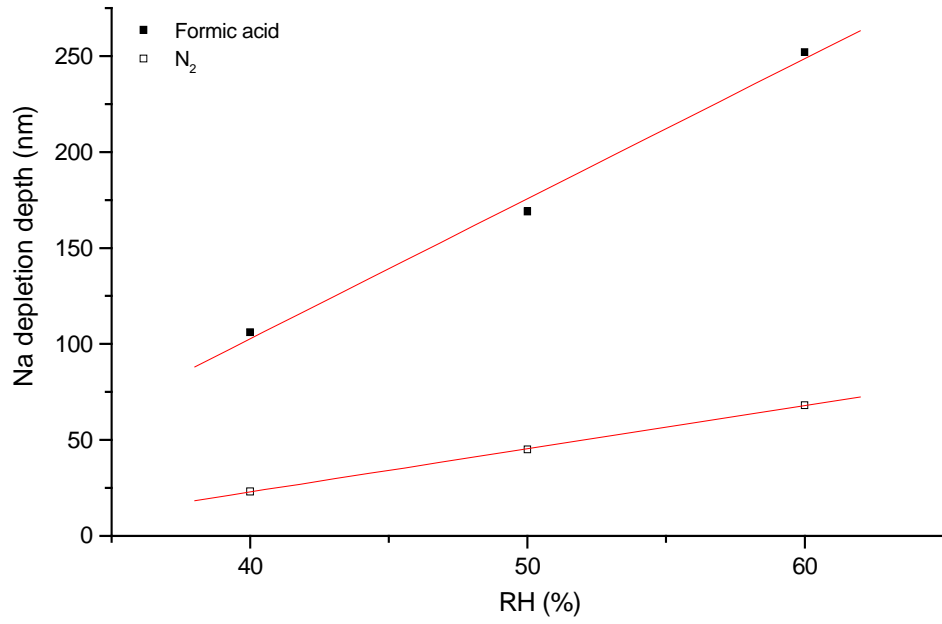


Figure V- 16: Correlation between the sodium depletion depth and the RH in the formic acid and N<sub>2</sub> atmosphere.

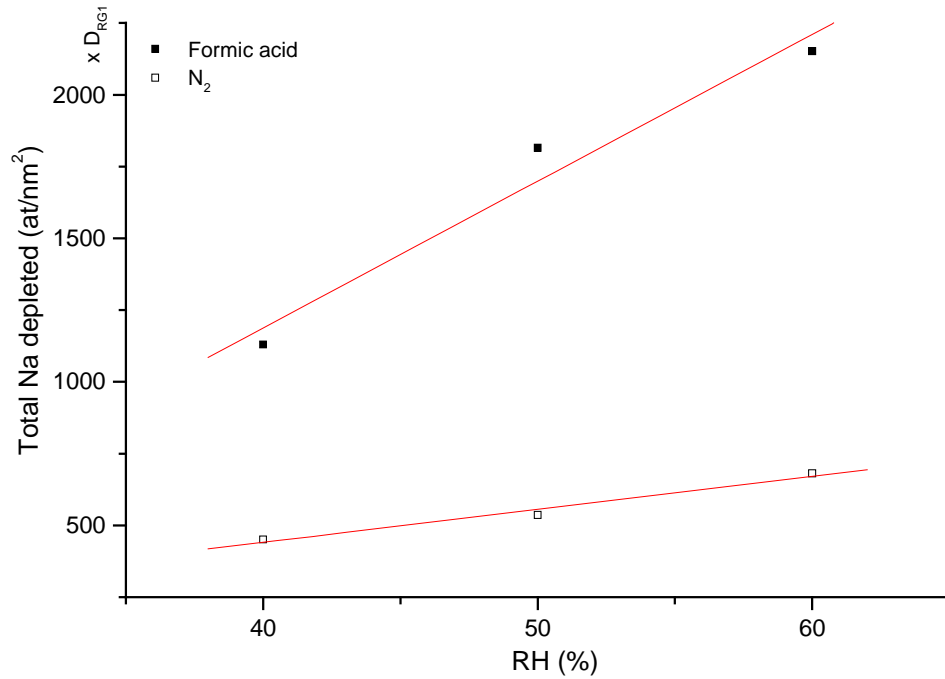


Figure V- 17: Correlation between the total sodium depleted and the RH in the formic acid and N<sub>2</sub> atmosphere (D<sub>RG1</sub> is the atomic density of the RG1 glass).

The same experiment was undertaken on the stable RRn glass replica for comparison. Because of the high durability of the glass, only little sodium depletion was produced after 6 weeks exposure compared to the RG1 glass (Figure V- 18). The profiles visually show that formic acid atmospheres induced more sodium leaching than N<sub>2</sub> atmospheres. However, the profile variations were too small to extract quantitative data to compare these 2 atmospheres or compare the effect of the different RHs.

In order to examine the effect of different polluted atmospheres on the RRn glass, the alteration was accelerated using the accelerated ageing experiments (100 % RH, 60 °C). The effect of acetic acid, formic acid and formaldehyde pollutants, used singly or mixed, was examined and compared to the effect of non-polluted atmospheres. The sodium depth profiles measured by SIMS after exposure to the different atmospheres are compared in Figure V- 19. The results confirm that acidic atmospheres induce greater sodium depletion, in the altered layer and in depth, than non-polluted atmosphere. The remaining sodium concentration in the altered layer is just below 1 at% for the glasses exposed to acids and around 3 at% for the glass exposed to non polluted atmosphere. These values are slightly higher than the values obtained for the RG1 glasses exposed to 100 % RH and saturated CO<sub>2</sub> atmospheres under ambient temperature. The fact that more sodium was retained in the RRn altered layer on which a much higher temperature was applied indicates that the composition, and so the stability, of the glasses controlled the amount of sodium leached within the layer as well as the acidity of the solution. The results confirm that formic acid causes more alteration to the glass than acetic acid, because of its higher dissociation constant; and the presence of higher concentration of combined pollutants does not increase the alteration significantly, as a result of the saturation of the solution. Finally, the same alteration is produced by formaldehyde and ambient air (no pollutant), which suggests that formaldehyde has no impact on the alteration. The effect of formaldehyde on the RG1 glass under ambient conditions will be examined in the next section.

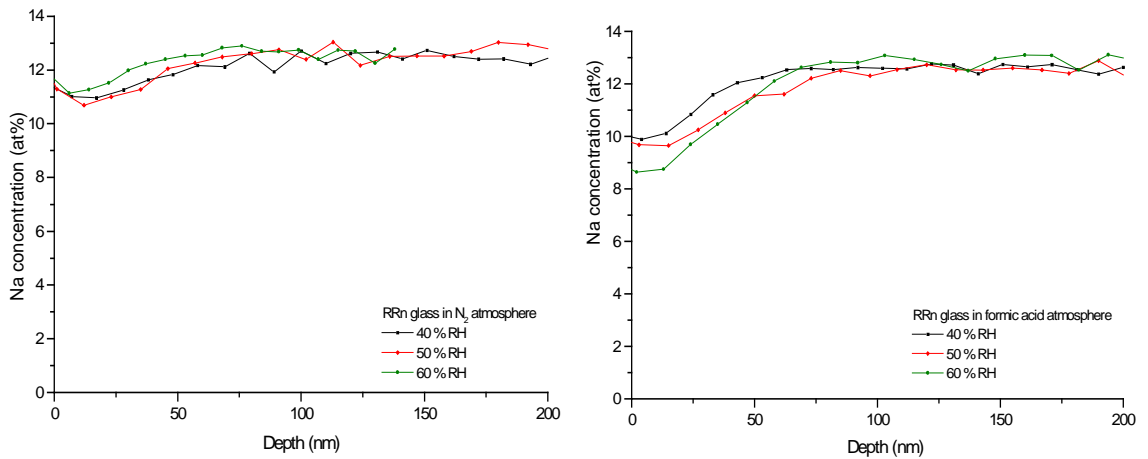


Figure V- 18: Sodium depth profiles of RRn glasses exposed to N<sub>2</sub> and formic acid atmosphere at 40, 50 and 60 % RH.

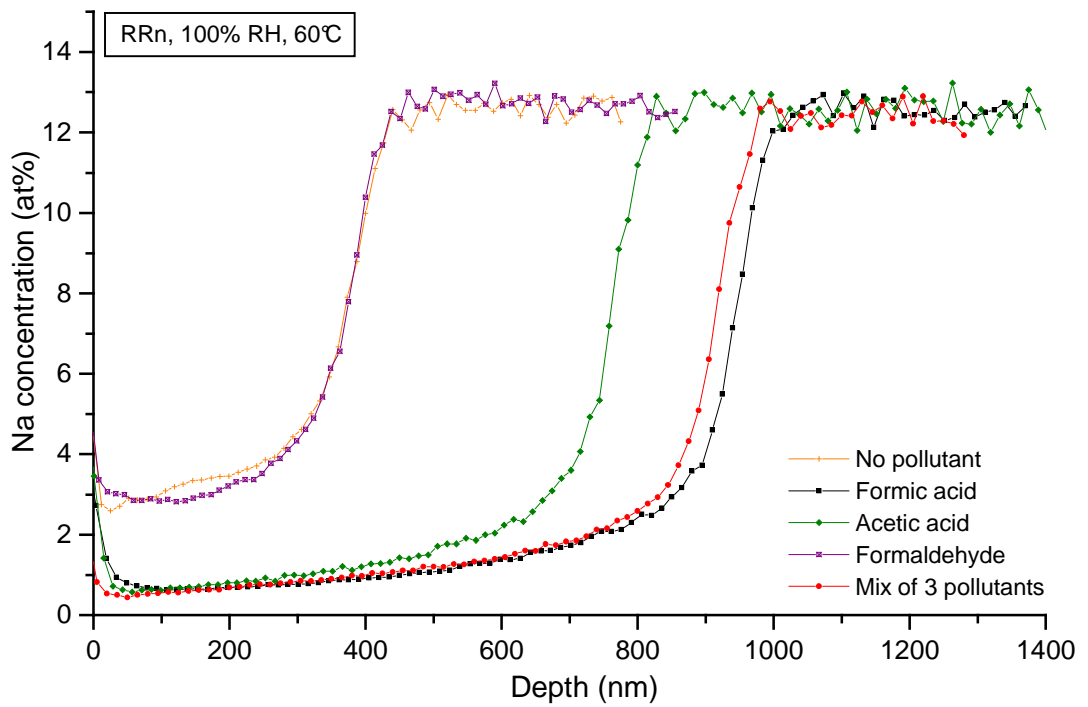


Figure V- 19: Sodium depth profiles of the RRn glasses exposed to different polluted and non polluted atmosphere at 60 °C and 100 % RH.

### V- 3.4 Progress of the alteration with time

The previous experiments clearly established that organic pollutants and more exactly acid pollutants affect the alteration process of soda silicate glasses. In this section, the evolution of the alteration with time was examined in artificial (desiccators) and real (museum) ageing conditions. For the artificial experiments, atmospheres polluted with formic acid or formaldehyde was compared to non-polluted atmospheres with ambient air or saturated  $N_2$ . Formic acid was chosen over acetic acid as it interacted predominantly with the glass.

#### V- 3.4.1 Surface deposits

Information on the effect of the atmosphere and the alteration process were gained from visual observation of the surface. An almost instantaneous whitening of the surface was observed when the RG1 glass was placed in the formic acid atmosphere (Figure V- 20).



Figure V- 20: Photograph of the RG1 glass fragments appearance before (transparent squares) and after exposure to formic acid atmosphere (white squares) on the bottom of an upturned beaker.

The evolution with time of the visual appearance of the glass surface is presented for non-acid polluted atmospheres (Figure V- 21) and acid-polluted atmospheres (Figure V- 22). Although the microscope images were obtained as soon as the fragments were taken out of their atmosphere, the contact with the external environment caused crystallisation or deliquescence of the surface deposits. In order to analyse the products by Raman spectroscopy, the surface deposits were dried using silica gel.

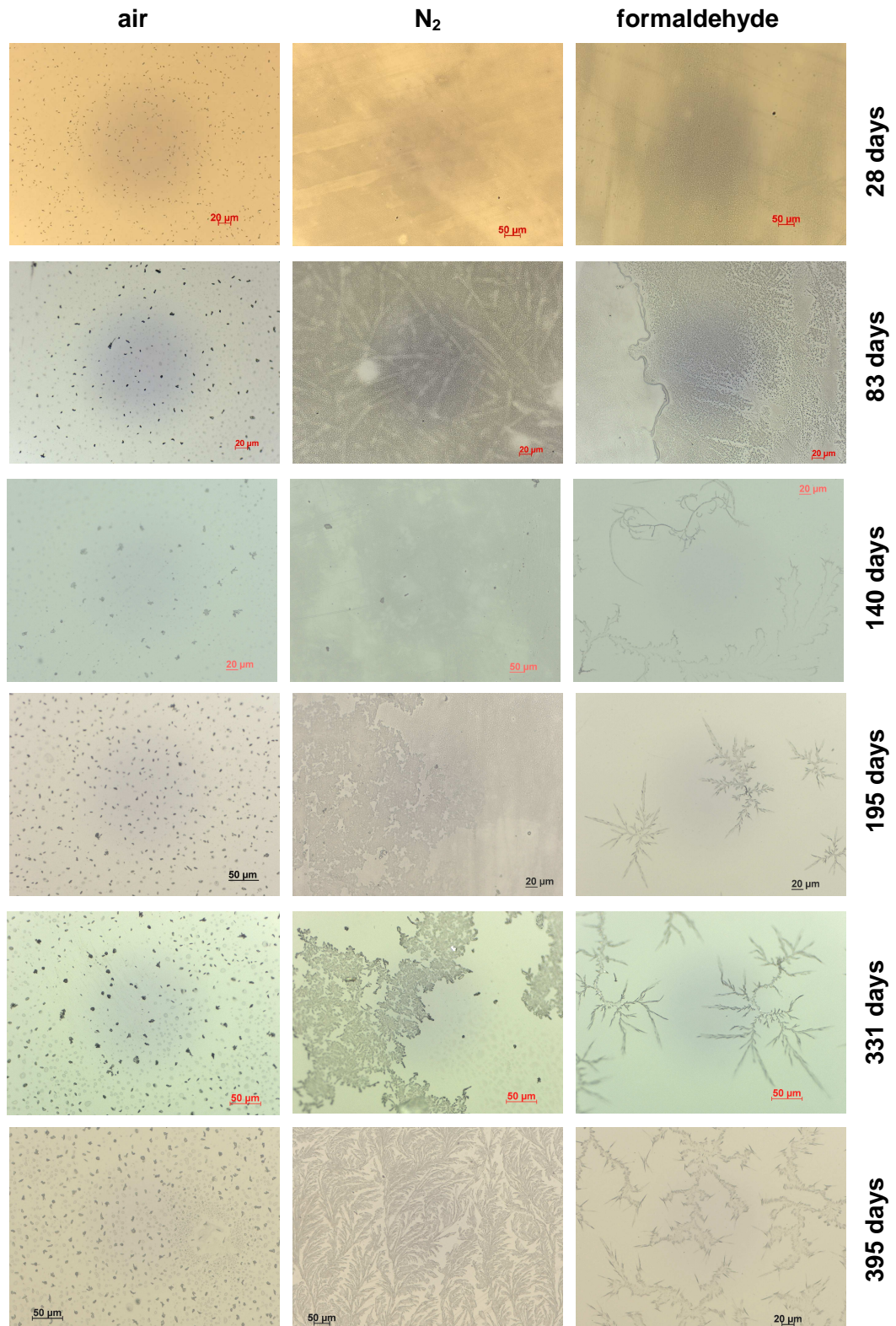


Figure V- 21: Light microscopy images of the RG1 glass surface after exposure to ambient air, N<sub>2</sub> and formaldehyde atmospheres for increasing duration (the background colours variation and the central dark spot are caused by the microscope instrument).

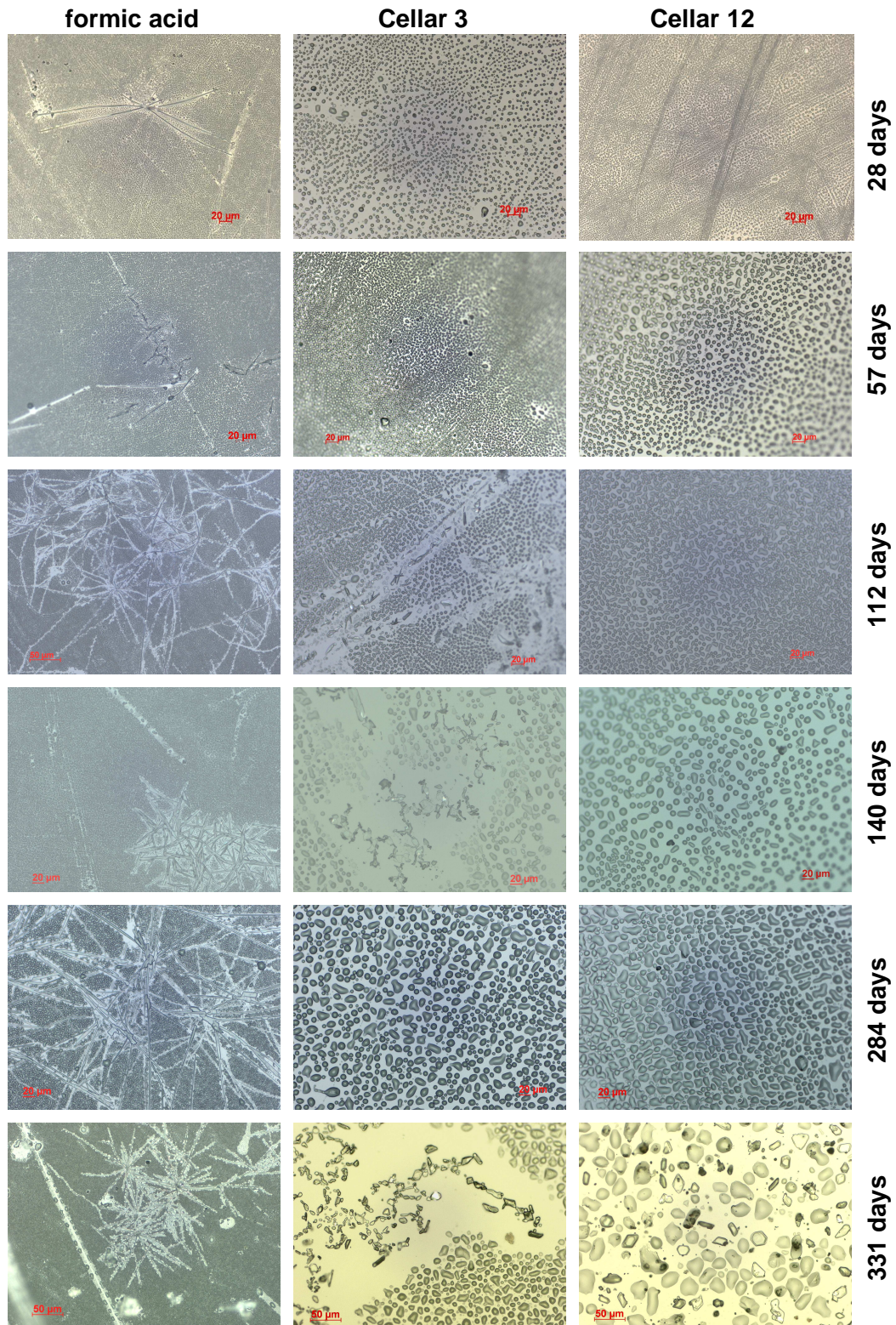


Figure V- 22: Light microscopy images of the RG1 glass surface after exposure to formic acid, cellar 3 and cellar 12 atmospheres for increasing duration (the background colours variation and the central dark spot are caused by the microscope instrument).

In ambient air, crystalline products formed on the glass surface from the first month of exposure (Figure V- 21). With time these crystals increased in size and density. Only after 8 months of exposure was the size of a few crystals large enough to be analysed by Raman spectroscopy. The analysis suggested the presence of a sulphate, sodium carbonate and possibly sodium acetate. In contrast, the surface of the glasses exposed to N<sub>2</sub> and formaldehyde atmospheres was opacified by a fog-like deposit at the surface created by densely packed fine liquid droplets (Figure V- 21). The track patterns observed on the samples exposed for 28 days to these atmospheres may correspond to a preferential arrangement of these droplets on invisible traces left after wiping the glass during the cleaning and drying process. This fog layer remained for several months before reacting and forming crystalline products, different between the two atmospheres. The crystalline products formed in the formaldehyde atmosphere have a dendrite like shape compared to the feather-like crystals formed in N<sub>2</sub> atmospheres. Only the dendrite crystals could be analysed and were identified as sodium formate phase I'. Consequently, the fog layer observed may correspond to sodium hydroxide droplets created through the leaching reaction induced by the humidity. As the solution concentration increased it reacted with pollutants, either formaldehyde in the desiccators or ambient air pollutants after opening the desiccators, to form the crystalline products observed. These visual observations suggest that formaldehyde is rather inert as it favours the attack of the glass by humidity and so the NaOH build up at the surface like N<sub>2</sub>. Formaldehyde possibly react with NaOH when a sufficient concentration is reached, to form sodium formate phase I'. This observation suggests that formaldehyde reacts through the Cannizzaro reaction rather than through preliminary formation of formic acid by oxidation.

In the formic acid, cellar 3 and cellar 12 atmospheres the appearance of the glass surface after exposure was very similar with an important concentration of droplets (Figure V- 22). The crystals obtained after drying the droplets were identified mainly as sodium formate II in all three atmospheres (see chapter III). The glasses exposed to the cellars atmosphere also showed the presence in minor concentration of sodium acetate anhydrate and trihydrate, sodium carbonate, sodium formate phase I'. The presence of mainly formates in the crystalline products of the glass exposed to cellar atmospheres where acetic acid dominate (see chapter II, Table II-2), confirms that formic acid predominates in the water film. Thus, formic acid controls the leaching reaction by controlling the acidity of the water film

### V- 3.4.2 *Elemental modification: Artificial ageing experiments (series 3)*

The purpose of the artificial experiments, set up in desiccators, was to be a reference for the samples aged in the museum atmosphere, by controlling the environmental conditions at 19 °C and 48 % RH from the start of the experiments. Unfortunately, in the course of the 13 months experiment, the air conditioning system of the laboratory failed over several months, causing large variations in temperature. After 4.5 months (135 days) the temperature first increased to 22 °C over 1 month; it was stable again at 18-19 °C for 2.5 months before dropping to 15 °C for about 1.5 month (Figure V- 23 *bottom*). These temperature fluctuations affected the progress of the alteration in all atmospheres which will be discussed.

During the time of the exposure, only alkali ions in the glass were affected by the leaching reaction, causing the formation of hydrated and alkali-depleted layers. The progress of the glass alteration in each atmosphere was followed by plotting the sodium alteration depth as a function of time in Figure V- 23. The results confirm that the alteration of the glasses is greatly accelerated by the presence of formic acid compared to formaldehyde, ambient air or N<sub>2</sub> atmospheres. The alteration mechanisms are different between the N<sub>2</sub> and ambient air atmospheres. While the alteration in the N<sub>2</sub> atmosphere follows the square root of time relation, indicative of a diffusion controlled process; the alteration produced in the ambient air is irregular and less extensive. This indicates that the low CO<sub>2</sub>, SO<sub>2</sub> levels in ambient air have slowed down the alteration process by reacting with the NaOH film at the glass surface and forming the carbonates and sulphate crystals previously identified. These products may have acted as a protective barrier towards further leaching. The supply of these pollutants was renewed regularly when the desiccators was opened for sampling, allowing a continuous reaction between the pollutants and the NaOH solution. In contrast the saturated N<sub>2</sub> atmosphere favoured the continuous leaching of the glass by the humidity, inducing the alkaline solution build up at the surface. The progress of the alteration in formaldehyde atmosphere followed that of the N<sub>2</sub> atmosphere in the first 6 months and then that of the ambient air atmosphere, which is consistent with the visual observations. This confirms that that formaldehyde has no impact on the leaching process and that the fog-layer corresponds to fine droplets of NaOH formed through leaching by the humidity. Thus, it suggests that the pollutants in the ambient air and the formaldehyde are beneficial to the conservation of glasses as they do not affect the leaching reaction but neutralise the hydroxide solution that causes dissolution of the silicate matrix.

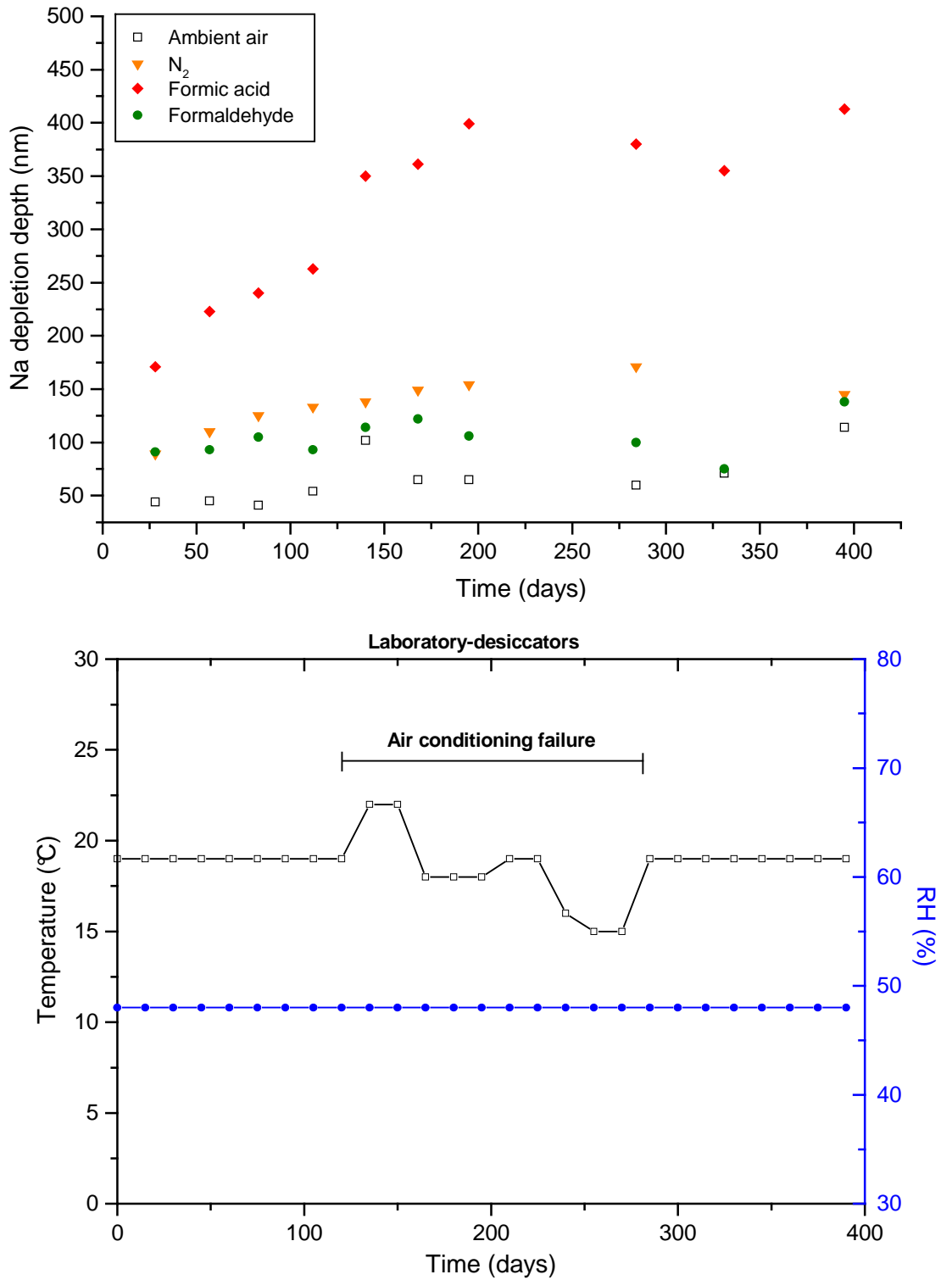


Figure V- 23: Artificial ageing experiments with time of RG1 glass. Top: alteration variation with time in the different atmospheres. Bottom: Environmental conditions variation with time.

The sodium and potassium profiles were plotted and their variation with time are presented for the glass exposed to N<sub>2</sub> (Figure V- 24), formic acid (Figure V- 25), formaldehyde (Figure V- 26) and ambient air atmospheres (Figure V- 27). With time the alteration progressed in depth and the amount of alkali in the altered layer decreased. After a certain period the leaching of alkali slowed down and reached a steady state (Figure V- 23), as expected for a diffusion-controlled process. This evolution was clearly visible on the sodium and potassium profiles. When the leaching was rapid at the beginning, the profiles were marked by the presence of a strong K peak, the decrease of the alkali concentration within the altered layer and the progress in depth of the reaction front (Figure V- 24 and Figure V- 25). As the reaction reached a steady state the sodium concentration in the altered layer increased slightly and the K peak disappeared, supporting a decrease of the ion-exchange activity.

The chemistry of the atmosphere induced differences in the altered layer formed, as observed in the previous experiments and in chapter IV. The altered layers formed in the ambient air, N<sub>2</sub> and formaldehyde atmospheres all display the same characteristics. The remaining sodium content in the altered layers stabilises at similar values, with 4 at% for the glass exposed to the N<sub>2</sub> atmosphere (Figure V- 24), and 5 at% for the glasses exposed to the ambient air or the formaldehyde atmosphere (Figure V- 26 and Figure V- 27). Moreover, they all display enrichment in alkali at the surface, characteristic of the gel layer. This enrichment is particularly important in the glasses exposed to N<sub>2</sub> (Figure V- 24), where the absence of pollutants favoured NaOH solution build up which enhanced the dissolution of the silicate network. In contrast, the pollutant in ambient air and formaldehyde atmospheres reacted with NaOH solution reducing the gel layer formation (Figure V- 21). The decrease of the altered layer depth for the glass exposed to N<sub>2</sub> atmosphere for 395 days (Figure V- 23) was caused by an underestimation of the gel layer thickness in which faster sputter rates are expected.

In the formic acid atmospheres, the leaching reaction is maintained and greatly accelerated, causing larger depletion of alkali in depth and within the layer (Figure V- 25). Thus the sodium content in the altered layer of the glasses exposed to formic acid reaches 1 at%. Oscillations are observed at the near surface of the K profiles where the K peak intensity decreased as the leaching reaction reached a steady state. These oscillations were also observed in the potassium profile of the glass exposed to saturated CO<sub>2</sub> atmosphere (Figure V- 10), but never for glasses exposed to non-acid atmospheres. Therefore these

oscillations, which significance has not been interpreted yet, are a characteristic feature of the steady state for glass altered in acid atmospheres.

The temperature fluctuations caused by the air conditioning system disturbed the reaction processes in all atmospheres. The glass exposed to formic acid atmospheres, where the leaching reaction was greater, responded more rapidly and to a greater extent to the change than the other atmospheres, as can be seen from the plot of the alteration progress (Figure V- 23), and in the sodium and potassium profiles (Figure V- 25). The temperature increase after 135 days greatly increased the alteration, when the alteration in most glasses was close to reaching the steady state. The reappearance of a strong K peak on the profile of the glass exposed for 140 days (just after the temperature change) suggests that the modification has disturbed the equilibrium that was developing and in some way re-activated the rapid ion-exchange reaction observed at the beginning of the exposure. Similarly, the small peak formed in the sodium profile, just after the bulk concentration is reached, gets more intense after the temperature increase as at the beginning of the exposure. The temperature decrease also re-activated the alteration process as a result of condensation formed on the surface, which is observed on the glass surface exposed to ambient air for 330 and 395 days (Figure V- 21).

A series of artificial ageing experiments was set up separately to examine the development of the alteration in the first weeks of exposure. The profiles of sodium and potassium and their evolution with time are given for the samples exposed to N<sub>2</sub> and formic acid atmospheres (Figure V- 28). No significant variation could be monitored on the glasses exposed to N<sub>2</sub> atmospheres, even with nanometre depth resolution (Figure V- 6). In contrast the glasses exposed to the formic acid atmosphere display important modification in their sodium and potassium profiles (Figure V- 28). The observation of a significant leaching in depth and the decrease of the remaining sodium content in the altered layer as well as the presence of an intense Na peak and K peak, are all characteristic signs that a rapid diffusion reaction through ion-exchange is taking place. We note that in this early period of the reaction, the S-shape in the sodium profile is not as well defined as in the glasses exposed over longer period, due to the rapid progress of the reaction.

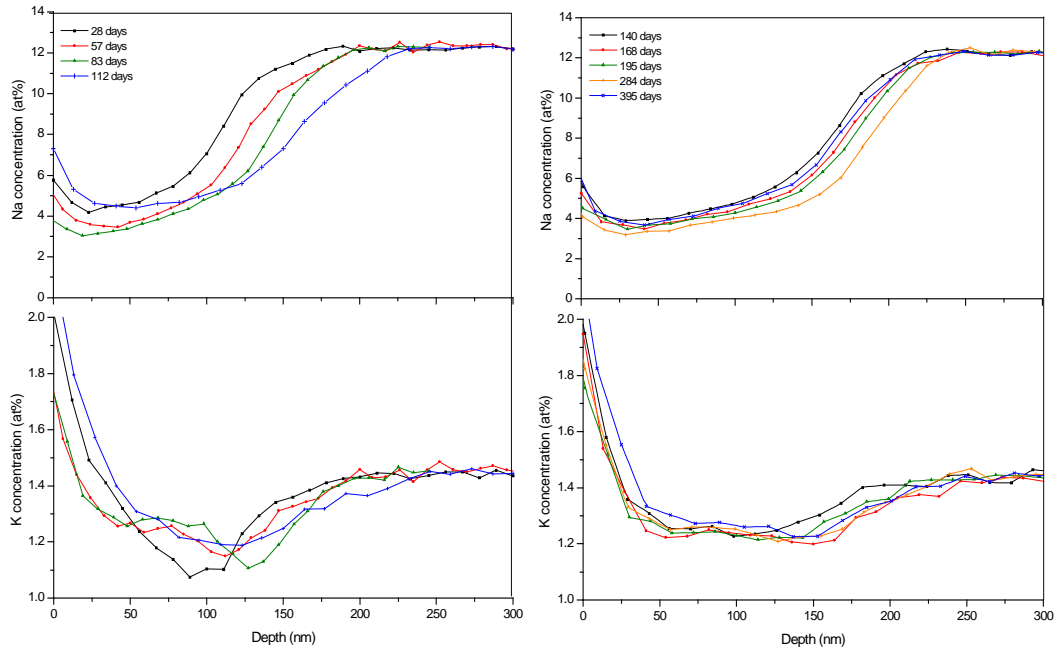
Saturated N<sub>2</sub> atmosphere

Figure V- 24: Sodium and potassium depth profiles evolution of the RG1 glasses exposed to saturated N<sub>2</sub> atmosphere over 13 months.

## Formic acid atmosphere

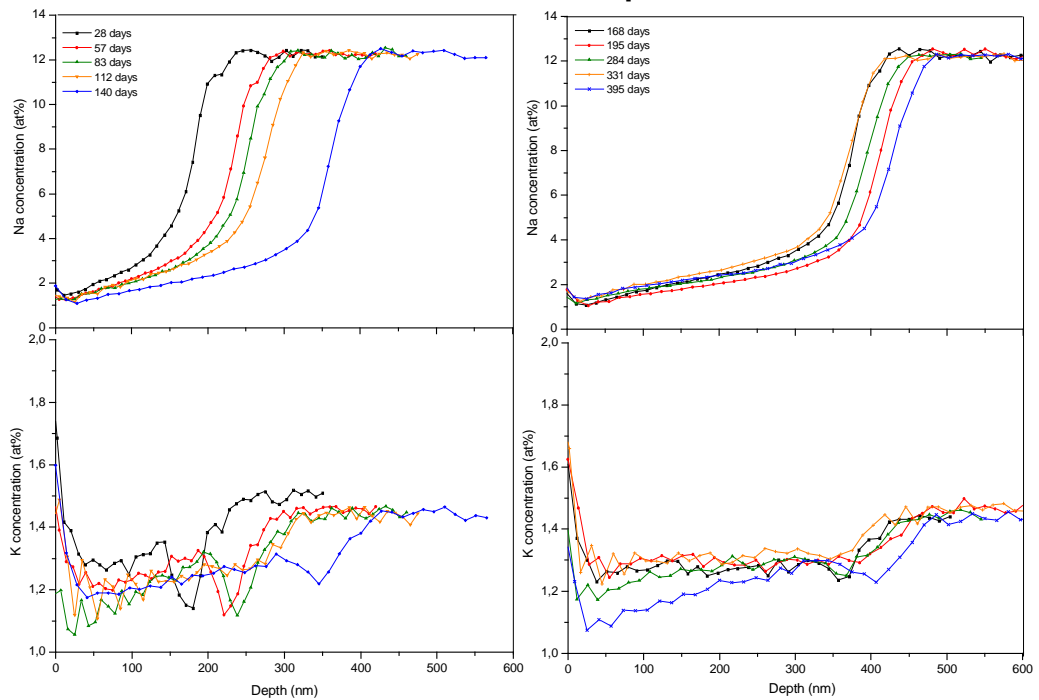


Figure V- 25: Sodium and potassium depth profiles evolution of the RG1 glasses exposed to formic acid atmosphere over 13 months.

## Formaldehyde atmosphere

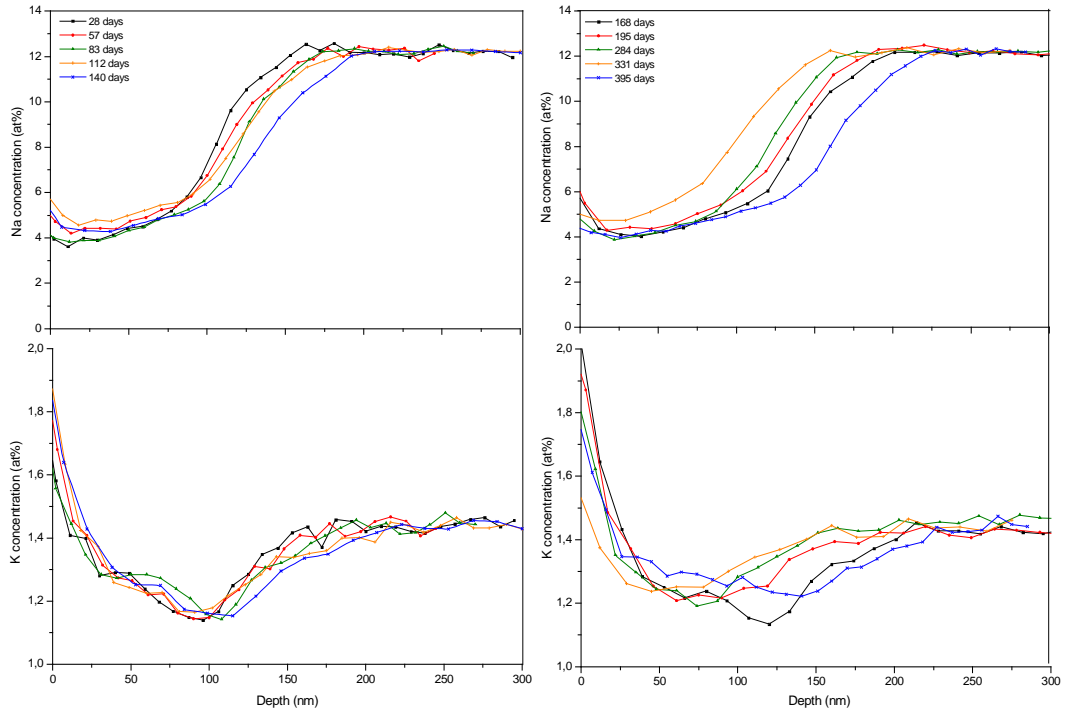


Figure V- 26: Sodium and potassium depth profiles evolution of the RG1 glasses exposed to formaldehyde atmosphere over 13 months.

## Ambient air atmosphere

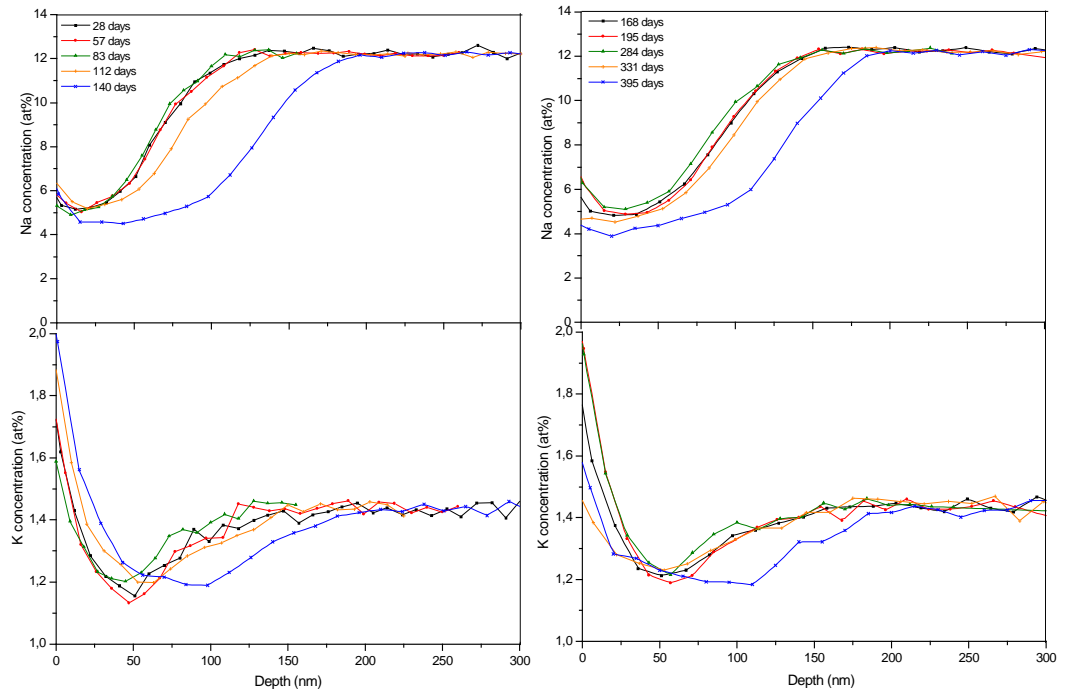


Figure V- 27: Sodium and potassium depth profiles evolution of the RG1 glasses exposed to ambient air atmosphere over 13 months.

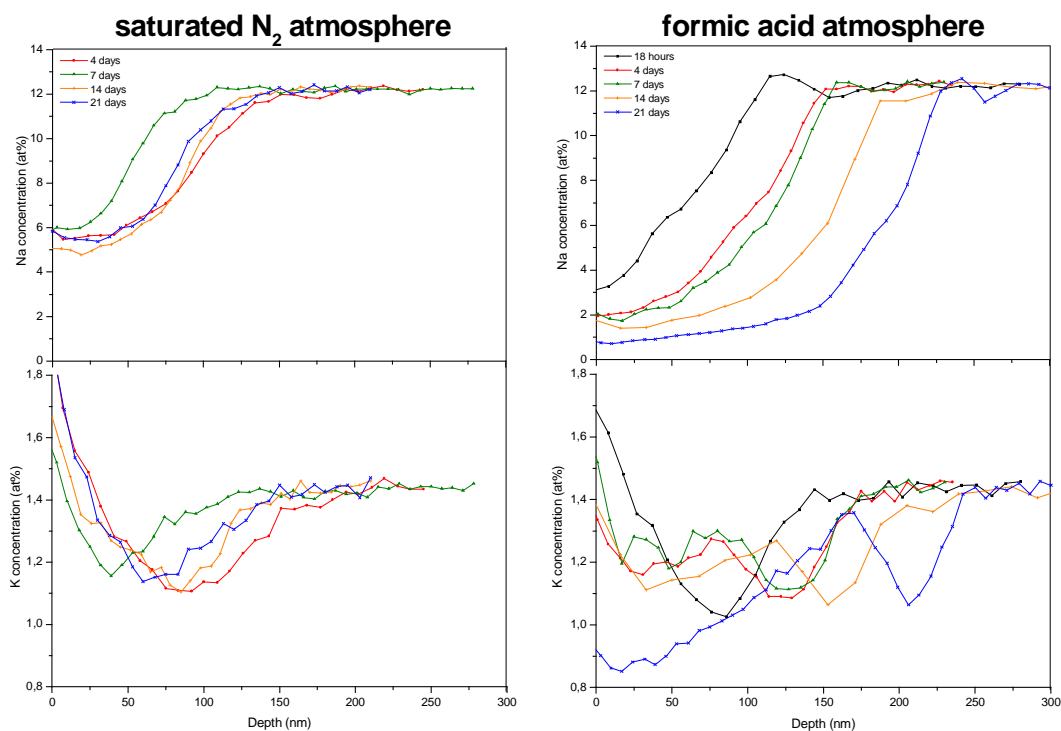


Figure V- 28: Sodium and potassium depth profiles evolution of the RG1 glasses exposed to saturated  $N_2$  and formic acid atmospheres over 3 weeks.

### V- 3.4.3 Elemental modification: Real ageing experiments

The glass fragments exposed in the cupboards of cellars 3 and 12 of the NMS were subjected to the high concentration of pollutants emitted by the wooden cabinets as well as the daily and yearly temperature and RH fluctuations. The concentration of all pollutants monitored in the cupboard in cellar 3 was approximately twice that monitored in cellar 12. In both cupboards, acetic acid was present in major concentration levels with formaldehyde and formic acid present at much lower concentration (Chapter II, Table II-2). The environmental conditions did not show large fluctuations, thanks to the buffering effect provided by the wood of the cabinets. However, in both cupboards, the RH increased significantly during the summer months. The conditions in cellar 3 were around 23 °C and 40-45 % RH compared to 20-22 °C and 43-53 % RH in cellar 12. The progress of the alteration and the environmental conditions variations with time are presented in Figure V- 29 for cellar 3 and Figure V- 30 for cellar 12. The variation with time of the Na and K profiles are presented in Figure V- 31 and Figure V- 32 for the glasses exposed in cellar 3 and 12 respectively.

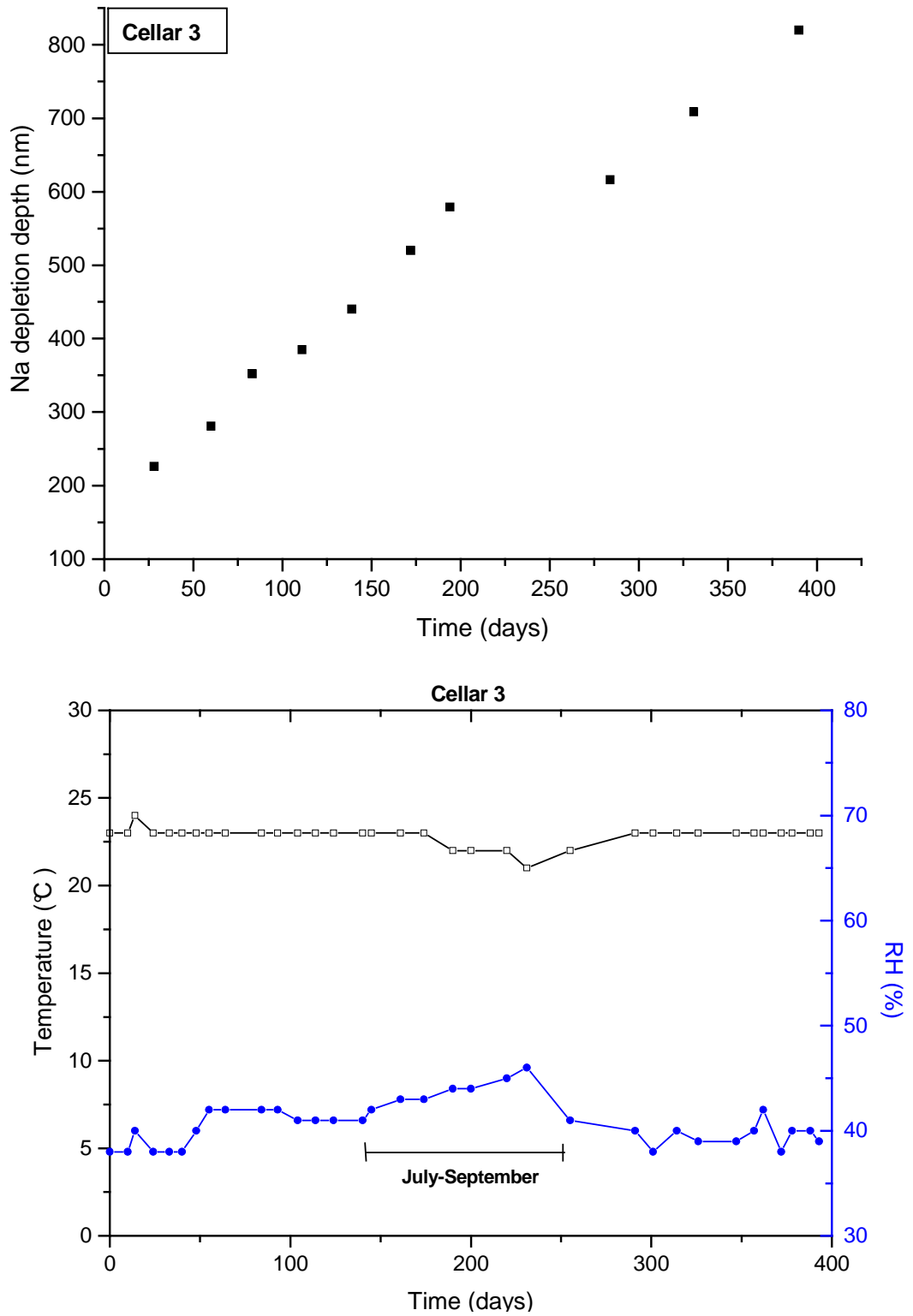


Figure V- 29: Ageing RG1 glasses in cellar 3. Top: alteration variation with time. Bottom: Environmental condition variations with time.

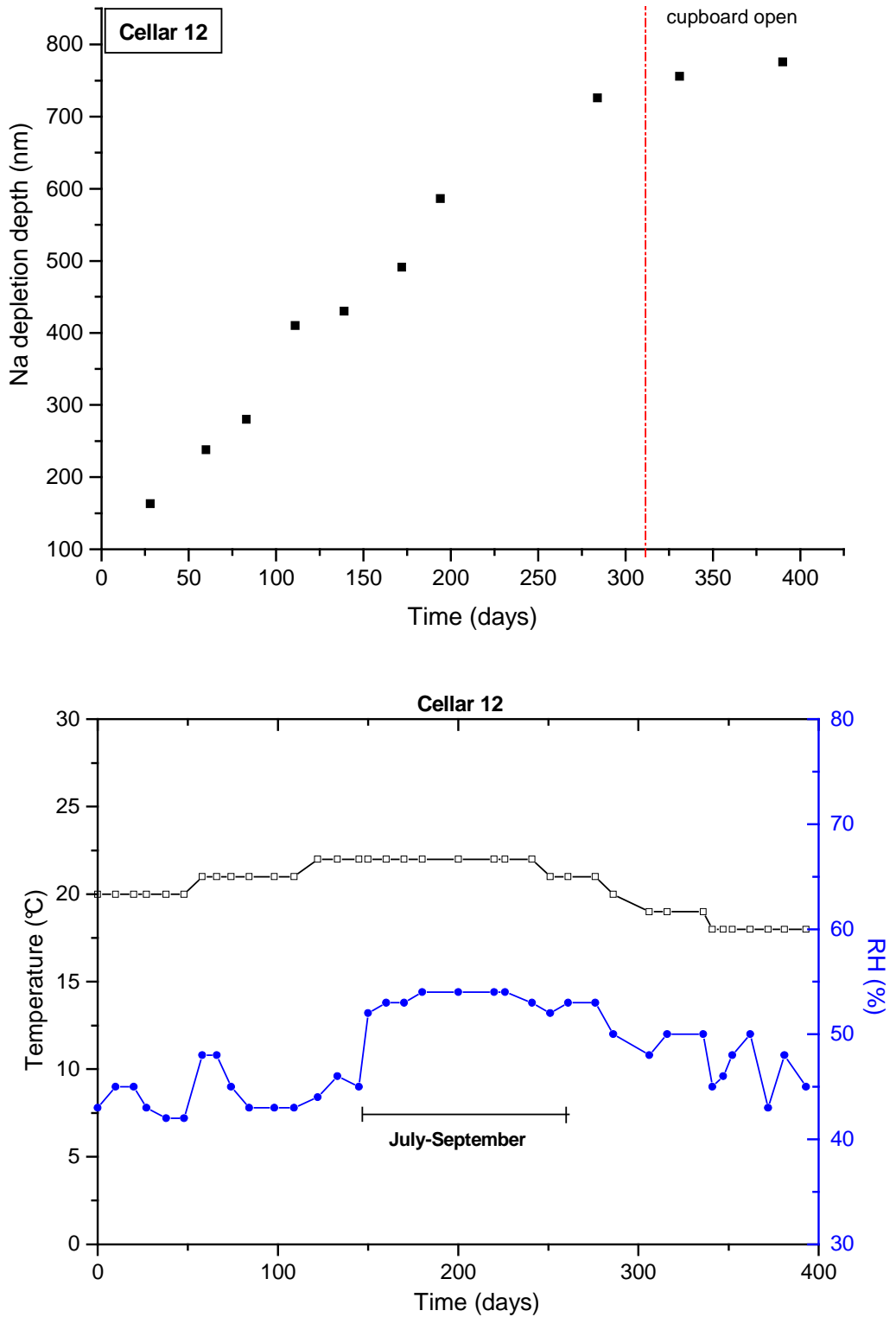


Figure V- 30: Ageing RG1 glasses in cellar 12. Top: alteration variation with time. Bottom: Environmental condition variations with time.

The sodium and potassium profiles for cellar 3 and 12 and their variations are identical to that obtained in the formic acid atmosphere with a sodium concentration of 1 at% in the altered layer and the concentration oscillation for potassium at the near surface at the steady state. This clearly confirms that acids are responsible for the glass alteration in the museum cupboards and showcases. The fluctuations in RH and temperature affected the development of the alteration, as indicated by the discontinuities observed on the graphs (Figure V- 29 and Figure V- 30). In particular we note a decrease of the alteration rate for the glasses exposed in cellar 3 after the RH went down after 250 days (Figure V- 29), while the RH and temperature increase in cellar 12 from day 150 increased the rate of the alteration (Figure V- 30). The modification in the sodium and potassium profiles are marked by the reappearance of the K peak as in the sample exposed for 284 days in cellar 3 (Figure V- 31) or the samples exposed for 172, 194 and 284 days in cellar 12 (Figure V- 32). These modifications indicate that a rapid ion-exchange was reactivated with the RH increase over the summer, increasing the leaching of alkali in depth and within the altered layer. The differences in RH and temperature between the different atmospheres influenced the amount of alkali leached and so the remaining concentration of alkali in the altered layer. This is particularly evident from the K profile between the formic acid (Figure V- 25), cellar 3 (Figure V- 31) and cellar 12 (Figure V- 32) atmospheres. The higher conditions in Cellar 12 during the summer (22 °C, 53 % RH), caused greater leaching, with the potassium content in the altered layer reaching 0.9 at%.

Due to the move of the objects in cellar 12 to a new store, the cupboard was emptied of its objects and it was left open from day 310. The glass fragments were then exposed to the circulating ambient air of the room, greatly reducing their interaction with organic pollutants emitted by the wooden cabinets. Figure V- 30 and Figure V- 32 indicate that the progress of the alteration decreased as a result, with the slow down of the reaction front advance and a slight increase of the sodium concentration in the altered layer. Interestingly, the potassium concentration in the near surface greatly increased, similarly to the glass exposed to ambient air, N<sub>2</sub> or formaldehyde (Figure V- 24 and Figure V- 26). Consequently the altered layer of the glass tends towards a new equilibrium in agreement with the chemistry of the new atmosphere.

**Cellar 3**

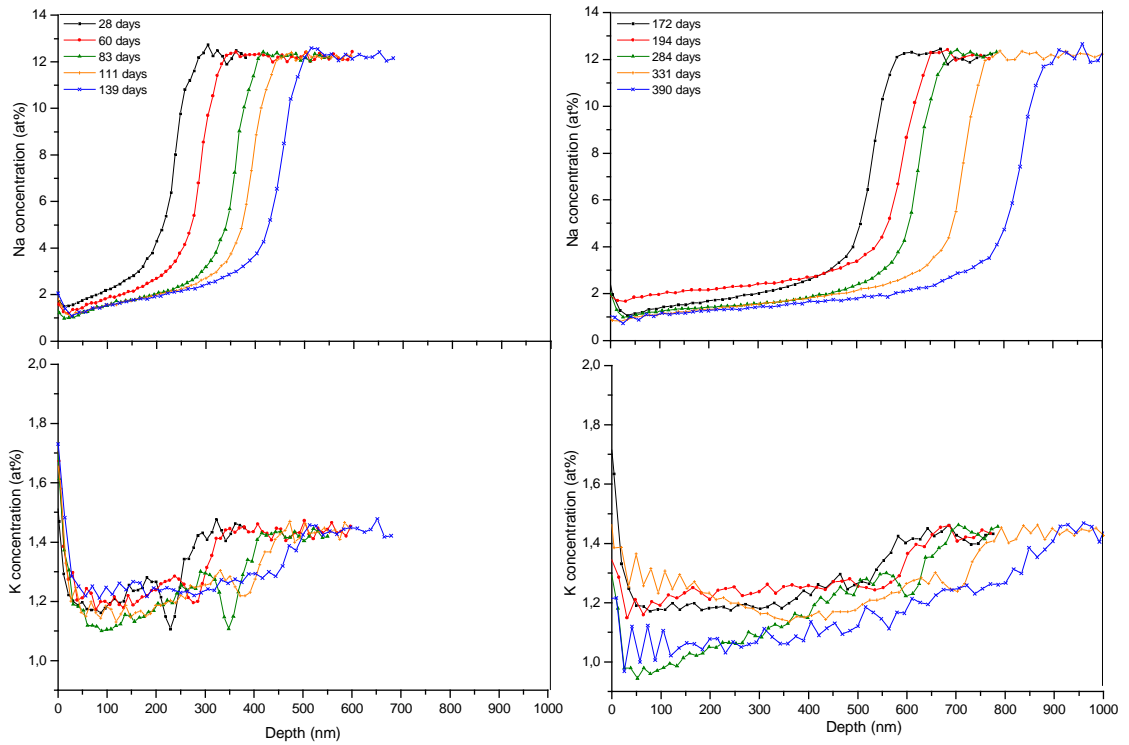


Figure V- 31: Sodium and potassium depth profiles evolution of the RG1 glasses exposed to cellar 3 atmosphere over 13 months.

**Cellar 12**

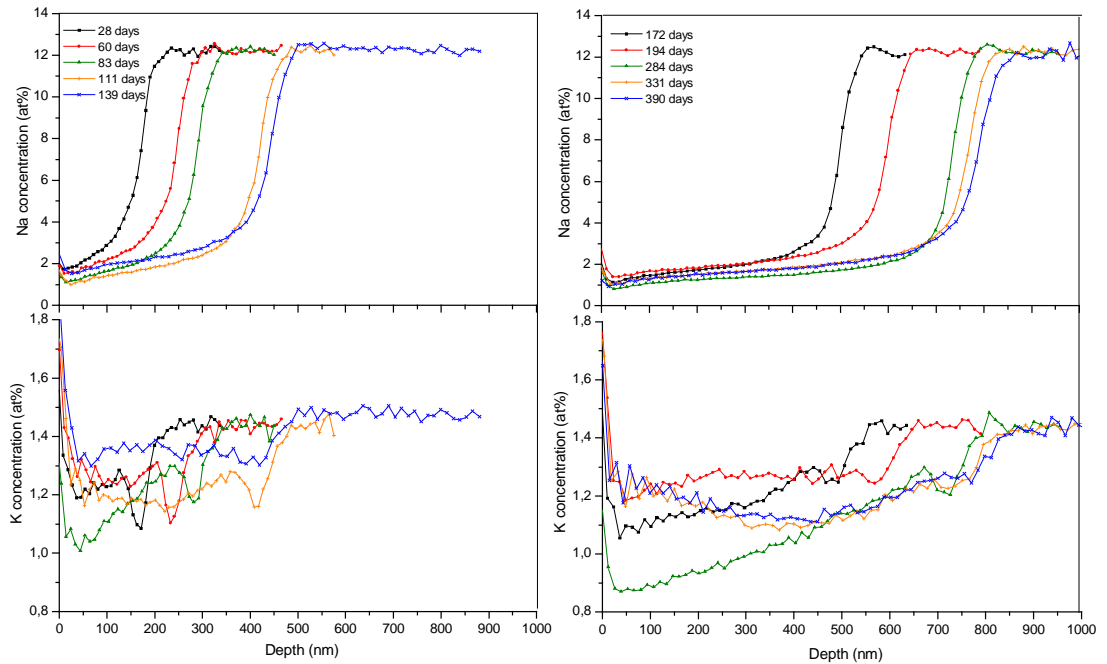


Figure V- 32: Sodium and potassium depth profiles evolution of the RG1 glasses exposed to cellar 12 atmosphere over 13 months.

As in the artificial ageing experiments, the development of the alteration in the first weeks of exposure was examined by exposing glass fragments between day 102 and day 123 of the main experiment. The environmental conditions for that period were approximately 23 °C, 41 % RH in cellar 3 and 21 °C, 43 % RH in cellar 12. The profiles of sodium and potassium and their evolution with time are given in Figure V- 33. for the samples exposed to cellar 3 and cellar 12 atmospheres. The development of the alteration is similar in both atmospheres due to their similar environmental conditions over that period. As in the artificial ageing experiments the profiles display the signs characteristic of a rapid ion-exchange reaction.

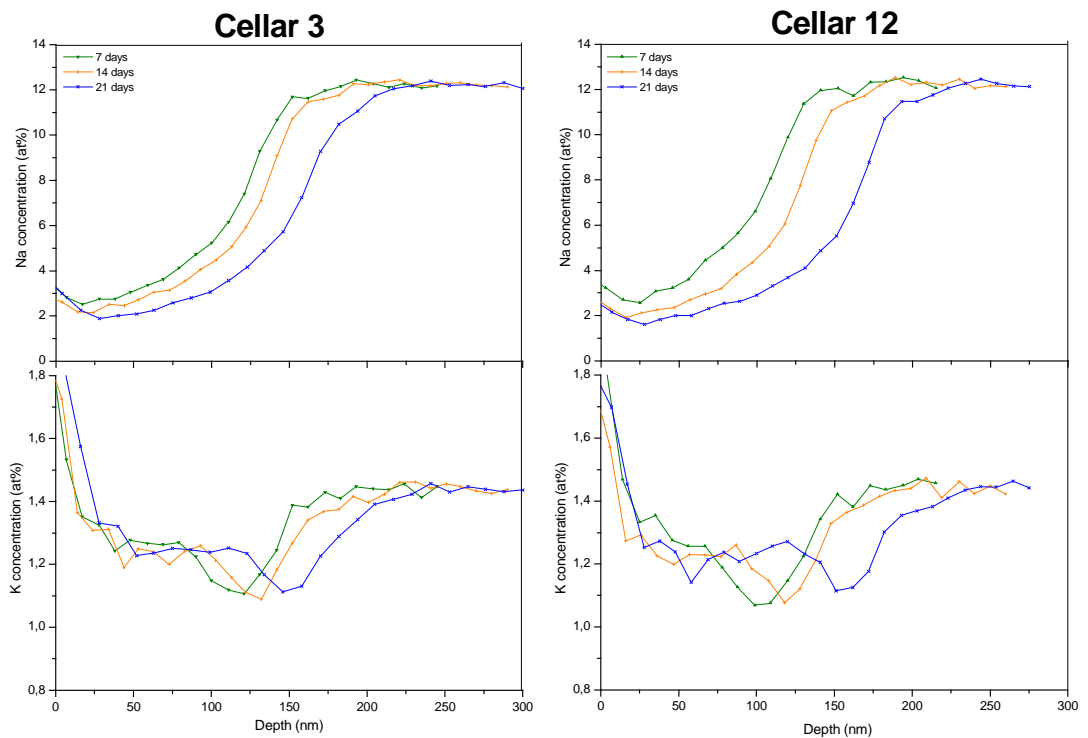


Figure V- 33: Sodium and potassium depth profiles of the RG1 glasses exposed to cellar 3 and cellar 12 atmospheres over 3 weeks.

### V- 3.4.4 Comparison of the artificial and real ageing experiments

The alteration of the glass under ambient temperatures was mainly controlled by the leaching of alkali ions, whatever the chemistry of the atmospheres. However the RH, temperature and the presence of pollutants modified the kinetics of this leaching reaction.

Considering that a fixed amount of pollutant was only introduced at the start of the artificial ageing experiments and not renewed, a constant pollutant concentration in the desiccators could not be maintained. Consequently, the  $30.5 \mu\text{g m}^{-3}$  concentration corresponds to the formic acid concentration at the start of the experiment. This concentration decreased with time as the pollutant was consumed through the reaction with the glass. The last two measurements of the glasses exposed to cellar 12 atmospheres, when the cupboard was left open, were omitted in the determination of the kinetics.

Because the leaching of alkali is a diffusion controlled reaction, the Na depletion depths were plotted as a function of the square root of time for the glasses exposed to cellar 3, cellar 12,  $\text{N}_2$  and formic acid atmospheres over 13 months (Figure V- 34). A similar plot was obtained for the alteration produced over 3 weeks in the same atmospheres (Figure V- 35). For each atmosphere a line was fitted to the data, and the corresponding equations are given in Table V- 2.

Table V- 2: Regression equations of the lines for the correlations of the sodium depletion depth with  $t^{1/2}$  in the different atmospheres (Figure V- 34 and Figure V- 35); with x corresponding to the  $t^{1/2}$  (days)<sup>1/2</sup> and y the sodium depletion depth (nm).

Atmosphere	13 months period		3 weeks period	
$\text{N}_2$	$y = 7x + 57$	$R^2 = 0.993$	Not available	
Formic acid	$y = 27x + 17$	$R^2 = 0.973$	$y = 41x + 3$	$R^2 = 0.995$
Cellar 3	$y = 40x - 17$	$R^2 = 0.989$	$y = 19x - 58$	$R^2 = 0.967$
Cellar 12	$y = 50x - 139$	$R^2 = 0.988$	$y = 32x + 8$	$R^2 = 0.983$

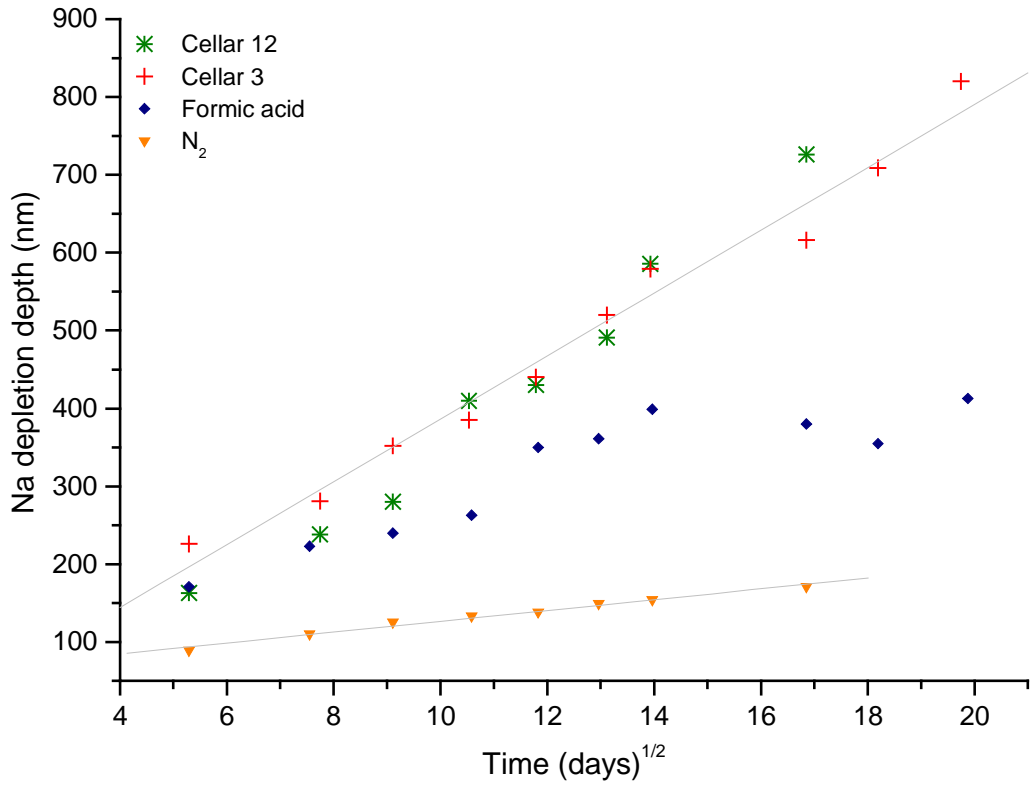


Figure V- 34: Correlation of the sodium alteration depth with  $t^{1/2}$  in N<sub>2</sub>, formic acid, cellar 3 and cellar 12 atmospheres over 13 months.

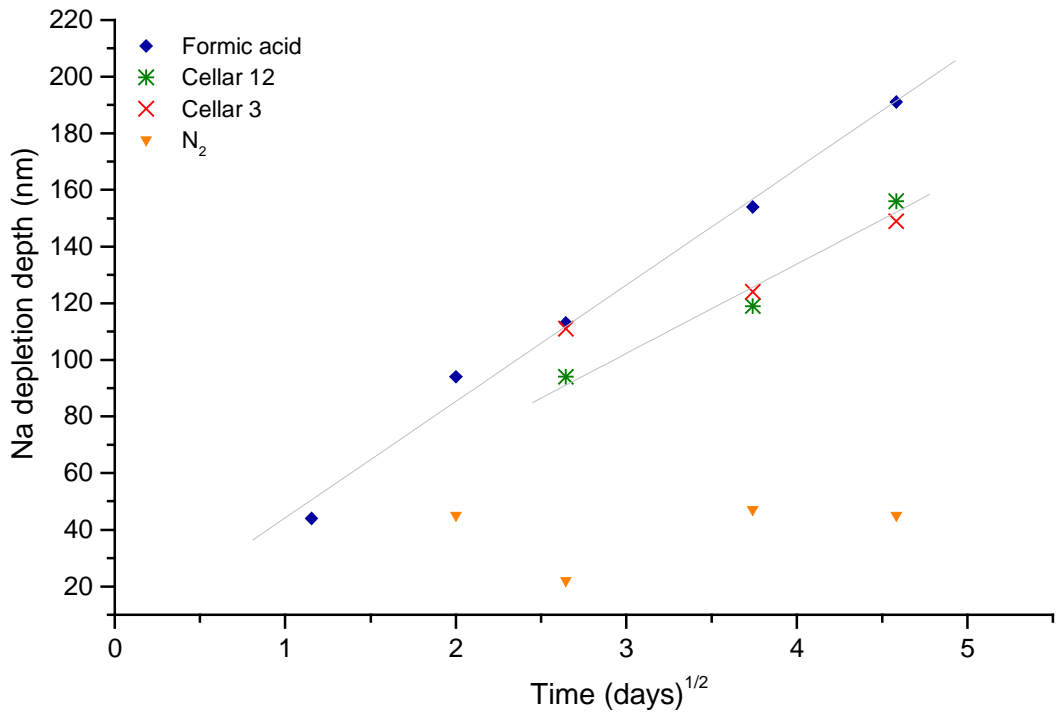


Figure V- 35: Correlation of the sodium alteration depth with  $t^{1/2}$  in N<sub>2</sub>, formic acid, cellar 3 and cellar 12 atmospheres over 3 weeks.

The alteration in the N<sub>2</sub> atmosphere is clearly proportional to the square root of time, which confirms that the reaction was diffusion controlled over the 13 months exposure. The alteration in the acid polluted atmosphere is accelerated by a minimum of 4 times compared to an inert atmosphere. However, in the acid polluted atmospheres, temperature and/or RH fluctuations affected the alteration rate over the 13 months exposure and deviations to the fitted lines are observed. It was discovered that better correlations were obtained by plotting the Na depletion depth directly as a function of time (Figure V- 36). The last measurements from the glass exposed to the formic acid atmosphere, were omitted as they correspond to the steady state.

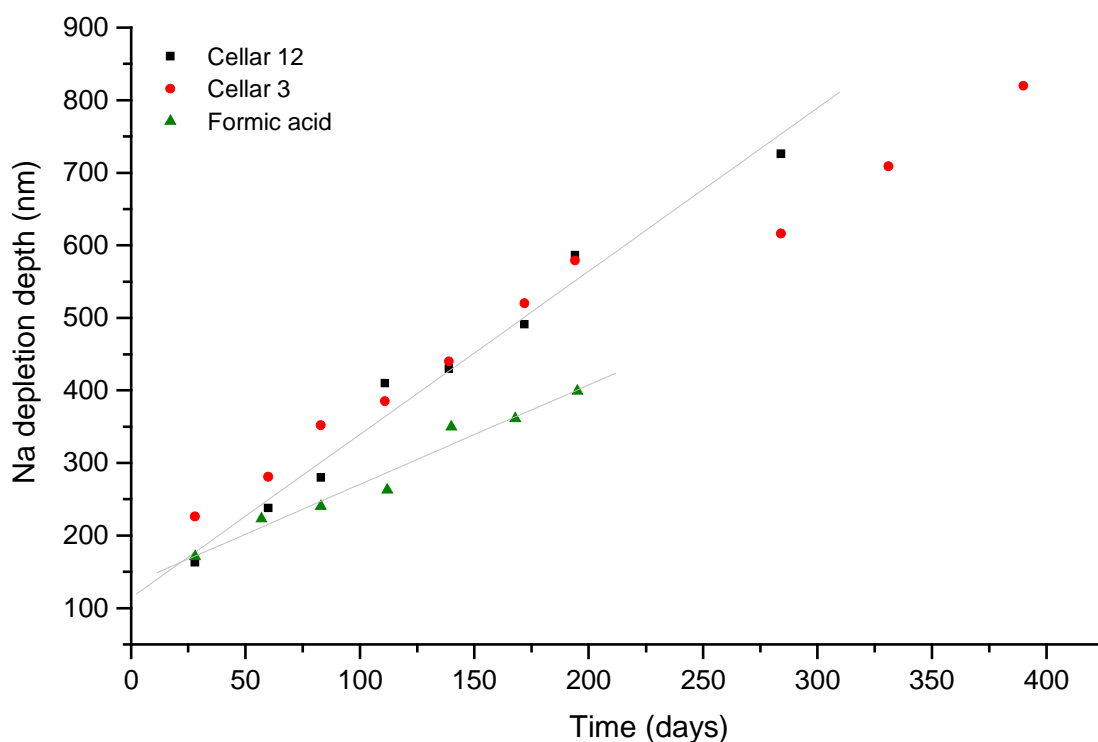


Figure V- 36: Correlation between the sodium alteration depth and the time, in formic acid, cellar 3 and cellar 12 atmospheres over 13 months.

The regression equations of the fitted lines for each atmosphere are:

$$\text{Formic acid} \quad y = 1.4 x + 133 \quad R^2 = 0.984$$

$$\text{Cellar 3} \quad y = 1.6 x + 214 \quad R^2 = 0.986$$

$$\text{Cellar 12} \quad y = 2.3 x + 114 \quad R^2 = 0.990$$

with x corresponding to the t (days) and y the sodium depletion depth (nm).

The correlations indicate that the alteration in the cellars as well as in the artificial formic acid atmospheres over 13 months is semi-linear with time. The diffusion reaction still controls the alteration but the reaction could never slow down because of the continuous fluctuations in the environment which re-activated the rapid ion-exchange reaction. This is supported by the 3 weeks experiments in which the alteration produced by formic acid is proportional to the square root of time, owing to the stable environmental conditions during these experiments.

The equations of the fitted line are consistent with the environmental conditions present in the different atmospheres which influenced the rate of the alteration. Thus, the alteration is expected to progress by 1.6 nm per day in cellar 3, which fluctuated around 23 °C and 41 % RH and by 2.3 nm per day in cellar 12, which fluctuated around 21°C and 48 % RH. Based on this data, it is possible to estimate that a glass with a composition similar to RG1 will develop an altered layer with a thickness of 37 µm (as in the British decanter) in 63 years in cellar 3 and 44 years in cellar 12. These values are consistent with the estimated exposure of the objects to these polluted environments.

The pollutant concentration did not appear to have an impact on the kinetics of the alteration since the progress of the alteration is faster in cellar 12 which had lower pollutant concentrations than cellar 3. Instead, the faster alteration in cellar 12 is controlled by the higher humidity of the atmosphere. Moreover, the correlation established over a year indicates that the alteration produced by the formic acid and cellar 12 atmospheres were similar in the first 3 months when their environmental conditions were close (Figure V- 36). After that period, the modifications of the RH and temperature changed the rate of the alteration and consequently their progress diverged. The 3 weeks experiment displays the same parallel between formic acid and cellar 12 atmospheres (Figure V- 35). The similarity between the two atmospheres indicates that the formic acid concentration in laboratory experiments ( $30.5 \mu\text{g m}^{-3}$ ) caused as much damage as the concentration in cellar 12, where the formic acid concentration was 6 times higher. The formic acid concentration used in the experiments is below the detection limits of ion chromatography (IC) used in museums to determine the level of organic pollutants and then identify problematic storage. This result suggests that formic acid concentration just below the IC detection limit would not be detected although they cause as much damage to unstable glass objects as high concentrations.

## V- 4. Conclusion

Water, present in the atmosphere as humidity, is the principal factor controlling the alteration of unstable glasses, as shown by the alteration experiments in N<sub>2</sub> atmospheres. This investigation confirmed the existence of two alteration mechanisms in ambient conditions: the selective leaching of alkali with formation of a hydrated layer; and the network dissolution. In the first stages, the leaching reaction predominates, with the amount of alkali leached proportional to the square root of time, and then at long-term the dissolution reaction dominates when the leaching reaction has reached the steady state. The results showed that the chemistry of the atmosphere greatly influences the kinetics of the process as well as the composition of the altered glass.

The water film created by the relative humidity provides the contact interface between the pollutants present in the atmosphere and the glass. An increase of the RH, increases the number of layers at the glass surface, accelerating the alkali leaching proportionally. We noted that the alteration process was slowed down when the glass was exposed to ambient air (renewed regularly) compared to an inert atmosphere. The low levels of pollutant present in the air (CO<sub>2</sub>, SO<sub>2</sub>...) reacted with the NaOH solution formed at the surface by water, stopping the network attack through dissolution.

In the presence of organic pollutants, emitted by the cabinets of the NMS, the leaching reaction is accelerated and amplified, and the dissolution reaction does not take place. This study clearly showed that formaldehyde does not act on the leaching reaction which means that formic acid (which accelerates it) is not created through oxidation. On the other hand, it reacts at the surface with NaOH, induced by water, to form sodium formate phase I' through the Cannizzaro reaction. Consequently, formaldehyde would be beneficial to the glass as it neutralise NaOH (as ambient air) avoiding the dissolution of the silicate network.

The similarity between the alterations formed in the cellars and the formic acid atmospheres confirms that organic acids are responsible for the accelerated alteration. Acid pollutants increase and maintain the acidity of the surface water film which accelerates and maintains the selective leaching of alkali ions in the glasses. Thus, in acidic atmospheres the leaching reaction always predominates, as observed in the previous chapter. The kinetics of the leaching reaction is increased by approximately 4 times in formic acid atmospheres

compared to non-polluted atmospheres. Acid pollutants not only increase the depth of the alteration, but they also increase the amount of sodium extracted within the altered layer. Therefore, the composition of the glass altered layer formed in acid polluted atmospheres has a sodium concentration ~1 at%, compared to ~5 at% in non-acidic atmospheres. This result is consistent with the composition of the glass objects from the NMS. The altered layer is then highly depleted in alkali and hydrated. The water and the low alkali level remaining in the glass may facilitate the ionic exchange and the leaching of the remaining bulk glass.

The more acidic the pollutant, the more leaching is induced. This result is different from the alteration in solution where the pH between 1 and 9 has little influence on the leaching reaction. The results indicated that the concentration of  $H^+$  and/or  $H_3O^+$  controls the atmospheric alteration, and this concentration depends on the number of water layers at the surface and the dissociating constant of the H-bearing species. The concentration of the pollutant has little or no influence on this alteration, particularly at the lower RH. The proposed explanation for this phenomenon is based on the saturation of the water film by the dissolved pollutants. The small volume of water present at the glass surface implies that the water layer rapidly reaches saturation in dissolved pollutants, even at low concentration. The amount of pollutant required to reach saturation decreases with RH and the surface area of the glass. In addition, there exists a competition between the different pollutants which may be explained by the difference in the acid-ionisation constant of these pollutants. In mixed polluted atmospheres, whatever the pollutant proportions, formic acid will always predominate in the film, possibly because it is incorporated faster in the film, creating mostly formates. This phenomenon explains the presence of mainly formates on the NMS glasses in atmospheres where acetic acid predominates. Consequently, formic acid is the second factor, after water, controlling the alteration.

The results showed that formic acid concentrations as low as  $30.5 \mu\text{g m}^{-3}$  produce as much damage as highly polluted atmospheres. The value of  $30.5 \mu\text{g m}^{-3}$ , for formic acid, is below the detection limits of ion chromatography currently used to monitor pollutant concentration in museums. This information is worrying from the preventive conservation of objects since it indicates that such atmospheres, damaging to the unstable objects, could not be identified.

The leaching reaction is diffusion controlled, so the amount of alkali extracted and the thickness of the altered layer is proportional to the square root of time, when the

environmental conditions (RH and temperature) are stable as in laboratory experiments. This was the case in the study of the glass weathering in moist and polluted air with SO<sub>2</sub> and NO<sub>2</sub> [9]. However controlled laboratory experiments are not representative of museum atmospheres where environmental conditions are far from controlled and daily, monthly and yearly fluctuations occur. The present investigation showed that the fluctuations greatly affected the leaching reaction progress and so the kinetics of the alteration. Each time fluctuations occurred, the equilibrium reached is disturbed and the rapid ion-exchange reaction is re-activated in the glass, causing an acceleration of the alteration. Although the alteration continuously tends toward an equilibrium in the glass, stabilising the alteration, it seems that this equilibrium is never reached owing to the constant fluctuations in the museums. This is amplified when the leaching is extensive, as in acidic atmospheres. Moreover, the crystallisation at the glass surface is expected to influence the equilibrium, favouring further leaching.

Consequently, the alteration in museums polluted by organic acids is constantly increasing and never reaches the steady state. From the 13 months experiments it was possible to establish that the alteration progressed by 1.6 nm per day in cellar 3 and by 2.3 nm per day in cellar 12 for the RG1 glass composition. These values indicate that only 50 years is required to reach an altered layer of 40 µm (thickness measured on some NMS objects), which is consistent with the exposure time of the objects to this polluted atmosphere. The difference in alteration kinetics between the two cellars is associated with the environmental conditions rather than the pollutant concentration difference. Finally, if a glass previously altered in an acidic atmosphere is placed in a non-acidic atmosphere, the equilibrium within the altered layer is disturbed and modification will take place in order to reach a new equilibrium in agreement with the chemistry of the new atmosphere.

## V- 5. References

- 1 Ryan J.L., The atmospheric deterioration of Glass: Studies of decay mechanisms and conservation techniques, *PhD thesis*. University of London (1996).
- 2 Fearn S., McPhail D., and Oakley V., Room temperature corrosion of museum glass: an investigation using low-energy SIMS, *App. Surf. Sci.* **231-232** (2004) 510.
- 3 Fearn S., McPhail D., and Oakley V., Moisture attack on museum glass measured by SIMS, *Phys. Chem. Glasses.* **5** (2005) 505.
- 4 Salem A.A., Stinger G., Grasserbauer M., Shreiner M., Giessler K.H., and Rauch F., SIMS and RBS analysis of leached glass: reliability of RSF method for SIMS quantification, *J. Mater. Sci.* **7** (1996) 373.
- 5 Schreiner M., Woisetschläger G., Schmitz I., and Wadsak M., Characterisation of the surface layers formed under natural environmental conditions on medieval stained glass and ancient copper alloys using SEM, SIMS and atomic force microscopy, *J. Anal. At. Spectrom.* **14** (1999) 395.
- 6 Hervig R.L., Mazdab F.K., Williams P., Guan Y., Huss G.R., and Leshin L.A., Useful ion yields for Cameca IMS 3f and 6f SIMS: Limits on quantitative analysis., *Chem. Geol.* **227** (2006) 83.
- 7 Craven J., Secondary Ion Mass Spectrometry (SIMS), unpublished manual, School of Geosciences, The University of Edinburgh, undated.
- 8 Smets B.M.J., and Lommen T.P.A, SIMS and XPS investigation of the leaching of glasses, *Verres Réfract.* **1** (1981) 84.
- 9 Cummings K., Lanford W.A., and Feldmann M., Weathering of glass in moist and polluted air, *Nucl. Instrum. Meth. B.* **136-138** (1998) 858.
- 10 Schnatter K.H., Doremus R.H., and Lanford W.A., Hydrogen analysis of soda-lime silicate glass, *J. Non-Cryst. Solids.* **102** (1988) 11.
- 11 Rudd G.I., Garofalini S.H., Hensley D.A., and Mate C.M., Atomic Force Microscopy and X-Ray Photoelectron Microscopy investigation of the onset of reactions on alkali silicate glass surfaces, *J. Am. Ceram. Soc.* **10** (1993) 2555.
- 12 Trens P., Denoyel R., and Guilloteau E., Evolution of surface composition, porosity and surface area of glass fibers in a moist atmosphere, *Langmuir.* **12** (1996) 1245.
- 13 Otha K., Ogawa H., and Mizuno T., Abiological formation of formic acid on rocks in nature, *Appl. Geochem.* **15** (2000) 91.
- 14 Peng C., and Chan C. K., The water cycles of water-soluble organic salts of atmospheric importance, *Atmos. Environ.* **35** (2001) 1183.

- 15 Saliba N.A., Yang H., and Finlayson-Pitts B.J., Reaction of gaseous nitric oxide with nitric acid on silica surfaces in the presence of water at room temperature, *J. Phys. Chem. A*. **105** (2005) 10339.
- 16 Sumner A.L., Menke E.J., Dubowski Y., Newberg J.T., Penner R.M., Hemminger J.C., Wingen L.M. Brauers T., and Finlayson-Pitts B.J., The nature of water on surfaces of laboratory systems and implications for heterogeneous chemistry in the troposphere, *Phys. Chem. Chem. Phys.* **6** (2004) 604.

## GENERAL CONCLUSION

The aim of this research was to investigate the role of organic pollutants in the alteration of historic soda silicate glasses, concentrating on the predominant pollutants emitted by wooden showcases: formic acid, acetic acid and formaldehyde.

The research focused mainly on investigating the alteration of the composition and chemical structure of the glass using Raman spectroscopy, Secondary Ion Mass Spectrometry (SIMS) profiling and electron microprobe (EPMA). The glass appearance and the crystalline products were examined complementarily by optical microscopy, Scanning Electron Microscopy (SEM) and Raman spectroscopy to assist the interpretation. The National Museums of Scotland (NMS) glass collection was used as a basis for this investigation since part of the collection was affected by a widespread alteration involving organic pollutants. In addition, replica glasses, aged in real or artificial environments, were used to examine the role of the different factors involved, the mechanisms and kinetics of the alteration.

The investigation showed that Raman spectroscopy can be applied *in-situ* and non-destructively to glass objects to gain information about their stability, degree of deterioration and the origin of the alteration. It was found that the stability of glass, which is linked to its composition, could be assessed from its Raman spectrum, sometimes using simply the spectra profiles or after decomposition of the spectra. A spectral decomposition method was developed for alkali silicate spectra, and correlations were established between the decomposed vibrational components and the composition of the glass. From these data, a relation was established, which can be used to assess the stability of soda silicate glass. The work concentrated on soda silicate glass compositions but has shown the value of extending it to other glass compositions, in particular potash silicate glasses, which are even more unstable and have been widely used in historic buildings and objects.

The examination of the altered glass layer indicated that the structure and composition are characteristic of the alteration process and the chemistry of its environment. The characteristics related to the appearance, Raman spectrum, composition and crystalline

products have been determined and were presented for soda silicate glasses altered through selective leaching (with and without acid pollutant) or congruent dissolution.

The application of SIMS depth profiling to aged glasses was very successful in determining the mechanisms of the alteration. It was possible to follow the progress of the alteration and obtain information on the chemical concentration of the altered layer as well as the state of the leaching reaction. The SIMS measurements clearly showed that the concentration in  $H^+$  and/or  $H_3O^+$ , influenced by the relative humidity and the pollutant acidity, controls the atmospheric alteration of glass by leaching.

The research presents experimental evidence that organic acid pollutants have a dramatic effect on the alteration of unstable soda silicate glasses, and are responsible for the widespread alteration of part of the NMS glass collection. Therefore storage of unstable glasses in wooden cabinets or showcases emitting organic pollutants must be avoided. The organic acidic pollutants increase the acidity of the water film formed on the glass surface by atmospheric humidity, and this subsequently accelerates and amplifies the leaching reaction. This work revealed that formic acid is the pollutant responsible of the alteration as it dominates in the water film, even when present in small concentration in the atmosphere. This finding explains the predominance of crystalline formate compounds formed at the glass surfaces. Contrary to general belief, formaldehyde is not the culprit of the alteration of glass exposed to organic polluted atmosphere, as it was shown to have no effect on the leaching process.

The alteration is aggravated where there are humidity and temperature fluctuations (as recorded in many museum storage or display environments), as these are responsible for maintaining a continuous leaching reaction. Consequently the kinetics of the alteration progress linearly with time and does not follow the square root of time relation expected from a diffusion-controlled process and generally assumed for the alteration of glasses in museums. This research provided an exploratory work of the kinetics and mechanisms of the atmospheric alteration of glasses and it would need to be extended further using fully controlled experiments to obtain a detail understanding of the leaching reaction process, its kinetics and the role of the controlling factors. Knowledge on the role of the reaction zone and the altered layer, in particular, would help interpret the features and shape observed in the SIMS depth-profiles and explains the effect of the elements remaining in the altered layer.

As a result of the continuous leaching in the polluted atmosphere, thick leached and hydrated layers have developed at the surface of the unstable NMS glass objects. Subsequent dehydration of these layers, arising from humidity decrease or temperature increase, is responsible for the strong cracking observed. This cracking, known as crizzling in museums, is the main problem for the conservation of the objects as it disfigures the glass and can lead to its complete disintegration.

The study of the effect of the environment on the hydrated layers would be needed to understand the mechanics of these layers, examining in particular the stress induced in the glass and its altered layer and the cracking process. Moreover, the use of solid-state Nuclear Magnetic Resonance (NMR) in parallel to Raman spectroscopy could provide more information on the structure of these layers, before and after drying, and enhance interpretation of the origin of the variations observed in the Raman spectra. This information would help determine in more detail the mechanisms involved in the drying and cracking process of these glasses. Detailed research of these aspects would allow developing conservation treatments and storage conditions which are adapted to the altered objects.

Finally, the examination of the crystalline deposits evidenced the existence of new formate compound phases and the role of the humidity in the transformation of these phases. Moreover these crystalline deposits created striking patterns or peculiar crystals at the glass surface. Complementarily techniques such as X-ray Diffraction (XRD) and NMR would be needed to determine the structure of these new phases and experimental work on the crystal synthesis is required to assess their formation process and their stability under ambient conditions.

# **APPENDICES**

## APPENDIX - I : Cation radii

Atom	Electronegativity	Ionic charge	Effective ionic radii (pm)			
			Coordination number			
			4	6	8	12
Arsenic	2.18	+3		58		
		+5	33.5	46		
Barium	0.9	+2		136	142	160
Calcium	1.0	+2		100	112	135
Copper	1.9	+2	57	73		
Iron	1.83	+2		61		
		+3		55		
Lead	1.8	+2	98	119	129	149
Lithium	0.98	+1	59	76		
Magnesium	1.31	+2	57	72	89	
Manganese	1.55	+2	66	67	96	
		+3		58		
		+6	25.5			
Potassium	0.82	+1	137	138	151	164
Silicon	1.92	+4	26			
Sodium	0.93	+1	99	102	118	139

Data from Dean J.A., *Lange's Handbook of Chemistry*, 15<sup>th</sup> edition, Mc Graw Hill (1999).

## APPENDIX - II : Ambient experiments

### Series 2 : Effect of RH and organic pollutants

Introduced atmosphere	40 % RH	50 % RH	60 % RH
N <sub>2</sub>	x	x	x
50 µl formic acid	x	x	x
50 µl acetic acid	x	x	failed
50 µl formic acid + 100 µl acetic acid		x	x

- Replica glasses used : RG<sub>1</sub> and RR<sub>n</sub>
- Duration : 6 weeks

### Series 3 : Progress of the alteration with time

Sample	Duration (days)	
	Ageing in desiccators	Ageing in museum
4D	4	-
W1	7	7
W2	14	14
W3	21	21
T1	28	28
T2	57	60
T3	83	83
T4	112	111
T5	140	139
T6	168	172
T7	195	194
T8	284	284
T9	331	331
T10	395	390

- Replica glass used : RG<sub>1</sub>
- Atmospheres:  
*Ageing in desiccators* : laboratory ambient air (LA), nitrogen (N<sub>2</sub>), formic acid (FA) and formaldehyde (F).  
*Ageing in Museum* : Cellar 3 (C3) and Cellar 12 (C12)

## APPENDIX - III : Accelerated experiments

Duration	Non polluted	Formic acid	Acetic acid	Formaldehyde	Formic acid + acetic acid + formaldehyde	Wood
1 week	RG <sub>1</sub>	RG <sub>1</sub> (h+d)	-	-	-	-
2 weeks	RG <sub>1</sub>	RG <sub>1</sub> (h+d)	-	-	-	-
3 weeks	RG <sub>1</sub>	RG <sub>1</sub> (h+d)	-	-	-	-
4 weeks	RG <sub>1</sub> , RRn	RG <sub>1</sub> (h+d)	RG <sub>1</sub> , RRn	RG <sub>1</sub> , RRn	RG <sub>1</sub> , RRn	RG <sub>1</sub>
6 weeks	RRo (dried)	RRo	-	-	-	-
8 weeks	RG <sub>1</sub> (dried)	-	-	-	-	-
3 months	-	RG <sub>1</sub> (h+d)	-	-	-	-

- Glass used RG<sub>1</sub>, RRo or RRn as stated.
- Pollutant quantity introduced: ~15 µl or ~30 µl of each pollutant ; or 2 g of MDF wood
- Temperature: 60 °C, except 50 °C for RG<sub>1</sub> aged 3 months
- Humidity: ~100 % RH
- ‘dried’ means that the water from the humidity in the tube was completely consumed, and the altered layer was dry on opening.
- ‘(h+d)’ means that half of the sample was stored in ambient air and the other half stored in dry silica before analyses.

## APPENDIX - IV : Crystalline products on glasses

Raman peak position ( $\text{cm}^{-1}$ ) and intensities of the formate and acetate compounds identified in the crystalline deposits from altered glasses in chapter III.

Na HCOO phase II	Na HCOO phase I'	Sodium calcium formate	Formate Y	Na CH <sub>3</sub> COO anhydrous	Na CH <sub>3</sub> COO trihydrate
			3540 m		3429 w/br
			3350 m/br		3282 w 3175 w
			3119 m/br	3008 vw 2932 m	2935 s
2830 m		2852 w	2854 s	2845 vw	
	2815 w 2785 m	2813 vw			
		2756 vw 2731 vw	2758 m		
2718 w	2685 w				
			1467 w		
		1403 w 1396 m		1452 vw 1419 vw	1417 m
	1388 vs		1390 s		
1368 s	1368 s	1382 m			
1356 vs	1360 m	1367 vs			
		1351 m 1341 m	1348 vs	1352 vw 1340 vw	1350 m
1073 w	1065 m	1073 vw			
				1013 vw 925 vs	1020 vw 932 vs
			880 vs 780 w		
770 vw	778 w 770 w	769 vw		665 m 624 vw	658 vw 624 vw
			270 w		
245 m					180 w/br
	150 s			154 w	159 w
135 s		138 m			

Intensity : vs : very strong, s : strong, m : medium, w : weak, vw : very weak, br : broad, sh : shoulder.

## APPENDIX - V : Publications

### Refereed papers

Robinet L., Coupry C., Eremin K., and Hall C., Raman investigation of the structural changes during alteration of historic glasses by organic pollutants, *J. Raman Spectrosc.* 37 (2006) *in press*.

Robinet L., Coupry C., Eremin K., and Hall C., The use of Raman spectrometry to predict the stability of historic glasses, *J. Raman Spectrosc.* 37 (2006) 789.

Robinet L., Fearn S., and Eremin K., Understanding glass deterioration in museum collections: a multi-disciplinary approach, ICOM Committee for Conservation triennial meeting (14<sup>th</sup>), The Hague, *James & James*, London (2005) 139.

Robinet L., Eremin K., Fearn S., Pulham C., and Hall C., Understanding glass deterioration in museum collections through Raman spectroscopy and SIMS analysis, *Mat. Res. Soc. Symp.* P 852 (2005) 121. – [award for the best student paper]

### Other technical publications

Carmichael H., Disintegration mystery cracked, *Chemistry World.* 2, 11 (November 2005) 13. <http://www.rsc.org/chemistryworld/News/2005/September/26090501.asp>

Prost A., Le bois des vitrines des musées contribue a la corrosion des objets en verre, Actualités scientifiques au Royaume-Uni, *Ambassade de France au Royaume-Uni.* (October 2005) 39. [http://www.ambascience.co.uk/article.php3?id\\_article=557](http://www.ambascience.co.uk/article.php3?id_article=557)

Wood R., Keeping a weather-eye on ancient glass, *Materials World.* (March 2005) 29. <http://www.cmse.ed.ac.uk/MatWorld-Mar05.pdf>

## Conferences

### Presentations

Robinet L., Eremin K., Coupry C., and Hall C., L'altération des verres historiques du musée national d'Ecosse: causes et conséquences, *Réunion plénière du GdR 2114 Chimart*. Paris, 25-26 January 2006.

Robinet L., and Eremin K., Glass alteration in the presence of organic pollutants: understanding the chemical and structural modifications, *Glass Science in Art and Conservation*. Lisbon, 19 - 20 September 2005.

Robinet L, Fearn S, and Eremin K., Understanding glass deterioration in museum collections: a multi-disciplinary approach, *ICOM Committee for Conservation triennial meeting (14<sup>th</sup>)*. The Hague, 12-16<sup>th</sup> September 2005.

Robinet L., Coupry C., and Hall C., Examination of the chemical structure of deteriorating museum glass by Raman spectroscopy, *3<sup>rd</sup> International conference on the application of Raman spectroscopy in Art and Archeology*. Paris, 31 August-3 September 2005.

Robinet L., Eremin K., Fearn S., Pulham C., and Hall C., Understanding Glass Deterioration in Museum Collections through Raman Spectroscopy and SIMS analysis, *Material Research Society Symposium*, Boston, 29<sup>th</sup> November – 3<sup>rd</sup> December 2004.

### Posters

Robinet L., Coupry C., Eremin K., Etude des modifications de structure d'un verre historique altéré. Profil d'altération mesure *in-situ* et sur coupe. *Colloque Imagerie et Cartographie en spectroscopie vibrationnelle organisé par le Groupe Français de Spectroscopie Vibrationnelle (GFSV)*. Les Houches, 26-28 January 2005.

Robinet L., Eremin K., Hall C., Pulham C., and Lacombe N., Raman spectroscopy for the study of deteriorating glass in museum collections, *The XIX<sup>th</sup> International conference on Raman spectroscopy (ICORS)*. Surfers Paradise, 8-13 August 2004.

**RESUME DETAILLE**  
**EN FRANCAIS**

## INTRODUCTION

L'étude de l'altération des collections verrières du musée national d'Ecosse (NMS) a clairement montré que les polluants organiques interagissent avec le verre produisant la formation de dépôts cristallins en surface. Cependant l'effet de ces polluants sur la structure elle-même n'est pas connue. Quelques études ont rapporté une altération similaire et ont affirmé que le formaldéhyde au sein des polluants organiques était responsable de l'altération sans tenir compte des polluants acides. Etant donné que le rôle de ces polluants sur l'altération des verres n'a jamais été examiné, il n'était pas possible de faire des recommandations concernant le traitement et la conservation future des verres du NMS.

Le but de cette étude a donc été d'étudier le rôle des polluants organiques sur l'altération des verres instables comparativement à une atmosphère non-polluée. Ce travail se concentre sur l'altération des verres à composition sodique instable et examine le rôle de l'acide formique, l'acide acétique et le formaldéhyde. Les analyses sont basées sur des objets en verres issus des collections du NMS et des verres répliques vieillies dans des atmosphères réelles et artificielles. La recherche focalise sur les modifications de la structure chimique du verre avec l'altération.

Le *chapitre I* revient sur l'état de connaissances concernant la structure du verre, sa composition, son altération, l'altération des collections verrières du NMS et les polluants organiques. Le *chapitre II* présente les matériaux étudiés, les procédures expérimentales et les différentes techniques d'analyses appliquées. Un court *chapitre III* examine les dépôts cristallins afin de compléter les résultats des autres analyses. Dans le *chapitre IV*, la spectroscopie Raman est appliquée pour examiner le lien entre les données spectrales et la composition/stabilité des verres; ainsi que les modifications de structure par l'altération sur des verres historiques et des verres vieillies artificiellement. Enfin, les mécanismes et les cinétiques de l'altération, basés sur les profils de concentration SIMS des verres vieillies artificiellement, sont présentés en *chapitre V*.

## I - ETAT DE L'ART

### Structure d'un verre

Dans les verres silicates il existe un ordre à courte distance avec l'arrangement des atomes en tétraèdres  $\text{SiO}_4$ , mais sans ordre à moyenne et longue distance. Ces unités  $\text{SiO}_4$  forment la structure de base des verres silicates c'est pourquoi Si est nommé le *formateur* du réseau. Ces tétraèdres sont liés à leur sommet, ne partageant qu'un seul oxygène, qui est nommé *oxygène pontant* (BO). L'introduction de cations dans le verre, principalement alcalins ( $\text{Na}^+$ ,  $\text{K}^+$ ) et alcalino-terreux ( $\text{Ca}^{2+}$ ,  $\text{Mg}^{2+}$ ) modifie les propriétés du verre aussi les nomme-t-on *modificateurs* de réseau. Ces cations dépolymérisent la structure en cassant des liaisons Si-O et créent des liaisons plus ioniques entre le cation et l'oxygène. Les oxygènes liés à ces cations sont nommés *oxygènes non-pontants* (NBO). Les unités silicates peuvent avoir entre 0 et 4 NBOs et la notation  $Q^n$  est utilisée pour différencier chacune de ces espèces, où  $n$  correspond au nombre d'oxygènes pontants. La concentration et le type de cation influencent la distribution de ces espèces  $Q^n$ . En fonction de leur structures électroniques, les cations affectent les énergies de liaisons des Si-O différemment, ce qui modifie la structure du réseau au travers des longueurs et des forces des liaisons, de la coordination du cation, de l'angle des liaisons Si-O-Si.

### Altération des verres

La composition du verre et la présence d'eau sont les deux facteurs principaux responsables de l'altération des verres. Plus un verre contient de cations modificateurs, plus sa structure est dépolymérisée et donc ouverte, ce qui favorise la mobilité des cations et l'altération du verre. Les cations ne réagissent pas avec l'eau de façon égale. En général, plus le rapport charge sur rayon ionique des cations diminue, plus le verre sera altéré. Ainsi, les alcalins sont facilement extraits du réseau, tandis que les alcalino-terreux augmentent la durabilité des verres. Pour cette raison les alcalino-terreux, ainsi que l'aluminium et le plomb sont nommés *stabilisateurs*. Cette différence est associée aux différentes mobilités des cations, liées aux forces de liaison de ces cations avec les NBOs.

Deux mécanismes sont impliqués lors de la réaction de l'eau avec le verre : la **lixiviation** sélective des alcalins et la **dissolution** du réseau silicate. Suivant la période dans le temps et surtout le pH de la solution d'attaque, l'un ou l'autre mécanisme domine l'altération.

Lors de la **lixiviation**, il y a formation de silanols après extraction sélective des alcalins, ce qui implique une hydratation du verre. La lixiviation en présence d'eau se fait au travers de 3 réactions simultanées :

- *L'échange ionique* : quand les alcalins sont remplacés par  $H^+$  ou  $H_3O^+$ , en gardant la neutralité électrique en chaque point.
- *L'hydratation* : quand l'eau pénètre dans le verre sous forme moléculaire
- *L'hydrolyse* : quand l'eau casse les liaisons Si-O-Si.

Comme ces 3 réactions font intervenir des mécanismes de diffusion, la quantité d'alcalins extrait par la lixiviation est proportionnelle à la racine carrée du temps. La lixiviation domine l'altération dans les premiers temps de contact avec l'eau puis la vitesse d'extraction ralentit avec le temps jusqu'à atteindre un état stable. La lixiviation favorise une augmentation du pH par formation d'hydroxydes d'alcalins (NaOH, KOH) en surface. Par suite de la lixiviation, le réseau silicate se réarrange par condensation des silanols pour former de nouvelles liaisons Si-O-Si.

Lors de la **dissolution**, il y a coupure des liaisons Si-O-Si et tous les éléments du réseau peuvent passer en solution, c'est pourquoi elle est dite congruente. Cette réaction domine à long terme, après stabilisation de la réaction de lixiviation, ou en présence de pH supérieur à 9. En solution basique, la dissolution est accélérée par l'attaque nucléophile et progresse proportionnellement avec le temps. Le verre dissous forme un gel qui est riche en espèces silicates hydratées. Après condensation, ce gel forme un matériau amorphe hydraté.

La réaction du verre avec l'atmosphère est favorisée par la présence d'un film d'eau à la surface du verre, dont l'épaisseur augmente avec l'humidité ambiante. Le processus d'altération est influencé par différents facteurs que sont : les conditions statiques ou dynamiques, l'aire de la surface du verre par rapport au volume de la solution, l'humidité relative qui contrôle le nombre de couche d'eau adsorbée en surface, la température, les polluants, et la nature des particules.

### **Altération des verres du musée national d'Ecosse (NMS)**

Un examen en 1996 des collections verrières du Musée National d'Ecosse (NMS) a révélé que les verres des collections Britanniques, Chinoises et Islamiques du 19<sup>ème</sup>-20<sup>ème</sup> siècle étaient touchés par une altération étendue inhabituelle avec formation de dépôts cristallins, craquelures, ou perte d'écailles. Une étude scientifique par le département 'Conservation and Analytical Research' du NMS a conclu que l'altération résultait d'une combinaison de facteurs :

- une composition instable : généralement riche en sodium et pauvre en calcium,
- une humidité relative (RH) et une température fluctuantes,
- des concentrations élevées de polluants organiques: l'acide acétique, l'acide formique et le formaldéhyde émis par les vitrines en bois où les objets sont exposés ou stockés.

Malgré une concentration largement majoritaire d'acide acétique dans l'atmosphère, seuls des cristaux de formates de sodium sont identifiés à la surface des verres.

### **Polluants organiques**

Les polluants organiques volatiles sont un problème majeur dans les musées car ils altèrent un grand nombre de matériaux inorganiques. Il s'agit principalement de formaldéhyde, d'acides acétiques et formiques. Ce sont les matériaux utilisés pour fabriquer les vitrines (bois, résines, colles, peintures...) qui constituent la source principale de ces composés. Le processus d'altération par l'aldéhyde n'est pas bien connu. Celui-ci peut soit former l'acide formique par oxydation, soit réagir avec NaOH selon la réaction de Cannizzaro en formant des formates.

## **II - EXPERIMENTATION ET INSTRUMENTATION**

La collection verrière du NMS a servi de base pour cette recherche. Par ailleurs, ce travail s'installe dans la continuité des recherches effectuées par Ryan et Fearn sur l'altération atmosphérique des verres instable dans les musées. Lors de leurs études ils ont utilisé un verre réplique **RG1** avec une composition riche en sodium et pauvre en calcium, proche de la composition des verres altérés du NMS. Nous avons choisi d'utiliser ce même verre, qui nous a été fourni par Fearn, pour examiner l'effet des polluants sur son altération.

### **Matériaux**

Les matériaux choisis sont présentés selon les différentes problématiques étudiées :

Etude du lien composition – stabilité – spectre Raman : Des échantillons ont été prélevés sur des objets stables et instables au sein des collections Britanniques et Islamiques.

Etude des changements de structure avec l'altération : basée sur l'analyse d'une bouteille à décanter Britannique et une bouteille Islamique du NMS (Figure II.2). Les deux objets ont une composition riche en sodium mais diffèrent par le type de cation stabilisateur présent.

Etude de la corrosion cristalline : Les produits cristallins proviennent de verres Britanniques, Islamiques et Chinois des collections du NMS, ainsi que des produits cristallins prélevés sur des objets du ‘Corning Museum of Glass’.

Etude du rôle des polluants – expériences de vieillissement : Le verre **RG1** qui a une composition instable riche en sodium et faible en calcium a servi de base pour les expériences de vieillissement artificielles. Deux répliques de verres sodiques additionnelles, l’un stable avec une plus forte proportion de calcium **RRn**, et l’autre instable avec une faible quantité de magnésium **RRo** sont utilisées dans certaines expériences pour comparaison. Tous ces verres ont été fabriqués par soufflage ce qui leur confère une plus grande ressemblance avec les verres historiques, par rapport aux blocs de verres faits en laboratoire. Leur composition élémentaire mesurée par microsonde électronique est présentée dans le tableau II.1.

### **Expériences de vieillissement**

Vieillissement en condition ambiante : Les verres répliques ont été altérés dans des dessiccateurs où la température, l’humidité relative et la concentration des polluants introduits étaient contrôlées. L’influence des paramètres suivants sur l’altération a été examinée : l’humidité, le type de polluant, sa concentration, le CO<sub>2</sub> en présence de lumière, et le temps. Le montage des expériences est présenté en figure II.4 et un résumé des expériences est donné en annexe II.

Des verres ont été altérés en atmosphère réelle en plaçant des échantillons de verre **RG1** aux côtés des objets au sein de deux armoires du NMS, nommées cellar 3 et 12 dans cette étude, qui émettent des quantités élevées de polluants. Les concentrations correspondantes sont indiquées dans le tableau II.2 ainsi que la disposition des échantillons en figures II.5 et II.6. Des verres **RG1** ont été exposés en parallèle dans les dessiccateurs et les armoires pendant 13 mois.

Vieillissement en conditions accélérées : Les 3 verres répliques ont été altérés par exposition à une atmosphère saturée en eau avec ou non des polluants, après suspension du fragment de verre par un bouchon silicone dans un tube en verre de 50 mL (Figure II-7). Le tube a été maintenu à une température de 60°C pour des durées de 1-8 semaines (Annexe III).

## Techniques d'analyses

Deux techniques d'analyses principales ont été choisies pour cette étude :

- La spectroscopie Raman pour examiner les modifications de structure du verre sur des objets du musée et des verres vieillis en conditions accélérées. Cette technique a été choisie car elle permet d'effectuer des analyses *in-situ* et non destructive, critères essentiels pour les musées.

- La microsonde ionique SIMS: pour suivre l'altération à partir des profils de concentration des éléments dans les verres vieillis en conditions ambiantes. L'intérêt du SIMS est de pouvoir observer les modifications de dizaine de nanomètres créées dans le verre à condition ambiante.

La microsonde électronique (EPMA) a été utilisée de façon complémentaire pour obtenir la composition élémentaire des verres étudiés. Le microscope électronique à balayage a été appliqué principalement pour obtenir des images de la surface ou de la coupe transversale des verres.

## III - PRODUITS CRYSTALLINS SUR LES VERRES

Ce chapitre a confirmé que l'altération causée par les polluants émis par les vitrines et armoires de stockage affectent aussi bien les verres Britanniques que les verres Chinois et Islamiques de composition instable dans la collection du NMS. Une altération identique touche les collections du Corning Museum of Glass. Dans tous les cas les composés formates sont majoritaires, avec principalement le sodium de formate II et minoritairement le sodium de formate I' et un formate de sodium et calcium. La présence de la phase I' du formate du sodium à la surface de certains objets a été confirmée à partir de la comparaison des spectres Raman d'un échantillon provenant d'un objet et du formate de sodium refroidi après chauffage au delà de 240°C. Il a été déterminé que la présence des phases I' ou II du formate de sodium dans les produits est liée à l'humidité relative de l'environnement. Les produits cristallins formés en surface des verres vieillis dans les atmosphères artificielles sont en accord avec les produits présents sur les objets de musée. La différence notée entre les produits formés lors des vieillissements en condition ambiante et accélérée pour les atmosphères à polluant mixte indique que la compétition entre les polluants est affectée par les conditions de température et d'humidité.

## IV - LA STRUCTURE CHIMIQUE DES VERRES SODIQUES

### Lien stabilité-composition-spectre Raman

Cette étude a montré que la spectrométrie Raman peut informer sur la stabilité d'un verre sans nécessiter la détermination de la composition élémentaire complète. Une première distinction peut être faite sur le profil du spectre entre les verres calciques ou au plomb, tous deux stables et les verres alcalins qui ont une stabilité mixte (figure IV.4). Dans le cas des verres alcalins une analyse spectrale est requise pour obtenir des informations sur les différentes unités vibrationnelles associées type d'alcalin et la concentration des cations. Pour cette raison une méthode de décomposition a été mise au point pour les spectres de ces verres et a conduit à des corrélations établies à partir des composantes spectrales obtenues (Table IV.3 and Figure IV.7).

La position de la bande à  $550\text{ cm}^{-1}$  a été corrélée directement au degré de polymérisation du verre avec la concentration en silice du verre (Figure IV.8). Par conséquent cette bande est aussi directement corrélée à la charge totale des cations modificateurs. Cette méthode est particulièrement adaptée pour comparer des verres issus d'un groupe de composition similaire, comme les verres alcalins.

Une autre corrélation a été établie entre la charge totale des cations modificateurs et l'intensité relative de la bande à  $950\text{ cm}^{-1}$ , associée à la vibration des espèces  $Q^2$  (Figure IV.9). Cette bande est principalement influencée par la concentration en cations doublement et triplement chargés, les stabilisateurs.

Le rapport des aires des bandes  $(A_{900}+A_{950}+A_{990})/(A_{900-1150})$  du spectre Raman est proposé pour déterminer la stabilité des verres sodiques (figure IV.10). Bien que cette méthode de décomposition spectrale nécessite d'autres vérifications, elle montre que la spectroscopie Raman peut aider les musées à évaluer la composition générale de leur objets en verre et la stabilité de leurs verres sodiques.

### Modification de la structure avec l'altération

Cette étude présente les différences de modifications produites entre les processus d'altération en atmosphère humide et en atmosphère humide polluée par la présence d'un acide. Chaque atmosphère génère des modifications d'apparence et de structure caractéristiques, décrites ci-dessous.

### Atmosphère humide et polluée par un acide

Dans une atmosphère acide, le processus de lixiviation des alcalins est continu et la dissolution est négligeable. Après altération en atmosphère acide, le verre apparaît visuellement inchangé, en gardant sa transparence, car le réseau Si-O-Si n'a pas été altéré. Cependant à cause de sa forte hydratation, le verre est sensible à la déshydratation qui provoque l'extraction des molécules d'eau de la structure et favorise probablement d'autres réactions de polymérisation entre silanols. Tout séchage important du verre par exposition à une humidité relative basse ou une augmentation de température crée d'importantes craquelures qui modifient irrémédiablement l'apparence visuelle du verre (Figure IV.18). Ces fractures peuvent amener le verre à sa complète désintégration.

Au sein de la structure en surface, la lixiviation entraîne la diminution des espèces  $Q^3$  associées aux alcalins et la formation d'espèces silanols (Figure IV.20). Ces modifications sont principalement observées dans le spectre Raman par la diminution d'intensité des bandes associées à la vibration des espèces  $Q^3$ , à environ  $550\text{ cm}^{-1}$ , pour les déformations et  $1100\text{ cm}^{-1}$ , pour les élongations. Les cations polyvalents stabilisateurs, tels que le calcium, le magnésium et le plomb, sont retenus dans la structure à cause de leur plus forte interaction avec les NBOs. Par conséquent, les espèces  $Q^2$  principalement associés à ces cations restent présentes dans la structure. Ces espèces  $Q^2$  présentent des bandes de vibration dans le spectre Raman dans la région  $900\text{-}1000\text{ cm}^{-1}$ , qui apparaissent sous la forme de deux composantes autour de  $950$  et  $990\text{ cm}^{-1}$  quand le cation associé est le calcium, ou une simple composante plus fine à  $990\text{ cm}^{-1}$  quand le cation associé est le plomb ou le cuivre. L'hydratation de la structure par formation de silanols et d'eau moléculaire est mise en évidence par la présence d'une bande large dans la région  $3000\text{-}3800\text{ cm}^{-1}$  du spectre Raman. Celle-ci est associée à la présence de nouvelles bandes plus ou moins visibles à  $970\text{-}1000\text{ cm}^{-1}$ ,  $1070\text{-}1080\text{ cm}^{-1}$  and  $1630\text{ cm}^{-1}$ . Lors de l'altération, la majorité des silanols formés polymérisent, en réagissant entre eux, et forment de nouvelles liaisons Si-O-Si ainsi que des anneaux  $D_1$  à 4 tétraèdres silicates. La polymérisation est détectée sur le spectre Raman par une augmentation du massif de vibration de déformation des Si-O-Si entre  $200$  et  $600\text{ cm}^{-1}$ . Dans certains cas, on note la présence de groupes formates au sein de la structure, ce qui suggère que l'acide formique pénètre au sein de la couche altérée, pouvant éventuellement catalyser la condensation des silanols comme c'est le cas dans les sol-gels.

### Atmosphère humide non polluée

En l'absence d'un polluant acide qui conserve l'acidité du film d'eau à la surface du verre, la lixiviation qui a lieu au début de l'altération entraîne la formation rapide d'une solution très basique de NaOH à la surface du verre. En présence de cette solution basique la réaction de dissolution du réseau silicate prédomine. Les produits de cette dissolution n'étant pas éliminés, comme lors d'une altération en solution, un gel se forme en surface contenant des espèces silicates hydratées  $\text{HSiO}_3^-$  and  $\text{SiO}_3^{2-}$  ainsi que les cations dissous.

Après altération en atmosphère humide, l'apparence visuelle du verre en surface est très modifiée, et cette apparence varie avec le temps et les conditions d'exposition. On note principalement une perte de transparence de la surface et la formation d'iridescences dans les premiers temps de l'altération (Figures IV.25). Avec le temps, la couche altérée s'épaissit, devient opaque et l'aspect d'un gel est clairement visible (Figures IV.26 et IV.27). Dès que ce gel sèche, lors d'une baisse d'humidité ou une augmentation de température, il se solidifie par condensation des espèces présentes dans le gel et forme un nouveau matériau amorphe avec une importante porosité. Des produits cristallins se forment à la surface ou sont emprisonnés à l'intérieur de ce matériau s'il y a contact avec l'air avant que la condensation ne soit complète. Par rapport à la structure du verre sain, la structure de ce nouveau matériau amorphe est fortement hydratée et davantage dépolymérisée puisqu'elle contient majoritairement des espèces  $Q^2$  ( Figures IV.29) Deux modifications visuelles et spectrales sont caractéristiques d'une altération par dissolution : l'apparition d'une nouvelle bande autour de  $670\text{-}680\text{ cm}^{-1}$  dans le spectre Raman et la formation d'un réseau de cupules à l'interface entre la couche altérée et le verre (Figures IV.27). Entre le gel/matériau amorphe et le verre sain il existe une couche de verre lixiviée de ses alcalins. Ainsi un verre ayant été exposé à une atmosphère humide non polluée par un acide est composé de trois couches : le verre sain, une couche de verre lixiviée et un nouveau matériau amorphe en surface.

### **Conclusion pour les verres historiques**

Les modifications de structure et d'apparence des objets du NMS sont similaires à celles produites par vieillissements en atmosphère humide et acide. Ce résultat confirme que les polluants organiques agissent sur le processus d'altération ; il suggère que les polluants acides sont responsable de l'altération des verres historiques du NMS. Par ailleurs ces résultats indiquent qu'il est possible de déterminer si un verre a été soumis à l'action d'une atmosphère acide ou non. Ces informations sur les modifications de structure et l'épaisseur de la couche altérée peuvent être obtenue *in-situ* et de façon non-destructive par spectroscopie Raman. Etant

donné que la réaction de dissolution est favorisée par l'augmentation de la température, cette altération n'est pas représentative de la situation à température ambiante. En revanche, la structure de la couche altérée obtenue dans des conditions réelles est vraisemblablement similaire à celle obtenue dans cette étude.

## V - MECANISME ET CINETIQUE DE L'ALTERATION

Lors de l'altération atmosphérique des verres sodiques, seuls les profils de concentration des alcalins, sodium et potassium, et de l'hydrogène sont modifiés. L'examen de ces profils a donné des informations sur la structure de la couche altérée et le processus d'altération ; et la mesure de la quantité d'ions sodium extrait et de l'épaisseur de la couche altérée a permis de quantifier et suivre l'avancée de l'altération.

L'examen de l'altération des verres dans une atmosphère inerte avec  $N_2$  à différentes humidités relatives indique que l'eau présente dans l'atmosphère est le facteur principal contrôlant l'altération des verres de composition instable. Les résultats de cette étude confirment l'existence des deux mécanismes d'altération à condition ambiante : la réaction de lixiviation avec extraction des alcalins et formation d'une couche hydratée; et la réaction de dissolution caractérisée par un enrichissement en alcalins à la surface. De plus, on observe une prédominance de la réaction de lixiviation au début de l'altération, avec une quantité d'alcalins extraite proportionnelle à la racine carrée du temps, puis à long terme, lorsque la lixiviation approche un état stable, la dissolution prédomine. Cependant la chimie de l'atmosphère influence la cinétique de ce processus ainsi que la composition de la couche de verre altérée.

Le film d'eau formé par l'humidité sur la surface sert d'interface de contact entre les polluants dans l'atmosphère et le verre. La hausse de l'humidité augmente le nombre de couches d'eau ce qui accélère la réaction de lixiviation proportionnellement (Figure V.16). On note que le processus d'altération est ralenti pour un verre exposé à l'air ambiant par rapport à un verre exposé à une atmosphère inerte ( $N_2$ ). Les faibles concentrations en  $CO_2$ ,  $SO_2$  contenus dans l'air réagissent avec la solution de NaOH formée en surface par l'eau, inhibant la dissolution du réseau silicate.

En présence des polluants organiques émis par les vitrines, la réaction de lixiviation est accélérée et amplifiée, et la réaction de dissolution n'a pas lieu. Cette étude a clairement montré

que le formaldéhyde n'agit pas sur la réaction de lixiviation, ce qui signifie que l'acide formique (qui l'accélère) n'est pas formé par oxydation. En revanche il réagit en surface avec la solution de NaOH induite par l'humidité, pour former du formate de sodium phase I' par la réaction de Cannizzaro. Par conséquent, le formaldéhyde et l'air ambiant ont un effet plutôt bénéfique pour le verre car ils neutralisent le NaOH empêchant la dissolution du réseau silicate.

L'augmentation d'altération observée pour les verres exposés aux atmosphères des vitrines est similaire à celle induite par l'acide formique, ce qui confirme que les acides sont responsables de cette accélération. Ces acides augmentent et maintiennent l'acidité de la solution en surface, ce qui accélère et maintient la réaction lixiviation. En atmosphère acide, la réaction de lixiviation reste toujours prédominante et sa vitesse est multipliée en moyenne par 4 par rapport à une atmosphère non acide. Non seulement les polluants acides augmentent la profondeur d'altération, mais ils augmentent aussi la quantité de sodium extrait au sein de la couche altérée. Ainsi la composition d'un verre altéré en atmosphère acide a une concentration en sodium ~1 at% par rapport à ~5 at% en atmosphère non acide (air ambiant, N<sub>2</sub> ou formaldéhyde) (Figures V.24 et V.25). La couche altérée formée est donc très appauvrie en alcalins et très hydratée. L'eau et la faible concentration en alcalins restant dans la couche peuvent servir à faciliter l'échange ionique et la lixiviation entre le verre sain et l'extérieur.

Plus le polluant est acide, plus il est dissocié, et plus grande est l'altération. Cependant l'augmentation de la concentration en polluant a peu ou pas d'influence sur l'altération, particulièrement à faible humidité relative. L'explication proposée pour ce phénomène est associée à la saturation du film par les polluants. Le faible volume que représente ce film signifie que la saturation en polluants dissous est atteinte rapidement même à faible concentration. La quantité de polluants nécessaire pour atteindre la saturation diminue avec l'humidité relative et l'aire de la surface d'échange du verre. Par ailleurs, il existe une compétition entre les différents polluants qui peut être expliquée par la différence de vitesse d'incorporation de ces polluants dans le film d'eau. Quelles que soient les proportions de chacun des polluants, les composés formates sont majoritaires car l'acide formique prédomine dans le film. Ce phénomène expliquera alors la présence majoritaire de composés formates sur les verres du NMS dans des atmosphères où l'acide acétique prédomine. Ainsi l'acidité du polluant, et dans ce cas l'acide formique est le seconde facteur, après l'eau, qui contrôle l'altération.

Les résultats ont montré qu'une concentration aussi faible que  $30.5 \mu\text{g}/\text{m}^3$  d'acide formique dans l'atmosphère produit autant de dommage que les concentrations six fois plus élevées des vitrines. Cette faible concentration est en dessous des limites de détection de la chromatographie ionique, technique généralement utilisée pour mesurer les taux de polluants dans les musées. Cette donnée est inquiétante d'un point de vue conservation des objets car elle indique que de telles atmosphères, néfastes pour des verres de composition instable, ne pourraient pas être identifiées.

La réaction de lixiviation est contrôlée par diffusion et la quantité d'alcalins extraite est proportionnelle à la racine carrée du temps quand les conditions environnementales (humidité et température) sont stables, comme c'est le cas généralement lors d'expériences en laboratoire. Cependant les conditions contrôlées du laboratoire ne sont pas représentatives de l'atmosphère du musée où les conditions sont loin d'être contrôlées et où des fluctuations quotidiennes, mensuelles et annuelles ont lieu. Cette étude a montré que ces fluctuations affectent de façon importante l'avancement de la réaction de lixiviation et donc la cinétique de l'altération. Chaque fois qu'une fluctuation a lieu, l'équilibre qui se développe est perturbé et un échange ionique rapide est réactivé dans le verre, causant une accélération de l'altération. Cette perturbation est visible dans les profils de concentration SIMS des verres par la réapparition du pic K au niveau du front d'échange dans le profil de concentration du potassium, pic caractéristique d'un échange ionique conséquent (Figures V.31 et V.32). Bien que la réaction de lixiviation tend vers l'installation de l'équilibre et la stabilisation de l'altération, il semble que cet équilibre n'est jamais atteint pour les verres exposés aux atmosphères de musées, dû aux incessantes fluctuations. Ceci est d'autant plus vrai dans les atmosphères acides où la réaction de lixiviation est importante. Par ailleurs, la cristallisation de produits d'altération en surface va aussi déplacer l'équilibre vers une augmentation de la lixiviation.

Par conséquent, l'altération des verres exposés à des polluants organiques acides dans les musées augmente constamment et ne se stabilise jamais (Figure V.36). Les expériences effectuées sur 13 mois ont permis d'établir que l'altération progresse de 1.6 nm par jour dans l'armoire 3 et de 2.3 nm par jour dans l'armoire 12 pour un verre de composition RG1. Ces valeurs indiquent qu'il faut en moyenne 50 ans pour obtenir une couche d'altération épaisse de  $37 \mu\text{m}$  (épaisseur d'altération du décanter), ce qui est cohérent avec la durée d'exposition des objets du NMS à cette atmosphère. La différence de cinétique d'altération entre les deux atmosphères est liée aux différences de conditions environnementales plutôt qu'à la différence de concentration en polluants. Enfin si un verre altéré en atmosphère acide est placé dans une

atmosphère non acide, la couche altérée va chercher à atteindre un nouvel équilibre en rapport avec la chimie de la nouvelle atmosphère.

## **CONCLUSION**

Cette étude a mis en évidence le rôle néfaste des polluants organiques acides dans l'altération des verres sodiques. Ces polluants acides combinés aux conditions environnementales fluctuantes entretiennent une altération continue par lixiviation qui induisent la formation de couches hydratées et dépourvues d'alcalins à la surface du verre. Cette couche est sensible à la déshydratation qui génère des craquelures pouvant amener à la désintégration complète de l'objet. Par conséquent, l'exposition des verres instables aux polluants organiques, lors du stockage dans des vitrines en bois par exemple, doit impérativement être évité.

Afin de pouvoir développer des traitements de conservation et des conditions de stockage appropriés pour les objets en verre altérés, il serait nécessaire d'étudier par la suite l'effet de l'environnement sur ces couches altérées, en examinant en particulier le comportement mécanique de ces couches. Il serait aussi essentiel d'acquérir de plus amples informations sur la structure de cette couche et ses modifications, en utilisant par exemple la RMN du solide en parallèle de la spectroscopie Raman.

Enfin, cette recherche s'est limitée à l'étude des verres sodiques sur lesquels il a été possible de développer l'application de la spectroscopie Raman, une méthode non-destructive, pour obtenir des informations sur la composition, stabilité et altération des verres. Il serait intéressant d'élargir cette étude à d'autres compositions, en particulier les verres potassiques qui sont encore plus instables et qui ont été largement utilisés au sein des monuments historiques ou pour les objets historiques.